A Cold-active Transglutaminase:
Purification, Characterization, Expression & Application in Producing Food Hydrogels

by

Yi Zhang

Department of Food Science and Agricultural Chemistry
McGill University, Montreal

June 2019

A thesis submitted to McGill University in partial fulfillment of the requirements for the degree of Doctor of Philosophy in Food Science and Agricultural Chemistry

ABSTRACT

Transglutaminase (TGase, EC 2.3.2.13) catalyzes acyl transfer reactions between the γ-carboxamide groups of peptides bound glutamine residues (acyl donors), and primary amines or water molecules (acyl acceptors). TGase can form cross-linkages in proteins that are useful in modification of food proteins structure and functions. In this study, TGase was purified from Antarctic krill (*Euphausia superba*) using salt fractionation and DEAE-Sephacel chromatography. The purified TGase had specific activity of 53.5 U/mg and MW of 78 kDa using SDS-PAGE. The TGase was active within an optimal temperature range of 0–10 ^{o}C and was Ca^{2+} dependent. The high catalytic activity at cold temperatures enabled the TGase to effect crosslinking of food proteins at low temperatures. Addition of the purified TGase at 0.1 U/mg into cold-set gelatin hydrogels significantly improved its textural properties including gel strength, setting time and melting temperature ($p < 0.05$). The studies on thermostability and kinetics found the cold-active TGase was quite stable at 0 to 40 ^{o}C and was readily inactivated above 60 ^{o}C. The conformational states and structural changes of the TGase as a function of incubation temperatures were identified using fluorescence spectroscopy. The gene encoding the krill TGase was identified using RNA sequencing, and the amino acids sequence was deduced as 753 residues. A homologous tertiary structure of the krill TGase was built using bioinformatics tools. The conserved domains and catalytic triad Cys333–His403–Asp426 were identified from the structure model, and the possible molecular interactions helped to explain the thermostability of this TGase enzyme. To utilize the cold-active TGase for commercial applications, there is the need for heterologous expression for large-scale production of the enzyme, as well as the production of substrates for enzyme catalysis. A gelatin high in α-chain was produced from thorny skate fish as substrate for TGase. Optimized conditions of the alcalase-assisted process produced 32% of α-chain containing 34% glycine and 16% imino acids determined by UPLC. FTIR spectroscopy, DSC and TGA were used to characterize the amide absorption bands and thermal decomposition. The α-chain gelatin hydrogel (1%, w/v) could withstand a wide range of temperatures, and exhibited high emulsifying activity, viscosity and stable gel clarity from 35 to 80 ^{o}C. Antioxidative peptides were also produced from Atlantic sea cucumber as substrates for TGase via proteolysis by alcalase and trypsin. The peptide sequences were characterized using LC-MS/MS and their *in vivo* functions were predicted using molecular docking analysis onto MPO enzyme. The cold-active TGase was expressed in *E. coli* and the recovered enzymes were used for forming antioxidant peptides/gelatin hydrogels.

RÉSUMÉ

La transglutaminase (TGase, EC 2.3.2.13) catalyse les réactions de transfert d'acyle entre les groupes γ-carboxamide de résidus de glutamine liés aux peptides (donneurs d'acyle), et d'amines primaires ou de molécules d'eau (accepteurs d'acyle). La TGase peut former des liaisons croisées dans les protéines utiles dans la modification de la structure et des fonctions des protéines alimentaires. Dans cette étude, de la TGase a été purifiée à partir du krill antarctique (*Euphausia superba*) par fractionnement de sel et chromatographie DEAE-Sephacel. La TGase purifiée avait une activité spécifique de 53,5 U / mg et un poids moléculaire de 78 kDa en utilisant SDS-PAGE. La TGase était active dans un intervalle de température optimale de 0 à 10°C et était dépendante du niveau de Ca2+. La forte activité catalytique à température froide a permis à la TGase d'effectuer les liaisons croisées des protéines alimentaires à basse température. L'addition de la TGase purifiée à 0,1 U / mg à des hydrogels de gélatine durcis à froid a considérablement amélioré ses propriétés texturales, notamment la résistance du gel, le temps de durcissement et la température de fusion ($p < 0,05$). Les études sur la thermostabilité et la cinétique ont montré que la TGase active à froid était assez stable entre 0 et 40°C et qu'elle s'inactive facilement à une température supérieure à 60°C. Les états conformationnels et les modifications structurelles de la TGase en fonction des températures d'incubation ont été identifiés par spectroscopie de fluorescence. Le gène codant pour la TGase du krill a été identifié à l'aide du séquençage de l'ARN et la séquence d'acides aminés a été déduite à 753 résidus. Une structure tertiaire homologue de la TGase du krill a été construite à l'aide d'outils bioinformatiques. Les domaines conservés et la triade catalytique Cys333–His403–Asp426 ont été identifiés à partir du modèle de structure et les interactions moléculaires possibles ont permis d'expliquer la thermostabilité de cette enzyme TGase. Pour pouvoir utiliser la TGase active à froid dans des applications commerciales, il est nécessaire d'avoir une expression hétérologue pour la production à grande échelle de l'enzyme, ainsi qu'à la production des substrats pour la catalyse enzymatique. Une gélatine riche en chaîne α a été produite à partir de poisson épineux en tant que substrat de la TGase. Les conditions optimisées du processus assisté par alcalase ont produit 32% de la chaîne α contenant 34% de glycine et 16% d'iminoacides, déterminée par UPLC. FTIR, DSC et TGA ont été utilisés pour caractériser les bandes d'absorption d'amide et la décomposition thermique. L'hydrogel en gélatine à chaîne α (1%, poids / volume) est capable de résister à un large intervalle de températures et présente une activité émulsifiante et une viscosité élevées, ainsi qu'une clarté de gel stable de 35 à

80°C. Des peptides antioxydants ont également été produits à partir du concombre de mer de l'Atlantique en tant que substrats de la TGase par protéolyse de l'alcalase et de la trypsine. Les séquences peptidiques ont été caractérisées à l'aide de LC-MS/MS et leurs fonctions *in vivo* ont été prédites à l'aide d'une analyse de couplage moléculaire sur enzyme MPO. La TGase active à froid a été exprimée dans *E. coli* et les enzymes récupérées ont été appliquées pour former des peptides antioxydants / hydrogels de gélatine.

CONTRIBUTION OF AUTHORS

Chapter I is a general introduction on the characteristics and functions of the enzyme TGase for food modification, as well as the rational and objectives of the studies entailed in the thesis.

Chapter II provides a detailed literature review of the enzyme. PhD candidate Y Zhang reviewed the literature and drafted the review papers based on the guidance of Professor B K Simpson. Dr. S He and Prof. T Geary contributed academic discussion and paper revision.

Chapters III – IX represent the research work based on various experiments. PhD candidate Y Zhang designed and performed the experiments, analyzed the data, and drafted the manuscripts. Professor B K Simpson supervised the research work, provided the research materials and facilities, guided the lab performance and data analysis, revised the manuscripts. Dr. S He contributed academic discussion and some training. Professor P Dutilleul guided the statistics work and revised related manuscripts. Dr. C Li contributed academic discussion and some training. Professors V Orsat & M J Dumont provided some research facilities for the experiments. Dr. E Bonneil provided some analysis on peptide work. Professors T Geary & A Jardim provided some research facilities for the experiments and some training.

Chapter X is a summary of the general conclusions and recommendations for further studies on the topic.

PUBLICATIONS

1. **Y Zhang**, B K Simpson. High thermal stability for a cold-active protein-crosslinking transglutaminase: from kinetics to structural analysis. (To be submitted to Food Chemistry)
2. **Y Zhang**, B K Simpson. Food-related Fish/shellfish transglutaminase: A review. (Submitted to Critical Reviews in Food Science and Nutrition on March 30, 2019)
3. **Y Zhang**, S He, E Bonneil, B K Simpson. Generation of antioxidative hydrolysates from Atlantic sea cucumber using alcalase versus trypsin: *in vitro* activity, *de novo* sequencing, and *in silico* docking for *in vivo* function prediction. (Submitted to Food Chemistry on 26 April, 2019)
4. **Y Zhang**, H Gohou, S Klomklao, B K Simpson. Microbial enzymes from fish processing discards. In book: Byproducts from Agriculture & Fisheries: Adding Value for Food, Feed, Pharma and Fuels, (B K Simpson, A N A Aryee, F Toldrá, Eds.). 2019: 259-275.
5. **Y Zhang**, J Zhang, B K Simpson. An introduction to agricultural and fishery wastes. In book: Byproducts from Agriculture & Fisheries: Adding Value for Food, Feed, Pharma and Fuels, (B K Simpson, A N A Aryee, F Toldrá, Eds.). 2019: 1-18.
6. **Y Zhang**, T Geary, B K Simpson. Genetically modified food enzymes: A review. Current Opinion in Food Science, 2019, 25: 14-18.
7. **Y Zhang**, P Dutilleul, C Li, B K Simpson. Alcalase-assisted production of fish skin gelatin rich in high molecular weight (HMW) polypeptide chains and their characterization for film forming capacity. LWT - Food Science and Technology, 2019, 110: 117-125.
8. **Y Zhang**, B K Simpson, M J Dumont. Effect of beeswax and carnauba wax addition on properties of gelatin films: A comparative study. Food Bioscience, 2018, 26: 88-95.
9. **Y Zhang**, P Dutilleul, V Orsat, B K Simpson. Alcalase assisted production of novel high alpha-chain gelatin and the functional stability of its hydrogel as influenced by thermal treatment. International Journal of Biological Macromolecules, 2018, 118: 2278-2286.
10. **Y Zhang**, S He, B K Simpson. Enzymes in food bioprocessing – Novel food enzymes, applications, and related techniques. Current Opinion in Food Science, 2018, 19: 30-35.
11. **Y Zhang**, S He, B K Simpson. A cold active transglutaminase from Antarctic krill (*Euphausia superba*): purification, characterization and application in the modification of cold-set gelatin gel. Food Chemistry, 2017, 232: 155-162.
12. N A Ackaah-Gyasi, **Y Zhang**, B K Simpson. Enzymes inhibitors: food and non-food impacts.

In book: Advances in Food Biotechnology, 2015: 191-206.

13. N A Ackaah-Gyasi, P Patel, **Y Zhang**, B K Simpson. Current and future uses of enzymes in food processing, In book: Improving and Tailoring Enzymes for Food Quality and Functionality, 2015: 103-122.

ACKNOWLEDGMENTS

My sincere thanks go to my supervisor, Professor Benjamin K. Simpson, for his encouragement, support, intellectual guidance and critical comments.

I am also grateful to the following professors and staff in our Faculty for their advice and training, especially Prof. P Dutilleul in the Department of Plant Science, Profs. T Geary & A Jardim in the Parasitology Institute, Profs. V Orsat and M J Dumont and M Ngadi in the Department of Bioresource Engineering. My comprehensive committee members in the Department of Food Science, Profs. V Yaylayan, S Bayen and S Kermasha, as well as my oral defense committee members Profs. Y Wang and A Ismail.

To the lab colleagues that I met during my studies, especially Dr. S He, Dr. H Fan, Dr. N A Ackaah-Gyasi, Dr. C Li, and P Sully, as well as the colleagues in the labs in Parasitology and Bioresource Engineering. My infinite thanks to my extended family members (uncles, aunts, cousins, nieces and nephews) and friends for their support.

Last but not least, my special thanks to my parents. I could not get this far without their love.

This thesis is dedicated to my respected teacher, beloved parents and good friends.

TABLE OF CONTENT

LIST OF FIGURES

LIST OF TABLES

LIST OF ABBREVIATIONS

ALC ……...……. Average of the local confidence
BLAST ……....…… Basic local alignment search tool
CDD ……. Conserved domain database
CID ……...… Collision-induced dissociation
COS …….……. Chitosan oligosaccharide
DEAE …… Diethylaminoethanol
DHA …….…… Docosahexaenoic acid
DMC ……..... N,N'-dimethylated casein
DNA ……. Deoxyribonucleic acid
DPPH ……... 2,2-diphenyl-1-Picrylhydrazyl
DSC ……..... Differential scanning calorimetry
EAA ……... Essential amino acids
EAI ……..... Emulsifying activity index
EC …… Enzyme commission
EEM ……..…….. Excitation – emission matrix
ESI ……..... Emulsifying stability index
FCCCD ……..… Face-centered central composite design
FTIR …… Fourier transform infrared
GDP ……..... Guanosine 5′-diphosphate
GMO …….. Genetically modified organisms
GO ……..... Gene ontology
GSH ……...… Glutathione
GSSG ……..…… Oxidized glutathione
GTP …… Guanosine-5′-triphosphate
IAA ……..…. Iodoacetic acid
IPTG …… Isopropyl β-$_D$-1-thiogalactopyranoside
KAAS …….….. KEGG automatic annotation server
KEGG ……...…. Kyoto encyclopedia of genes and genomes
KOG ……..….. Eukaryotic orthologous groups

LC-MS/MS …….. Liquid chromatography-tandem mass spectrometry
LOX ……..……. Lipoxygenase
MDC …… Monodansylcadaverine
MPO …….. Myeloperoxidase
MW ……...…… Molecular weight
MWCO ……. Molecular weight cut-off
NCBI ……...… National center for biotechnology information
NEAA ……..... Non-essential amino acids
NEM ……...……. *N*-ethylmaleimide
NI ……...… Nucleotide sequences
NMR ……..... Nuclear magnetic resonance
NR ……... Non-redundant protein sequences
OFR ……..……. Open reading frame
PCMB …….…… Parachloro mercuri benzoate
PCR …….…… Polymerase chain reaction
PDB ……...… Protein data bank
PITC ……...…… Phenylisothiocyanate
PMSF ……..……. Phenylmethylsulfonyl fluoride
POD ……..... Peroxidase
PPO ……...… Polyphenol oxidase
PTC ……...……. Phenylthiocarbamoyl
RNA ……...…… Ribonucleic acid
ROS ……...…… Reactive oxygen species
RSM ……..…….. Response surface methodology
SDS-PAGE ……. Sodium dodecyl sulphate - polyacrylamide gel electrophoresis
TCA …….. Trichloroacetic acid
TGA ……. Thermogravimetric analysis
TGase ……..……. Transglutaminase
UPLC ……...… Ultra performance liquid chromatography
WHO ……..……. World health organization

CHAPTER I. GENERAL INTRODUCTION

This thesis is on the purification, characterization and application of transglutaminase (TGase) from the cold-adapted marine species known as Antarctic krill (*Euphausia superba*), and its production in recombinant form in *Escherichia coli*. The enzyme is ubiquitous and widely distributed in animals, plants and microorganisms. The systematic name is protein-glutamine γ-glutamyl transferase, and it catalyzes acyl transfer reactions between the γ-carboxamide groups of peptide bound glutamine residues (as acyl donors), and primary amines or water molecules (as acyl acceptors). The enzyme is capable of forming inter- or intra- molecular cross-linking of protein via ε-(γ -Glu)-Lys bonds (Fleckenstein et al., 2004), which is a useful way to modify the physical and functional properties of foods. With the growing developments in food processing and food product development, there has been corresponding increase in the need for TGase for the production of cheese and dairy products, imitation seafood products, restructured meats, meat analogs from plant proteins, pasta, tofu, noodles, etc. Commercial TGases are mostly derived from guinea pig liver and microorganisms (Zhu and Tramper, 2008). The supply from these traditional sources is inadequate to meet the growing industrial need for the enzyme. Thus, newer sources of the enzyme are needed; in particular, those endowed with unique properties to suit particular applications, as well as novel strategies to produce the enzymes cost effectively.

TGases from aquatic species have been studied in more than 20 species from both the freshwater and marine habitats, such as carp, sardine, squid, and red bream. They differ from their terrestrial counterparts, in terms of structural and functional properties. For instance, marine species from the cold habitats, are acclimated to cold temperatures and their enzymes are stable and active at cold temperatures. The cold active enzymes have high catalytic activity at low temperatures and are heat-labile due to their flexible enzyme structures. These cold active enzymes have great potential for applications in the food industry; however, relatively few studies have been conducted with respect to the TGases from cold-adapted organisms.

Antarctic krill, a dominant species in the Antarctic Ocean, is a small shrimp-like invertebrate. In addition to its use as human food, Antarctic krill has also been studied as source for protease enzymes such as trypsins, chymotrypsins and carboxypeptidases, and xylanases. These enzymes were found to perform better catalytically in cold temperatures compared with the commercially available counterparts from mammals and microorganisms. Although there have been no studies on Antarctic krill TGase, the enzyme has been purified from other aquatic animals like botan shrimp, scallop, squid, carp, rainbow trout and atka mackerel (Nozawa et al., 1997a).

There are numerous potential applications of cold active TGases in low temperature food processing such as the production of surimi, ice cream, cold beverages, cold-set gels, and cold-cast films, etc. TGase has also been used to enzymatically modify gelatin by forming cross-linked bonds to enhance the rheological properties. Gelatin can set to elastic gels and films on cooling below 35^{o}C from disordered molecules to ordered network predominantly by hydrogen bonds, where TGase would introduce additional covalent cross-links to improve gelation. Microbial TGase has been used to prepare soy protein cold set gels, and porcine myofibrillar protein gels; thus, it is of interest to study the relative performance of cold active TGase from marine species in forming cold-set protein gels. The thermostability of cold-active enzymes is important for their utilization in food processing as it influences the structural and functional properties of the enzyme. Gelatin can cold-set as hydrogels with high water holding capacity, biodegradability and biocompatibility. Gelatin hydrogel is currently used as food ingredient such as food thickener and gelling agent.

In this study, it was intended to purify TGases from the cold-adapted Antarctic krill and characterize it with respect to its kinetic properties, and responses to pH and temperatures, activators and inhibitors. It was also intended to use molecular biology and bioinformatics techniques to produce and characterize the recombinant form of the enzyme. The enzymes thus produced were then to be verified for their potential for food and related applications on a fish gelatin for making cold-set gelatin gels and films.

Thus, the objectives of the research were to:

1. purify novel cold-active transglutaminases (TGases) from Antarctic krill, and investigate the biochemical properties and thermostability of the cold-active TGase via kinetic measurements, and conformational change using fluorescence spectroscopy.
2. extract gelatins that form strong hydrogels as substrates of TGase using green procedures.
3. use enzyme-assisted methods to produce antioxidative peptides as substrates of TGase.
4. obtain the gene sequence encoding the TGase, and analyze its sequence and predict the structure by bioinformatics, and express the TGase in *E. coli* and use it to incorporate antioxidant peptides in gelatin hydrogels at low temperatures.

CHAPTER II. LITERATURE REVIEW

2.1. Trends in food enzymes

Enzymes are biocatalysts that can be applied in the food industry as efficient, safe, and environment-friendly alternatives to conventional food processing. The industrial enzymes market was valued US $6.1 billion in 2017 and is expected to reach US $8.5 billion by 2022 (Ferrer et al., 2016). The food industry holds a large share of this output. Enzymatic bioprocessing methods are currently used to produce various foods including dairy, baking, beverages & brewing, fats & oils, meat, and functional foods. Apart from their usage as processing aids, enzymes are also naturally present in foods where they elicit both desirable and undesirable effects. Examples of desirable enzymes and their effects in foods include, endogenous β-glucosidase, polyphenol oxidase (PPO), peroxidase (POD), esterase that influence ripening and flavors generation (Hbaieb et al., 2017; Ramírez et al., 2016); cathepsins in myofibrillar protein hydrolysis in fermented products (Yang et al., 2015), as well as proteases and transglutaminases in food texture modification. Examples of the undesirable effects of enzymes in foods such as dark discolorations in fresh fruits, vegetables and raw crustacea caused by endogenous PPO or rancidity caused by endogenous lipase and lipoxygenase (LOX). Enzyme kinetic modeling has been an important strategy for exploring the behavior of enzymes on substrates under various reaction conditions to achieve the goal of producing high quality and affordable food products using classical enzymes. Some recent research on modeling systems include hydrolases (e.g., pepsin, trypsin, amylase, alcalase, cellulase, lipase) the hydrolysis / digestion of protein, starch and lipid (Do et al., 2016; Morales-Medina et al., 2018); inactivation of POD, PPO and LOX (Şakiroğlu et al., 2016; Stephany et al., 2016); as well as using specific enzymes to remove undesirable compounds in foods such as chlorogenic acid lactones in coffee (Kraehenbuehl et al., 2017), and biogenic amines in fermented foods (Şahin-Ercan et al., 2016). There are more than 55 different enzymes products used in food processing (Van Oort, 2010), and the number is increasing with the discovery of more novel food enzymes. In this study, some new trends on enzymatic processing are summarized which include: novel or improved enzymes that are better suited to particular food processing environments, as well as recently developed enzyme inactivation and enzyme immobilization techniques.

2.1.1. Novel food enzymes

Novel enzymes are generally associated with unique properties or functions such as low-temperature activity, thermostability, pH adaption, and others like tolerance to high salinity, pressure, solvents, metal ions and inhibitors. These novel enzymes are valuable in food

bioprocessing. For instance, cold-active enzymes enable catalysis to occur at low temperatures. Cold-active enzymes are generally also heat-liable due to their flexible structures resulting in their easy inactivation by mild heat treatment. Living organisms inhabiting extreme environments (a.k.a. extremophiles) have been shown to be excellent sources of novel enzymes (a.k.a. extremozymes) that can retain their integrity and function under extreme reaction conditions. Both bioprospecting and artificial design are used to discover novel or improved food enzymes. Conventional screening approaches involving enzyme purification and activity determination are a valuable strategy to obtain new enzymes from animal, plants and microorganisms. In addition, metagenomic screenings have been used as effective tools for the discovery of any biotechnological relevant *enzymes* including hydrolases and oxidoreductases (Thies et al., 2016). For this, environmental samples from extreme environments are used to establish a metagenomic library from extracted DNAs to screen the genes encoding new enzymes (Ferrer et al., 2016). Protein engineering has been used to design enzymes for specific reactions using molecular biology approaches such as site-specific mutagenesis.

In food processing, proteases are widely used for meat tenderization, curdling of milk, beverage clarification, de-bittering, texturization, deproteinization, and to produce flavor. Proteases have been used for decades in the cheese industry for milk clotting. Nonetheless, there is still increasing demand for novel milk coagulating enzymes in the dairy industry. In this regard, a new milk-clotting protease was recently discovered as an alternative to rennet for the development of cream cheese product (Lemes et al., 2016). A new milk-clotting enzyme for manufacturing soft cheese from cow milk and goat milk was reported from sunflower seeds (Nasr et al., 2016). Proteases are also used to produce protein hydrolysates for incorporation in foods such as infant formula. Such hydrolyzed formula milks are easier to digest and have reduced allergenic potential (Fleischer et al., 2016). A novel cold-active serine protease isolated from *Chryseobacterium* sp. facilitated tenderization of meat during refrigerated storage to improve both the texture and taste of the meat (Mageswari et al., 2017). A thermostable acidic protease with optimal catalytic activity at pH 5.0 and 55 °C (Souza et al., 2017) was considered to be useful in coagulation of casein in cheese production, and for the degradation of proteins for juice and wine clarification. Other novel proteases found recently include a highly thermostable alkaline caseinolytic protease with maximal activity at pH 7 and 80 °C (Dadshahi et al., 2016), a new alkaline trypsin (Bkhairia et al., 2016) with antithrombotic and anticoagulant properties purified from the edible medicinal plant *Aster*

koraiensis Nakai (Choi et al., 2017), an aspartic protease for pork tenderization and for the preparation of turtle peptides (Sun et al., 2017b), a salt-stable protease that is useful in low-salt fish sauce fermentation (Gao et al., 2017), and an inexpensive fungal protease with high catalytic activity over broad pH and temperature ranges (Novelli et al., 2016).

Glycoside hydrolases hydrolyze glycosidic bonds and are widely used in syrup, beverage (beer, wine), and dough production. A new low-temperature mashing system containing diverse amylolytic enzymes was applied to produce wort on a commercial scale cost-effectively (Holmes et al., 2017). Amylases hydrolyze starches to produce simple sugars in varying degrees. For instance, a novel recombinant α-amylase produced maltose more efficiently from liquefied corn starch than β-amylase (Jeon et al., 2016). Recombinant amylases, especially from fungi origin or from malted cereals, are abundantly used presently in baking. Production of α-amylase can be accomplished inexpensively from agri-residues such as wheat bran via solid-state fermentation. Amylases have a broad range of applications in the food and brewing industries, as well as in baking and the preparation of digestive aids. Amylases also have extensive applications in starch saccharification, in the textile and detergent industries. Moreover, a novel thermophilic β-glucosidase showed high selectivity for the synthesis of prebiotic galactotrisaccharide (Yang et al., 2018). A polydatin-β-d-glucosidase that facilitates resveratrol preparation (Zhou et al., 2016) and an amylase used in cake formulation (El Abed et al., 2017), were also reported recently.

Lipases act on various kinds of esters to produce acids and alcohols. They are usually used to enrich flavor and generate meaty or fruity aromas in meats, cereals, fruit juices, alcoholic beverages, and dairy products. A new lipase was isolated from the liver of seabass and used to defat seabass skin more effectively than isopropanol (Sae-Leaw and Benjakul, 2018). A new thermostable and solvent-resistant recombinant lipase was produced from *Rhodothermus marinus* with potential for food lipid processing and aroma improvement (Memarpoor-Yazdi et al., 2017).

Transglutaminases (TGases) are transferases and catalyze acyl transfer reactions between the γ-carboxamide groups of peptide-bound glutamine residues (acyl donors), and primary amines or water molecules (acyl acceptors). They form inter- or intra- molecule cross-linkages in proteins via ε-(γ-Glu)-Lys bonds which is useful for modifying the physical and functional properties of foods. A cold-active TGase with an optimal temperature of 0-10 °C was recently purified from Antarctic krill and shown to be capable of potentiating cold-set gelling of fish gelatin (Zhang et al., 2017b). A new bacteria strain *Streptomyces* sp. CBMAI 1617, was recently shown to produce

high-yield TGase that enabled the preparation of wheat protein and flour based doughs similar to commercial TGase (Ceresino et al., 2018). TGase is very versatile and is used in the food industry to: improve the texture, appearance, firmness, and shelf life of meat; enhance the firmness of fish products; improve the quality and texture of dairy products; improve the mechanical properties of protein-based biodegradable films; and improve the texture and volume of baked goods. Because of the increasing use of TGase in the food industry, it is to be expected that some common diets on the market would contain residual amounts of the enzyme. In addition to the food uses, TGase is also used extensively as a biocatalyst in the biomedical and biotechnology fields. Nonetheless, TGase catalyzed reactions in proteins generate isopeptide bonds that are different from conventional peptide bonds. The isopeptide bonds may not lend themselves to degradation in the same way as regular peptide bonds; thus, it is possible that reaction products differ in important respects in terms of conformation, sizes, degree of cross-linking, digestibility and possible allergenicity. Studies have established a direct correlation between the proliferation in celiac disease and the higher consumption of the enzyme ingested through baked goods such as breads (Porcelli et al., 2016), which poses the question as to whether the use of TGase as a food processing aid has triggered an increase in the incidence of gluten intolerance in consumers.

2.1.2. Enzymes in new food applications

Enzymes can be used to enhance the production of nutrient-dense foods; i.e., foods that are high in nutrients but low in calories. Enzymes could achieve this by breaking down rigid plant-based foods to release the nutrients such as vitamins and minerals; hydrolyzing anti-nutritive substances such as phytates and enzyme inhibitors; via transformation of substrates as in the formation of allicin; or by simply concentrating or stabilizing beneficial components in foods. Peptide ligation mediated by enzymes such as sortase, butelase or trypsiligase is a valuable strategy to prepare complex peptides as nutritional food additives (Schmidt et al., 2017). Docosahexaenoic acid (DHA) in fish oils can be concentrated using commercial *Candida antarctica* lipase A and TL 100L lipase due to their selectivity of hydrolysis, which is useful for food fortification and pharmaceutical applications (Akanbi and Barrow, 2017). A new date fruit product enriched in soluble dietary fiber with antioxidant and prebiotic effects was produced using enzymatic conversion from insoluble dietary fiber (Mrabet et al., 2017).

New food products can be prepared with improved physicochemical and mechanical properties by enzymatic treatments. Branching and debranching enzymes affect the ratio of α-1,4 and α-1,6-

glycosidic bonds in starch which decides the structure and performance of resultant food products. A highly branched dextrin was prepared from high-amylose maize starch using a waxy rice branching enzyme (Tian et al., 2016). TGases were added in goat's whey cheese (Karzan et al., 2016) and meat products (Hong et al., 2016), etc., and the corresponding products showed enhanced sensory, texture properties and yield.

Bioactive compounds separation and extraction can be assisted by enzymes to increase the yield, purity, and efficiency. Bioactive compounds such as phenolics, flavorings and colorants can be extracted by diverse combination techniques, e.g., enzyme-assisted three-phase partitioning, microwave-assisted enzymatic extraction, ultrasound-assisted enzymatic extraction, or enzyme-assisted supercritical fluid extraction (Marathe et al., 2017). Recently, Chinook salmon lipase was immobilized and used to produce dairy products with distinct flavors by altering free fatty acid composition (Kurtovic et al., 2016). Phenolics extracted from the by-products of winemaking using enzymes, showed antioxidant and enzyme inhibitory effects (i.e., inhibition of alpha-glucosidase and lipase activities) (de Camargo et al., 2016). Enzymatic extraction in combination with pressurized liquids was used to recover phlorotannin from the brown marine algae. Phlorotannins have important pharmacological activities including antioxidant, anti-HIV, antidiabetic, anticancer, anti-inflammatory and enzyme inhibitory properties, and are touted as a potential functional ingredient in marine medicinal foods (del Pilar Sánchez-Camargo et al., 2016). Chitooligosaccharides (COSs) are bioactive compounds that have been shown to have antimicrobial and immuno-stimulating effects with potential for several applications such as in tumor growth inhibition, mineralization to increase bone strength, prevention of malaria, wound dressing, and in food preservation via their antifungal effects (Aam et al., 2010). They are water-soluble and are commonly incorporated into dairy products and beverages. COSs have been prepared from shrimp chitosan using enzymes such as chitinases and chitosanases, and also by non-specific enzymes lysozyme, papain, or cellulase (Laokuldilok et al., 2017).

Enzyme treatment sometimes aim to relieve the safety risks of food products, in terms of breaking down the harmful bacteria or undesirable compounds such as biogenic amines, gluten, lectins, acrylamide, cyanogenic glucosides, glucosinolates, protease inhibitors, etc. Some enzymes such as cellulase combined with surfactants were shown to drastically remove *Salmonella* biofilm under meat processing, which could be a new strategy to control *Salmonella* outbreak (Wang et al., 2016a). An immobilized lysozyme exhibited effective lysis of lactic bacteria *Oenococcus oeni*

in white and red wines (Cappannella et al., 2016). A zearalenone-degrading enzyme was immobilized as a novel detoxifying agent (He et al., 2016). Furthermore, degradation of gluten in grain products can be achieved with enzymes such as trypsin, chymotrypsin, pepsin, etc. (Colgrave et al., 2017) which benefits consumers who are gluten intolerant. High-quality gluten-free products such as sourdough bread, pasta and beer were produced using new approaches with suitable peptidases (Scherf et al., 2016). Asparaginase may reduce acrylamide formation in cooked foods by converting asparagine to aspartic acid, while maintaining sensory quality (Xu et al., 2016).

2.1.3. Innovative enzyme-related effects in food bioprocessing

Enzymes need to be inactivated in food processing to either curtail their undesirable effects (e.g., some enzymes such as POD, PPO, LOX or lipase), or prevent continued activity of desirable enzymes in food products after they have been used to achieve the desired transformation (e.g., proteases, amylases, TGases). Both chemical and physical procedures are developed for enzyme inactivation. Thermal treatment is the conventional inactivation method, followed by high pressure, microwave, and infrared or ultraviolet light treatments. In recent years, some new non-thermal technologies have emerged. Examples of non-thermal strategies to inactivate enzymes include the use of high intensity light pulses, pulsed electric fields, and ultrasound to effectively terminate proteolysis (Arroyo et al., 2017); ohmic heating consisting of passing an electric field through foods to inactivate PPO and POD in sugarcane juice (Brochier et al., 2016); pulsed light has also been used to inactivate horseradish POD (Pellicer and Gómez-López, 2017).

There are also novel enzyme immobilization approaches been continuously developed to enable recovery and reuse of enzymes, as well as their removal from food products to stop continued hydrolysis or pose potential problems like allergenicity. Different commercial food enzymes such as lipase, glucose isomerase, lactase, protease, invertase have been immobilized for producing corresponding food products, namely, interesterification of oils/fats, high-fructose corn syrup, lactose, amino acids, and invert sugar. The development of immobilized enzymes is based on three immobilization mechanisms, i.e., mild adsorption using charges or polarity of enzymes, covalent binding/cross-linking of enzymes to surfaces or to the enzymes themselves, and entrapment / microencapsulation. Developments in enzyme immobilization include the discovery of various innovative carriers that are cheaper, inert, stable, reusable, efficient, or permit catalysis to occur under harsh reaction conditions. Enzymes have been immobilized onto biotinylaminopropyl celite, thionyl chloride-activated controlled-pore glass, nylon, and on microelectrodes. Other carriers that

have been used are poly(ethylene glycol) crosslinked to albumin, poly (carbamoyl sulfonate) hydrogels, and polyethyleneimine-coated magnetite particles (Datta et al., 2013).

2.1.4. Genetically modified food enzymes

According to the definition of genetically modified organisms (GMOs) by World Health Organization (WHO), the term "genetically modified enzymes" can be used to refer to situations in which the DNA encoding the enzyme of interest has been artificially altered. Non-genetically modified enzymes remain the major source for the food enzyme market, which includes endogenous enzymes produced from animals, plants and microorganisms. Modern food processing tends to be sophisticated and precise, and sometimes requires extreme conditions such as high temperature, high pressure, extreme pH, salinity and the use of solvents. However, native enzymes often have limitations that need to be improved to suit specific food processing environments. Genetic modification aims to rationally improve enzymes to enhance characteristics such as purity, yield, specificity, catalytic efficiency, stability, surface property and multifunctionality, as well as enable cost-effective production and sustainable development for food processing.

The strategy for producing genetically modified food enzymes is based on genetic engineering and requires comprehensive understanding and integration of bioinformatics, enzymology, biophysical chemistry and molecular biology, etc. Most genetically modified enzymes are expressed in well-established standard microbial model systems such as *E. coli* and *Pichia pastoris*. There are a few strategies for producing genetically modified enzymes depending on information known about the target enzyme and the purpose of its use:

(i) Gene sequence optimization is commonly used for heterologous expression of recombinant enzymes to optimize codon bias of the host cell, as well as to limit mRNA secondary structure that could inhibit translation (Rosano and Ceccarelli, 2014). These changes usually increase yield, while the amino acid sequence remains the same.

(ii) Gene truncation or fusion requires knowledge of the relationship between amino acid sequence and enzyme function. Gene truncation involves eliminating DNA sequences that are not functionally important, enabling the enzyme to be expressed in higher yield or with higher activity; gene fusion constructs a gene with 2 or more enzyme DNA sequences so that the recombinant enzyme has multiple functions (Dediu, 2015).

(iii) Site-directed mutagenesis is a rational design process based on in-depth knowledge of the target enzyme in terms of structure, catalytic mechanism, active site, etc. DNA sequence(s)

encoding specific amino acid(s) that are related to activity or structural stability is (are) replaced, inserted or deleted to produce enzymes with desired or improved properties (Hua et al., 2018).

(iv) Directed evolution, a non-rational design process that requires no prior knowledge of the target enzyme, is an *in vitro* accelerated process that mimics natural evolution for generating enzymes. It consists of two key processes: genetic diversity generation for constructing combinatorial libraries, and high-throughput screening or selection. The first process can be achieved by random mutagenesis using error-prone PCR techniques, or gene recombination using representative DNA-shuffling techniques (Labrou, 2010). The second process for identifying or isolating improved variants may be quite difficult to perform, so that developing efficient screening protocols has been a primary goal of innovation (Packer and Liu, 2015).

(v) Semi-rational design involves mutations based on sequence, structure or computational models, followed by small-scale mutagenesis and screening methods (Hua et al., 2018). An example of semi-rational design is site saturation mutagenesis, in which a mutant library is created containing all possible substitutions at one or more target positions in a gene sequence (Özgün et al., 2016).

The material presented here summarizes novel food enzymes produced by genetic modification, especially using strategies (ii) - (v) and discusses their improved properties as well as applications and potential applications in food processing.

2.1.4.1. Genetically modified carbohydrases/glycosidases

Carbohydrases are among the most widely-used enzymes in the food industry, being employed in baking, brewing, flavor production (e.g., sweetener production), prebiotics (*e.g.* galactooligossacharides, fructooligossacharides, chitooligosaccharides), etc. Some of these enzymes break down polysaccharides into simple sugars. Alpha-amylase (EC 3.2.1.1) is ubiquitous in the starch industry; the commercially available *Bacillus licheniformis* α-amylase is thermostable but acid-sensitive. Novel *Bacillus licheniformis* α-amylases obtained using directed evolution by replacing active site domain His residues with Arg and Asp residues had higher activity at pH 4.5 than the wild type enzyme (Liu et al., 2014a; Liu et al., 2017c), which enhances starch liquefaction, saccharification and fermentation processes in which the pH of starch slurry is usually < 6.0 (Cates et al., 2010). A modified *Rhizopus oryzae* α-amylase obtained using site-saturation mutagenesis of His 286 had a higher optimum temperature (60 ^{o}C) and lower optimum pH (4.0–4.5) than the wild-type enzyme (Li et al., 2018b), properties better suited for use in high

maltose syrup production. A mutant *Aspergillus aculeatus* β-glucosidase (EC 2.3.1.21) obtained using site-saturation mutagenesis had improved hydrolytic efficiency especially to cellobiose, and was used to accelerate the saccharification of alkaline-pretreated bagasse (Baba et al., 2016). The substrate specificity of *Thermotoga maritima* β-glucosidases after genetic modification was enhanced for quercetin glucosides (Sun et al., 2014), suggesting its usage in producing aglycones that have high pharmaceutical activity. Endo-β-1,4-xylanase (EC 3.2.1.8) cleaves the β-1,4 glycosidic linkages in xylans. A variant of this enzyme generated using site-directed mutagenesis exhibited higher specific activity and was utilized in the production of xylooligosaccharides from wheat straw under thermal and alkaline conditions (50–65 ^{o}C, pH 7–10) (Faryar et al., 2015). Novel endo-β-1,4-xylanases with modification in secondary binding sites also showed increased specificity toward water-insoluble (but not water-soluble) wheat arabinoxylan, and its application in bread making resulted in increased loaf volumes (Leys et al., 2016). An engineered β-1,3-1,4-glucanase (EC 3.2.1.73), hydrolyzing β-1,3-1,4-glucan usually found in avena, rice, oats and barley, had improved catalytic efficiency, thermostability and halostability following replacement of hydrophobic Lys 48 with Ala and Leu (Lee et al., 2017). *Bacillus* spp. is the main source of β-1,3-1,4-glucanase used in malt extract production in the brewing industry, and novel β-1,3-1,4-glucanases were produced by replacing Lys with Ser to form rigid β-sheet structures. The modified glucanases functioned effectively under industrial operating conditions with improved optimal temperature and thermostability (Niu et al., 2015).

Some types of carbohydrases hydrolyze disaccharides into monosaccharides. For example, a novel *Saccharomyces cerevisiae* invertase (EC 3.2.26) was engineered to have optimal pH and stability ranges for the breakdown of sucrose into glucose and fructose; the enzyme was modified by the substitution of hydrophilic residues in the active site region or peripheral loops with hydrophobic amino acids (Mohandesi et al., 2017). Another genetically modified invertase with high transfructosylating activity was used for simple and efficient production of prebiotic fructooligosaccharides (Marín-Navarro et al., 2015). Commercial β-galactosidase or lactase (EC 3.2.1.23) is commonly applied in lactose-free milk product processing, in which the process temperature is relatively low. A variant of β-galactosidase obtained using directed evolution had high activity in industrial-type conditions for milk processing, i.e., substrate lactose, buffer pH 6.75, and 8 °C (Rentschler et al., 2016). To improve the transglycosylating activity of this enzyme, a thermoresistant *Thermotoga maritima* β-galactosidase modified using rational design was

obtained with better specificity for the biosynthesis of galacto-oligosaccharides, a prebiotic compound (Talens-Perales et al., 2016).

2.1.4.2. Genetically modified proteases/peptidases

The major use of proteases in the food industry is hydrolysis of protein matrices to enhance flavor, texture or functional properties in diary, meat and fish products. Commonly used food proteases are derived from animals (such as trypsin, chymotrypsin, chymosin/rennet, pepsin), plants (such as papain, bromelain, ficin), and microorganism (such as the microbial acid protease Flavourzyme® from *Aspergillus oryzae* and proteinase A from *S. cerevisiae*; bacteria neutral proteases produced by *Bacillus circulans* BM15 and *Streptomyces nogalator* AC 80; and bacteria alkaline proteases produced by *Aspergillus niger* and *Bacillus subtilis*).

Unlike food carbohydrases and lipases, animal/plant-derived food proteases are generally less commonly found in genetically modified forms, probably because the versatile properties of the native proteases are adequate to suit most required temperature and pH conditions in food processing, and their catalytic mechanism has been well investigated. It could also be due to the very ample availability of microbial proteases for industrial uses**.** Another reason could be the limitations posed for efficient expression of proteases derived from animal or plant sources in microbial systems.

Recent research on modified food proteases from *Aspergillus* and *Bacillus* species indicates that engineered metalloproteases obtained through site-saturation mutagenesis of His224 had improved affinity for substrate, making the synthesis of *Z*-aspartame more cost-effective (Zhu et al., 2018). An acid protease from a mutant *A. oryzae* strain was produced using solid state fermentation with potato pulp powder, with enhanced glycine releasing activity (Murthy and Kusumoto, 2015). A truncated neutral protease from *A. oryzae* had optimum pH of 8.0 and optimum temperature of 55 ^{o}C, and its enzymological characterization suggested that it was efficient in antihypertensive peptide production, debittering, and food oil processing (Ke et al., 2012).

Bacillus spp. are the main producers of alkaline proteases with high thermal and pH stabilities. Subtilisin natto kinase, a serine protease from *B. subtilis* var. *natto*, was modified by site-directed mutagenesis to obtain higher specific activity and oxidative stability, and may be useful as a potential cardiovascular drug due to its strong fibrinolytic activity (Weng et al., 2015). The cold activity at 10 ^{o}C and alkali-resistant properties of a *Bacillus alcalophilus* alkaline protease were improved through directed evolution using error-prone PCR (Liu et al., 2014b) for use in cold-

temperature food processing. Similarly, an alkaline serine protease from mesophilic *Bacillus pumilus* was engineered to have increased hydrolytic efficiency at 15 ^{o}C without compromising thermostability (Zhao and Feng, 2018). Modified proteases are also applied in the detergent industry. An alkaline protease isolated from an oil-polluted mud flat metagenome by random mutagenesis displayed robust compatibility with laundry detergents at low temperature (30 °C) and alkaline pH range (pH 8.0–11.0) (Gong et al., 2017).

2.1.4.3. Genetically modified lipases

Lipase (EC 3.1.1.3) is the most common biocatalyst for lipid (fats and oils) modification. *Bacillus* lipases display activities over wide pH and temperature ranges, and some possess fatty acid specificity. Lipase A from *B. subtilis* was expressed as a fusion protein with cell wall mannoprotein Pir4 resulting in an immobilized lipase, and was used as a leavening agent to enhance rheological and aromatic properties of bread (Paciello et al., 2015). The secretion of *Rhizopus oryzae* lipase was improved by rational design of the *N*-glycosylation sites, which could meet the industrial demand for *Rhizopus* lipase, especially for the edible oil and fat industries (Yu et al., 2017b). *Candida rugosa* lipase isozymes modified by site-directed mutagenesis had high catalytic efficiency for producing fatty acid methyl esters and diglycerides as food emulsifiers, as well as for the conversion of crude *Jatropha curcas* seed oil into biodiesel (Chang et al., 2014; Kuo et al., 2015). *Malassezia globose* lipase with specific activity especially on mono- and diacylglycerol was modified with enhanced thermostability to meet industrial-scale requirements, making it a potential biocatalyst for synthesis of diacylglycerols in edible oils with health benefits (Gao et al., 2014). Engineered thermostable T1 lipases had low activity toward long-chain triacylglycerols; thus, they are potential biocatalysts to enhance flavor in dairy products by generation of short-chain fatty acids from milk fats (Tang et al., 2017). A *Thermomyces lanuginosus* lipase modified using semi-rational design was targeted to enhance methanol tolerance for potential use in biofuel production from waste food oils and grease (Tian et al., 2017).

2.1.4.4. Other genetically modified food enzymes

A D-psicose 3-epimerase (EC 5.1.3.31) modified by site-directed mutagenesis displayed high substrate-binding affinity, catalytic efficiency and thermostability in catalyzing the isomerization of D-fructose to D-psicose, an ultra-low-calorie sweetener with desirable physiological properties (Zhang et al., 2016b). Similarly, engineered *Caldicellulosiruptor saccharolyticus* cellobiose 2-epimerases (EC 5.1.3.11) showed increased specific activity to directly convert lactose into

lactulose without co-production of epilactose, and its application will boost the commercial availability of lactulose, a non-digestible disaccharide used as a prebiotic food additive and medicine (Shen et al., 2016). A novel trehalose synthase (EC 2.4.1.245) from *Picrophilus torridus* was prepared by replacing Pro residues to increase thermostability and catalytic efficiency, and was used to convert maltose from low-value agricultural products such as sweet potato starch to high-value trehalose (Chou et al., 2010). *Yersinia* phytases (EC 3.1.3.8) were genetically manipulated using site-directed mutagenesis to improve pepsin and trypsin resistance and thermostability, enabling potential use for efficient hydrolysis of phytic acid to inorganic phosphate to improve nutrient uptake from foods (Niu et al., 2017). A novel di-D-fructose dianhydride I (DFA I)-forming inulin fructotransferase was engineered using rational design to improve its catalytic behavior, including activity and thermostability, so that it could produce prebiotic DFA I in industrial processes using inulin as substrate (Yu et al., 2017a). Nitrilase (EC 3.5.5.1), which converts nitriles into corresponding carboxylic acids, was genetically modified to achieve higher activity for stereospecific production of (*R*)-(−)-mandelic acid, useful in the production of pharmaceuticals (Liu et al., 2014c). A mutant *Aspergillus niger* α-L-rhamnosidase with improved thermostability and substrate affinity reduced bitterness caused by naringin in orange juice (Li et al., 2018a). 1,4-*α*-glucan branching enzyme (EC 2.4.1.18) was engineered by Met349 mutation to achieve higher activity for the formation of α-1,6-glucosidic linkages, and could form highly branched potato starch (Liu et al., 2017b). A novel *Bacillus stearothermophilus* NO2 cyclodextrin glycosyltransferase was produced through iterative saturation mutagenesis around the catalytic residues, and was used to produce 2-*O*-*α*-D-glucopyranosyl-L-ascorbic acid, which has great advantages in food processing due to its stability and facile degradation to L-ascorbic and glucose (Tao et al., 2018).

2.1.4.5. Safety concerns

Genetically modified food enzymes are currently produced from GMOs. Safety concerns have been raised regarding potential contamination of food with bacterial toxins or mycotoxins, allergens or uncharacterized extraneous substances as impurities (De Santis et al., 2018; Srivastava, 2019). Genetic modification of enzymes may also change their allergenic properties, posing new potential health risks. For instance, type I sensitisation was found in a study of 813 exposed industrial workers using genetically modified enzymes (Budnik et al., 2017). Thus, prior to marketing, genetically modified food enzymes need approval from various regulatory bodies such

as the US Food and Drug Administration, the Association of Manufacturers and Formulators of Enzyme Products and the European Food Safety Authority, through processes that vary in different countries. In addition, ethical and religious concerns have been raised for genetically modified enzymes. For instance, it has been suggested that raw materials or ingredients used in fermentation of microorganisms to produce enzymes should be halal (Ermis, 2017).

2.2. Introduction of TGase

Transglutaminase (TGase) with the systematic name protein-glutamine-γ-glutamyltransferase, is assigned Enzyme Commission number EC 2.3.2.13, where EC 2 denotes they are transferases; EC 2.3 indicates they are acyl transferases; and EC 2.3.2 indicates that they are aminoacyl transferases. TGase catalyzes modification of protein molecules via covalent inter- and intra-molecular cross-linkages between the γ-carboxamide group of mid-chain glutamine residues with the free NH_2 group of peptide-bound primary amines or the ε-NH_2 group of lysine residues (Li et al., 2013). TGases are also known to hydrolyze γ-carboxamide groups of glutamine residues in protein molecules (Nandakumar and Wakayama, 2015). This γ-glutaminyl-peptide / amine-γ-glutamyl transferase cross-linking reaction is pH-dependent and can form isopeptide bonds within or between polypeptide chains. It can also result in integration of polyamines into proteins through glutamine side chains (Wilhelm et al., 1996). These behaviors of TGases have significant impacts on food quality such as texture, gelation stability, food consistency and mouthfeel among others. Thus, TGases have been used in a plethora of food applications in the food industry for the manufacture of baked goods, dairy products, muscle food products, imitation food products, as well as fruit and vegetable products (Fernandes, 2016; Kieliszek and Błażejak, 2017; Yokoyama et al., 2004).

2.2.1. Animal, plant and microorganisms TGases

TGases are ubiquitous in living organisms, i.e., animal, plant and microorganisms (bacteria, fungi and algae); and they show structural as well as subtle functional differences. They also differ in their availability for commercial applications based on their sources.

TGases have been characterized in vertebrates, with the first mammalian TGase reported in guinea pig liver (Clarke et al., 1959) and shown to catalyze integration of polyamines into glutamine residues of protein molecules (Wilhelm et al., 1996). Animal TGases described so far have been shown to be of 9 different types (eight active and one inactive). The 8 active forms are Factor XIII, TGM1, TGM2, TGM3, TGM4, TGM5, TGM6 and TGM7, and the inactive form is

designated as Band 4.2 (Luciano and Arntfield, 2012; Thangaraju et al., 2017). They are reported to be Ca^{2+} dependent and they all share identical active sites with a catalytic triad comprised of cysteine, histidine and aspartate (or cysteine, histidine and asparagine) despite having different primary structures (Beninati and Piacentini, 2004). Factor XIII is found in blood plasma where it catalyzes cross-linking of fibrin leading to blood coagulation (Ariëns et al., 2002; Laki and Lorand, 1948). Factor XIII is a tetramer of 320 kDa with two A and two B subunits. The A subunits contain the catalytic sites while B subunits are considered as carriers of the A subunits (Radek et al., 1993). TGases have been reported in the tissues and body fluids of several vertebrate and invertebrate animals (**Table 2.1**).

TGases have also been well characterized from several higher and lower plant sources (**Table 2.1**). Plant TGase was first reported in *Pisum sativum* seeds (Icekson and Apelbaum, 1987), and has since been reported in other plant parts including the leaves, seeds and roots of sugar beet (*Beta vulgaris*), soybean (*Glycine max*), broad bean (*Vicia faba*), wheat (*Triticum aestivum*), barley (*Hordeum vulgare*) chrysanthemum (*Chrysanthemum morifolium*), white lupine (*Lupinus albus*), rice (*Oryza sativa*), maize (*Zea mays*), Jerusalem artichoke (*Helianthus tuberosus),* and rosemary leaves (*Rosmarinus officinalis*) (Aribaud et al., 1995; Bernet et al., 1999; El-Hofi et al., 2014; Falcone et al., 1993; Kang and Cho, 1996; Lilley et al., 1998; Siepaio and Meunier, 1995; Signorini et al., 1991). In plants, TGases participate in photosynthesis (Della Mea et al., 2004), cell death (Del Duca et al., 2014) and pollination (Gentile et al., 2012). Plant TGases have low homologies with animal or microbial TGases but similar catalytic sites also comprised of the catalytic triad Cys–His–Asp as found in rice (Campos et al., 2013), as well as activation by the requisite Ca^{2+} concentration (El-Hofi et al., 2014). Plant TGase activity can be stimulated by Ca^{2+} ions; however, plant TGases do not have an absolute requirement for Ca^{2+} ions as do animal TGases. A study by Kang and Cho (1996) in fact suggested that plant TGases may be inhibited by Ca^{2+} ions at concentrations greater than 2 mM (Serafini-Fracassini et al., 1995). Other investigators have also shown Ca^{2+} ions to have an inhibitory effect at concentrations greater than 2 mM (Aribaud et al., 1995; Kang and Cho, 1996). The sequences of plant TGases have little homology with their animal counterparts, except for the catalytic triad (Serafini-Fracassini and Del Duca, 2008). Nonetheless, plant TGases have not been extensively characterized with respect to structure and function as compared with animal or microbial TGases; nor have their applications for food modifications been fully explored (Luciano and Arntfield, 2012). This is probably due to TGases being present

in low amounts in the various plant parts thus far studied (Serafini-Fracassini and Del Duca, 2008).

The exorbitant costs of producing TGases from animal and plant sources inspired a search for TGases from microbial sources (Kieliszek and Misiewicz, 2014). Microbial TGases (or mTGases) constitute the most abundant types of commercially available TGases. They have been reported from several sources (**Table 2.1)**. The first mTGase (also the first non-animal TGase) was purified from a soil bacterium *Streptoverticillium* sp. S-8112 (Ando et al., 1989). mTGases have been found in several bacteria (**Table 2.1**), and they generally have low molecular weight (MW), and are monomeric protein molecules with MW of about 38 kDa (Ando et al., 1989). The mTGases bear structural differences compared to their counterparts from animal and plant sources. Their function is independent of Ca^{2+} and GTP (guanosine-5′-triphosphate) and they also have much broader substrate specificity and lower deamidation activity (Kashiwagi et al., 2002; Ohtsuka et al., 2001). Because of their availability in relatively larger quantities and higher degree of purity, mTGases are being exploited as multipurpose modern research tools for manifold applications in the food and allied industries, such as a cross-linking agent for bonding proteins, peptides, or smaller molecules and other polymers together, and/or for site-specific covalent fusion of therapeutic proteins to polyethylene glycol to produce derivatives with improved clinical properties (Fontana et al., 2008; Maso et al., 2018). In order to meet the growing demands for the enzyme, recombinant TGases are being produced via genetic manipulations in host microorganisms such as *Aspergillus*, *Bacillus*, *Escherichia coli* and yeast (Cubiro et al., 2007; Li et al., 2013; Liu et al., 2011; Salis et al., 2015; Yu et al., 2008).

2.2.2. TGase production

There has been extensive research conducted on the preparation of TGases from animal and plant tissues as well as from traditional microorganisms. Purified TGase can be obtained using neutral salt or cold solvent precipitation techniques followed by chromatographic separation methods. Ion exchange chromatography, especially weak anion exchangers such as diethylaminoethyl (DEAE)-Sephacel have been widely used to purify TGase from animal and plant tissues (Tseng et al., 2008; Worratao and Yongsawatdigul, 2005). Gel filtration chromatography using resins such as Sephacryl S-200 HR and Sephacryl S-300 HR have also been used for TGase purification purposes (Hemung and Yongsawatdigul, 2008a; Nozawa et al., 2001a). Affinity chromatography is efficient based on specific interaction(s) between the enzyme and its ligand (substrate, inhibitor or co-factor). In this regard, casein-CNBr activated Sepharose 4B

column, phenylalanine-CH Sepharose 4B column, and GTP-agarose column have been applied to purify TGase from rat liver and guinea pig liver (Achyuthan and Greenberg, 1987; Brookhart et al., 1983; Croall and DeMartino, 1986).

Microbial fermentation has shown great value in industrial preparation of TGase. *Streptomyces* spp. and *Bacillus* spp. strains are commonly used to produce mTGase (Bahrim et al., 2010; Cui et al., 2007; Zilhao et al., 2005) by the successive steps of screening, fermentation, centrifugation and purification (Kieliszek and Misiewicz, 2014). In particular, since the demand for TGase is growing due to its potential applications in food processing, biotechnological and medical industries (Hitomi et al., 2016; Santhi et al., 2015), recombinant TGases from mammals, fish and plants have been investigated and produced in various host organisms (Hansson et al., 2002; Ikura et al., 2002). Genetic modification techniques have been used to alter TGases to improve their catalytic properties. For example, a novel TGase engineered using rational mutagenesis and random mutagenesis exhibited higher specific activity than its wild type counterpart (Yokoyama et al., 2010); and a new thermostable TGase with 12-fold higher half-life at 60 ^{o}C compared to the natural one was produced from random and saturation mutagenesis (Buettner et al., 2012).

2.2.3. Catalytic mechanism

TGase catalyzes transfer reactions between the acyl groups in glutamine and the amine groups in alkyl amines to form a cross-linked molecule N^5-alkyl-glutamine with ammonia molecule as co-product. The substrate recognition mechanism by TGase is still less well understood. However, there is common consensus that TGase exhibits strong selectivity for glutamine residues in protein substrates which act as acyl donor. Studies with tissue TGase (tTGase, tTG or TG2) and Factor XIII TGase (FXIII) suggest preferred amino acids sequences of 4-12 amino acids residues containing glutamine (Hitomi et al., 2009; Sugimura et al., 2006). Lysine is the usual acyl acceptor for the cross-linkage reaction catalyzed by tTGase and FXIII, and these two TGases have clear preference for the residues preceding lysine in proteins, which are serine, alanine, leucine, tyrosine and asparagine (Grootjans et al., 1995). Various groups like carboxyl groups, aromatic groups and saccharides can be incorporated into glutamine containing proteins with appropriate primary amines as spacers (Ohtsuka et al., 2000). Different from tTGase, mTGase has broader tolerance to both natural and non-natural acyl-acceptor substrates such as some esterified α-amino acids (Gundersen et al., 2014).

The catalysis process of TGase is closely related to its three-dimensional structure. Components

such as Ca^{2+}, guanine nucleotides (i.e., GTP, GDP (guanosine 5′-diphosphate), GMP (guanosine 5′-monophosphate) can modulate both structure and function of TGase. For example, the transamidation activity of tTGase is allosterically activated by Ca^{2+} but inhibited by GTP, GDP and GMP. Thioredoxin has been shown to activate extracellular tTGase (Jin et al., 2011). Crystal structures of TGases derived from humans including Factor XIII, human TGase 2 and TGase 3 (Ahvazi et al., 2002; Han et al., 2010; Yee et al., 1994), red sea bream fish liver tTGase (Noguchi et al., 2001) and *Streptomyces mobaraense* TGase (Kashiwagi et al., 2002) have been reported. Taking red sea bream liver TGase as an example, it contains 4 domains with a total of 695 amino acid residues (Noguchi et al., 2001). The β-sandwich domain consists of 1 α-helix and 2 four-stranded sheets; the core domain consists of 11 α-helices and 12 β-sheets. Barrels 1 and 2 domains consist of 7 β-sheets, respectively; and the active site is Cys_{272}–His_{332}–Asp_{355} located in the core domain (Noguchi et al., 2001). Its catalysis process is postulated thus: firstly, three calcium ions bind to residues in the core domain, which can either drag the structure or rotate the structure slightly (Ahvazi et al., 2002) under low concentration of guanine nucleotides such as GTP and GDP (Ahvazi et al., 2004); secondly, a glutamine residue arrives in the acyl binding site located around the two-barrel domains which probably causes large conformational change of the enzyme; thirdly, the structural change damages the disulfide bonds between Cys_{272} and Cys_{333} around the active site, as well as the hydrogen bond between Cys_{272} and Tyr_{515} to totally expose the active site (Noguchi et al., 2001). TGase then switches from a compact inactive form to an extended active conformation; fourthly, a glutamine residue arrives at the active site in the core domain to form the covalent acyl-enzyme intermediate between the acyl groups from substrates with the thiol group from cysteine in the enzyme (Keillor et al., 2014), and this process is considered to be the rate-limiting step (Iismaa et al., 2003); finally, nucleophilic substrates such as lysine, primary amines and even water, bind to the acyl-enzyme or thioester intermediate and attack the thioester carbonyl to displace the thiol group in the enzyme (Siegel and Khosla, 2007) to generate the isopeptide crosslink in the final product.

The comparison on the structures of red sea bream TGase, human Factor XIII, and human TGase 3 binding of calcium shows that their structures are similar, and their active sites are conserved in amino acids sequence. However, there are a few structural and electrostatic differences especially in the catalytic sites, which may cause the easier activation, broader substrate specificity and lower inhibitor selectivity for tTGase (Noguchi et al., 2001). Tissue TGase has been demonstrated to

catalyze various reactions based on the substrates type, making it also function as a deamidase (Ohtsuka et al., 2001), GTPase (Fesus and Piacentini, 2002), kinase (Mishra and Murphy, 2006) and protein disulfide isomerase (Hasegawa et al., 2003).

2.3. Enzymatic Properties of Fish/shellfish TGases

TGase is one of the two members of the transpeptidase family of enzymes, the other being γ-glutamyl transpeptidase (Myhrman and Bruner-Lorand, 1970). A γ-glutamyl transpeptidase from lobster muscle was found to have similar characteristics to guinea pig liver TGase and human Factor XIII (Myhrman and Bruner-Lorand, 1970), which represents the first evidence of fish/shellfish derived TGase. As shown in **Table 2.2**, there are reports describing the isolation and characterization of TGases from different fish/shellfish species (Binsi and Shamasundar, 2012; Hemung and Yongsawatdigul, 2008a; Nozawa et al., 1997a). Fish/shellfish TGases show significant sequence homology, conserved regions and similar structures because they share a common evolutionarily ancestor from the ocean. For example, salmon TGase has 62.4% similarity in amino acid sequence to red sea bream TGase, while it showed only 43.5% and 34.4% of sequence similarities with guinea pig liver TGase and Factor XIII, respectively (Sano et al., 1996). The physiological function of TGase in fish/shellfish species include blood coagulation, muscle cell healing, tissue differentiation and development, immune response and stress response (Arockiaraj et al., 2013; Chen et al., 2014a; Maningas et al., 2008; Nozawa and Seki, 2002). The basic properties of TGases from fish/shellfish species, guinea pig liver TGase, and human (Factor XIII) are compared in **Table 2.2**.

2.3.1. Overall structure

The sea bream TGase appears to be the only one among all the fish/shellfish TGases with its crystal structure fully characterized to disclose it as a monomer with a tertiary structure that is relatively loose and relaxed versus mammalian TGases (Noguchi et al., 2001). It is comprised of four domains and a catalytic triad active site (Cys–His–Arg) located in the α-helix, random coil and β-sheet, respectively; as well as a shallow and narrow shaped binding pocket for the substrate. In recent years, bioinformatics approaches have been found to be useful for studying enzymes. It uses the obtained gene or amino acid sequences to analyze homology of enzymes from different sources, as well as to predict and study the enzyme structure, to obviate the high cost and limited access to X-ray crystallographic and nuclear magnetic resonance (NMR) methods for protein structural studies. TGases from salmon (*Onchorhynchus keta*) liver (Sano et al., 1996), freshwater

crayfish (*Pacifastacus leniusculus*) (Wang et al., 2001), giant tiger shrimp (*Penaeus monodon*) (Chen et al., 2005a), Chinese shrimp (*Fenneropenaeus chinensis*) (Liu et al., 2007), zebrafish (*Danio rerio*) (Deasey et al., 2012), white shrimp (*Litopenaeus vannamei*) and freshwater prawn (Arockiaraj et al., 2013) have been cloned and characterized by bioinformatics. For example, the predicted 3D structure of prawn TGase was generated by I-TASSER program based on the homologous similarities in protein databases (Arockiaraj et al., 2013). From such bioinformatics studies, it was established that fish TGase exhibited high similarities with crustacean TGase such as white shrimp, and the conservation of amino acids mostly occurred in the core domain, based on multiple sequences alignments.

2.3.2. Activity

TGases from different fish/shellfish species show different catalytic properties and activities, which may be due to acclimation to different habitats. A common method for determining TGase activity from marine species is via fluorescence spectrophotometric measurement of incorporation of monodansylcadaverine (MDC) into N,N'-dimethylated casein (DMC) (Takagi et al., 1986). Variations in the purification and activity assays used by different researchers may result in differences that make their comparisons difficult. By using the same purification and assay methods for 6 fish/shellfish TGases, it was established that botan shrimp (*Pandalus nipponensis*) TGase had the highest specific activity of 22.9 U/mg, followed by TGases from carp (*Cyprinus carpio*; 8.6 U/mg), scallop (*Patinopecten yessoensis*; 2.2 U/mg), rainbow trout (*Oncorhynchus mykiss*; 1.17 U/mg), atka mackerel (*Pleurogrammus azonus*; 1.1 U/mg) and squid (*Todarodes pacificus*; 0.046 U/mg) in decreasing order of activity (Nozawa et al., 1997a). Another study found that TGase from Mozambique tilapia (*Oreochromis mossambicus*) showed highest specific activity of 69.14 U/mg, followed by TGases from Indian oil sardine (*Sardinella longiceps*; 66.34 U/mg), common carp (*Cyprinus carpio*; 49.33 U/mg) and bigeye snapper (*Priacanthus hamrur*; 47.44 U/mg) (Binsi and Shamasundar, 2012).

2.3.3. Molecular weight

Molecular weights (MW) of TGases from different fish/shellfish species have been verified by SDS-PAGE, and results found that their MW ranged from 73 to 95 kDa, e.g., 77 kDa for walleye pollack (*Theragra chalcogramma*) liver TGase (Kumazawa et al., 1996) and 94 kDa for squid (*Todarodes pacificus*) gill TGase (Nozawa et al., 2001a). Recently, a TGase from Antarctic krill (*Euphausia superba*) showed MW of 78 kDa (Zhang et al., 2017b) and crayfish (*Pacifastacus*

leniusculus) TGase had MW of 86 kDa (Sirikharin et al., 2018). TGase genes were cloned from fish/shellfish species by polymerase chain reaction (PCR), and the encoded amino acid sequence used to deduce the theoretical MW of these TGases, e.g., the MW of TGases from freshwater crayfish (*Pacifastacus leniusculus*) and Chinese shrimp (*Fenneropenaeus chinensis*) were calculated from their cDNAs as 86.03 kDa (Wang et al., 2001) and 84.96 kDa (Liu et al., 2007), respectively.

2.3.4. Isoelectric point

The isoelectric point (pI) of TGase was obtained by isoelectric focusing (IEF), where the purified TGase migrated in a pH gradient under the influence of electric current. The pI values of the TGases were determined as follows: tropical tilapia (*O. niloticus*) TGase, 6.53 (Worratao and Yongsawatdigul, 2005); and for lobster TGase, 5.9 (Myhrman and Bruner-Lorand, 1970); which are lower than that of TGase from guinea pig liver (pI 8.9). Besides, theoretical pI values can be deduced from the pKa values of the constituent amino acids. By using gene cloning method, pI values were reported as 5.61 for Chinese shrimp (*Fenneropenaeus chinensis*) (Liu et al., 2007), and 5.5 for freshwater prawn (Arockiaraj et al., 2013).

2.3.5. pH optima and stability

At different pH values, the side chain residues of the amino acids in an enzyme may carry different charges. If the charge of enzyme and substrate molecules formed at certain pH values favor the catalytic reaction, the overall reaction is optimal at that particular pH value. As shown in **Table 2.2,** TGases are active within a relatively narrow pH range of neutral to slightly alkaline. Tropical tilapia (*O. niloticus*) TGase showed highest activity at pH 7.5 (Worratao and Yongsawatdigul, 2005). Threadfin bream (*Nemipterus* sp.) liver TGase showed optimum activity from pH 8.5 to 9.0 (Hemung and Yongsawatdigul, 2008a). However, optimal pH values of enzymes depend on different factors such as nature of substrate, temperature, ionic strength, presence and absence of activators or inhibitors, etc. Thus, it is inaccurate to compare the optimal pH of TGases from different sources under different reaction conditions. Extreme pH (pH<2 and pH>12) environments can cause ionization of amino acid side chains and even unfolding of enzyme structure. The stable pH range of squid gill TGase is 7.5–9.0 at 25 ^{o}C within 1 h incubation, while TGase from microorganism *Streptoverticillium* is stable between the pH range of 5–9, when reaction was carried out for 10 min at 37 °C (Ando et al., 1989).

2.3.6. Thermal optima and stability

TGases derived from fish/shellfish display differences in temperature optima and thermal stabilities which may be related to their habitat temperatures (Ashie and Lanier, 2000; Uresti et al., 2006). The optimal temperatures for TGases from selected marine species were reported as 4 °C for Antarctic krill (*Euphausia superba*) TGase (Zhang et al., 2017b) and crayfish (*Pacifastacus leniusculus*) TGase (Sirikharin et al., 2018), 20 °C for squid (*Todarodes pacificus*) gill TGase (Nozawa et al., 2001a), 35 °C for both grey mullet (*Mugil cephalus*) (Lee et al., 1998) and European sardine (*Sardina pilchardus*) TGases (Batista et al., 2002), 37 °C for bigeye snapper (*Priacanthus hamrur*), Indian oil sardine (*Sardinella longiceps*) and carp (*Cyprinus carpio*) TGases, 40 °C for Japanese oysters (*Crassostrea gigas*) (Kumazawa et al., 1997), 50 °C for tropical tilapia (*O. niloticus*), and 55 °C for red sea bream (*Pagrus major*). The optimal temperatures for TGases from most species listed above were lower than those from terrestrial organisms which are usually around 50 °C (Ando et al., 1989; Motoki and Seguro, 1998), suggesting that the habitat temperature plays an important role in modulating enzyme function.

Nonetheless, TGases active at low temperatures invariably are less stable at high temperatures. For example, while the optimal temperature for tilapia TGase is 50 °C with 65% activity retention at 60 °C, carp TGase showed optimal temperature at 37 °C but only retained 29% activity at 60 °C (Binsi and Shamasundar, 2012). Besides, the presence of calcium seems to improve the stability of TGase against thermal denaturation (Nozawa et al., 2001a). In general, TGase loses activity at temperatures above 70 °C (Yokoyama et al., 2004) accompanied with a conformational change from ordered secondary structure to an unordered structure (Cui et al., 2008). The thermal properties of enzymes to some extent determine their suitability for industry application, thus it is necessary to investigate TGase activities in extreme cold and warm temperatures to provide the basic knowledge needed to rationalize their use in potential applications.

2.3.7. Activators

Calcium dependence is an important property for TGases from aquatic species, with the degree of dependence varying with calcium concentration from 0.5 to 50 mM (Binsi and Shamasundar, 2012; Hemung and Yongsawatdigul, 2008a; Yasueda et al., 1994). The wide difference may be due to species variation, but it is also likely that different reaction conditions and procedures used in assaying enzyme activities play a role. For example, a TGases reaction solution with high EDTA level and low NaCl concentration turned out to need more calcium ions to activate the enzyme

(Faye et al., 2010; Nozawa et al., 2005). In addition, NaCl had an activating effect on marine invertebrate TGases, but not freshwater shellfish TGases (Nozawa et al., 2001b). This observation may be because of their open blood vascular system surrounded by high salt containing seawater. Moreover, increase of NaCl level could reduce the required amount of $CaCl_2$ to fully activate squid gill TGase; on the other hand, NaCl could rapidly inactivate the enzyme in the absence of substrates (Nozawa et al., 2001a). Metal ions, e.g., Sr^{2+} also activate TGases from marine, freshwater and guinea pig liver by inducing subtle conformation changes in the enzyme structure to expose the catalytic triad (Kumazawa et al., 1996; Worratao and Yongsawatdigul, 2005).

2.3.8. Inhibitors

Various compounds have been studied for the inhibition of purified aquatic animal TGases. They include ethylene diamine tetra acetic acid (EDTA), ethylene glycol tetraacetic acid (EGTA), dithiothreitol (DDT), lysine-HCl, ammonium chloride (NH_4Cl), ammonium sulfate ($(NH_4)_2SO_4$), phenylmethylsulfonyl fluoride (PMSF), parachloro mercuri benzoate (PCMB), iodoacetic acid (IAA), and *N*-ethylmaleimide (NEM) (Hemung and Yongsawatdigul, 2008a; Nozawa et al., 2001a; Worratao and Yongsawatdigul, 2005). Among these compounds, IAA, NEM and PCMB were the most potent inhibitors because these chemicals are sulfhydryl alkylating agents which react with the thiol group of cysteine in the active site of the enzyme. EDTA and EGTA are usually added into the extraction buffer to prevent the TGase from self-aggregation; however, they are well known calcium ion chelating agents that prevent TGase transformation into its active structure. DDT shows slight to no interruption of TGase activity; and it is commonly included in the extraction buffer since it prevents metal catalyzed oxidation of cysteine at the active site of TGase (Kwon et al., 1994). Lysine-HCl serves as a competitive inhibitor for hydroxyl amine-HCl which acts as substrate in some activity assays (Binsi and Shamasundar, 2012). NH_4Cl reduces TGase activity by generating excess ammonium ions to reverse the catalysis of TGase, because NH_4^+ is also a product of the acyl transfer reaction. PMSF, a well-known serine protease inhibitor, showed slight or no inhibition of TGase from aquatic animals, which may be because PMSF reacts with the histidine residue in the active site of fish TGase, but at the same time, it can prevent enzyme degradation by endogenous serine proteinases (Worratao and Yongsawatdigul, 2005). Metal ions such as Cu^{2+}, Zn^{2+}, Fe^{2+} and Co^{2+}, which have strong affinity for sulfhydryl groups can inhibit TGases from aquatic animals (Hemung and Yongsawatdigul, 2008a).

Table 2.1

TGases from selected animal, plant and microorganisms.

Species	Part	Reference
Animal source		
Bovine	snout	(Buxman and Wuepper, 1976)
Canine heartworm (*Dirofilaria immitis*)	-	(Chandrashekar et al., 1998)
Chicken	gizzard	(Puszkin and Raghuraman, 1985)
Filaria worm (*Brugia malayi*)	-	(Devarajan et al., 2004)
Filaria worm (*Onchocerca volvulus*)	-	(Lustigman et al., 1995)
Frog	liver	(Assisi et al., 1999)
Guinea pig	liver	(Folk and Cole, 1965)
Human	platelet	(Puszkin and Raghuraman, 1985)
Porcine	skin	(Ando et al., 1988)
Rabbit	liver	(Abe et al., 1977)
Rat	brain	(Ohashi et al., 1995)
Plants source		
Apple (*Malus domestica*)	pollen	(Del Duca et al., 1997)
Barley (*Hordeum vulgare*)	leaves; roots	(Lilley et al., 1998)
Chrysanthemum (*Chrysanthemum morifolium*)	leaves	(Aribaud et al., 1995)
Garden pea (*Pisum sativum*)	seeds	(Icekson and Apelbaum, 1987)
Jerusalem artichoke (*Helianthus tuberosus*)	tubers	(Serafini-Fracassini and Del Duca, 2008)
Maize (*Zea mays*)	calluses;	(Bernet et al., 1999)
Rosemary leaves (*Rosmarinus officinalis*)	leaves	(El-Hofi et al., 2014)
Sugar beet (*Beta vulgaris*)	leaves	(Signorini et al., 1991)
Soybean (*Glycine max*)	leaves	(Kang and Cho, 1996)
Tobacco (*Nicotiana tabacum*)	flowers	(Serafini-Fracassini et al., 2002)
Wheat (*Triticum aestivum*)	leaves; roots	(Lilley et al., 1998)
White lupine (*Lupinus albus*)	seedlings	(Siepaio and Meunier, 1995)
Microbial sources		
Bacillus circulans		(De Souza et al., 2006)
Bacillus subtilis		(Kobayashi et al., 1998)
Enterobacter sp. C2361		(Bourneow et al., 2011)
Physarum polycephalum		(Klein et al., 1992)
Streptomyces hygroscopicus		(Cui et al., 2007)
Streptomyces lydicus		(Færgemand et al., 1997)
Streptomyces mobaraense		(Yang et al., 2011)
Streptomyces netropsis		(Yu et al., 2008)
Streptomyces platensis		(Lin et al., 2006)
Streptococcus suis		(Yu et al., 2015)
Streptoverticillium ladakanum		(Ho et al., 2000)

Table 2.2

Enzymatic properties of TGases obtained from fish/shellfish.

Fish/shellfish Source	MW (kDa)	Activity (U/mg)	pI	Opt pH	Opt Temp (°C)	Stability at 50 °C	Opt [Ca^{2+}] (mM)	Reference
Antarctic krill (*Euphausia superba*)	76	53.52	-	8-9	0-10	-	10	(Zhang et al., 2017b)
Atka mackerel (*Pleurogrammus azonus*)	-	1.10	-	-	-	-	-	(Nozawa et al., 1997a)
Bigeye snapper (*Priacanthus hamrur*)	73-95	47.44	-	-	37	89%	50	(Binsi and Shamasundar, 2012)
Botan shrimp (*Pandalus nipponensis*)	-	22.90	-	-	-	-	-	(Nozawa et al., 1997a)
Carp (*Cyprinus carpio*)	73-95	49.33	-	-	37	87%	50	(Binsi and Shamasundar, 2012)
Cod (*Gadus morhua*)	-	-	-	-	-	-	-	(Malinowska-Pańczyk and Kołodziejska,
Crayfish (*Pacifastacus leniusculus*)	86	-	-	8.5	22	-	-	(Sirikharin et al., 2018)
European sardine (*Sardina pilchardus*)	-	-	-	-	35	26%	-	(Batista et al., 2002)
Grey mullet (*Mugil cephalus*)	-	-	-	7.7	35	-	-	(Lee et al., 1998)
Indian oil sardine (*Sardinella longiceps*)	73-95	66.35	-	-	37	75%	50	(Binsi and Shamasundar, 2012)
Japanese oysters (*Crassostrea gigas*)	84	156.6	-	8.0	40	60%	-	(Kumazawa et al., 1997)
Lobster (*Homarus americanus*)	200	-	5.	-	-	-	-	(Myhrman and Bruner-Lorand, 1970)
Rainbow trout (*Oncorhynchus mykiss*)	-	1.17	-	-	-	-	-	(Nozawa et al., 1997a)
Red sea bream (*Pagrus major*)	78	-	-	9.0-9.5	55	84%	0.5	(Yasueda et al., 1994)
Salmon (*Salmo salar*)	-	-	-	-	-	-	-	(Malinowska-Pańczyk and Kołodziejska,
Scallop (*Patinopecten yessoensis*)	-	2.2	-	8.0	-	-	50	(Nozawa et al., 1997a)
Squid (*Todarodes pacificus*) gill	94	216.3	-	7.5-8.0	20	80%	50	(Nozawa et al., 2001a)
Threadfin bream (*Nemipterus* SP.) liver	95	3920	-	8.5-9.0	50	-	1	(Hemung and Yongsawatdigul, 2008a)
Tilapia (*Oreochromis mossambicus*)	73-95	69.14	-	-	50	97%	50	(Binsi and Shamasundar, 2012)
Tropical tilapia (*O. niloticus*)	85	196.9	6.	7.5	50	-	1.25	(Worratao and Yongsawatdigul, 2005)
Walleye pollack (*Theragra chalcogramma*) liver	77	-	-	9.0	50	-	-	(Kumazawa et al., 1996)
Comparison with other common sources								
Guinea pig liver	85	-	-	7.0-7.5	-	-	-	(Connellan et al., 1971; Larre et al., 1993)
Human blood (Factor XIII)	300	-	-	-	-	-	-	(Bishop et al., 1990)
Streptoverticillium mobaraense	40	-	8.	6.0-7.0	50	74%	-	(Ando et al., 1989)

CONNECTING STATEMENT 1

Chapter III is the preliminary work on transglutaminase. The enzyme was extracted and purified from a cold habitat marine species – Antarctic krill. The purified TGase was characterized for its catalytic properties including activity at low temperatures. Its application in preparing cold-set gelatin gel was investigated to confirm is catalytic prowess at low temperature.

This chapter constitutes the text of a paper published as:

Y Zhang, S He, B K Simpson. A cold active transglutaminase from Antarctic krill (*Euphausia superba*): purification, characterization and application in the modification of cold-set gelatin gel. Food Chemistry, 2017, 232: 155-162.

For this paper, PhD candidate Y Zhang designed and performed the experiments, analyzed the data, and drafted the manuscript. Co-author Dr. S He contributed academic discussion and some training. Co-author/corresponding author Professor B K Simpson supervised the research work, provided the research materials and facilities, guided the lab performance and data analysis, revised the manuscript.

CHAPTER III. A COLD ACTIVE TRANSGLUTAMINASE FROM ANTARCTIC KRILL (*Euphausia superba*): PURIFICATION, CHARACTERIZATION AND APPLICATION IN THE MODIFICATION OF COLD-SET GELATIN GEL

3.1. Abstract

Transglutaminase (TGase) was purified from whole Antarctic krill (*Euphausia superba*) using ammonium sulfate fractionation and DEAE-Sephacel chromatography. The purified enzyme had specific activity, purification fold and yield of 53.518 U/mg, 10.272 and 10.992%, respectively. The MW of the purified Antarctic krill TGase was estimated to be 78 kDa using SDS-PAGE. The optimal pH and temperature for the activity of the purified TGase were pH 8.0–9.0 and 0–10^{o}C, respectively. However, the TGase activity reduced to 50% at a higher temperature of 45^{o}C. The cations Ca^{++} and Na^{+} activated the purified TGase activity optimally at levels of incorporation of 10 mM and 1.8 mM, respectively. Addition of TGase at 0.1 U/mg increased the gel strength ($p < 0.05$), setting temperature, setting time ($p < 0.05$) and melting temperature ($p < 0.05$) of cold-set gelatin gel.

3.2. Introduction

TGase can form inter- or intra- molecule cross-linkages in proteins via ε-(γ-Glu)-Lys bond formation. This reaction is very useful for modifying the physical and functional properties of foods. The need for TGase for commercial use is increasing in tandem with the advances in food processing and food product development. Furthermore, TGases suited for low-temperature applications are scarce. Even though TGase has been found in animals, plants and microorganisms, commercial TGases are derived from limited sources, mainly from guinea pig liver and microorganisms such as *Streptoverticillium* sp. and *Streptomyces* sp. (Zhu and Tramper, 2008). Thus, there is the need to discover newer sources of the enzyme cost-effectively for industrial use, particularly TGases endowed with distinct properties that would make them better suited for applications under certain reaction conditions. TGases from aquatic species have been studied for the past two decades from at least 20 sources. The sources include both freshwater and marine species such as carp, sardine, squid, red sea bream (Binsi and Shamasundar, 2012; Hemung and Yongsawatdigul, 2008b; Nozawa et al., 1997b; Worratao and Yongsawatdigul, 2005). TGase from marine species have been found to be different from their counterparts in terrestrial animals, plants and microorganisms, in terms of both structure and characteristics. Marine species that inhabit cold environments, e.g., the polar seas and deep seas, are optimally adapted to cold temperatures and their enzymes are stable and active at cold temperatures. The cold active enzymes have been reported to have high catalytic activity at low temperatures and are highly heat-labile due to their more flexible enzyme structures (Cavicchioli et al., 2002). For example, an extracellular esterase

purified from a psychrophilic bacterium with an optimum activity at 40°C was found to display ~50% of the maximum at 4°C (Hong et al., 2012); however no such similar work has been reported for psychrophilic TGases.

Antarctic krill (*Euphausia superba*) is a dominant species in the Antarctic ocean. It is a small shrimp-like invertebrate, and the estimated annual catch was relatively stable at about 1.2×10^5 tons for the period spanning 1990 until 2009, but has since increased to more than 2×10^5 tons / yr because of intensified harvesting by countries like Japan, Norway, China, and Russia (Nicol et al., 2012). Apart from serving as human food, Antarctic krill has also been studied as source for various enzymes including trypsins, chymotrypsins, carboxypeptidase (Sjödahl et al., 2002), as well as xylanases (Lee et al., 2006), and these enzymes showed high activity at low temperatures. Biochemical properties of TGase in shrimp were characterized with respect to blood coagulation, immune function against infection, and carbohydrate metabolism maintenance under cold stress (Arockiaraj et al., 2013; Chen et al., 2014b; Maningas et al., 2008). There are several potential applications of cold active TGase in low temperature food processing, such as: preparation of surimi (Kaewudom et al., 2012), ice cream (Rossa et al., 2012), kefir (Wróblewska et al., 2009), cold-set gel (Hong and Chin, 2010; Zhang et al., 2016a). They have also been used to make cold-cast films (Lukasik and Ludescher, 2006). Cold active TGases also have potential for non-food low temperature applications in the biomedical, cosmetic and textile industries. However, very few studies have been conducted on TGases from cold-adapted species thus far.

Gelatin is a soluble protein prepared by partial hydrolysis of collagen with widespread utility in food industry, and TGase has been used to enzymatically modify gelatin by forming cross-links to enhance its rheological properties. Gelatin can set to elastic gel on cooling below 35°C from disordered molecules to ordered network predominantly by hydrogen bonds, where TGase would introduce additional covalent cross-linkages to improve gelation (Babin and Dickinson, 2001). Since microbial TGases have been used in the preparation of cold set gels from soy protein (Zhang et al., 2016a) and porcine myofibrillar protein (Hong and Chin, 2010), it is fascinating to study the effect of cold active TGase from marine species on cold-set protein gels, e.g., gelatin gels.

3.3. Materials and methods

3.3.1. Samples and chemicals

Antarctic krill (*Euphausia superba*) was purchased from a fish market in Qingdao Harbor, China. The samples were frozen at -40°C overnight and freeze-dried. The freeze-dried krill was further

milled into powder form using a high-speed blender and stored at -20°C under vacuum. The chemicals used in the present study were all analytical grade and were all purchased from Sigma-Aldrich Inc. (St. Louis, MO, USA). They include ammonium sulfate ($(NH_4)_2SO_4$), barium chloride ($BaCl_2$), calcium chloride ($CaCl_2$), copper chloride ($CuCl_2$), N, N'-dimethylated casein (DMC), dithiothreitol (DTT), ethylene diamine tetra acetic acid (EDTA), ethylene glycol bis(2-aminoethlyether)-N,N,N',N'-tetraacetic acid (EGTA), iodoacetic acid (IAA), magnesium chloride ($MgCl_2$), manganese chloride ($MnCl_2$), monodansylcadaverine (MDC), N-ethylmaleimide (NEM), para-chloromercuribenzoic acid (PCMB), phenylmethylsulfonyl fluoride (PMSF), sodium chloride (NaCl), tris-HCl, and zinc chloride ($ZnCl_2$).

3.3.2. Purification of TGase

All the extraction and purification steps used for the recovery of Antarctic krill TGase were carried out at 4°C.

Preparation of crude TGase extract. Antarctic krill was powdered in liquid N_2, and the powder was stirred for 30 min in extraction buffer (10 mM Tris-HCl, pH 8, containing 5 mM NaCl, 5 mM EDTA, 2 mM DTT) in the ratio of (1:10 w/v). The homogenate was centrifuged at 10,000 g for 30 min at 4°C using a refrigerated centrifuge (Marathon 21000R, Fisher Scientific, Pittsburgh, USA). The supernatant was used as crude TGase extract.

Ammonium sulfate precipitation. Solid ammonium sulfate was added slowly to the crude TGase extract to 25% saturation at 4°C with gentle stirring for 30 min, and the precipitate formed was collected by centrifugation at 10,000 g for 30 min. Precipitates at 35%, 45%, 55%, 65%, 75%, and 85% saturation were collected successively; and the precipitates were dissolved in deionized water (1:1 w/v) and subjected to ultrafiltration with a 30 kDa MW cut off (MWCO) membrane (Millipore, USA). TGase activity and protein concentration were measured as described below, and the fraction from the $(NH_4)_2SO_4$ saturation step with the highest specific enzyme activity was re-dissolved in minimum amount of buffer and designated as the $(NH_4)_2SO_4$ fraction and used for ion exchange (IEX) chromatography.

DEAE-Sephacel chromatography. The $(NH_4)_2SO_4$ fraction was diluted in extraction buffer to a protein concentration of 1.0 mg/mL, and then applied onto a DEAE-Sephacel (GE healthcare, Sweden) column (2.5 × 27 cm) equilibrated with the buffer. Elution was performed at a constant flow rate of 1 mL/min. After washing with the elution buffer to remove unbound components in the sample, the bound components were eluted with a linear gradient of 0–1 M NaCl. Fractions of

3.5 mL were collected and measured at 280 nm for protein content and assayed for TGase activity as described below. The fractions with TGase activity were pooled and concentrated using a 30 kDa MWCO ultrafiltration membrane (Millipore, USA).

3.3.3. Determination of TGase activity

The TGase activity was measured according to the method of Tagaki et al. (1986), with slight modification. The reaction mixture comprised of 1 mg/mL DMC, 15 μM MDC, 3 mM DTT, 5 mM $CaCl_2$, 50 mM Tris-HCl (pH 7.5), and 100 μL TGase. The reaction was performed at 25°C for 10 min and stopped by adding EDTA solution to a final concentration of 20 mM. Fluorescence intensity (FI) of MDC incorporated into DMC was measured with F2000 fluorescence spectrophotometer (Hitachi, Ltd, Tokyo, Japan) at excitation and emission wavelengths of 350 and 480 nm, respectively. FI values of blanks (FI_0) were carried out in a similar procedure but deionized water was used to replace TGase. Enhancing factor (EF) was determined to be 1.877 in this study. One unit of TGase enzyme activity was defined as the amount of enzyme that catalyzed the incorporation of 1 nmole of MDC into DMC during 1 min at 25°C. TGase activity was calculated per Equation 1. Protein content was determined with a Pierce BCA protein assay kit (Thermo Scientific, USA); and specific activity, fold purification, and yield at each step were determined using Equations 2, 3, and 4, respectively.

$$\text{TGase activity (1 U)} = \frac{(\text{FI}-\text{FI}_0)\times 15{,}000\ \text{nmol}\times 2\ \text{mL}\times 10^{-3}}{\text{FI}_0\times 10\ \text{min}\times 1.877} \quad (1)$$

$$\text{Specific activity (U/mg protein)} = \frac{\text{Total TGase activity}}{\text{Total protein}} \quad (2)$$

$$\text{Purification fold} = \frac{\text{Specific activity at a particular step}}{\text{Specific activity of crude TGase}} \quad (3)$$

$$\text{Yield of TGase (\%)} = \frac{\text{Total activity of a particular step}}{\text{Total activity of crude TGase}} \quad (4)$$

3.3.4. SDS-PAGE

SDS-PAGE was performed using 5% stacking gel and 10% resolving polyacrylamide gels. Samples from each purification step were boiled in Laemmli sample buffer (Bio-Rad Laboratories, USA) for 5 min prior to application in the gel wells. High MW calibration standards (GE Healthcare UK Limited, UK) comprised of myosin (220 kDa), α_2-macroglobulin (170 kDa), β-galactosidase (116 kDa), transferrin (76 kDa) and glutamic dehydrogenase (53 kDa).

3.3.5. Characterization of TGase

Effect of pH. The optimal pH was determined by preparing the substrates for the TGase assay

in different buffers ranging from pH 4–9. The pH 4–6.5 buffers were prepared using 100 mM acetate buffer; the pH 7–7.5 buffers were prepared with 50 mM Tris-HCl; and pH 8–9 buffers were prepared from 50 mM borate buffer. All reactions were carried out using 1 mg/mL DMC, 15 μM MDC, 3 mM DTT, 5 mM $CaCl_2$, and 100 μL TGase at 25ºC for 10 min. The relative TGase activity (%) was calculated using the highest TGase activity obtained as 100%.

Effect of temperature. TGase activity was studied over a wide temperature range (0, 4, 10, 20, 30, 37, 45, 55, 65ºC) and assaying for TGase activity at the selected temperatures. The reaction mixture comprising of 1 mg/mL DMC, 15 μM MDC, 3 mM DTT, 5 mM $CaCl_2$, 50 mM Tris-HCl (pH 7.5), were incubated at the corresponding temperatures for 5 min before adding 100 μL TGase. The relative TGase activity (%) was calculated using the highest TGase activity obtained as 100%.

Effect of $CaCl_2$ and NaCl. The effect of $CaCl_2$ at different concentrations of 0, 5, 10, 20, 50 mM were studied in the presence of 1 mg/mL DMC, 15 μM MDC, 3 mM DTT, 50 mM Tris-HCl (pH 7.5), and 100 μL TGase at 25ºC for 10 min. The effect of NaCl at different concentrations of 0, 0.6, 1.2, 1.8 and 2.4 mM were also studied in the presence of 1 mg/mL DMC, 15 μM MDC, 3 mM DTT, 5 mM $CaCl_2$, 50 mM Tris-HCl (pH 7.5), and 100 μL TGase at 25ºC for 10 min. The relative TGase activities (%) were calculated using TGase activity without the Ca^{++} or NaCl as 100%.

Effect of inhibitors and other metal ions on TGase activity. The following inhibitors, EGTA, IAA, NEM, $(NH_4)_2SO_4$, PCMB and PMSF; and the following compounds, $MnCl_2$, $MgCl_2$, $BaCl_2$, $CuCl_2$, $ZnCl_2$, were separately added at a final concentration of 10 mM into the reaction system containing 1 mg/mL DMC, 15 μM MDC, 3 mM DTT, 5 mM $CaCl_2$, 50 mM Tris-HCl (pH 7.5), and 100 μL TGase. The reaction was performed at 25ºC for 10 min. The residual TGase activity (%) was calculated using the TGase activity without the inhibitors or metal ions as 100%.

3.3.6. Preparation and characterization of cold-set gelatin gels modified with TGase

Commercial gelatin was dissolved in distilled water at 50ºC to obtain a final concentration of 6.67% (w/v) and then stirred for 30 min at 25ºC. Purified TGase from Antarctic krill was added at concentrations of 0, 0.05, 0.1, 0.5 and 1.0 U/g gelatin with continuous stirring for another 10 min at 25ºC. Gelatin solutions were then cooled at 4ºC for 18 h to form gels.

Gel strength. Gel strength was measured based on standard method of the Gelatin Manufacturers Institute of America (GMIA, 2006). After cold setting, samples were immediately removed from the refrigerator and gel strength was measured with a Texture analyzer (TA-XT2i,

Stable Micro System Ltd., Surrey, UK) fitted with a 1.27 cm diameter cylindrical probe at a test speed of 1 mm/s. The maximum force (g) required for the probe to penetrate the gel by 4 mm was recorded as the gel strength.

Setting temperature and time. Gelatin solutions (6.67%) were prepared in test tubes (12 mm × 95 mm) at final volumes of 5 mL and measured for setting time and temperature by the method of Muyonga et al. (2004) with slight modification. For setting temperature, samples were transferred into in a water bath of 40°C. A thermometer and a glass rod were inserted in the gel solutions. The water bath was cooled gradually by 1°C at 15 s intervals. The glass rod was lifted at 5 s intervals. The temperatures (°C) at which gelatin no longer dripped from the tip of glass rod was recorded as the setting temperature. To measure the setting time, samples were transferred into a water bath of 10°C. A glass rod was inserted and lifted at 1 s intervals. The time (s) at which the gelatin was unable to detach the rod was recorded as the setting time.

Melting temperature. Melting point was determined based on the BS755 method (BSI755, 1975) with slight modification. Gelatin solutions (6.67%) were prepared in test tubes (12 mm × 95 mm) and cold set at 4°C for 18 h. Five drops of a mixture of chloroform and methylene blue dye were added to the gelatin gels, and the gels were then placed in a thermostatic bath at 4°C and heated by increments of 0.2°C / min. The melting point (°C) was considered as the temperature at which the stained droplets began to move into the gel.

3.3.7. Statistical analysis

All measurements were carried in triplicates, and the data obtained were analyzed using SPSS software version 12.0.

3.4. Results and Discussion

3.4.1. TGase purification

The crude TGase extract was subjected to fractionation with solid $(NH_4)_2SO_4$ in the range of 25 to 85% saturation. As shown in **Figure 3.1a**, the TGase fraction precipitating at 65% saturation was the most active based on relative specific activities (19.98±2.24 U/mg). The purification scheme summarized in **Table 3.1** shows a purification fold and yield of TGase after $(NH_4)_2SO_4$ fractionation were 3.84 and 33.64%, respectively. In the purification of TGase from *Streptoverticillium ladakanum*, ammonium sulfate precipitate at 55–75% saturation that was used for further chromatographic purification had a purification fold of only 1.8 (Tsai et al., 1996). Similarly, the 80% $(NH_4)_2SO_4$ fraction from the purification of Japanese oyster (*Crassostrea gigas*)

TGase, showed a purification fold of 1.6 (Kumazawa et al., 1997). However, there is a drawback with using ammonium sulfate precipitation to purify TGase, partially due to the fact that excess ammonium ions are capable of inhibiting the acyl reaction catalyzed by TGase (Benjakul et al., 2004), resulting in the low TGase activity recovery. Thus, in the present study ultrafiltration was introduced to remove the residual $(NH_4)_2SO_4$ from the extract. The ultrafiltrated TGase solution after $(NH_4)_2SO_4$ precipitation was applied to a DEAE Sephacel column and the fractions eluted from the column with 0 to 0.5 M NaCl, were measured for absorbances at 280 nm and TGase activities (**Figure 3.1b**). TGase activities were found in 2 peaks, i.e., a large peak from the fractions eluted at 0.13–0.15 M NaCl, and a smaller peak from the fractions eluted at 0.23–0.24 M NaCl. Previous research reported TGase from tropical tilapia eluted at 0.15–0.20 M NaCl by DEAE Sephacel column (Worratao and Yongsawatdigul, 2005), while TGase from squid, scallop and carp dorsal muscle eluted at 0.16, 0.12 and 0.3 M NaCl, respectively, by using DE-52 cellulose column (Nozawa et al., 1997b). TGase from Antarctic krill presented two peaks in this study, similar to TGase purified from Japanese oyster that also appeared as two peaks using a Q-Sepharose FF column (Kumazawa et al., 1997). Thus, it is possible that more than one type of TGase isozyme exist in the tissues of Antarctic krill. Research has found that two types of shrimp TGases involved in blood coagulation were encoded at different chromosomal locations (Chen et al., 2005b). In the present study, the fractions that eluted between 0.13 to 0.15 M NaCl were collected and pooled, and the specific activity of the pooled fraction was measured as 53.52 U/mg, which is comparable to the values of 47.44, 66.35, 69.14 and 49.33 U/mg reported for dialyzed DEAE-cellulose fractions from bigeye snapper, oil sardine, tilapia and common carp, respectively (Binsi and Shamasundar, 2012). As shown in **Table 3.1**, the purification fold and yield at the IEX step were 10.272 and 10.992%, respectively.

3.4.2. Molecular weight

The purity of TGase was confirmed using SDS-PAGE (**Figures 3.2a** and **3.2b**). There were fewer protein bands observed in the 65% saturated $(NH_4)_2SO_4$ precipitation step, compared to that in crude TGase extract (**Figure 3.3a**). Furthermore, in the elution at 0.13–0.15 M NaCl, only one band was observed, suggesting that purified TGase was obtained (**Figure 3.2b**). The MW of Antarctic krill TGase was estimated as 78 kDa by SDS-PAGE, which is similar to those of walleye pollock liver and red sea bream TGases which were reported as 77 kDa and 78 kDa, respectively (Kumazawa et al., 1996; Yasueda et al., 1995), but smaller than those of tropical tilapia, squid, and

threadfin bream liver TGases which were reported as 85 kDa, 94 kDa and 95 kDa, respectively (Hemung and Yongsawatdigul, 2008b; Nozawa et al., 2001a; Worratao and Yongsawatdigul, 2005).

3.4.3. Effect of pH

Antarctic krill TGase activity was studied under different pH conditions. As shown in **Figure 3.3a**, the krill TGase activity was optimal (80–100%) over the pH range of pH 6 to 9. The broad optimum range of 6 – 9, comprises of 2 peaks corresponding to optimum values of 6.5 (minor) and 8.0 (major). This observation could suggest 2 isoforms of the enzyme. Nonetheless, the results from the SDS-PAGE (**Figure 3.2b**) suggest a single band for the TGase enzyme. Thus, the multiple pH optima observed, may be attributed to effects of ionizations of acidic and basic groups in the free enzyme, substrate or enzyme substrate complexes (Dixon et al., 1979; Mattock et al., 1970). The maximum activity was at pH 8.0, and the pH activity profile was similar to those reported for threadfin bream liver TGase (optimal pH 8.5–9.0), scallop, carp and Japanese oyster (optimal pH 8.0), as well as walleye pollock liver (optimal pH 9.0) (Hemung and Yongsawatdigul, 2008b; Kumazawa et al., 1996; Kumazawa et al., 1997; Nozawa et al., 1997b). Antarctic krill lives in sea water which normally has a pH of 8.0, but can be higher depending on the photosynthetic activity in sea-ice (Thomas and Dieckmann, 2002). Thus, its extracellular enzymes such as TGase, are considered to conform and function well in ambient weak alkaline pH environments. With the broad pH activity profile extending to the alkaline range, Antarctic krill TGase can be used in applications such as alkali-soluble protein modification, and wool textile modification, etc.

3.4.4. Effect of Temperature

The effect of different temperatures on the activity of purified Antarctic krill TGase is presented in **Figure 3.3b**. Antarctic krill TGase showed relative activities of 96.50±1.57%, 100±1.61%, and 95.65±2.01% at 0°C, 4°C and 10°C, respectively, and then gradually declined with increasing temperature from 10°C to 65°C. Based on its higher catalytic activity at low temperatures, Antarctic krill TGase with optimal temperature of 4°C, can be referred to as a cold active enzyme, or psychrophilic enzyme. TGase purified from squid (*Todarodes pacificus*) gill exhibited low optimal temperature of 20°C (Nozawa et al., 2001a); however, the counterparts from microbial sources like *Streptoverticillium mobaraense*, and from some marine sources like walleye pollock liver or threadfin bream liver exhibited much higher optimal temperatures around 50°C (Hemung and Yongsawatdigul, 2008b; Kumazawa et al., 1996; Lu et al., 2003). The optimal temperature of

TGase may be also related to its habitat temperatures. Antarctic krill has adapted to live in the Antarctic zone where the surface polar sea temperature is -2^{o}C, and about -10^{o}C at greater depths (Thomas and Dieckmann, 2002). A trypsin-like proteinase isolated from Antarctic krill exhibited 60 times higher catalytic activity than its bovine counterpart at 1–3^{o}C (Sjödahl et al., 2002). It is recognized that cold-active enzymes have flexible structure compared with their mesophilic and thermophilic counterparts. This flexibility contributes to the high catalytic activity as well as the high temperature instability of cold active enzymes. The Antarctic krill TGase was relatively more active from 0–10^{o}C, while its relative activity at 45^{o}C, 55^{o}C and 65^{o}C, declined to 50%, 47% and 44%, respectively. This observation differs from what was observed with bigeye snapper TGase which was optimally stable of 37^{o}C and retained 89% stability at 50^{o}C (Binsi and Shamasundar, 2012). It is suggested that the Antarctic krill TGase starts to unfold at relatively lower temperatures making it more heat labile versus bigeye snapper TGase.

3.4.5. Effect of $CaCl_2$ and NaCl

Calcium ions are said to activate TGase by inducing a conformational change in its active site to enable it to bind better with substrates. This Ca^{++} dependency is found for some other TGases such as human Factor XII and fish TGase, but not in microbial TGases. The effects of Ca^{++} at concentrations of 0, 5, 10, 20, 50 mM are presented in **Figure 3.3c**, which shows TGase activity increasing with Ca^{++} concentration up to 10 mM, and then declining thereafter. The relative activity with varying Ca^{++} levels was highest (148.01±7.06%) at $CaCl_2$ concentration of 10 mM, but lowest (75.87±0.76%) at 50 mM $CaCl_2$. However, a previous report on squid and scallop TGases observed optimal Ca^{++} concentration of 50 mM (Nozawa et al., 2001a; Nozawa et al., 1997b), whereas the TGases from threadfin bream liver, red sea bream, and carp showed highest activities at Ca^{++} concentration less than 1 mM (Hemung and Yongsawatdigul, 2008b; Nozawa et al., 1997b; Yasueda et al., 1995). It would seem from this that, the dependency of TGase on Ca^{++} for activity may vary from specie to specie. It is also possible that the flexible structure of cold active Antarctic krill TGase was compacted by extensive binding and made more rigid at the higher Ca^{++} levels to adversely affect its catalytic activity.

The extracellular fluids of most marine invertebrates are isotonic to that of the surrounding seawater. Thus, their endogenous enzymes are probably halophilic and dependent on salt for activity. Halophilic enzymes normally require high NaCl concentrations to be active and stable. In this study, the effect of NaCl concentrations of 0, 0.6, 1.2, 1.8, 2.4, and 3.0 mM on Antarctic krill

TGase activity is presented in **Figure 3.3d**. Results indicated that for the range of NaCl concentration investigated, the level of NaCl producing the highest relative TGase activity (139.29±0.74%) was 1.8 mM. Ortega et al. (2011), have attributed the capacity of halophilic enzymes to retain structural integrity and remain active to their enzyme proteins having a higher glutamate and aspartate amino acid contents. The result found in the present study is consistent with previous observations made with scallop, botan shrimp, and squid TGases which showed increased activity by adding 0.5 M NaCl (Nozawa et al., 1997b), unlike TGases derived from freshwater species such as tilapia that are inactivated by NaCl (Worratao and Yongsawatdigul, 2005).

3.4.6. Effect of inhibitors and metal ions

The effect of selected inhibitors on Antarctic krill TGase activity is presented in **Table 3.2** and shows a decreasing order of inhibition capacity as: PCMB > IAA > NEM > PMSF > EGTA > $(NH_4)_2SO_4$. These compounds were investigated for various reasons; e.g., PCMB, an organomercury compound, reacts with thiol groups to form mercaptan complex, and thus it inhibits the activities of enzymes that are dependent on thiol groups. IAA is an alkylating agent that can alkylate cysteine residues and impair disulfide bond formation, thus its use would help to verify the relative contribution of disulfide bonds to the stability and activity of the enzyme. NEM is reactive towards thiol groups via its imide functional group, and its use provides information on the importance, if any, of sulfhydryl groups to functional integrity of the enzyme. These three inhibitors are considered as the strongest inhibitors among those studied, and similar to what was observed with other TGases derived from aquatic animals (Hemung and Yongsawatdigul, 2008b; Nozawa et al., 2001a). PMSF inhibits serine proteases irreversibly by sulfonating serine residues at the enzymes' active site and inhibits cysteine proteases reversibly by binding their thiol groups. EGTA has high affinity to Ca^{++} chelator to remove the Ca^{++} ions required for catalysis by forming stable EGTA-Ca complex. For $(NH_4)_2SO_4$, NH_4^+ ions produced as a by-product of the acyl transfer reaction may inhibit the enzyme. Nonetheless, these two compounds inhibit TGase to a much lesser degree.

Table 3.2 also shows that the inhibition of Antarctic krill TGase by metal ions decreased in the following order: Cu^{2+} > Zn^{2+} > Ba^{2+} > Mn^{2+} > Mg^{2+}, which was similar to previous reports (Hemung and Yongsawatdigul, 2008b; Worratao and Yongsawatdigul, 2005). Cu^{2+} and Zn^{2+} ions have strong affinity for the thiol group of cysteine in the catalytic triad of TGase, while other metal

ions might have slight interaction with the amino acids in TGase (Cui et al., 2007).

3.4.7. Modification of cold set gelatin gels

The purified Antarctic krill TGase was added in gelatin solutions to study the effect on gelatin properties such as gel strength, melting temperature, setting temperature and setting time. As shown in **Table 3.3**, addition of TGase generally enhanced the cold-set gelatin gel properties. Gel strength increased significantly ($p < 0.05$) with TGase addition of 0.1 U/mg compared with that of the cold-set gelatin gel without TGase. However, high concentration of TGase such as 0.5 U/mg and 1.0 U/mg resulted in a decrease in gel strength, which was probably due to damage to the intra molecular aggregation in the gel network by excessive covalent bonds produced by TGase (Norziah et al., 2009). The addition of 0.1 U/mg TGase increased the setting temperature by 16.50±0.10°C, and the melting temperature by 28.70±0.17°C ($p < 0.05$), compared with the samples without enzyme that had 15.97±0.15°C and 27.20±0.17°C setting and melting temperatures, respectively. However, excess TGase addition above 0.1 U/mg reduced the rigidity of the triple-helix structure of gelatin resulting in relatively lower setting and melting temperatures. Addition of TGase with 0.05, 0.1 and 0.5 U/mg significantly gave a shorter setting time ($p < 0.05$), which is attributed to increase in number of interactions formed with TGase at 4°C. Previous studies have showed that TGases from aquatic species could increase setting and gelling abilities of fish mince (Binsi and Shamasundar, 2012). Microbial TGase was also able to modify the bloom strength, gelling point, melting point of gelatin gels. The modification effect was dependent on the TGase addition, gelatin quality as well as incubation conditions.

3.5. Conclusion

Transglutaminase (TGase) purified from Antarctic krill exhibited unique properties compared with its counterparts from terrestrial animals, plants and microorganisms. The purified TGase exhibited optimal activity at weakly alkaline pH (pH 8.0–9.0) and low temperature (0–10°C). The enzyme activity was enhanced by Ca^{++} and Na^{+} in a concentration dependent manner up to maximum levels of incorporation of 10 mM (for Ca^{++}) and 1.8 mM (for Na^{+}), beyond which further additions of the cations was not useful. The Antarctic krill TGase was strongly inhibited by PCMB, IAA, NEM and Zn^{2+}, Cu^{2+} suggesting that the purified enzyme probably has cysteine in its catalytic site. Such distinct properties, especially the high activity at cold temperatures could enable the TGase to be used in cold reaction conditions, as shown in this study with the formation of gelatin gels at 4 °C with enhanced mechanical properties.

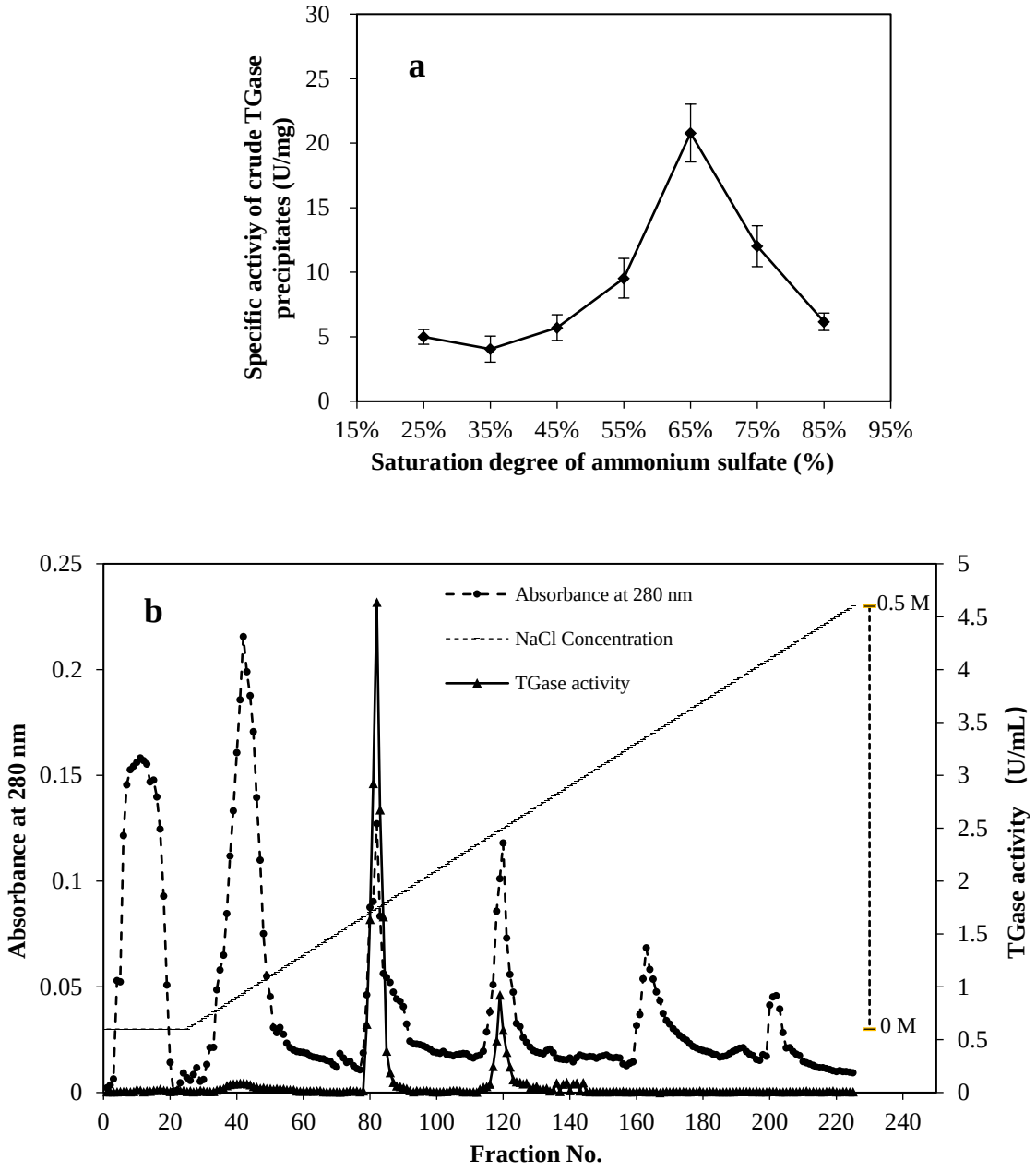

Figure 3.1. TGase purification. **a.** TGase specific activity of ammonium sulfate fractions at different saturation. **b.** The elution fractions of DEAE-Sephacel column.

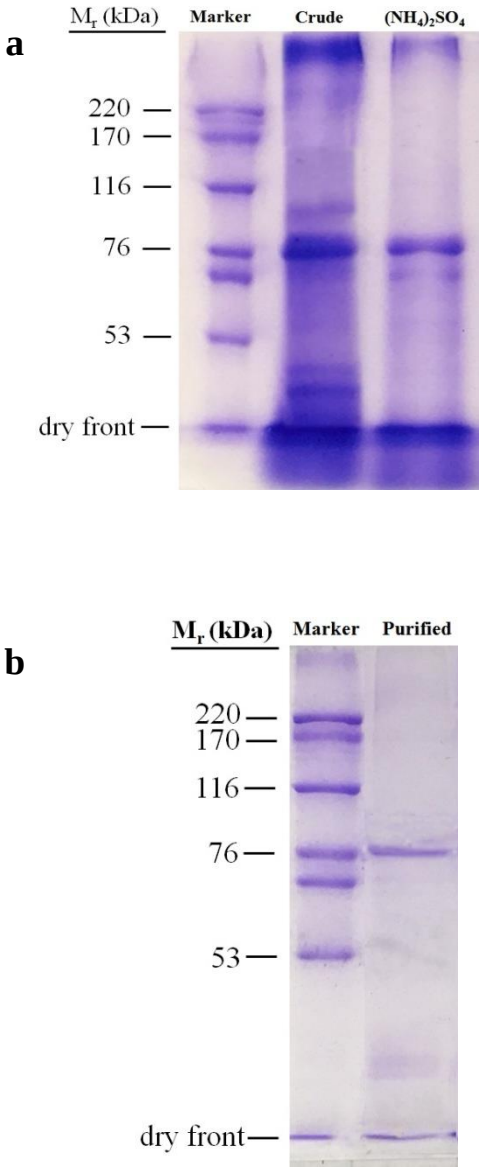

Figure 3.2. SDS-PAGE protein pattern of TGase. **a.** Lane 1: standard marker, Lane 2: crude TGase extract, Lane 3: ammonium sulfate fraction at 65% saturation. **b.** Lane 1: standard marker, Lane 2: fractions at 0.13-0.15 M NaCl.

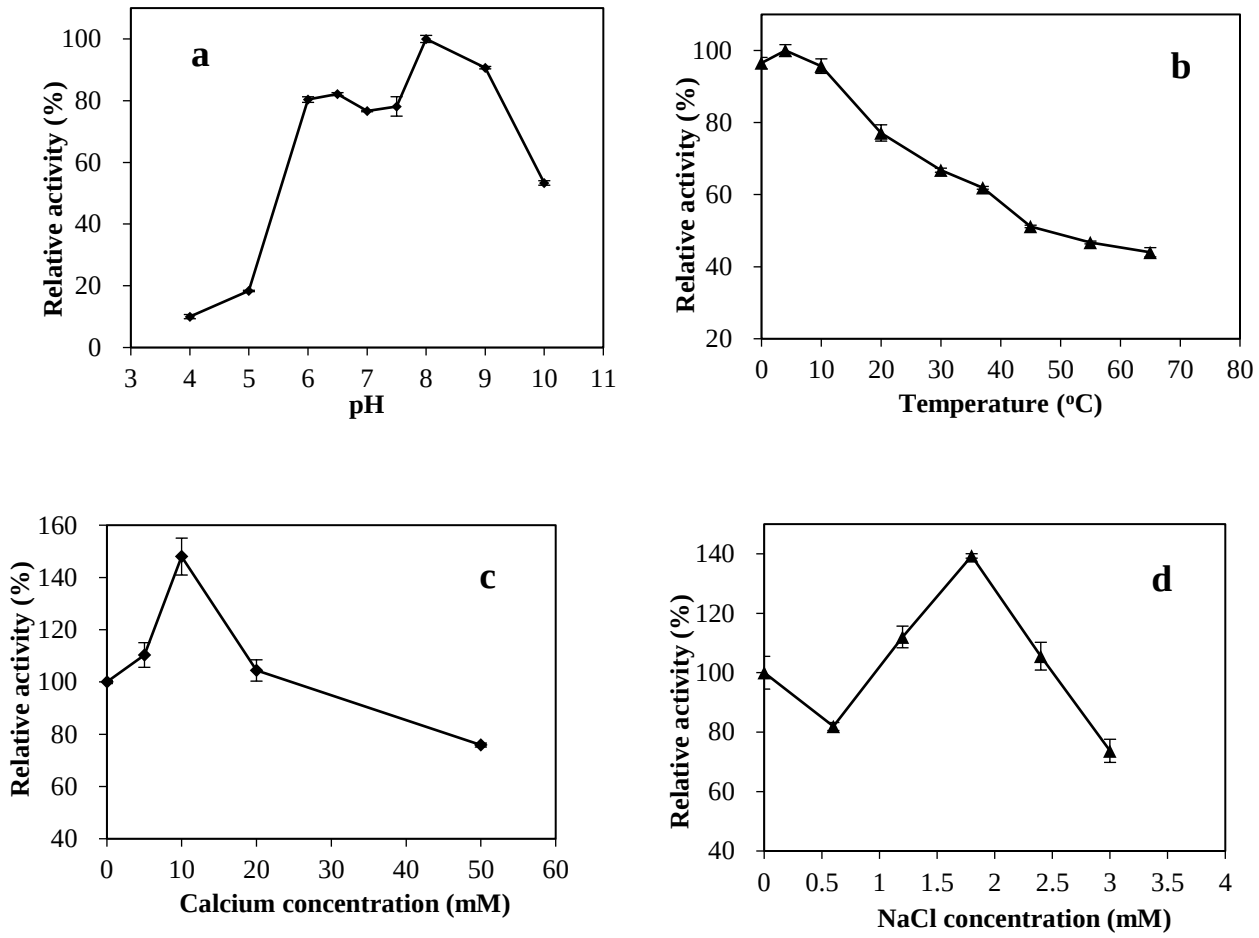

Figure 3.3. Characterization of purified TGase from Antarctic krill. **a**. Effect of pH. **b**. Effect of temperature. **c.** Effect of $CaCl_2$ concentration. **d.** Effect of NaCl concentration.

Table 3.1

Purification of TGase from Antarctic krill.

Purification Step	Total protein (mg)	Total activity (U)	Specific activity (U/mg)	Purification fold	Yield (%)
Crude extract	87.819	457.561	5.210	1.000	100.000
$(NH_4)_2SO_4$ precipitation	7.704	153.943	19.982	3.835	33.644
DEAE-Sephacel	0.940	50.293	53.518	10.272	10.992

Table 3.2

Effect of inhibitors and metal ions on TGase activity.

Inhibitors & Metal ions	Residual activity (%)
IAA	28.75 ± 1.70
EGTA	42.93 ± 0.18
PCMB	1.62 ± 0.39
PMSF	40.79 ± 1.31
$(NH_4)_2SO_4$	65.58 ± 0.25
NEM	34.38 ± 2.76
Zn^{2+}	20.12 ± 2.90
Cu^{2+}	19.78 ± 4.31
Ba^{2+}	22.55 ± 0.99
Mn^{2+}	30.65 ± 4.57
Mg^{2+}	53.52 ± 0.48

Values given are means ± standard deviations.

Table 3.3

Properties of gelatin with addition of TGase purified from Antarctic krill.

	Gel strength (g)	Setting Temperature (°C)	Setting time (s)	Melting Temperature (°C)
Gelatin + 0 U/mg TGase	229.55 ± 2.62^{c}	15.97 ± 0.15^{ab}	18.47 ± 0.25^{a}	27.20 ± 0.17^{c}
Gelatin + 0.050 U/mg TGase	231.55 ± 1.63^{c}	16.17 ± 0.23^{ab}	16.47 ± 0.15^{c}	28.03 ± 0.31^{ab}
Gelatin + 0.1 U/mg TGase	255.45 ± 1.20^{a}	16.50 ± 0.10^{a}	15.90 ± 0.36^{c}	28.70 ± 0.17^{a}
Gelatin + 0.5 U/mg TGase	246.15 ± 2.33^{b}	16.30 ± 0.26^{ab}	16.03 ± 0.25^{c}	27.77 ± 0.38^{bc}
Gelatin + 1.0 U/mg TGase	241.10 ± 1.13^{b}	15.87 ± 0.21^{b}	17.27 ± 0.25^{b}	27.33 ± 0.15^{c}

Values were given as mean ± standard deviation. Values with the same superscript letters in a row were not significantly different ($p < 0.05$).

CONNECTING STATEMENT 2

Chapter IV is a study on the thermostability of the purified cold-active TGase designed to provide the requisite information needed to rationalize / justify its utilization in food processing. It entailed investigation of the kinetics of thermal inactivation of the cold-active TGase, as well as the conformational changes of the TGase induced by various heat treatments using fluorescence spectroscopy. Homologous structure of the TGase was constructed using the sequence based on transcriptome analysis to disclose the relationship between structural change and thermostability of the enzyme.

This chapter constitutes a paper to be submitted to Food Chemistry journal for consideration for publication:

Y Zhang, B K Simpson. High thermal stability for a cold-active protein-crosslinking transglutaminase: from kinetics to structural analysis.

PhD candidate Y Zhang designed and performed the experiments, analyzed the data, and drafted the manuscript. Professor B K Simpson supervised the research work, provided the research materials and facilities, guided the lab performance and data analysis, revised the manuscript.

CHAPTER IV. HIGH THERMAL STABILITY FOR A COLD-ACTIVE PROTEIN-CROSSLINKING TRANSGLUTAMINASE: FROM KINETICS TO STRUCTURAL ANALYSIS

4.1. Abstract

The thermo stability of Antarctic krill TGase that catalyzes protein crosslinking reactions at low temperatures was studied. The analyses included kinetics of thermal inactivation, conformational changes via fluorescence spectroscopy, and *in silico* structural analysis using transcriptomics. Kinetics of inactivation studies showed the TGase was stable in the temperature range of 0 to 60 ^{o}C for 2 to 20 days but was readily inactivated above 60 ^{o}C. Fluorescence spectroscopy phase diagram suggested the existence of three conformational states as a function of temperature (0–100 ^{o}C, i.e., nature, intermediate molten globule, and inactive unfolded (U) states). 3D fluorescence spectra showed tertiary structure change dominated at 40 ^{o}C, secondary structure change at 60 ^{o}C, and irreversible structure disruption at 80 ^{o}C. The gene sequence of the TGase was firstly identified using transcriptomics, and a homologous structure was constructed. The conserved catalytic triad of the TGase was Cys333–His403–Asp426, and the catalytical mechanism was proposed. The possible molecular interactions involving disulfide bonds around core domain suggested the thermostability of this TGase.

4.2. Introduction

Transglutaminases (EC 2.3.2.13), also known as TGases or TGs, are a family of closely related transferase enzymes that catalyze post-translational modification of protein molecules via protein-protein crosslinks between γ-carboxamide groups of glutamyl residues and the ε-amino of lysyl residues. They are ubiquitous and widely distributed in a variety of organisms ranging from microorganisms, to plants, and animals (both vertebrates and invertebrates). TGase catalyzed reactions result in stable isopeptide bonds that are highly resistant to hydrolytic degradation by proteases. This feature enables TGases to participate in diverse physiological functions in living organisms including processes such as: blood clotting, wound healing, apoptosis, and sperm production in humans and animals (Agarwal et al., 2016; Panner Selvam and Agarwal, 2018); post-translational modification of proteins via polyamines inter- or intra-molecular cross-linkages in plants during their growth and development, as well as stabilization and photoprotection of various components of photosynthesis (Serafini-Fracassini and Del Duca, 2008). Although TGases have been found in microorganisms, their exact physiological role is still unclear, apart from studies that suggest that microbial TGases participate in cell differentiation (Zhang et al., 2009) and in cross-linking multiprotein surface structural protein coat that protects bacterial spores (Henriques and Moran, 2007).

Advantage has been taken of the highly stable isopeptide bonds that are formed by TGases to bind proteins together, improve texture or create new products in various industrial processes such as food processing (e.g., in dairy, baked goods, soy proteins, meats and meat analogs, surimi, edible films), textile manufacture (e.g., wool, leather, silk), and in biomedicine (e.g., collagen- and other biopolymer-based scaffolds and hydrogels, protein-DNA conjugation, protein fluorescent labelling, and antibodies functionalization) (Mehta and Eckert, 2005; Nemes et al., 2005; Savoca et al., 2018).

In the industrial setting, enzyme stability and activity are necessary for effective biocatalysis. Thus, reaction conditions such as pH, temperature, presence / absence of inhibitors or activators, water activity, and ionic strength, etc., that can elicit changes in the structural integrity of the enzymes can ultimately impact catalytic functioning. Enzymes from species acclimated to different temperature regimes have developed various strategies to drive reaction rates in their respective habitats (Georlette et al., 2004; Hoyoux et al., 2004). While enzymes from cold-adapted species have relatively higher catalytic activities at low temperatures, their homologs from warm-temperature acclimated species have relatively higher activities at higher temperatures. These differences are made possible by their structural and stability differences. While the cold-active enzymes have more flexible catalytic centers and low thermal stabilities, their warm-temperature counterparts have relatively more rigid catalytic centers and high thermal stabilities (Coker, 2016; Littlechild, 2015).

The practical significance of this differing stabilities of cold versus warm temperature adapted enzymes is that they can be uniquely suited to distinct applications. For instance, thermostable enzymes have advantages in processes that take place at higher temperatures by increasing substrates solubility and conversion rates into finished products, or by reducing viscosity of the reaction media. Examples include uses in baking, starch liquefaction / saccharification, mashing (brewing), starch and fuel viscosity reduction, pulp and paper modification, synthesis in organic solvents (e.g., synthesis of penicillin or aspartame), transesterification reactions (biodiesel), production of enantiopure fine chemicals, and thermophilic DNA polymerase reactions in molecular biology. Cold-active but heat-labile enzymes have advantages in reactions that take place at lower temperatures by reducing undesirable side reactions, protecting heat-labile essential components, reducing energy cost and curtailing microbial activity and metabolism. Examples include: alcoholic and non-alcoholic beverages (e.g., fermentation of beer and wine, fruit juice

processing, chill-proofing of beer), breadmaking, meat tenderization, cold water detergents (various lipases, protease, amylases, cellulases), bioenergy, biomedical and pharmaceutical applications, molecular biology (for dephosphorylation of 5' end of linearized fragments of DNA, release of uracil from uracil-containing DNA, digestion of DNA and RNA (de Miguel Bouzas et al., 2006; Rigoldi et al., 2018; Sarmiento et al., 2015).

4.3. Materials and methods

4.3.1. Chemicals

Frozen Antarctic krill was obtained from Dalian, China and stored at –80 °C before transcriptome assay. Agarose, calcium chloride ($CaCl_2$), N, N'-dimethylated casein (DMC), dithiothreitol (DTT), ethylene diamine tetra acetic acid (EDTA), monodansylcadaverine (MDC), sodium chloride (NaCl), Tris-HCl (all analytical grade) were purchased from Sigma-Aldrich Inc. (St. Louis, MO, USA).

4.3.2. Thermal stability test

TGase activity was measured using reaction mixture comprised of 1 mg/mL DMC, 15 µM MDC, 3 mM DTT, 5 mM $CaCl_2$, 50 mM Tris-HCl (pH 7.5) and 100 µL purified TGase (Zhang et al., 2017b). The reaction was performed at 25 °C for 10 min and stopped by adding EDTA solution to a final concentration of 20 mM. Fluorescence intensity (FI) of MDC incorporated into DMC was measured with F2000 fluorescence spectrophotometer (Hitachi, Ltd, Tokyo, Japan) at excitation and emission wavelengths of 350 and 480 nm, respectively. FI values of blanks (FI_0) were carried out by a similar procedure but deionized water was used to replace TGase. Enhancing factor (EF) was determined to be 1.877 in this study. One unit of TGase enzyme activity was defined as the amount of enzyme that catalyzed the incorporation of 1 nmole of MDC into DMC during 1 min at 25 °C. TGase activity was calculated by Equation (1).

$$\text{TGase activity (1 U)} = \frac{(FI-FI_0)\times 15{,}000\ \text{nmol}\times 2\ \text{mL}\times 10^{-3}}{FI_0\times 10\ \text{min}\times 1.877} \quad (1)$$

Previously purified TGase was pre-incubated in 50 mM Tris-HCl (pH 7.5) containing 5 mM $CaCl_2$ at a wide temperature range of 0, 20, 40, 60, 80 and 100 °C. After pre-incubation for different time intervals of 0, 5, 15, 30, 60 min, and 1, 2, 4, 8, 12 h, aliquots of TGase were withdrawn, cooled or warmed rapidly, and their relative activities were measured at 25 °C as previously described. Residual activity of TGase was measured as the percentage of activity remaining after incubation, taking the activity of TGase without pre-incubation as 100%.

4.3.3. Kinetics model

As often reported in the literature for enzyme inactivation studies (Anthon and Barrett, 2002; Aymard and Belarbi, 2000; Oancea et al., 2008), first-order kinetics (Equation 2 below) was used to describe the thermal inactivation of TGase. The rate constant *k* was calculated by the linear regression of $\ln(\frac{A_t}{A_0})$ versus t.

$$\ln(\frac{A_t}{A_0}) = -kt \quad (2)$$

where A_t is the residual activity (U), A_0 is the initial activity (U), *k* is the rate constant (h^{-1}) at the studied temperature, and t is the treatment time (h).

The half-life value ($t_{1/2}$) of inactivation given by Equation (3), was used to estimate the time (h) needed to reduce the initial activity by 50% at the corresponding temperatures.

$$t_{1/2} = \frac{\ln 2}{k} \quad (3)$$

The decimal reduction time (*D* value) expressed as Equation (4) was used to estimate the time (h) needed to reduce the initial activity by 90% at the corresponding temperatures.

$$D = \frac{\ln 10}{k} \quad (4)$$

The temperature sensitivity parameter (Z_T value) expressed as Equation (5) was used to describe the temperature (^oC) needed to reduce the D value by one log-circle (90%). Z_T value can be calculated by plotting logD versus temperature Tm (^oC).

$$\log D = -\frac{Tm}{Z_T} \quad (5)$$

Arrhenius Law expressed by Equation (6) was used to represent the temperature dependence of *k*. *Ea* can be calculated from the Arrhenius plot of ln*k* vs 1/T.

$$\ln k = -\frac{E_a}{RT} + \ln A \quad (6)$$

where E_a is the activation energy ($J \cdot mol^{-1}$), R is the universal gas constant (8.314 $J \cdot K^{-1} \cdot mol^{-1}$), T is the experimental temperature (K), A is the pre-exponential constant (h^{-1}).

4.3.4. Fluorescence spectroscopy analyses

To analyze the effect of thermal treatment on the structure of the cold-active TGase, 100 µL aliquots of purified TGase in 50 mM Tris-HCl (pH 7.5) containing 5 mM $CaCl_2$, were heated at temperatures 0, 20, 40, 60, 80 and 100 °C for 15min in water bath. After heating, the TGase enzymes were cooled or warmed quickly to 25 ^oC and centrifuged at 5000 g for 2 min to remove the precipitates. The fluorescence spectroscopy analysis was performed in 1 × 1 cm fluorescence

cuvette on a F2000 fluorescence spectrophotometer (Hitachi, Japan). Phase diagrams is a sensitive method to detect the folding/unfolding of proteins. It was built up based on Equation $I_{320nm} = a + b*I_{365nm}$ where I_{320nm} and I_{365nm} were the emission intensities of TGase at 320 nm and 365nm, respectively, when the excitation wavelength was set to 292 nm; a and b were the intercept and slope of the I_{320nm} versus I_{365nm} plot. Three-dimensional (3D) fluorescence spectra were performed with the emission and excitation wavelength range from 200 to 500 nm with an increment of 20 nm and scan speed of 1000 nm min^{-1}.

4.3.5. Transcriptome assay & bioinformatics analyses

4.3.5.1. Total RNA extraction

Total RNA was extracted from frozen Antarctic krill using a Total RNA Extractor (Trizol) kit (Shanghai Sangon, China). The concentration of extracted DNA was estimated using Qubit® RNA HS Assay Kits (Life Technologies, Foster City, CA, USA) on a Qubit 2.0 Fluorometer (Life Technologies). The integrity of extracted DNA was measured on a 1.0% agarose.

4.3.5.2. mRNA-Seq library construction & sequencing

The mRNA library was prepared with 3 µg total RNA using VAHTS™ mRNA-seq V2 Library Prep Kit for Illumina® (Vazyme Biotech Co., Ltd, Nanjing, China) following manufacturer's protocol. Briefly, mRNA was purified from total RNA using mRNA capture beads, and then fragmented. Random primers were used to synthesize the first strand cDNA, and subsequently the second strand cDNA was synthesized. The double strand cDNA was purified using VAHTS DNA clean beads. After end repair, dA-tailing, adapter ligation and cDNA purification, polymerase chain reaction (PCR) was performed using the purified ligation products, primer mix and DNA polymerase to amplify the library. The quality of the library was determined using Agilent 2100 bioanalyzer, and the library was sequenced using Illumina HiSeq 2000 sequencing system.

4.3.5.3. *De novo* assembly, gene annotation & identification of TGase genes

The assembly and functional annotation of each read were performed based on method described by Jeon et al. (2018). Raw reads were evaluated by FastQC and processed using Trimmomatic to obtain clean reads. The clean reads were performed by *de novo* assembling using Trinity software. High quality reads were mapped for assembly validation and aligned bowtie2 software. The unigenes were annotated mainly by NCBI Blast+ using 9 database including NR (non-redundant protein sequences), NI (nucleotide sequences), KOG (eukaryotic orthologous groups), Swiss-Prot, TrEMBL, PFAM (protein family), CDD (conserved domain database), GO

(gene ontology), and KEGG (Kyoto encyclopedia of genes and genomes) using KAAS (KEGG Automatic Annotation Server). The unigenes encoding TGase were selected by searching the annotation data, and the complete gene sequence was assembled manually and determined using NR/NT database, as well as ORFPredictor (https://bioinformatics.ysu.edu/tools/OrfPredictor.html) to identify the sequence with complete Open Reading Frame (OFR).

4.3.5.4. Characterization of Antarctic krill TGase sequence

The corresponding amino acid sequence of TGase was predicted using Translate tool at the ExPasy website (https://web.expasy.org/translate/). The physicochemical parameters including molecular weight and theoretical isoelectric point (PI) were analyzed by ProtParam tool at the ExPasy (https://web.expasy.org/protparam/). The motif sequences and conserved domains of TGase were identified using Interpro (http://www.ebi.ac.uk/interpro/). Transmembrane region was predicted using Phobius tool (http://phobius.sbc.su.se/). Signal peptide was analyzed using SigCleave tool at EMBOSS (http://www.bioinformatics.nl/cgi-bin/emboss/sigcleave). The similarities of its cDNA and amino acid sequences across a variety of species were analyzed using the BLAST search program (https://blast.ncbi.nlm.nih.gov/Blast.cgi). Multiple sequence alignments were constructed using ClustalW algorithm on Phylogeny (http://www.phylogeny.fr/one_task.cgi?task_type=clustalw).

4.3.6. *In silico* structural analysis

The tertiary structure of Antarctic krill TGase was predicted using MODELLER program. Homologous protein (template) was identified using HHpred server (https://toolkit.tuebingen.mpg.de/#/jobs/2566042). Validation of predicted 3D model was performed using VERIFY 3D and PROCHECK programs (http://servicesn.mbi.ucla.edu/). PyMOL Molecular Graphics System was used to generate the structural image.

4.4. Results and discussion

4.4.1. Thermal stability of cold-active TGase

The purified cold-active TGase was pre-treated at various temperatures (0, 20, 40, 60, 80, 100 ^{o}C) for various times (0-12 h), and the residual activities are shown in **Figure 4.1**. The residual activities of TGase decreased with increasing pre-incubation temperature and pre-incubation time (**Figure 4.1A**). The cold-active TGase was stable at 0 ^{o}C with 94.76% activity retained after 12 h. This observation was in accordance with results of TGases derived from other marine species to the effect that TGase activity scarcely changed at low temperatures of 0-6 ^{o}C (Kumazawa et al.,

1996; Nozawa et al., 2001a; Worratao and Yongsawatdigul, 2003). At 20 °C, 40 °C and 60 °C for 12 h incubation, the TGase showed residual activities of 83.55%, 75.12%, and 57.28%, respectively. From **Figure 4.1B**, the residual activities after 15 min were comparable at 0 °C, 20 °C, and 40 °C, and became slightly lower for 60 °C treatment where 92.94% activity remained. The Antarctic krill TGase exhibited higher thermal stability than that of a cold-active squid (*Todarodes pacificus*) gill TGase (Nozawa et al., 2001a), which had optimal temperature of 20 °C and was thermally stable from 0-50 °C with 80% residual activity after only 1 h incubation at 50 °C, pH 7.5. However, both our Antarctic krill TGase and the reported squid gill TGase showed higher thermal stability than their counterparts derived from other marine species such as sardine (*Sardina pilchardus*), walleye pollack (*Theragra chalcogramma*) liver, and tilapia (*Oreochromis niloticus*) that showed rapid loss of activities within a few minutes at 55 °C, 40 °C and 50 °C, respectively (Batista et al., 2002; Kumazawa et al., 1996; Worratao and Yongsawatdigul, 2003). Thus, the Antarctic krill TGase from this study exhibited both high catalytic activity at low temperatures (Zhang et al., 2017b) and thermal stability within a relatively broad temperature range (0-60 °C). Similar activity-stability relations have been found with cold-active enzymes such as isocitrate dehydrogenase, superoxide dismutase and alcohol dehydrogenase that exhibited comparable thermal stability as their mesophilic homologues (Fedøy et al., 2007; Kazuoka et al., 2007; Merlino et al., 2010).

Unlike the steady linear trend observed when the TGase was pre-incubated at 0-60 °C in **Figure 4.1A**, pre-incubation at 80 °C caused rapid loss of activity within the first 2 h with only 13.94% activity retained, and almost complete inactivation after 4 h. Furthermore, pre-incubation at 100 °C completely inactivated TGase within a short time (< 5 min). There was also irreversible protein denaturation induced by high temperature treatments at 80 °C for 4 h, and after minutes at 100 °C, which suggested denaturation of TGase enzyme due to the breakdown of covalent bonds. A few stabilizers have been reported to either protect the TGase from activity loss during heating or enhance its thermal stability. The presence of salts such as NaCl and $CaCl_2$ at moderate levels could stabilize fish TGase (Nozawa et al., 2001a) and guinea pig liver TGase (Nury et al., 1989), while the addition of polyols such as glycerol, polyethylene glycol and sorbitol could improve the thermal stability of microbial TGase (Cui et al., 2008).

4.4.2. Kinetics

The thermal stability data ranging between 0 and 100 °C in **Figure 4.1A** was investigated by

first-order kinetics, and the resulting model shown in **Figure 4.1C** suggested that the first-order model could fit the linear portion of thermal stability data, i.e., 0-60 °C for 0 to 12 h; 80 °C for 0 to 4 h. The corresponding kinetic parameters and determination coefficients are listed in **Table 4.1**. The R^2 values for the first-order model varied from 0.9640 to 0.986, indicating that first-order model was suitable to describe the inactivation of the cold-active TGase within the selected ranges. The same model was used previously for microbial TGases from *S. hygroscopicus* and *S. mobaraense* (Cui et al., 2008; Menéndez et al., 2006).

The inactivation rate constant k values increased from 0.0047 to 0.7632 h^{-1} when treatment temperature increased from 0 to 80 °C; and the $t_{1/2}$ values decreased significantly ($p < 0.05$) from 149.08 to 0.91 h (**Table 4.1**). When temperature was above 60 °C, the TGase was inactivated rapidly. The k and $t_{1/2}$ values at 60 °C were 0.0448 h^{-1} and 15.47 h, respectively, which indicated Antarctic krill TGase was more thermally stable than *S. hygroscopicus* TGase with k and $t_{1/2}$ values of 0.0828 min^{-1} and 8 min, respectively, at 60 °C (Cui et al., 2008). The k value at 80 °C was significantly higher than other k values ($p < 0.05$), suggesting that this cold-active TGase was relatively unstable and highly susceptible to heating at high temperatures above 80 °C. The D value is another important parameter used in the characterization of enzyme thermostability. Showing similar trend with $t_{1/2}$ values, D values decreased significantly from 495.24 to 3.02 h from 0 to 80 °C ($p < 0.05$). The cold-active TGase from Antarctic krill could be stable with 50% activity retained for approximately 6 days at 0 °C in aqueous solution containing 5 mM Ca^{2+}, compared to only 15 h and 1 h at 60 and 80 °C, respectively. It indicated that the thermal stability of the TGase was influenced by temperatures, even though it was considered as thermostable compared with characterized microbial TGases. The Z_T value describes the relationship between D value and temperature. It was obtained from **Figure 4.1D** as 40.65 °C. The activation energy for the cold-active TGase reaction in temperature range of 0 to 80 °C was calculated from the slope of Arrhenius plot (**Figure 4.1E**) and was found to be 641.35 $J \cdot mol^{-1}$. From the kinetic studies, it is deduced that the cold-active TGase was stable at 0 to 60 °C for ~2 to 20 days but could be inactivated within hours above 80 °C. This feature suggests that this enzyme would suit a range of food processing conditions such as cold-set protein gels. However, thermal stabilities of enzymes in real food matrices show different behaviors due to the influence of water molecules or other co-existing food components such as fats, carbohydrates, etc. (Oliviero et al., 2014). Enzyme inactivation is related with its conformational integrity, thus, the structural changes evaluated by

fluorescence spectroscopy and molecular dynamics are combined to explain the kinetics behavior of the cold-active but thermostable Antarctic krill TGase.

4.4.3. Structure – thermal stability analysis using fluorescence spectroscopy

Phase diagram was generated to analyze the conformational changes induced by thermal treatment of the Antarctic krill TGase. The thermal stability and kinetics data shown in **Figure 4.1** indicate that thermal treatment at temperatures above 0 ^{o}C had deactivating effect on TGase; thus, the corresponding plots of I_{320} versus I_{365} were used as a reliable method for characterizing the unfolding intermediate states of TGase. Phase diagrams (**Figure 4.2A**) showed the presence of non-linear dependencies, which reflected the sequential character of structural transformations (Kuznetsova et al., 2004). Each of the two linear portions, from 0 to 60 ^{o}C and from 60 to 100 ^{o}C, described the individual all-or-none- transition, suggesting the existence of three conformational states of TGases as a function of temperature from 0 to 100 ^{o}C. These three structural states were from active native (N) state, to intermediate molten globule (MG) state, up to completely inactive unfolded (U) state. Similar multistep unfolding was also observed in the denaturation of food enzymes such as methylesterase, peroxidase and tyrosinase (Ioniţă et al., 2014; Nistor et al., 2014; Stănciuc et al., 2015). Based on the results in **Figure 4.2A**, 0 ^{o}C was considered as the favorable temperature to stabilize the TGase structure in active form, where the highest fluorescence intensities were observed. Increasing the temperature up to 60 ^{o}C probably caused a looser packing of the protein molecules, with a sequential decrease of the fluorescence intensity. Thermal treatment above 60 ^{o}C caused large and irreversible structural change that resulted in the damage of forces such as hydrogen bonds, disulfide bonds and hydrophobic interactions, to unravel the tertiary and secondary structures.

Three-dimensional (3D) fluorescence spectrum exhibits fluorescence intensity on an excitation – emission matrix (EEM). Based on the evaluation of the intensity, peak appearance/disappearance, peak location, gradient and movement trend, more details on the conformational change of protein can be provided. The 3D fluorescence spectra and corresponding contour diagrams for the TGase solutions incubated at temperatures 0, 20, 40, 60, 80 and 100 ^{o}C are compared in **Figure 4.2B**. Four peaks (a, b, 1, 2) were observed in all graphs as a function of thermal treatment at different temperatures. Peaks a and b represented Rayleigh scattering peak ($\lambda_{excitation} = \lambda_{emission}$) and second-order scattering peak ($2\lambda_{excitation} = \lambda_{emission}$), respectively. Peaks 1 and 2 represented the characteristic fluorescence peaks for protein molecules. Peak 1 was associated with the

fluorescence spectral characteristics of Trp and Tyr residues indicating tertiary structural change; whereas peak 2 represented the fluorescence characteristics of the polypeptide backbone indicating the secondary structural change (Zaroog and Tayyab, 2012). The overall EEM pattern of the TGase molecules were similar with enzymes such as glucoamylase and peroxidase (Stănciuc et al., 2015; Zaroog and Tayyab, 2012), however, the wavelength values around the fluorescence peaks 1 and 2 might slightly alter due to the difference in enzyme molecules, solvent, and microenvironment of enzymes (Liu et al., 2013). As seen in **Figure 4.2B**, the 3D patterns of peaks 1 and 2 were similar for TGases treated at 0 ^{o}C and 20 ^{o}C, suggesting the enzyme had stable structure at such temperatures, which agreed with the findings for thermal stability (**Figure 4.1**) conducted in previous sections. There was an obvious decrease in fluorescence intensity of peaks 1 and 2 when temperatures were increased to 40 and 60 ^{o}C, and the decrease for peak 1 was larger than that of peak 2, suggesting there was conformational change when temperature increased from 40 ^{o}C and dominated by tertiary structure. TGase preincubated at 80 ^{o}C showed a significant decrease in intensities of peaks 1 and 2, accompanied by an obvious 20 nm red-shift for peak 1, as seen in the 3D fluorescence spectra. It suggested an unfolding process that resulted in an exposure of some buried Trp and Tyr residues as well as mobility of hydrophobic residues to polar environment, and the tertiary structure probably was irreversibly disrupted. For peak 2, a 5 nm red-shift was recorded, implying that the thermal treatment at high temperatures above 60 ^{o}C caused unfolding of polypeptide chains and a conformational change in secondary structure.

4.4.4. Identification of TGase genes from transcriptome data

Transcriptomics is an effective tool for obtaining TGase gene from Antarctic krill, as the overall RNA quality in the raw material was not good for PCR due to the long-term transportation from the Antarctic. Transcriptome data showed that there were 51,345,648 raw reads evaluated by FastQC and 47,565,606 clean reads obtained by Trimmomatic. After *de novo* assembling, 63,739 transcripts and 36,282 unigenes were generated and listed in **Table 4.2**. The unigene annotation statistics was summarized in **Table 4.3**. In total, there were 19,939 unigenes annotated in at least one database and 798 genes annotated in all databases, with respective percentage values of 54.96% and 2.20%. From the function annotation of all 36,282 unigenes, 5 unigenes numbered as #1, 2, 3, 4 and 5 were found with TGase function. The sequence of the 5 TGase unigenes and their function annotated from 9 database are shown in **Table 4.3**. These 5 TGase unigenes were found similar with TGase genes from various species, including Indian white prawn (*Fenneropenaeus indicus*),

white leg shrimp (*Litopenaeus vannamei*), giant river prawn (*Macrobrachium rosenbergii*) and Japanese tiger prawn (*Marsupenaeus japonicus*), that are close to Antarctic krill. The 5 identified TGase-related unigenes had length of 422, 1177, 660, 447 and 1689 bp, respectively; however, the Antarctic krill TGase gene should have a length of > 2000 bp because the molecular weight of purified Antarctic krill TGase was approximately 78 kDa (Zhang et al., 2017b). Based on the length of the 5 unigene, there are 26 sequence combinations with length of > 2000 base pair (bp), and each of the combined sequence was determined using both NR/NT database and ORFPredictor (data not shown). Only one gene sequence by combining unigene in order of #3, 2 and 1 was identified as a complete TGase gene using NCBI BLAST search program, and it was with a complete ORF.

4.4.5. Characterization of Antarctic krill TGase sequence

The cDNA sequence and the deduced amino acid sequence of identified TGase are shown in **Figure 4.3A**. The full length of Antarctic krill cDNA was 2259 bp with start codon ATG and stop codon TGA. The gene encoded TGase protein with 753 amino acids, and it had theoretical molecular weight of 85.139 kDa and estimated PI of 4.99. TGase domains were found using Interpro analysis, including a TGase N-terminal domain at positions 56–181, a TGase core domain at positions 318–426 where there was a TGase active site motif, GQCWVFAGVVNTVCRALG at 331–348, and a TGase C-terminal domain at positions 652–747. The domains were highlighted in green shade, and the catalytic triad was depicted in red shade, as shown in **Figure 4.3A**. Phobius analysis showed that Antarctic krill TGase was non-cytoplasmic protein and a transmembrane region located at position 330–349 was observed with a possibility of 2%. Extracellular TGases have been found presented with cross-linking ability of various proteins such as fibrin and collagen (Nurminskaya and Belkin, 2012). Besides, Antarctic krill TGase contained no signal peptide region. Nucleotide sequence similarity analysis with the BLAST algorithm showed that cDNA and deduced amino acid sequences of Antarctic krill TGase had high identity of 78.72% and 49.48%, respectively, with giant river prawn (*Macrobrachium rosenbergii*) TGase. Relatively lower identities of ~48% were found with TGases from Japanese tiger prawn (*Marsupenaeus japonicus*), signal crayfish (*Pacifastacus leniusculus*), red swamp crayfish (*Procambarus clarkii*), white leg shrimp (*Litopenaeus vannamei*), Asian tiger shrimp (*Penaeus monodon*). The above characterization results indicated that the assembled sequence was Antarctic krill TGase.

Multiple sequence alignment was conducted between Antarctic krill TGase and giant river

prawn TGase (GenBank ID: AIN46597.1), as well as a few TGases with solved structures such as Factor XIII from human (PDB ID: 4KTY), red sea bream TGase (1G0D) and TGase3 from human (1L9M). The full alignment was shown in **Figure 4.3B**, where the sequences with high identity were highlighted in blue shade. TGase catalytic core domains of all TGase enzymes from various sources were highly conserved, as can be seen the catalytic triad of TGase, Cys-His-Asp highlighted in yellow shade, and the amino acids involved in Ca^{2+} inactivation sites 1, 2 and 3 that highlighted in red, pink and olive shades.

4.4.6. Tertiary structure model & inferred catalytic mechanism

Homologous proteins returned from HHPred included 4KTY, 1G0D, 1L9M and 2Q3Z. Among these, 4KTY was the best template with a high probability and statistical significance (probability of 100, E-value of 9.6E-164, identities of 33%); moreover, 4KTY, human Factor XIII, was the first high-resolution crystal structure (1.98 Å) of TGase in active state (Stieler et al., 2013). The predicted tertiary structure of Antarctic krill TGase upon 4KTY is shown in **Figure 4.3C** (right) and it was used for subsequent molecular dynamic simulations. The validation studies indicated the built model was in good quality. As seen in **Figure 4.4**, VERIFY 3D image showed 81.52% of residues having a score of $\geqslant 0.2$ suggesting a good compatibility of the predicted model with the sequences in database; Ramachandran plot showed that 90.0% of residues were in most favored regions indicating a good-quality model was built for Antarctic krill TGase.

The overall predicted structure of Antarctic krill TGase was extended and flexible, as shown in **Figure 4.3C**. It contained four domains, i.e., β-sandwich, core, barrel 1 and barrel 2. The secondary structures of β-sandwich and barrel 1 & 2 domains were mainly β-sheets. To be specific, β-sandwich domain had 9 β-sheets and 1 α-helix, whereas the barrel contained 7 β-sheets, respectively. The core domain consisted of 11 α-helices and 11 β-sheets. Based on the alignment in **Figure 4.3B**, the conserved catalytic triad Cys333–His403–Asp426 for Antarctic krill TGase highlighted in magenta in **Figure 4.3C**, was located on α-helix, β-sheet, and random coil, respectively, in the core domain. The active site was wide, deep and exposed, resulting in ease of substrate binding. It has been reported that TGase underwent large structural change during activation by millimole of Ca^{2+} (Pinkas et al., 2007; Stieler et al., 2013). A predicted inactive structure of Antarctic krill TGase (**Figure 4.4C**), built from the inactive red sea bream TGase (1G0D) (Noguchi et al., 2001), was intact and the active site was remarkably covered.

The catalytic mechanism of Antarctic krill TGase can be postulated based on sequence and

structure comparison with human and fish TGases (Palanski and Khosla, 2018; Stieler et al., 2013), and it was considered highly related with structure. Briefly, Ca^{2+} binding to the Ca^{2+} binding sites could either drag and rotate the structure slightly, as well as the acyl donor residue arriving in the binding site would cause large conformational change. Those structural changes damage the disulfide bonds involving Cys439, Cys344 and Cys351, as well as hydrogen bonds, so the β-sandwich is dissociated, and two barrels are separated. Covalent acyl-enzyme intermediate is formed between the acyl groups of substrates with the thiol group of Cys333 in the active site. Nucleophilic substrates such as lysine, primary amines and water molecules, bind to the acyl-enzyme or thioester intermediates and attack the thioester carbonyl to displace the thiol group and to generate the isopeptide crosslinking in product.

4.5. Conclusion

Based on the thermo stability and kinetic model, the cold-active TGase from Antarctic krill was thermostable especially at temperatures 0-60 ^{o}C. To explain this, fluorescence spectroscopy was applied to characterize structural change when TGase was incubated at different temperatures. It suggested the existence of an intermediate molten globular state during unfolding, and peptide bond change occurring at 60 ^{o}C. Considering the difficulty to obtain the complete gene sequences of Antarctic krill TGase due to lack of fresh samples after long-distance transportation, transcriptomics was used to obtain the gene sequence and a homologous structure was constructed using human Factor XIII, PDB ID: 4KTY. The domains and catalytic triad were identified, as well as the possible molecular interactions around the domains. Such structural interpretation explained the reason for the thermostability of this cold-active TGase.

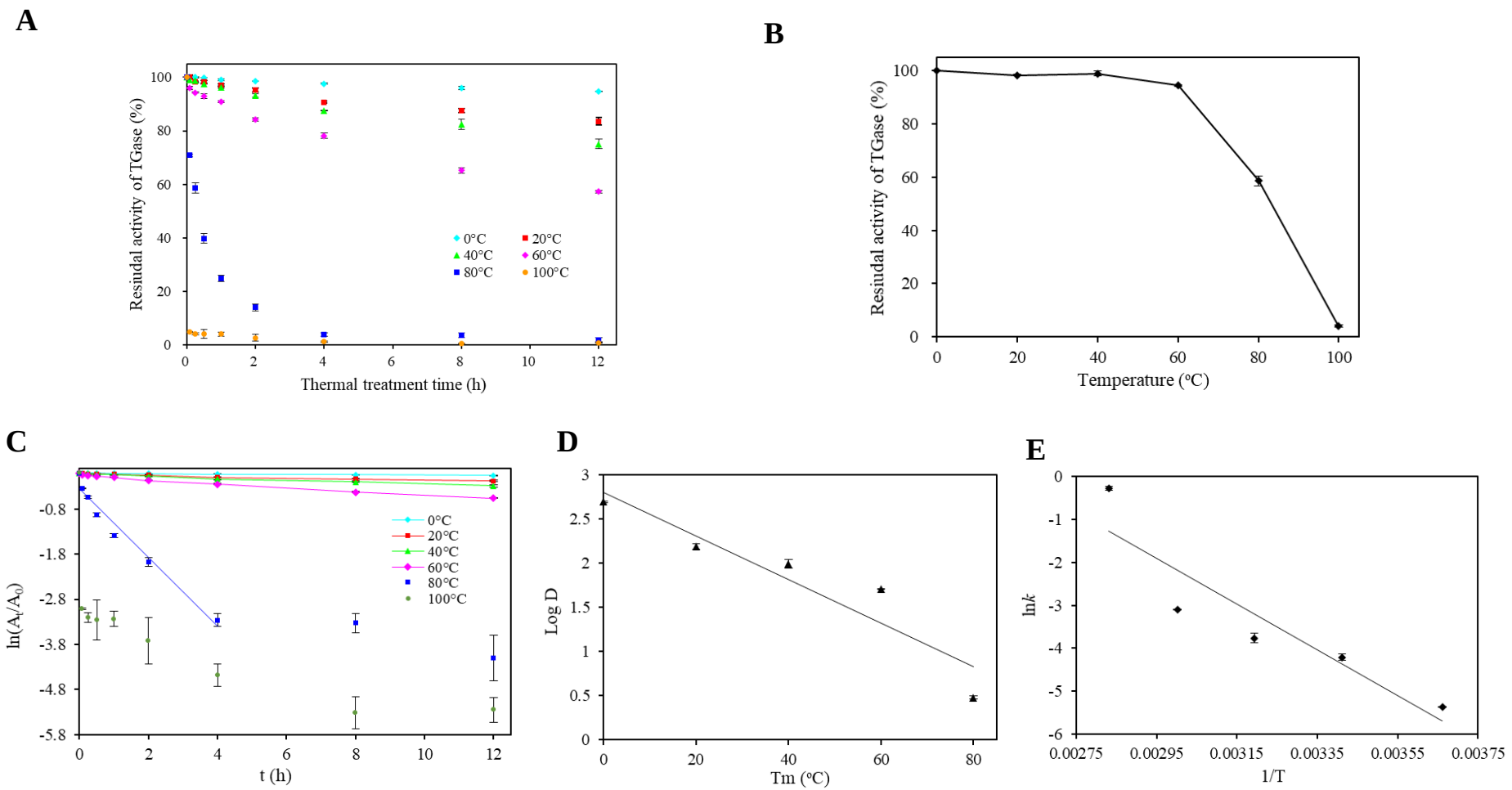

Figure 4.1. (A) Thermal stability of cold-active TGase: the residual activity of TGase (%) after treatments at 0, 20, 40, 60, 80, 100 ºC for 0, 5, 15, 30, 60 min and 1, 2, 4, 8, 12 h. **(B)** Effect of temperatures on thermal stability of cold-active TGase: the residual activity of TGase (%) after treatments at 0, 20, 40, 60, 80, 100 ºC for 15 min. **(C)** First-order kinetic model for thermal stability of cold-active TGase. **(D)** Plot of log D against temperatures for cold-active TGase. **(E)** Arrhenius plot of thermal inactivation of cold-active TGase.

A

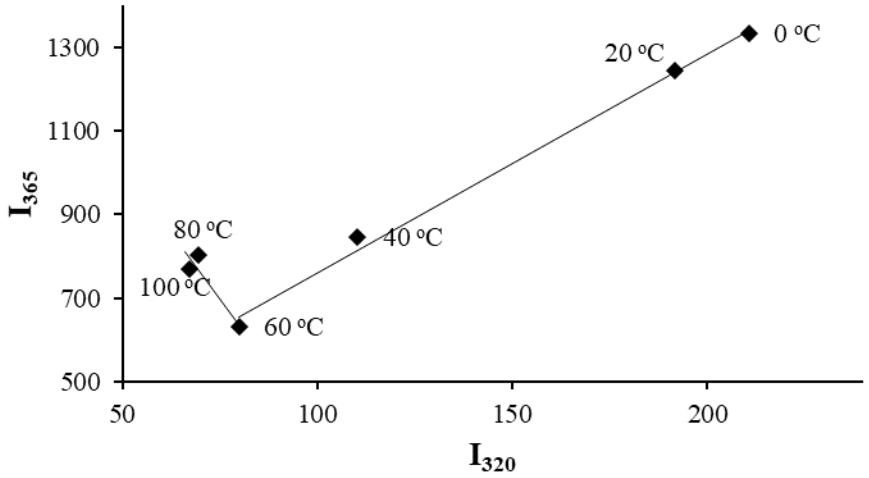
1300
1100
900
700
500
50
100
150
200
I_{365}
I_{320}
0 ºC
20 ºC
40 ºC
60 ºC
80 ºC
100 ºC

B

0 ºC

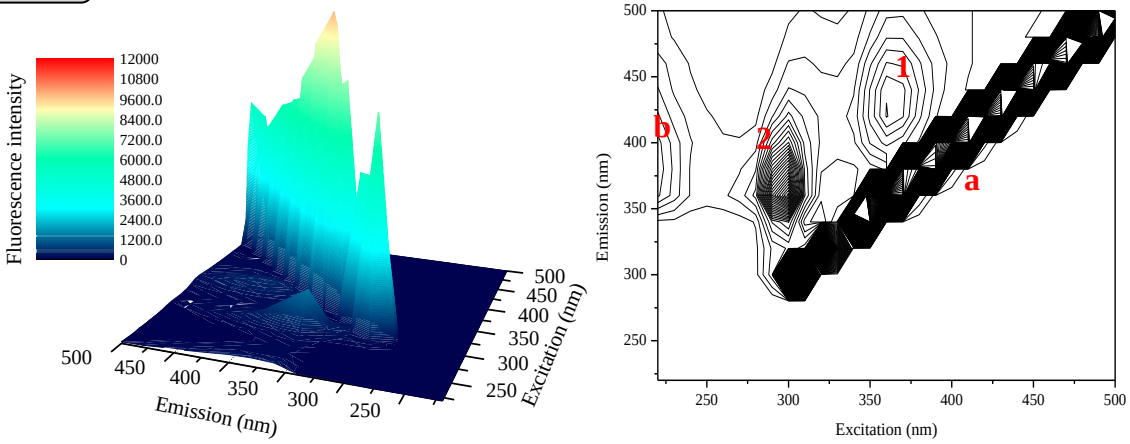
Fluorescence intensity
12000
10800
9600.0
8400.0
7200.0
6000.0
4800.0
3600.0
2400.0
1200.0
0
Emission (nm)
Excitation (nm)
Excitation (nm)
Emission (nm)
a
b
1
2

20 ºC

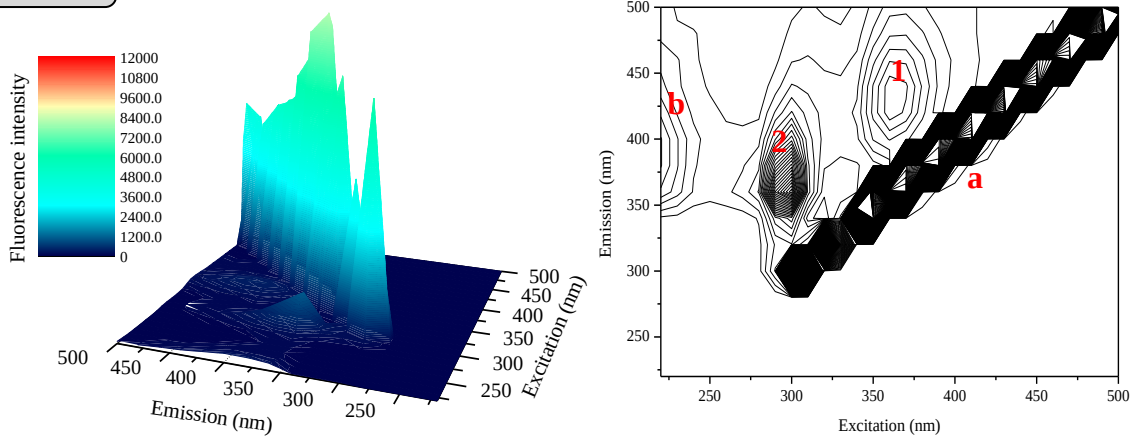
Fluorescence intensity
12000
10800
9600.0
8400.0
7200.0
6000.0
4800.0
3600.0
2400.0
1200.0
0
Emission (nm)
Excitation (nm)
Excitation (nm)
Emission (nm)
a
b
1
2

40 ºC

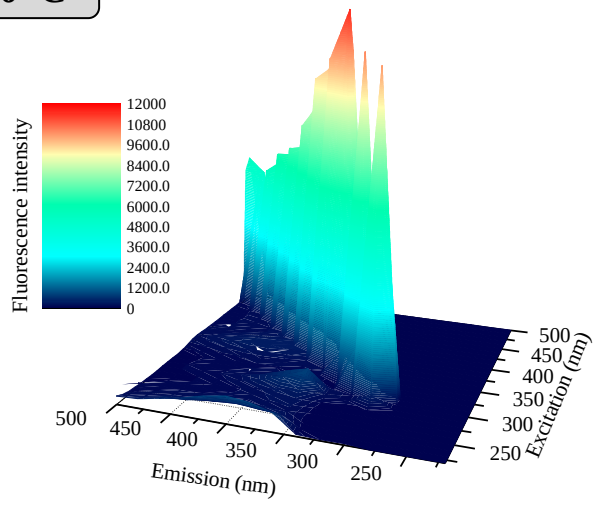

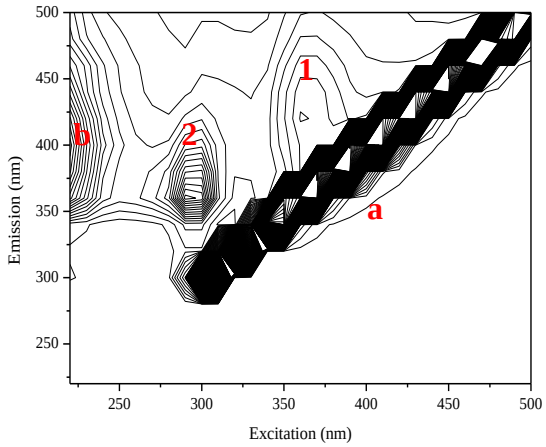

60 ºC

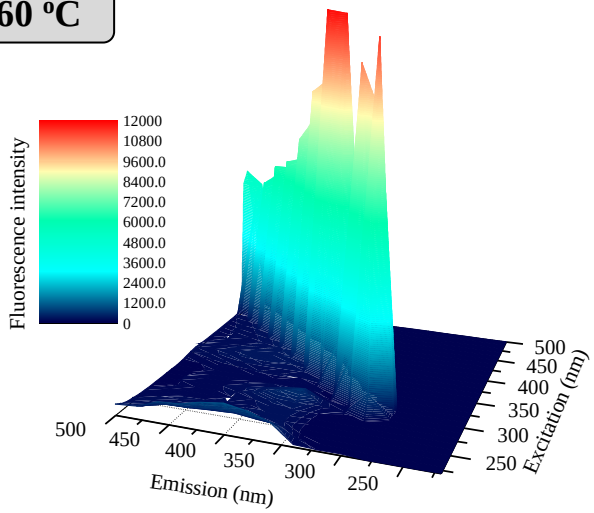

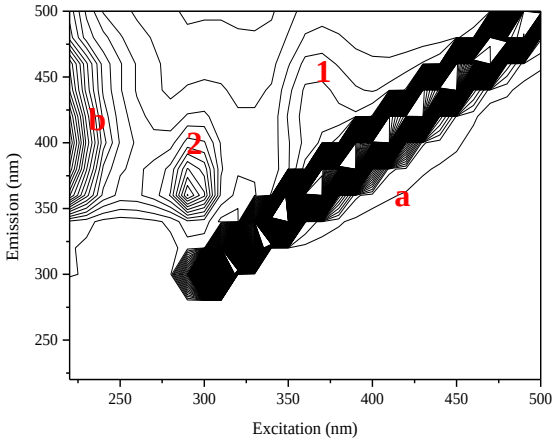

80 ºC

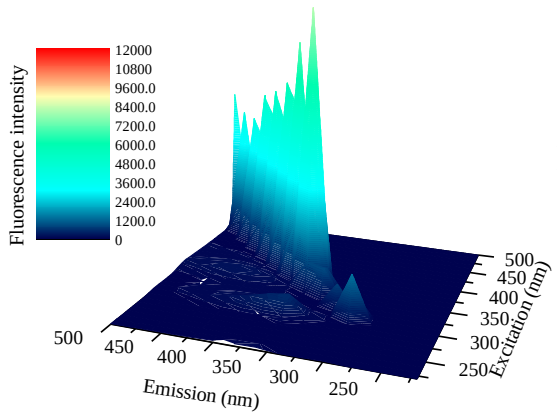

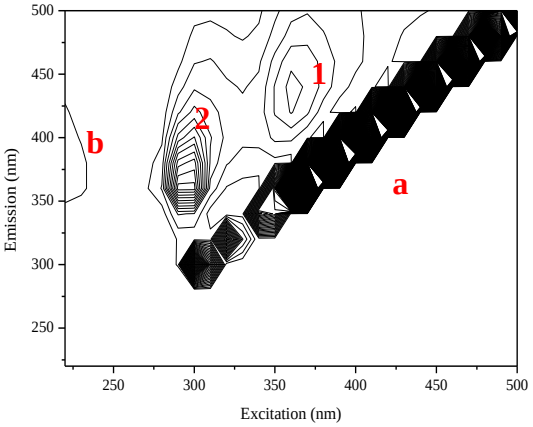

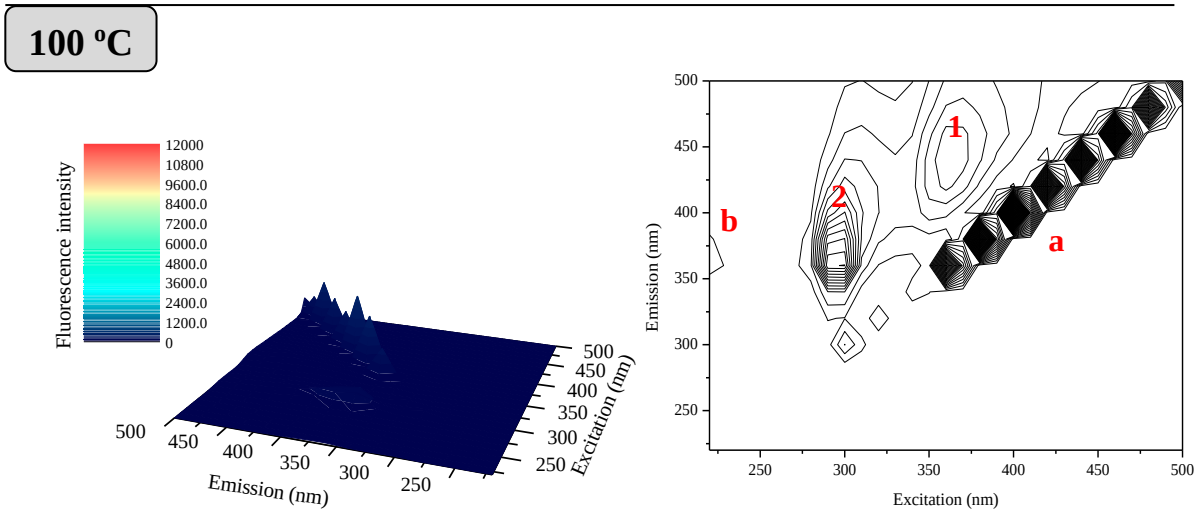

Figure 4.2. Fluorescence analysis on the conformational change of TGase induced by thermal treatment. (A) Phase diagram on the temperatures (0, 20, 40, 60, 80 and 100 ºC) and intrinsic fluorescence intensity of the TGase measured at 320 and 365 nm. (B) Three-dimensional fluorescence spectra and contour diagrams on the intrinsic fluorescence intensity measured from 220 to 500 nm for the TGase treated at temperatures (0, 20, 40, 60, 80 and 100 ºC).

A

```
atg gct cta aac ttc gga aac ttc  ttt gac ttt gat ttt  ttc gat aat ctg ttc aac aac ctg cga gat gaa aat acc ggg cgt cgt agg   90
 M   A   L   N   F   G   N   F   F   D   F   D   F   F   D   N   L   F   N   N   L   R   D   E   N   T   G   R   R   R    30
gag gat ggc agg gag ctt aca ttt atg gaa gaa gct gat gca aac aat gac ata gat gca gga gag gaa cgc ccg aga gtg aca tct gtt  180
 E   D   G   R   E   L   T   F   M   E   E   A   D   A   N   N   D   I   D   A   G   E   E   R   P   R   V   T   S   V    60
gat atg cag gct cga tcc aat gcg ctt aaa tgt aac tgt gag aaa ttt gaa cta gta gag agg agg gat gga cgt tca gtt att att cgt  270
 D   M   Q   A   R   S   N   A   L   K   C   N   C   E   K   F   E   L   V   E   R   R   D   G   R   S   V   I   I   R    90
cgt gga gcg acc ctc acc ctg gac gtc aca ttc aac tca cag ata gac ctc acg tct gga cag aaa cta gga ctt aca ttt tcc ttt ggg  360
 R   G   A   T   L   T   L   D   V   T   F   N   S   Q   I   D   L   T   S   G   Q   K   L   G   L   T   F   S   F   G    120
cga tca gcc aat atc ccc aat ggt acc caa gca aag ttg gat gtc aca ggc aag cag acg ttt gat gat gat acc gct cta tgg gat gtc  450
 R   S   A   N   I   P   N   G   T   Q   A   K   L   D   V   T   G   K   Q   T   F   D   D   D   T   A   L   W   D   V    150
cgg ttg gtt act cag gct gaa aat act tta acc ttg gag gtg cat gtc cca gta cat gtg atg gta ggc atc tgg cag tta act ata gag  540
 R   L   V   T   Q   A   E   N   T   L   T   L   E   V   H   V   P   V   H   V   M   V   G   I   W   Q   L   T   I   E    180
gtc tcc cct caa agt aat cct tca gct aaa cat gtg ttc cga cca gaa gaa aca tta tac ata ctc ttc aac cca tgg aac aaa gag gat  630
 V   S   P   Q   S   N   P   S   A   K   H   V   F   R   P   E   E   T   L   Y   I   L   F   N   P   W   N   K   E   D    210
gat gtg tac atg gag gaa gat gag cta cgg gaa gag tac atc ctc aat gac gtt ggg aag atc tgg gtt ggc aat tgg cgt tct aac ttt  720
 D   V   Y   M   E   E   D   E   L   R   E   E   Y   I   L   N   D   V   G   K   I   W   V   G   N   W   R   S   N   F    240
ggg agg tca tgg aac tat ggt cag ttt gat gat gct gta ctc cct gct tgt atg tat cta atg gag aat gca cgt ctc agg cca gaa gaa  810
 G   R   S   W   N   Y   G   Q   F   D   D   A   V   L   P   A   C   M   Y   L   M   E   N   A   R   L   R   P   E   E    270
agg gga gat gtt gtc aaa gtc agc agg gcc ata tca aag atg atg aac gtc aat gat gaa ggt ggt gtt gtt tgg ggc aga tgg gat ggc  900
 R   G   D   V   V   K   V   S   R   A   I   S   K   M   M   N   V   N   D   E   G   G   V   V   W   G   R   W   D   G    300
gaa tac cag gat ggc caa ggt cct agt tac tgg act ggg tct atc tcc atc tta gag cag tac atg tct aca aaa agg ggt gtc aag tat  990
 E   Y   Q   D   G   Q   G   P   S   Y   W   T   G   S   I   S   I   L   E   Q   Y   M   S   T   K   R   G   V   K   Y    330
gga cag tgc tgg gta ttt gca gga gtt gtt aac aca gtt tgt cgt gcc ctt ggc att cct tgt cgt cct gtt agc aat ttg aga tct gct 1080
 G   Q   C   W   V   F   A   G   V   V   N   T   V   C   R   A   L   G   I   P   C   R   P   V   S   N   L   R   S   A    360
cat gat aca aac cag tca ctc tcc att gac cag ttt ctc acc gag gat ggc act gat aga ctt agt gct aat gag gtg acc cgt aga gta 1170
 H   D   T   N   Q   S   L   S   I   D   Q   F   L   T   E   D   G   T   D   R   L   S   A   N   E   V   T   R   R   V    390
ttt aac tgg gga ttc tcg gat tcc atc tgg aat ttc cat gtc tgg aat gat gct tgg atg gcc cgg aaa gac ttg cct gat ggc tat gga 1260
 F   N   W   G   F   S   D   S   I   W   N   F   H   V   W   N   D   A   W   M   A   R   K   D   L   P   D   G   Y   G    420
ggt tgg cag gcc att gat tca acg cca cag gag cag agt ggt gga ctt ttc caa tgt gga cct gca tcc cat act gcc ata cta cta gga 1350
 G   W   Q   A   I   D   S   T   P   Q   E   Q   S   G   G   L   F   Q   C   G   P   A   S   H   T   A   I   L   L   G    450
aag act gaa cta aac tat gac atc aac ttc ctt gtt ggt gag gtc aat gct gac gtc atc aca tgg atc gtg gac cca aaa gca aaa ctg 1440
 K   T   E   L   N   Y   D   I   N   F   L   V   G   E   V   N   A   D   V   I   T   W   I   V   D   P   K   A   K   L    480
ggc ttt tct aaa gtc cgc gcc gac aaa ttc gat gtc gga cgt gaa ctt atc acc aaa gca cca gga tat aat gcc ttt ggc gac cga gac 1530
 G   F   S   K   V   R   A   D   K   F   D   V   G   R   E   L   I   T   K   A   P   G   Y   N   A   F   G   D   R   D    510
aag gta atc atc aat gat att tat aag tca cca gag gga tca gat gca aat agg ctc atg ctt aac tca gca gct agc agg tcc cgc act 1620
 K   V   I   I   N   D   I   Y   K   S   P   E   G   S   D   A   N   R   L   M   L   N   S   A   A   S   R   S   R   T    540
ggt cgg cta gct ttt gaa ttc tct gaa cct att gat gat gtg aaa ttc acc att gaa gat gtt gtc caa gtt cct atg ggt gat gat ttc 1710
 G   R   L   A   F   E   F   S   E   P   I   D   D   V   K   F   T   I   E   D   V   V   Q   V   P   M   G   D   D   F    570
tcc gtc aca gca aca gct aag aac gag agt gac tct act cgt aca gtt tgg atg aag atc tgt tgt gcc agt gag tac tac act ggt gtg 1800
 S   V   T   A   T   A   K   N   E   S   D   S   T   R   T   V   W   M   K   I   C   C   A   S   E   Y   Y   T   G   V    600
aga gca aac aga atc aaa tgg gta gac aca acc aag aat tct gaa tac tac gac aac ctg gtg gag tat gga atg atc aag ctt atg gct 1890
 R   A   N   R   I   K   W   V   D   T   T   K   N   S   E   Y   Y   D   N   L   V   E   Y   G   M   I   K   L   M   A    630
ctg tgt cat gtt gaa gag aca aca cag tca tgg att ggt gaa gat tct ttc cag gtt atc aag cct agg att aaa att gag cta cca gag 1980
 L   C   H   V   E   E   T   T   Q   S   W   I   G   E   D   S   F   Q   V   I   K   P   R   I   K   I   E   L   P   E    660
act gcc act gta gga aag gcc ata gta gtg aag ctg tct ttc aac aac ccc ctg gag act ata ttg aaa caa tgt tca ctg gtg gta gac 2070
 T   A   T   V   G   K   A   I   V   V   K   L   S   F   N   N   P   L   E   T   I   L   K   Q   C   S   L   V   V   D    690
gga cca ggc ctc ctc agg cca aag acc att cct atc agg gat gtg gaa gct aaa ggc gag atg agt tat gag tta aaa gta tac ccc aag 2160
 G   P   G   L   L   R   P   K   T   I   P   I   R   D   V   E   A   K   G   E   M   S   Y   E   L   K   V   Y   P   K    720
cgt ggc ggc agg aga act atc att gcc aca ttc aac tcc agg cag ttg gtt gac ctc act ggg tca aag aat att gat gtt gtt gag caa 2250
 R   G   G   R   R   T   I   I   A   T   F   N   S   R   Q   L   V   D   L   T   G   S   K   N   I   D   V   V   E   Q    750
gat gtt tga                                                                                                           2259
 D   V  stop                                                                                                          753
```

B

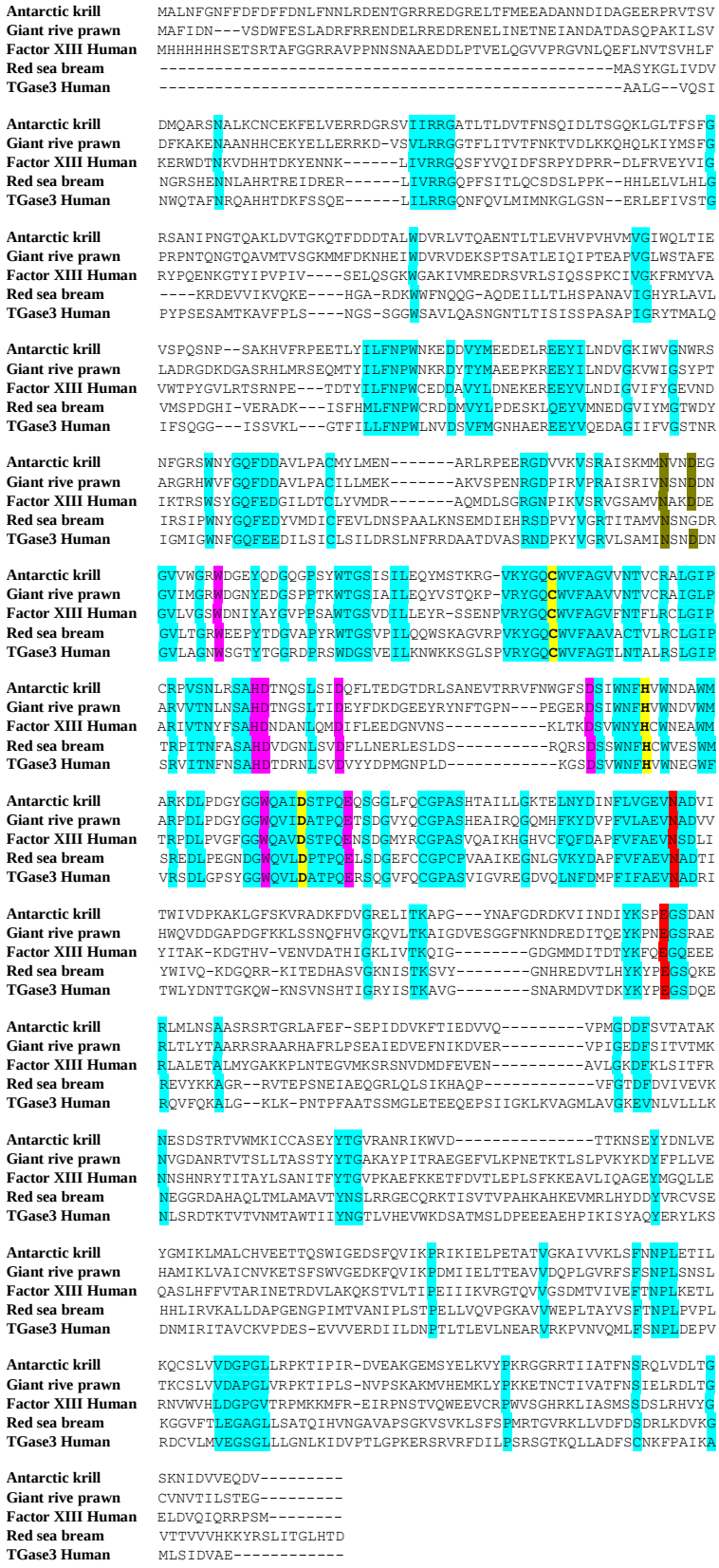
Antarctic krill
Giant rive prawn
Factor XIII Human
Red sea bream
TGase3 Human

C

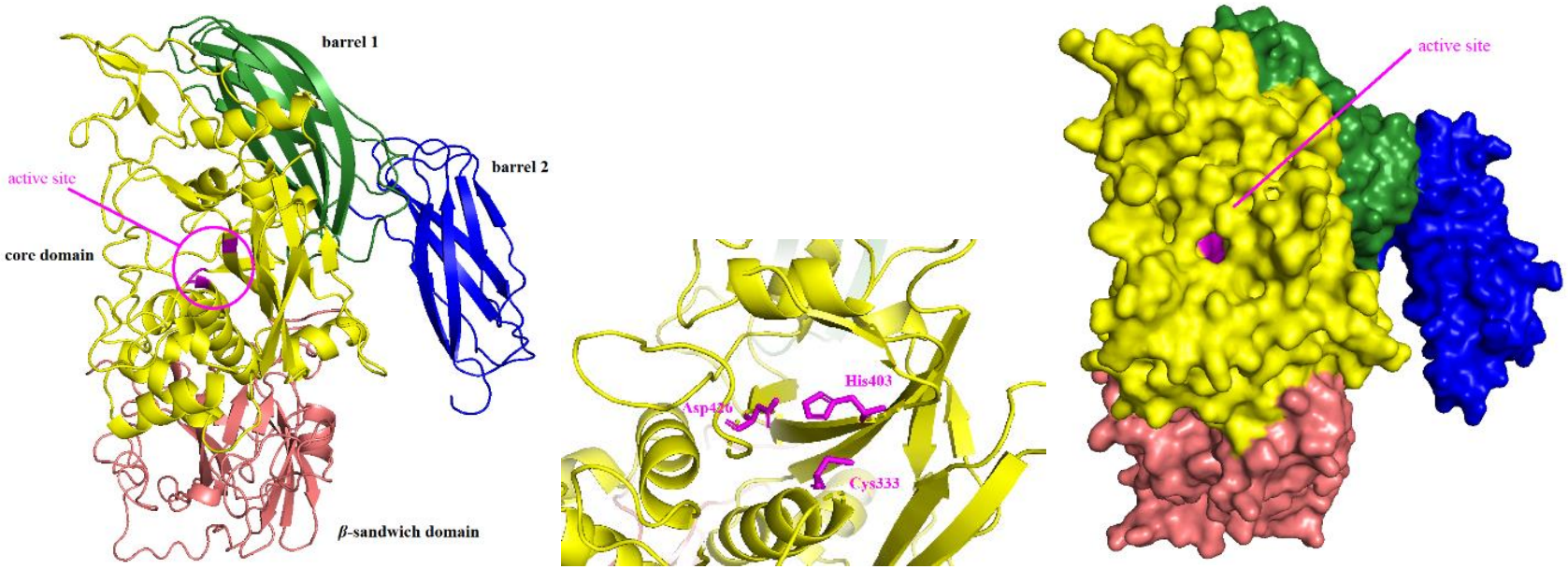

Figure 4.3. (A) Partial nucleotide and deduced amino acid sequences of Antarctic krill TGase, numbering on the right side. TGase core domain in green shade. Catalytic triad Cys333–His403–Asp426 in yellow shade. (B) Partial multiple sequence alignments. Conserved amino acids in blue shade. Catalytic triad in yellow shade. Ca^{2+} binding site 1 in red shade; Ca^{2+} binding site 2 in pink shade; Ca^{2+} binding site 3 in olive shade. (C) Predicted tertiary structure of Antarctic krill TGase. The four domains with secondary structures (left); active site (middle); surface of the overall structure (right).

A

81.52% of the residues have
averaged 3D-1D score >= 0.2

Pass

At least 80% of the amino acids have scored >= 0.2 in the 3D/1D profile.

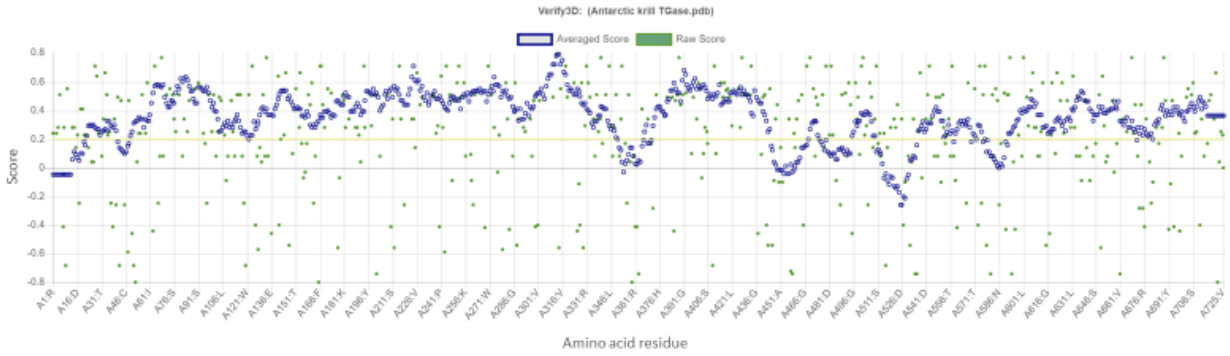

B

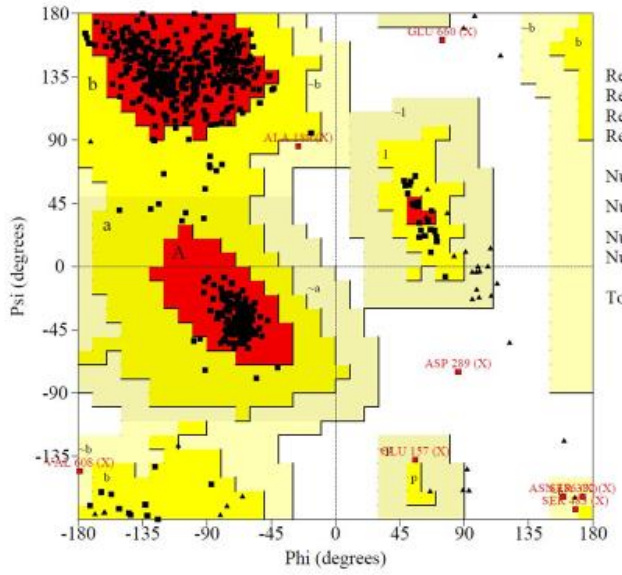

Plot statistics

Residues in most favoured regions [A,B,L]	579	90.0%
Residues in additional allowed regions [a,b,l,p]	56	8.7%
Residues in generously allowed regions [~a,~b,~l,~p]	6	0.9%
Residues in disallowed regions	2	0.3%
Number of non-glycine and non-proline residues	643	100.0%
Number of end-residues (excl. Gly and Pro)	2	
Number of glycine residues (shown as triangles)	53	
Number of proline residues	27	
Total number of residues	725	

Based on an analysis of 118 structures of resolution of at least 2.0 Angstroms and R-factor no greater than 20%, a good quality model would be expected to have over 90% in the most favoured regions.

C

Figure 4.4. (**A** & **B**) Validation of tertiary structure model of Antarctic krill TGase built upon human Factor XIII (4KTY): VERIFY 3D image & Ramachandran plot. (**C**) Predicted tertiary structure of inactive Antarctic krill TGase. The four domains with secondary structures (left); active site (middle); surface of the overall structure (right).

Table 4.1

Kinetic parameters of the cold-active TGase curved using first-order model.

T_m (°C)	k (h^{-1})	R^2	$t_{1/2}$ (h)	D value
0	0.0047 ± 0.0001^a	0.978	149.08 ± 2.27^a	495.24 ± 7.53^a
20	0.0149 ± 0.0011^a	0.964	46.80 ± 3.34^b	155.45 ± 11.10^b
40	0.0234 ± 0.0026^a	0.986	29.87 ± 3.35^c	99.23 ± 11.12^c
60	0.0448 ± 0.0003^a	0.982	15.47 ± 0.10^d	51.40 ± 0.32^d
80	0.7632 ± 0.0352^b	0.965	0.91 ± 0.04^e	3.02 ± 0.14^e

Table 4.2 Data from *de novo* assembly.

	Transcript	Unigene
Total No.	63,739	36,282
No. of length ≥500 bp	20,565	11,434
No. of length ≥1,000 bp	7,198	3,593
Total length	34,906,558	18,893,117
Average length	547.65	520.73
Maximum length	10,203	10,203
Minimum length	201	201
N50 length	674	624
N90 length	257	251

Table 4.3 Unigene annotation statistics.

Database	Number of unigenes annotated	Percentage (%)
NR	18,004	49.62
NI	3,936	10.85
KOG	11,275	31.08
Swiss-Prot	15,454	42.59
TrEMBL	18,763	51.71
PFAM	8,408	23.17
CDD	11,484	31.65
GO	17,594	48.49
KEGG	3,110	8.57
In at least one database above	19,939	54.96
In all database above	798	2.20

Table 4.4

The 5 unigenes related with TGase function.

# 1		
Unigene ID		TRINITY_DN4029_c0_g1
Sequence		ATTCTGAATACTACGACAACCTGGTGGAGTATGGAATGATCAAGCTTATGGCTCTGTGTCATGTTGAAGAGAC AACACAGTCATGGATTGGTGAAGATTCTTTCCAGGTTATCAAGCCTAGGATTAAAATTGAGCTACCAGAGACT GCCACTGTAGGAAAGGCCATAGTAGTGAAGCTGTCTTTCAACAACCCCCTGGAGACTATATTGAAACAATGTT CACTGGTGGTAGACGGACCAGGCCTCCTCAGGCCAAAGACCATTCCTATCAGGGATGTGGAAGCTAAAGGCG AGATGAGTTATGAGTTAAAAGTATACCCCAAGCGTGGCGGCAGGAGAACTATCATTGCCACATTCAACTCCAG GCAGTTGGTTGACCTCACTGGGTCAAAGAATATTGATGTTGTTGAGCAAGATGTTTGA
Length		422 bp
Annotation	NR	gi|270304351|gb|ACZ71260.1| hemocyte transglutaminase [*Fenneropenaeus indicus*] 2.09909e-42
	NT	-
	KOG	-
	Swiss-Prot	sp|Q05187|TGMH_TACTR Hemocyte protein-glutamine gamma-glutamyltransferase OS=*Tachypleus tridentatus* PE=1 SV=1 3.99462e-27
	TrEMBL	tr|D2K9J4|D2K9J4_FENIN Hemocyte transglutaminase (Fragment) OS=*Fenneropenaeus indicus* PE=2 SV=1 1.05077e-42
	PFAM	-
	CDD	-
	GO	GO:0003810, protein-glutamine gamma-glutamyltransferase activity; GO:0016020, membrane; GO:0018149, peptide cross-linking; GO:0046872, metal ion binding
	KEGG	-
# 2		
Unigene ID		TRINITY_DN15427_c0_g1
Sequence		GAAGAGTACATCCTCAATGACGTTGGGAAGATCTGGGTTGGCAATTGGCGTTCTAACTTTGGGAGGTCATGGA ACTATGGTCAGTTTGATGATGCTGTACTCCCTGCTTGTATGTATCTAATGGAGAATGCACGTCTCAGGCCAGAA GAAAGGGGAGATGTTGTCAAAGTCAGCAGGGCCATATCAAAGATGATGAACGTCAATGATGAAGGTGGTGTT GTTTGGGGCAGATGGGATGGCGAATACCAGGATGGCCAAGGTCCTAGTTACTGGACTGGGTCTATCTCCATCT TAGAGCAGTACATGTCTACAAAAAGGGGTGTCAAGTATGGACAGTGCTGGGTATTTGCAGGAGTTGTTAACAC AGTTTGTCGTGCCCTTGGCATTCCTTGTCGTCCTGTTAGCAATTTGAGATCTGCTCATGATACAAACCAGTCACT CTCCATTGACCAGTTTCTCACCGAGGATGGCACTGATAGACTTAGTGCTAATGAGGTGACCCGTAGAGTATTTA ACTGGGGATTCTCGGATTCCATCTGGAATTTCCATGTCTGGAATGATGCTTGGATGGCCCGGAAAGACTTGCCT GATGGCTATGGAGGTTGGCAGGCCATTGATTCAACGCCACAGGAGCAGAGTGGTGGACTTTTCCAATGTGGAC CTGCATCCCATACTGCCATACTACTAGGAAAGACTGAACTAAACTATGACATCAACTTCCTTGTTGGTGAGGTC

		AATGCTGACGTCATCACATGGATCGTGGACCCAAAAGCAAAACTGGGCTTTTCTAAAGTCCGCGCCGACAAAT TCGATGTCGGACGTGAACTTATCACCAAAGCACCAGGATATAATGCCTTTGGCGACCGAGACAAGGTAATCAT CAATGATATTTATAAGTCACCAGAGGGATCAGATGCAAATAGGCTCATGCTTAACTCAGCAGCTAGCAGGTCC CGCACTGGTCGGCTAGCTTTTGAATTCTCTGAACCTATTGATGATGTGAAATTCACCATTGAAGATGTTGTCCA AGTTCCTATGGGTGATGATTTCTCCGTCACAGCAACAGCTAAGAACGAGAGTGACTCTACTCGTACAGTTTGG ATGAAGATCTGTTGTGCCAGTGAGTACTACACTGGTGTGAGAGCAAACAGAATCAAATGGGTAGACACAACC AAGA
Length		1177 bp
Annotation	NR	gi|124518460|gb|ABN13875.1| hemocyte transglutaminase [*Litopenaeus vannamei*] 2.98174e-151
	NT	gi|684151940|gb|KM008611.1| *Macrobrachium rosenbergii* transglutaminase mRNA, complete cds 1.00031e-14
	KOG	-
	Swiss-Prot	sp|Q05187|TGMH_TACTR Hemocyte protein-glutamine gamma-glutamyltransferase OS=*Tachypleus tridentatus* PE=1 SV=1 6.37534e-113
	TrEMBL	tr|A8QL63|A8QL63_LITVA Hemocyte transglutaminase OS=*Litopenaeus vannamei* PE=2 SV=1 1.49261e-151
	PFAM	-
	CDD	-
	GO	GO:0003810, protein-glutamine gamma-glutamyltransferase activity; GO:0016020, membrane; GO:0018149, peptide cross-linking; GO:0046872, metal ion binding
	KEGG	-
# 3		
Unigene ID		TRINITY_DN2860_c0_g1
Sequence		ATGGCTCTAAACTTCGGAAACTTCTTTGACTTTGATTTTTTCGATAATCTGTTCAACAACCTGCGAGATGAAAA TACCGGGCGTCGTAGGGAGGATGGCAGGGAGCTTACATTTATGGAAGAAGCTGATGCAAACAATGACATAGA TGCAGGAGAGGAACGCCCGAGAGTGACATCTGTTGATATGCAGGCTCGATCCAATGCGCTTAAATGTAACTGT GAGAAATTTGAACTAGTAGAGAGGAGGGATGGACGTTCAGTTATTATTCGTCGTGGAGCGACCCTCACCCTGG ACGTCACATTCAACTCACAGATAGACCTCACGTCTGGACAGAAACTAGGACTTACATTTTCCTTTGGGCGATCA GCCAATATCCCCAATGGTACCCAAGCAAAGTTGGATGTCACAGGCAAGCAGACGTTTGATGATGATACCGCTC TATGGGATGTCCGGTTGGTTACTCAGGCTGAAAATACTTTAACCTTGGAGGTGCATGTCCCAGTACATGTGATG GTAGGCATCTGGCAGTTAACTATAGAGGTCTCCCCTCAAAGTAATCCTTCAGCTAAACATGTGTTCCGACCAG AAGAAACATTATACATACTCTTCAACCCATGGAACAAAGAGGATGATGTGTACATGGAGGAAGATGAGCTAC GG
Length		660 bp
Annotation	NR	gi|51338957|dbj|BAD36808.1| transglutaminase [*Marsupenaeus japonicus*] 2.17236e-42
	NT	-
	KOG	-

	Swiss-Prot	sp|Q05187|TGMH_TACTR Hemocyte protein-glutamine gamma-glutamyltransferase OS=*Tachypleus tridentatus* PE=1 SV=1 3.6547e-22
	TrEMBL	tr|Q68Y89|Q68Y89_PENJP Transglutaminase (Fragment) OS=*Penaeus japonicus* PE=2 SV=1 1.08745e-42
	PFAM	pfam00868, Transglut_N, Transglutaminase family. 8.7416e-10
	CDD	pfam00868, Transglut_N, Transglutaminase family. 3.65897e-09
	GO	GO:0003810, protein-glutamine gamma-glutamyltransferase activity; GO:0016020, membrane; GO:0018149, peptide cross-linking; GO:0046872, metal ion binding
	KEGG	-
# 4		
Unigene ID		>TRINITY_DN13007_c0_g1
Sequence		GATGTATTCGCCGTCTGTCATGTGACAGAGACCAGCTATAACTGGTATGATCAAGATAAGCTTCAAGTTCAGA AACCTATGATTGATGTTGATCTTCCATCAACTGCCACAGTGGGCCAGTCAATGTTAGTGACGTTGTCTTTCACC AATCCTCTTGACAGAGCCCTAACTCGCTGCTCAGTGGTTGTAGATGGACCTGGACTCACCAGACCCAAAACAG TTCAGCTCAGAGATGTAGCGGCCAAAGGTGAGATGCGGTATGAGTTGAAGGTGTTCCCAAAACGTGGAGGCA GAAGAACCATCATTGCTGCCTTCAACTCTAGAGAGCTGGTGGATCTCACTGGGTCTCAGAATGTGGATGTTATT GAGGCATAGAACAACTATTACTGCCTTCAACTCTAGAGAGCTGGTGGATCTCATTGGCTCTCAGAATGTGGAT GTTATTGA
Length		447 bp
Annotation	NR	gi|323695914|gb|ADX99580.1| transglutaminase [*Macrobrachium rosenbergii*] 1.80069e-31
	NT	-
	KOG	-
	Swiss-Prot	sp|Q05187|TGMH_TACTR Hemocyte protein-glutamine gamma-glutamyltransferase OS=*Tachypleus tridentatus* PE=1 SV=1 2.84753e-19
	TrEMBL	tr|F1JZV5|F1JZV5_MACRS Transglutaminase OS=*Macrobrachium rosenbergii* GN=TG PE=2 SV=1 9.01396e-32
	PFAM	-
	CDD	-
	GO	GO:0003810, protein-glutamine gamma-glutamyltransferase activity; GO:0016020, membrane; GO:0018149, peptide cross-linking; GO:0046872, metal ion binding
	KEGG	-
# 5		
Unigene ID		>TRINITY_DN17296_c0_g1
Sequence		GGAGAAACAGACGGAAAATCAAATGCATGACGAGCATTACGGTTTCTTCTAGCTGCTATATGGAGTGCTATTC TCGAGGCATCTGAGGTTTCTGCTGATTTGTATGAATCATTGACTATTTCCTTATCTCGTCCAAAGTAATCATCAT CCACTTCTCCAGGGCTTTTTGTGATGATCTGCTTTCCAACATGGTTTTTGTTGCTTCCAACTCTTTTAACTTTGTC ATCTTCCTTGTCATCTTTCTGCCAAGTGACAACATCAGCATTCACTTCAGCCAAGAGGAAATCCACATCATAGC

		CGAGGTCAGTCCGCCCAGTCTTAATAGCAACATGAGATGCAGGACCACATTGATAGATACCATTACTCTCCTC TTGAGGTGTGGCATCTATGGCCTGCCACCCACCATAGCCATCGGGAAGATCCCAACGAGCCATCCACACATCA TTCCACACATGGAAGTTCCAGATGCTATCGTGGAATCCACCTCCAATAGTATCAATCACATCATCCATGTCCTC ATACCCCAGTTCCTCTCCTTCTTCATCAACAAATTGATCAATTGTTAGGGACTTGTTGGTATCATGCGCAGAAT TAAGATTGGTGACAACACGTGAAGGGATCCCAAGGGCTCGACACACTGTGGTGACAAGGCAAGCAAAGACCC AGCATTGTCCGTATCGGACTGGTTTTCCAGAGGTGAGGTACTGCTCTAGAATTTTGATGGAGCCTGTCCAGTGG GTGGGTTTCTTCCCGTCATCATACTTTCCGTCCCATCGCCCAACAAGTACACCTGAATCGTCATTGCTATTTACC ATCTTTGAAATAGCCCTGCTGATCTTGACAGCATCCCCCTTCTCATCTGGCTTAAGGTTGGCCTTCTCTAGGAG ATAAACACAGGCAGGCAATACTGCATCATCAAATTGCCCAAACACCCACTGTCTGCCACGGGCAGTTGGGTAG CTCCCCACCCATACCTTTCCTATATCATTCAAAACATACTCATTCCGAAGCTCCTCCTCTTCTAGGTACACCTCA TCATCCTTACTCCAAGGGTTGAACAGTACATATATTTGGTCTGGGTGCCGGTACATATGTCTGGCTTTCTCATT GCTACGGGATGAAACCTCCACTGACAGCTTCCATACTCCGACTGGAGCATGGTGAGGGATCTGAACTTCAAGT GTAACGGTGTCAGCATCTTGAGTAGCAAATCTGACGTCCCACTCCTCCACGCTCTTGTCAAAGGTCTTCTTCCC TGTCACCAGCAGTCTAGCCTGAGTGCCTTTCACAACTGTAGGTCGAGCACCGAAAGAGAAGTAGAGCTGAACT TTGAGATTGTTTACACAGTCTGCTTCCTGGTTGAAGGTAATATTGAAGAACAAAGTACCTCCCCTCCTTAAAAC TAGTGTTGGCTTCTTCCTGTTGACGAGTTCAAACTTATCACAGTGACTGTTGAGGGCATTGGTCTTGGCCTGAA GATCTACTGACAATACCTTCGGCTTCACCTCCTCCACTTCATTCTCAGCCTCATCTGCATCTCTAATAACTTCTT CCTCATCCCGGTCCTCCTGGCGCCGGTCGTTGTTGTCGCGGCGTAACCCAGCAAACAGGTCTTCAAAGTAGTCA CCTACATCGGAGAAGAAGGCCATTCTGAATTGAGTGAGTGAGGGATCTTCACCCAGTGACCAC
Length		1689 bp
Annotation	NR	gi|633894294|emb|CCQ25772.1| transglutaminase [*Macrobrachium rosenbergii*] 0.0
	NT	gi|957850046|ref|XM_014820013.1| PREDICTED: *Priapulus caudatus* hemocyte protein-glutamine gamma-glutamyltransferase-like (LOC106815545), mRNA 1.84982e-13
	KOG	-
	Swiss-Prot	sp|Q05187|TGMH_TACTR Hemocyte protein-glutamine gamma-glutamyltransferase OS=*Tachypleus tridentatus* PE=1 SV=1 1.36618e-130
	TrEMBL	tr|A0A024GWU1|A0A024GWU1_MACRS Transglutaminase OS=*Macrobrachium rosenbergii* GN=tgm PE=2 SV=1 0.0
	PFAM	pfam00868, Transglut_N, Transglutaminase family. 2.88188e-12
	CDD	pfam00868, Transglut_N, Transglutaminase family. 1.20627e-11
	GO	GO:0003810, protein-glutamine gamma-glutamyltransferase activity; GO:0016020, membrane; GO:0018149, peptide cross-linking; GO:0046872, metal ion binding
	KEGG	-

CONNECTING STATEMENT 3

Chapter V is about the production of a TGase substrate, gelatin, from fish skin using the protease alcalase for subsequent application work in cold-set food hydrogel preparation and characterization. Protein gelation is useful in food processing because it can influence sensory and textural attributes of foods. Various factors including pH, temperature, minerals and ionic strength, and protein concentration, all influence the formation of protein hydrogels as well as their properties. The literature is replete with information on heat-induced gelation of proteins, while there is relative dearth of information about gelation of proteins at low temperatures (so-called cold-set gels). This part of the study was undertaken to investigate the capacity of cold-active TGase from Antarctic krill to enhance formation of cold-set hydrogels for potential food applications.

This chapter forms the text of a manuscript published as:

Y Zhang, P Dutilleul, V Orsat, B K Simpson. Alcalase assisted production of novel high alpha-chain gelatin and the functional stability of its hydrogel as influenced by thermal treatment. International Journal of Biological Macromolecules, 2018, 118: 2278-2286.

For this paper, PhD candidate Y Zhang designed and performed the experiments, analyzed the data, and drafted the manuscript. Professor P Dutilleul guided the statistics work and revised related manuscripts. Professors V Orsat provided some research facilities for the experiments. Professor B K Simpson supervised the research work, provided the research materials and facilities, guided the lab performance and data analysis, revised the manuscript.

CHAPTER V. ALCALASE ASSISTED PRODUCTION OF NOVEL HIGH ALPHA-CHAIN GELATIN AND THE FUNCTIONAL STABILITY OF ITS HYDROGEL AS INFLUENCED BY THERMAL TREATMENT

5.1. Abstract

High alpha-chain (α-chain) content is associated with superior quality gelatin. A production process involving mild alcalase treatment was optimized by RSM, and the α-chain was quantified based on SDS-PAGE. A novel fish skin gelatin high in α-chain (32% of total protein, 45 mg/g fish skin of yield) was produced at optimum conditions, i.e., 2.3 U/g alcalase addition to fish skin for 0.5 h at 25 ^{o}C, followed by water extraction at 67 ^{o}C for 7 h. The novel gelatin contained 34% glycine and 16% imino acids as determined by UPLC. FTIR analysis disclosed four characteristic infra-red amide absorption bands. DSC and TGA analysis revealed thermal decomposition at 215 ^{o}C. Novel gelatin hydrogel (1%, w/v) could withstand a wide range of temperatures, and exhibited high emulsifying activity and viscosity, as well as stable gel clarity from 35 ^{o}C to 80 ^{o}C. The high temperature treatment (95 ^{o}C) produced hydrogel with lower clarity and emulsifying activity but higher viscosity than at the other temperatures. All heat-treated gelatin hydrogels behaved as non-Newtonian fluids as per the Ostwald de Waele model. The novel high α-chain fish skin gelatin has potential broad application in food, pharmaceutical and biological industries.

5.2. Introduction

Previous research studies on fish skin gelatin mostly focused on the discovery of new sources to complement or replace mammalian gelatin for various religious, cultural and health reasons. However, the production design of high-quality gelatin has not been well studied. High quality attributes of commercial gelatin include properties such as gel strength, viscosity, setting rate, melting point and emulsification capacity (Karim and Bhat, 2009; Lassoued et al., 2014). These properties depend on both the amino acid composition and the polypeptide fraction distribution of the gelatin (i.e., α-chain, β-chain, γ-chain, and peptides) (Giménez et al., 2009a; Karim and Bhat, 2009). While different processes for gelatin production may not be expected to largely alter the amino acid composition, the processing conditions can nonetheless influence the size or the polypeptide fraction distribution of the gelatin, and thus influence the quality of the final product. Research has found that gelatins with high α-chain content exhibit superior gel strength and better physicochemical properties (Gómez-Guillén et al., 2002; Karim and Bhat, 2009). Each α-chain has a MW of about 80–125 kDa, and contains around 1,014 amino acids with repetitive Gly–Pro–X, or Gly–X–Hyp, where Gly is glycine, Pro is proline, Hyp is hydroxyproline, and X may be any other amino acid (Balti et al., 2011; Chen et al., 2015). A recent study reported the separation and characterization of α-chain subunits from tilapia fish skin gelatin, and proposed that α-chain

content is highly related with its functional properties (Chen et al., 2015). Nonetheless, α-chain degrades readily in aqueous solution; thus, it is crucial to rigorously control processing conditions to obtain highly intact α-chains to suit specific applications.

Hydrolysis of collagen based on chemical or enzyme treatments, as well as their combinations, have been used to produce gelatin. The most common proteases used thus far for producing gelatins include pepsin (Lassoued et al., 2014; Nalinanon et al., 2008), trypsin, bromelain, collagenase and neutrase (Alemán et al., 2011; Norziah et al., 2014). Alcalase has been used to produce hydrolysates or bioactive peptides from fish skin gelatin; however, the use of alcalase to directly produce fish skin gelatin is poorly researched. The advantages with alcalase versus other proteases include the facts that: alcalase is derived from *Bacillus licheniformis* and is commercially available and inexpensive; it is heat stable and effective for the hydrolysis of proteins at high temperatures; it is active, stable and functions well at alkaline pH, thus it can be used directly after alkaline pre-treatment for removal of non-collagen proteinaceous material without the need to adjust pH as is the case with pepsin. Alcalase can also act as an esterase, and can potentiate efficient stereoselective hydrolysis of amino esters, as well as transesterification and transpeptidation reactions (White and White, 1997). These multifunctional attributes of alcalase bode well for larger molecular size gelatin, and hence the textural properties of food products derived therefrom.

Gelatin is a thermo-reversible polymer that can cold-set as hydrogel with high water holding capacity, biodegradability and biocompatibility. Gelatin hydrogel is used in the food industry such as food ingredient (e.g., thickener, gelling agent), as well as in pharmaceutical and biomedical industries for applications such as drug delivery and artificial tissue (Dash et al., 2013; Koob and Hernandez, 2003). Hydrogels with low gelatin content are normally used for film / coating solutions by taking advantage of its functional and rheological properties (Hoque et al., 2010); while high gelatin containing hydrogels are used in tissue and material engineering as these latter ones need strong mechanical properties (Dash et al., 2013). Thermal treatment is common in industrial processing that involves the use of gelatin hydrogels. However, high temperatures above 35 ^{o}C break down the structural network of gelatin hydrogels leading to poor functionality which limits their potential applications (Dash et al., 2013). A few studies found that thermal treatment negatively influenced the stability of gelatin and gelatin hydrogels. For example, pre-heating at 75 ^{o}C led to interactions between the peptide chains of gelatin resulting in highly insoluble polymers (Rbii et al., 2011). Heat treatment of 3% fish gelatin solution negatively affected the properties of the

resulting gelatin films (Hoque et al., 2010). Chemical cross-linking of gelatin chains for preparing hydrogel has been well studied for the improvement of gel stability to resist to thermal degradation (Koob and Hernandez, 2003; Van Den Bulcke et al., 2000). However, hydrogels formed from gelatin high in α-chain favor the buildup of well-organized and firm gel network, and it is interesting to investigate the effect of varying thermal treatments on the integrity and functionality of the hydrogel prepared by gelatin high in α-chain.

5.3. Materials and methods

5.3.1. Fish skin preparation

Thorny skate fish (*Amblyraja radiata*) with an average length of 35 cm were purchased from a local fish market in Montreal, Canada. Thorny skate is an economically important cold-water fish widely found in the North Atlantic Ocean, and its skin is a good source material for producing gelatin due to its low fat and ash contents (Lee et al., 2011). Fish skins were manually separated from the muscle, cut into pieces (0.5 cm × 0.5 cm), frozen at −80 °C, and then freeze-dried and stored at −20 °C till needed.

5.3.2. Alcalase activity analysis

Alcalase (FoodPro alkaline protease, Danisco) activity was measured by the Folin-casein method (Xie et al., 2010). One unit of alcalase activity is defined as the amount of the enzyme that can hydrolyze casein to produce color equivalent to 1 µmole of tyrosine per min at pH 9.5 at 25 °C. Alcalase was inactivated by heating at 100 °C for 30 sec.

5.3.3. Gelatin production

The common approaches for gelatin production include the successive steps of removal of non-collagenous protein material, pre-treatment/swelling in alkali, hot water extraction, and drying. In this study, dried fish skins were firstly soaked in 0.1 M NaOH solution (1 : 50, w/v) for 2 h at 4 °C with continuous stirring and changes of the NaOH solution every 30 min. The NaOH-treated skins were washed with distilled water until pH 9.5 was obtained. Alcalase at different levels (0.2, 2.5, 4.8 U/g alkali-treated skin) were used to swell the skin matrix at 25 °C for different times (0.5, 3.0, 5.5 h). After enzymatic treatment, the fish skins were washed with distilled water until neutral pH was obtained. The swollen fish skins were soaked in distilled water with a skin to water ratio of 1:2.5 (w/v). The mixture was first placed at 100 °C for 30 sec to inactivate alcalase, and then gently agitated in a water bath at a speed of 20 rpm at different temperatures (40, 60, 80 °C) for different times (2, 6, 10 h) to produce gelatin. Finally, the gelatin solutions were filtered with a Büchner

funnel using a Whatman No. 4 filter paper. The filtrates were collected, freeze dried, and stored at 4 ^{o}C for further analysis.

5.3.4. Analysis of α-chain content in gelatin

The polypeptide fraction distribution of gelatin was verified by SDS-PAGE using Mini-PROTEAN Tetra Electrophoresis System (Bio-Rad Laboratories Inc.). Polyacrylamide gels comprised of 5% stacking and 10% resolving gels. Gelatin samples were mixed with Laemmli sample buffer and the mixture was heated at 100 ^{o}C for 5 min. Twenty microliter (20 µL) aliquots of the samples (1.5 mg protein/mL) were loaded in each well. The standard protein markers were used (GE Healthcare, Mississauga, ON, Canada). Total protein band intensity and α-chain band intensity for each gelatin sample were quantified by using Quantity One software (Bio-Rad). Total soluble protein content of the gelatin solution was measured using the bicinchoninic acid (BCA) assay (Pierce, Rockford). The α-chain percentage and α-chain yield of each gelatin sample were calculated using Equations (1) and (2), respectively:

$$\text{α-chain percentage in gelatin (\%)} = 100 \times \frac{\text{α-chain band intensity}}{\text{total protein band intensity}} \quad (1)$$

$$\text{α-chain yield (mg /g skin)} = \frac{\text{α-chain percentage (\%)}/100 \times \text{protein content in dry gelatin (mg/g)} \times \text{weight of dry gelatin (g)}}{\text{weight of dry skate fish skin (g)}} \quad (2)$$

5.3.5. Response surface methodology and design

A four-factor Face-Centered Central Composite Design (FCCCD) was applied with alcalase amount (U/g), alcalase treatment time (h), water extraction temperature (^{o}C) and water extraction time (h) as independent variables, and α-chain percentage (%) and α-chain yield (mg/g skin) as responses. The three uncoded levels corresponding to the codes (-1, 0, +1) of the four independent variables were calculated after completion of preliminary testing aimed to ensure that the responses could be observed within the search domain to be used for optimization under a face-centered central composite design. Using the 30 experimental combinations of values (**Table 5.1**), with 6 replicates of the center point (0, 0, 0) in coded form, the following second-degree polynomial model was fitted in a multivariate approach:

$$Y = \beta_0 + \beta_1 A + \beta_2 B + \beta_3 C + \beta_4 D + \beta_{11} A^2 + \beta_{22} B^2 + \beta_{33} C^2 + \beta_{44} D^2 + \beta_{12} AB + \beta_{13} AC + \beta_{14} AD + \beta_{23} BC + \beta_{24} BD + \beta_{34} CD \quad (3)$$

where Y is the response; A, B, C, D are the four independent variables, i.e., alcalase amount, alcalase treatment time, water extraction temperature and water extraction time, respectively; β_0 is the intercept; β_1, β_2, β_3, β_4 are the linear coefficients; β_{11}, β_{22}, β_{33}, β_{44}, the quadratic coefficients; and β_{12}, β_{13}, β_{14}, β_{23}, β_{24}, β_{34}, the bilinear coefficients. Quadratic or bilinear effects are required to

optimize a response. While quadratic effects (A^2, B^2, C^2, D^2 in Equation 3) are the first nonlinear effects in the polynomial family, the bilinear effects (AB, AC, AD, BC, BD, CD) represent the interactions between the four independent variables taken two by two.

5.3.6. Determination of amino acid composition

To analyze amino acids in high sensitivity, ACQUITY ultra-performance liquid chromatography (UPLC) system (Waters, MA, USA) equipped with Pico-Tag system and ACQUITY BEH C18 column (2.1 mm × 10 cm, Waters, MA, USA) was used. Gelatin powder was subjected to vapor phase hydrolysis using 6 M HCl with 1% phenol at 110 °C for 24 h under N_2 atmosphere. The gelatin hydrolysates were washed, re-dried, and derivatized with phenylisothiocyanate (PITC, Waters, MA, USA). The formed phenylthiocarbamoyl (PTC)-amino acids were dissolved in phosphate buffer (pH 7.4) and monitored at 254 nm. Pierce amino acid standard H was used as calibration standard. The elution conditions were: column temperature 48 ^oC; eluent A contained 0.14 M sodium acetate (pH 6.0), 0.05% triethylamine, 6% acetonitrile (Waters, MA, USA); eluent B contained 60% acetonitrile in water (Waters, MA, USA). A gradient elution with eluent B increasing was employed. Data were collected and analyzed using Empower 2 software (Waters, MA, USA).

5.3.7. FTIR analysis

FTIR spectroscopy was used to characterize the functional groups of gelatin (García-Saldaña et al., 2016), and the FTIR spectra were recorded on a Thermo Scientific Nicolet iS5 FTIR spectrometer (Thermo, Madison, WI) using an attenuated total reflectance diamond crystal. The spectra in the range of 400–4000 cm^{-1} with automatic signal gain were collected in 32 scans at a resolution of 8 cm^{-1} and were ratioed against a background spectrum recorded from the empty cell at 25 ^oC.

5.3.8. Thermal analysis

The thermal properties and stabilities of novel gelatin were determined using differential scanning calorimetry (DSC, Q2000, TA Instruments, New Castle, DE) and thermal gravimetric analysis (TGA, Q50, TA Instrument, New Castle, DE) (Apostolov et al., 1999). For DSC analysis, dry gelatin of 2–5 mg was placed in a Tzero aluminum sample pans hermetically sealed with lids with an empty sealed pan as reference. N_2 at a flow rate of 50 mL/min was used as a carrier gas. The sealed pan with samples were cooled to –50 ^oC at 10 ^oC/min and scanned from –50 ^oC to 250 ^oC at a heating rate of 10 ^oC/min. For TGA, dry gelatin of 5 mg was heated from 20 ^oC to 600 ^oC

at a rate of 10 °C/min. Nitrogen was used as the purge gas at a flow rate of 60 mL/min.

5.3.9. Gelatin hydrogel preparation and thermal treatment

Gelatin hydrogels were prepared by dissolving in distilled H_2O to obtain a final concentration of 1% (w/v) (Van Vlierberghe et al., 2010). The gelatin hydrogels were set at 25 °C and then incubated in a shaking water bath at 35, 50, 65, 80 and 95 °C, respectively, for 30 min. The heat-treated gelatin hydrogels were left to cool to 25 °C for 2 h before analysis for their functional properties.

5.3.10. Determination of functional properties

Clarity. Transparency of gelatin hydrogel was determined spectrophotometrically (Beckman DU 800, Fullerton) in 1 cm cuvettes by measuring the transmittance at 600 nm (T600) against distilled H_2O as reference at 25 °C (Sai-Ut et al., 2012). Each transparency value was calculated using Equation (4), where x was the cuvettes thickness (mm). The higher transparency value represents lower clarity of gel.

$$\text{Transparency value} = -\log(T600) / x \quad (4)$$

Emulsifying activity and stability. Emulsifying activity measurement was performed as per the procedure by Giménez et al., (2009a). Gelatin hydrogel (1 mL) and soybean oil (1 mL) were mixed in a beaker and homogenized at a speed of 20,000 rpm for 1 min. Next, 100 μL emulsion was taken from the bottom of the beaker at times zero and 10 min after homogenization and diluted to 10 mL with 0.1% SDS solution. The absorbances measured at times zero (A_0) and 10 min (A_{10}) were used to calculate the emulsifying activity index (EAI) and the emulsion stability index (ESI) from Equations (5) and (6), respectively.

$$\text{EAI } (m^2/g) = \frac{2\times 2.303\times DF\times A}{c\times\theta\times\phi} \quad (5)$$

where DF is the dilution factor (100); A is the absorbance at 500 nm; c is the protein concentration (g/m^3); θ is the oil volume fraction (0.25); and ϕ is the optical path of cuvette (m).

$$\text{ESI (min)} = \frac{A_0\times\Delta t}{\Delta A} \quad (6)$$

where $\Delta A = A_0 - A_{10}$, and $\Delta t = 10$ min.

Rheology and viscosity. Rheological properties of the gelatin hydrogels were measured with rheometer (Advanced Rheometer AR2000, TA Instrument, New Castle) (Moraes et al., 2009). Samples were stabilized at 25 °C for 30 min before analysis. The flow curves were obtained by increasing shear rate from 0 to 70 s^{-1}, 25 °C. The Power Law model (or Ostwald de Waele model)

as expressed in Equation (7) was used to describe the experimental data.

$$\sigma = K\gamma n \quad (7)$$

where σ is shear stress (Pa), K is consistency index (Pa s^n), γ is shear rate (s^{-1}), and n is flow behavior index. If n < 1, fluid is shear-thinning or pseudoplastic; n = 1 corresponds to Newtonian fluid; while n > 1 denotes fluid is shear-thickening or dilatant. Viscosity of 1% gelatin hydrogel was recorded at shear rate of 70 s^{-1} at 25 ^oC, and expressed in mPa·S.

5.3.11. Statistical analysis

Design Expert version 7.0.0 (Stat-Ease Inc., Minneapolis, MN) was used to perform surface response analysis, including the ANOVA decomposition and significance tests for model coefficients, the optimization of the response as a function of the independent variables, and the plotting of the fitted surface (Mead, 1988). Five determinations were performed for the functional properties of novel gelatin hydrogel, and comparisons of means were based on the least significant difference (LSD) computed with SPSS software version 22.0 (IBM SPSS Inc., Chicago, IL, USA).

5.4. Results and discussion

5.4.1. Alpha-chain percentage of fish skin gelatin

The α-chain content in gelatin is of prime importance as index of high-quality gelatin. The protein distribution of each gelatin produced under various conditions designed by FCCCD (**Table 5.1**) are shown in the SDS-PAGE patterns (**Figure 5.1**). The different protein patterns indicate that enzyme treatment and water extraction processes influenced the α-chain percentage, and thereby alter the quality of the gelatin. Response surface analysis data for the α-chain percentages of fish skin gelatin (**Table 5.2**; Response 1 section), indicates a very significant model (*p* value < 0.0001, *F* value = 26.41). The *p* values ≤ 0.05 indicated that the linear effect B, interaction terms AB, AC, BC, BD, CD, and quadratic effects C^2, D^2 were significant for the fitted model, as seen in Equation (8). The lack of fit was not significant (*p* = 0.3067), which indicates that the model fitted the data well. The R^2, adjusted R^2, and predicted R^2 values were, respectively, 0.9610, 0.9246, 0.7899, which is very satisfactory as the absolute maximum is 1.0. The so-called adequate precision (17.66) was much greater than 4, which is desirable.

$$\alpha - \text{chain percentage } (\%) = -77.04 + 4.328A + 6.463B + 2.460C + 6.458D - 0.3284AB - 0.03786AC + 0.05113AD - 0.05714BC - 0.1957BD - 0.04059CD - 0.3393A^2 - 0.3713B^2 - 0.01582C^2 - 0.2826D^2 \quad (8)$$

The maximum or optimum predicted α-chain percentage of 32.6% were obtained under the

following conditions: 3.0 U/g alcalase treatment for 0.6 h followed by water extraction at 64.2 °C for 6.87 h. As shown in **Figure 5.2a**, alcalase treatment time and water extraction temperature interacted strongly (p = 0.0002) with respect to the α-chain percentage of gelatin. An increase in water extraction temperature from 40 to 65 °C caused an increase in α-chain percentage. However, longer enzymatic treatment time combined with higher water extraction temperature negatively affected the α-chain percentage of gelatin. The reason for the decrease could be that longer enzymatic treatment caused more extensive hydrolysis of α-chain into peptides, while higher water temperatures for extraction produced more extensive denaturation and degradation of α-chain into low MW fractions (Sai-Ut et al., 2012). **Figure 5.2b** shows the effect of water extraction temperature and water extraction time on α-chain percentage of gelatin. These two variables also interacted significantly with each other (p < 0.0001). The highest α-chain percentage was observed at water extraction temperature of 60 °C for 6 h. Alcalase has broad specificity for protein substrates, leading to multiple cleavages in the amide bonds in collagen to form low MW peptides. Nonetheless, the capacity to act as an esterase could potentially cause the smaller molecules to reassemble to re-form larger molecules, as observed with the alpha chain gelatins. In this study, the amount of alcalase (0.2–4.8 U/g skin) used for producing α-chain is relatively small than other proteases with different substrate specificities such as trypsin, chymotrypsin, pepsin, aminopeptidases and carboxypeptidases. For instance, Chomarat et al. (1994) reported that pepsin addition of 10^5 U/g dry tissue produced a bovine skin gelatin with 34% α-subunit, and proctase with addition of 10^5 U/g dry tissue produced only 17% α-subunit.

5.4.2. Alpha-chain yield of fish skin gelatin

Alpha-chain yield is of high importance to the gelatin industry due to its effect on functional properties. As shown in **Table 5.2** (Response 2 section), the F value of 20.99 and the corresponding p < 0.0001 indicated that the response surface model fitted well the experimental data (Equation 9). The p values for linear effects A, B, C, D, interaction terms AB, AC (**Figure 5.2c**), BC (**Figure 5.2d**), BD, CD, as well as quadratic effects C^2, D^2, were significant (p < 0.05). The non-significant lack of fit (p = 0.3096) and the R^2 value of 0.9514 both confirmed an excellent fitting. The adjusted R^2 and predicted R^2 were 0.9061 and 0.7400, respectively, and the value of adequate precision was 13.834.

$$\alpha - \text{chain yield (mg/g skin)} = -108.0 + 4.723A + 8.676B + 3.034C + 11.46D - 0.4768AB - 0.05999AC + 0.08090AD - 0.08684BC - 0.2558BD - 0.04525CD - 0.3526A^2 - 0.3841B^2 -$$

$0.01823C^2 - 0.5768D^2$ (9)

For the maximum predicted α-chain yield of 45.65 mg/g skin, the optimal conditions were 1.1 U/g alcalase treatment for 0.5 h, followed by water extraction at 71.4 ^oC for 7.1 h. It is inferred from this observation that α-chain yield was significantly influenced by both alcalase treatment and water extraction. **Figure 5.2c** is a depiction of the data on α-chain yield as a function of alcalase amount and water extraction temperature, and it shows that water extraction temperature had a strong influence on α-chain yield. As water extraction temperature increased from 40–70 ^oC, α-chain yield also increased from 29.1 up to 43.6 mg/g skin when alcalase addition was 0.2 U/g, but higher extraction temperature > 70 ^oC decreased the α-chain yield. That may be due to a relatively lower breakdown of collagen molecules into water soluble peptides for gelatin extraction at the lower extraction temperatures (Sai-Ut et al., 2012). It is inferred from this observation that low amounts of alcalase added, especially 1.8 U/g, resulted in higher α-chain yields. **Figure 5.2d** is a summary of the interaction of alcalase treatment time and water extraction temperature and shows that longer enzyme treatment time reduced α-chain yield of gelatin, which may be due to loss of low MW peptides produced during the processing. This present study indicated that low alcalase amount plus short alcalase treatment time produced fish gelatins with higher α-chain yield.

5.4.3. Optimum conditions

The optimum conditions determined for the alcalase assisted extraction of gelatin were: pre-treatment using 2.3 U/g alcalase to fish skin for 0.5 h, followed by water extraction at 67 ^oC for 7 h. The maximum predicted α-chain percentage and α-chain yield were 32.4% of 45.1 mg/g skin, respectively. To verify the model, the gelatin was produced using the above optimum conditions and its protein pattern is shown in **Figure 5.3a**. Thus, the experimental results (32.5% of α-chain with yield of 45 mg/g skin) showed no significant differences from the predicted values. The optimum conditions found in this study have advantages over other previous optimization studies in terms of shorter enzyme treatment time, lower levels of enzyme added, or lower extraction temperatures. Petersen and Yates (1977) found that alcalase addition of 1.5 U/g at conditioning temperature of 25 ^oC for 17 h, pH 9.0 was a good combination to generate gelatin from collagen material. Optimum conditions for gelatin derived from cattle bones with the largest apparent viscosity were predicted as neutrase addition of 7.86 ppm for 14.9 h at 50 ^oC, followed by water extraction at 77.5 ^oC for 3 h (Hosseini-Parvar et al., 2009). Furthermore, the high level of α-chain contained in the optimized gelatin produced would result in better properties such as gelling,

viscosity and film making, than previous gelatins. The novel gelatin produced with the optimum conditions was used to prepare hydrogels for the characterization and functional properties analysis as influenced by thermal treatments.

5.4.4. Interactive effects between independent variables

From **Table 5.2**, it appears that for both responses (α-chain percentage and α-chain yield), 5 of the 6 bilinear effects are statistically significant ($p < 0.01$ or $p < 0.05$). The only bilinear effect that is statistically non-significant ($p \geq 0.05$) is AD (alcalase amount combined with water extraction time). It would not be possible to correctly optimize response 1 or response 2 in a purely univariate approach, i.e., studying a response as a second-degree polynomial function of only one independent variable. The selected four variables were related with two important processes (A, B for enzyme treatment; B, C for water extraction) in gelatin production. The effects of the two variables within each process were significantly interactive ($p < 0.01$ or $p < 0.05$; **Table 5.2**), which showed that the presence of a bilinear effect AB (i.e., the combination of alcalase amount with alcalase time) matters for the optimization of a response such as α-chain percentage or α-chain yield, and these responses are also dependent on CD (water extraction temperature combined with water extraction time). It can be concluded that the factors in either enzyme treatment or water extraction need to be combined for optimizing α-chain in gelatin. Moreover, pairs of variables from different process such as AC, BC and BD also significantly interacted for α-chain percentage and α-chain yield in gelatin. These effects are shown in **Figure 5.2a**, **5.2c** and **5.2d**, which present response surface plots of the second-degree polynomial function with two variables kept constant and the other two varying within the determined experimental ranges. Overall, it is strongly suggested that the two important processes (enzyme treatment and water extraction) significantly interacted for producing high level of α-chain in gelatin.

5.4.5. Amino acid composition

The amino acid composition of the novel gelatin is shown in **Figure 5.3b**. The analyses were done in triplicate and the results presented are mean values with standard deviations lower than 2%. Glycine content was the highest (343/1000), followed by alanine (96/1000) and proline (86/1000). The imino acids (i.e., proline and hydroxyproline) content of the gelatin was ~16%, which was similar to that of Type I collagen (15.3%) from common skate (*Raja kenojei*) skin (Hwang et al., 2007), but lower than that of cuttlefish skin gelatin (18%) and clown feather-back skin gelatin (20.7%) (Balti et al., 2011; Kittiphattanabawon et al., 2016). The structural stability of gelatin gel is

closely related with the high content of glycine-proline-hydroxyproline which results in the tight space between individual α-chain, and hydrogen bonds formed in the triple helix, especially due to the –OH group in hydroxyproline (Shoulders and Raines, 2009). Besides, no cysteine and tryptophan residues were observed, and similar findings were reported for gelatins isolated in other fish species (Shyni et al., 2014).

5.4.6. FTIR analysis

The FTIR spectrum of the novel gelatin is depicted in **Figure 5.3c**, and shows absorption regions of amide A, amide I, II and III bonds. The amide A band (3400–3440 cm^{-1}) relates to N–H stretching vibration, while a shift of this band to low frequency of 3303.7 cm^{-1} indicates the hydrogen bond formed from N–H group in gelatin (Doyle et al., 1975). Amide I band was found at 1643.7 cm^{-1} which is associated with C=O stretching vibration, which probably originated from the α-helix (Doyle et al., 1975) in gelatin. The amide II band observed at 1537.7 cm^{-1} denotes the N–H bending and C–N stretching vibrations; while the amide III band observed at 1235.5 cm^{-1} represents the C–N and N–H vibrations as well as wagging vibrations of CH_2 groups from Gly backbone and Pro side chain (Jackson et al., 1995). The fingerprint region observed at 1000–500 cm^{-1}, reflects the C–O skeletal stretching (Sow and Yang, 2015).

5.4.7. Thermal analysis

Figure 5.3d shows the TGA trace of the novel gelatin and indicates that the onset thermal decomposition temperature of gelatin was 213.4 ^{o}C and the derivative thermogravimetric curve, i.e., the rate of change of mass over temperature, was highest at a temperature of 314.6 ^{o}C. The results were similar with the TGA data reported in previous studies for bovine skin gelatin (Zheng et al., 2002). The gradual decrease of gelatin mass in the 20–100 ^{o}C range could be explained by the non-crystallized water left from the gelatin sample (Apostolov et al., 1999). This result is consistent with the DSC data shown in **Figure 5.3e**, which shows the degradation of the gelatin around 215 ^{o}C. Previous research showed the moisture content in gelatin largely influenced the DSC traces of gelatin (Sobral and Habitante, 2001). The melting temperature of the produced gelatin was 104.7 ^{o}C, which is similar to that of bovine gelatin (a_w = 0.336) with a melting temperature of 102 ^{o}C (Rahman et al., 2010).

5.4.8. Functional properties of novel gelatin hydrogel after thermal treatment

Hydrogels prepared using the high α-chain fish gelatin were investigated for the influence of thermal treatment on their clarity, emulsifying activity index (EAI), emulsifying stability index

(ESI), viscosity and rheology. These data obtained from these studies are presented in **Figure 5.4**, and discussed below:

Clarity. All the gelatin hydrogels after thermal treatments showed good clarity (transparency values < 0.01), suggesting the novel gelatin material produced in this study was clear. As shown in **Figure 5.4a**, the clarity of gelatin hydrogels treated at 35, 50, 65 and 80 ^{o}C were significantly higher compared with gelatin gels heated at 95 ^{o}C ($p < 0.05$). It is suggested that thermal processing at higher temperatures such as 95 ^{o}C may result in degradation of the α-chain, and subsequent cooling at 25 ^{o}C may result in aggregation of the gelatin molecules and the formation of gelatin-gelatin coacervates with larger size (Lau et al., 2000), to reduce the clarity of gelatin hydrogel.

Emulsifying activity and stability. Research has shown that emulsions stabilized with high MW gelatins contain less populations of large droplets compared with gelatin with low MW (Surh et al., 2006). In the present study (**Figure 5.4b** and **5.4c**), the emulsifying properties of the fish gelatin hydrogels were generally stable as a function of thermal treatment, suggesting that high α-chain fish skin gelatin produced in this study can be an effective emulsifier.

As shown in **Figure 5.4b**, the EAI of novel gelatin hydrogel increased from 35–50 ^{o}C and was the highest (10.75 ± 0.11 m^2/g protein) at 50 ^{o}C ($p < 0.05$), and then decreased after 50 ^{o}C. There were no significant differences in EAI values between gelatin gels treated at 35 ^{o}C and 80 ^{o}C ($p > 0.05$). Thermal treatment at 95 ^{o}C significantly ($p < 0.05$) decreased the EAI to 4.69 ± 0.31 m^2/g protein. This result suggests that thermal treatment at extremely high temperatures, above 95 ^{o}C for instance, may cause aggregation of the polypeptide molecules in gelatin gel, thereby destroying its emulsification capacity. Moreover, preparation of gelatin hydrogels at moderate temperatures, especially 50 ^{o}C, could generate flexible structures that would enable gelatin to form a viscoelastic membrane around the oil droplet and to easily stretch at the oil and water interface during emulsification process (Damodaran, 2005). Thus, the gelatin hydrogels displayed relatively high EAI after thermal treatment in the range of 35–80 ^{o}C.

All gelatin hydrogels treated at various temperatures showed good ESI values (**Figure 5.4c**). In this regard, gelatin gels heated at 50 ^{o}C exhibited the highest ESI value of 31.9 ± 4.99 min ($p < 0.05$). Other temperatures resulted in ESI values of 10–20 min without significant differences ($p > 0.05$). It is possible that thermal treatment at 50 ^{o}C for 30 min with the fish gelatin hydrogels resulted in more stable emulsions by generating repulsive interactions such as electrostatic and steric repulsion between oil droplets (McClements, 2004). It is worth noting that processing at 50

°C is favorable for both emulsifying activity and stability, which may be due to the conformational changes produced in the gelatin molecules at 50 °C.

Viscosity. Gelatin hydrogels with low viscosity exhibit brittleness, compared with gelatin hydrogels with high viscosity. As presented in **Figure 5.4d**, the viscosity of the high α-chain gelatin hydrogels was comparable for thermal treatments ranging from 35–80 °C, which suggests that the optimization produced gelatin with stable viscosity in texture. The highest viscosity value of 1.644 ± 0.020 mPa·S was found for gelatin hydrogels after being heated at 95 °C ($p < 0.05$). A previous study by Gudmundsson reported that viscosity measurements at 60 °C for cod gelatin gel showed protein degradation and a decrease in viscosity compared with 40 °C (Gudmundsson, 2002). For this study, it could be inferred that an increased aggregation of α-chain in gelatin produced at 95 °C may exist during cooling stage to result in an increased HMW fractions, and hence, an increase in the viscosity. Although processing at lower temperatures (35–80 °C) also increased denaturation and aggregation of gelatin, its conformational changes may have been reversed and restored during cooling period to 25 °C.

Rheology. The flow curves of the hydrogels prepared using optimized gelatin after thermal treatments are presented in **Figure 5.4e**. The rheological behavior suggests Non-Newtonian, dilatant behavior, with all flow behavior index (n) values greater than 1 in the application of the Power Law model. Dilatant fluids show increased viscosity with increasing shear rate, which have been observed in food polymers such as water-soluble pectin (Mierczyńska et al., 2015), whey protein (Foegeding and Mleko, 2002), and gelatin-riboflavin solutions (Demirbay et al., 2017). Food materials rich in starch exhibit dilatancy in the early stage of gelatinization, which may be a transition process for the transformation of the rheological behavior from dilatant to pseudoplastic (Rao, 2007). The high α-chain gelatin hydrogels treated at 95 °C showed the lowest 'n' value of 1.0875. All 'n' values gradually increased with decrease of heating temperatures, indicating that the novel gelatin hydrogels treated at 35 °C ('n' value of 1.1416) produced more non-Newtonian dilatancy property. The different rheological properties of high α-chain gelatin hydrogels may be explained by the size change and interactions of the α-chain in gelatin molecules caused by different heating temperatures.

5.5. Conclusions

This study successfully produced gelatin high in α-chain content with the aid of alcalase enzyme under mild reaction conditions. The amino acid composition, functional groups and thermal

properties of the gelatin were characterized, from which it is inferred that this high α-chain fish gelatin will favor stable network formation in hydrogels. The functional properties data also suggest that the hydrogels made from the gelatin could withstand thermal treatments over a wide temperature range from 35–80 ^{o}C, thus can suit various applications that require thermal treatments.

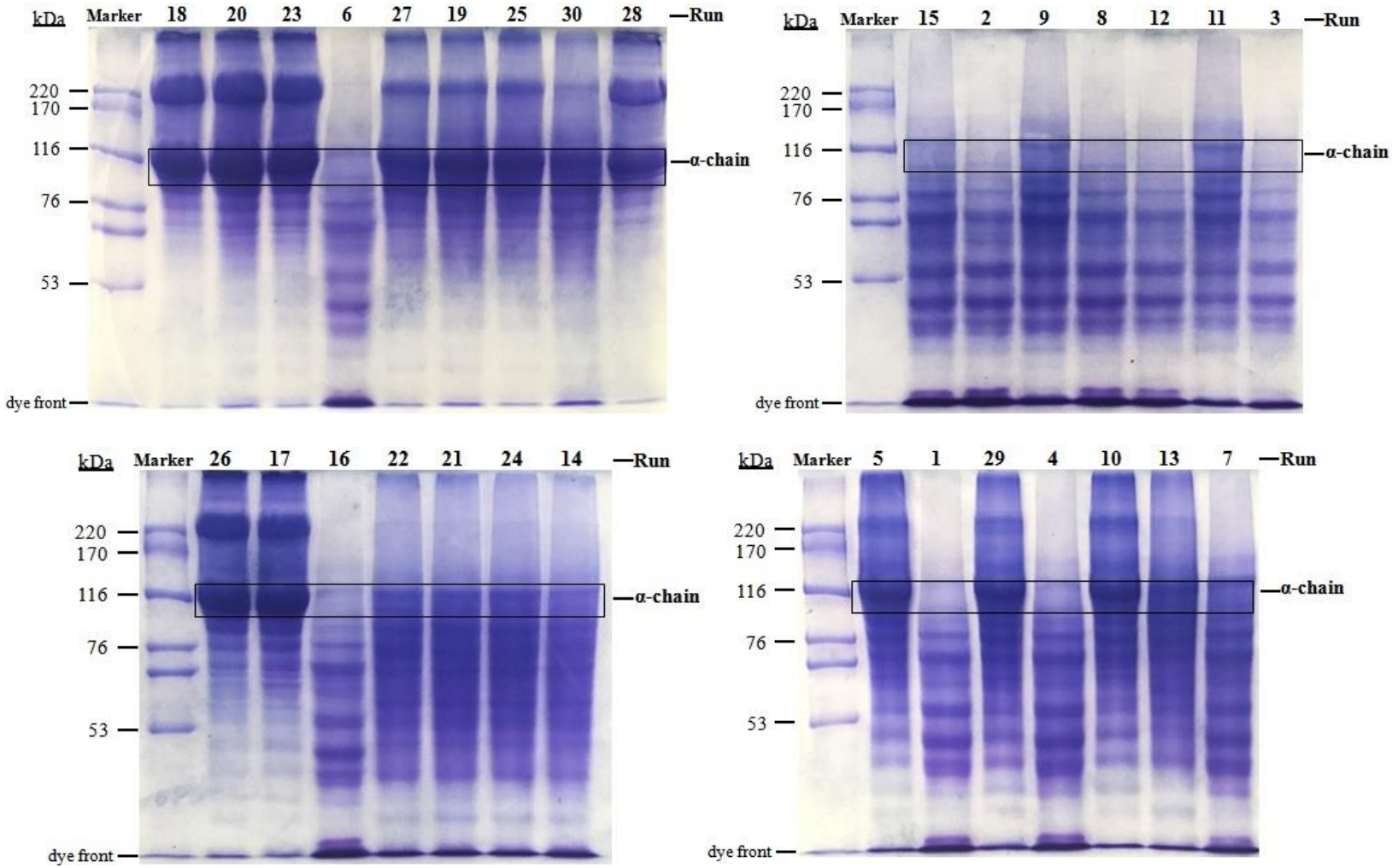

Figure 5.1. SDS-PAGE patterns of fish skin gelatin by alcalase-assisted production using face-centered central composite design.

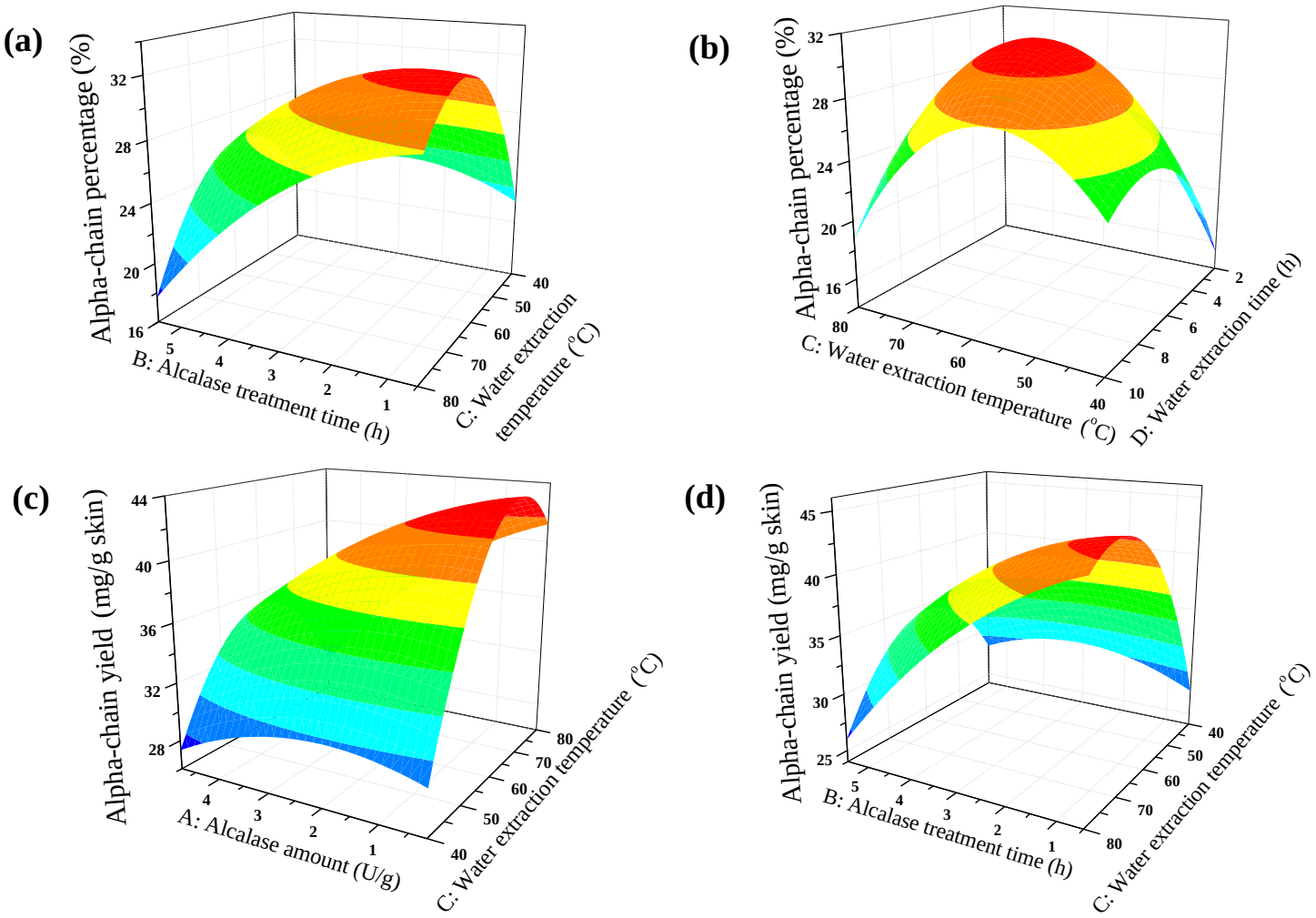

Figure 5.2. Three-dimensional (3D) response surface plots. (a) Alpha-chain percentage (%) as a function of alcalase treatment time (h) × water extraction temperature (°C); (b) Alpha-chain percentage (%) as a function of water extraction temperature (°C) × water extraction time (h); (c) Alpha-chain yield (mg/g skin) as a function of alcalase amount (U/g) × water extraction temperature (°C); (d) Alpha-chain yield (mg/g skin) as a function of alcalase treatment time (h) × water extraction temperature (°C).

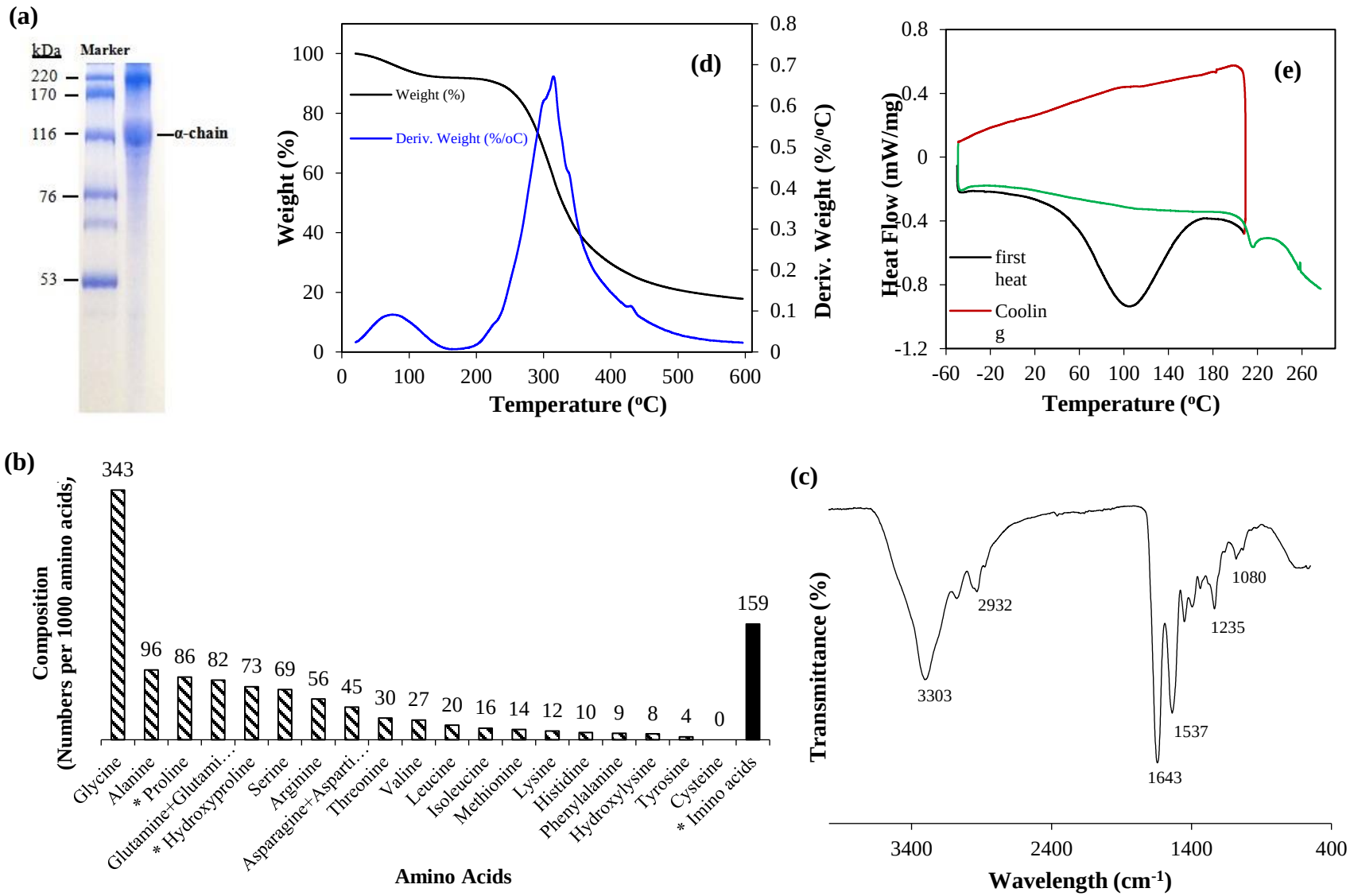

Figure 5.3. Characterization of the novel high α-chain fish skin gelatin produced at optimum conditions. (a) SDS-PAGE pattern; (b) amino acid composition; (c) FTIR spectrum; (d) TGA trace; and (e) DSC trace.

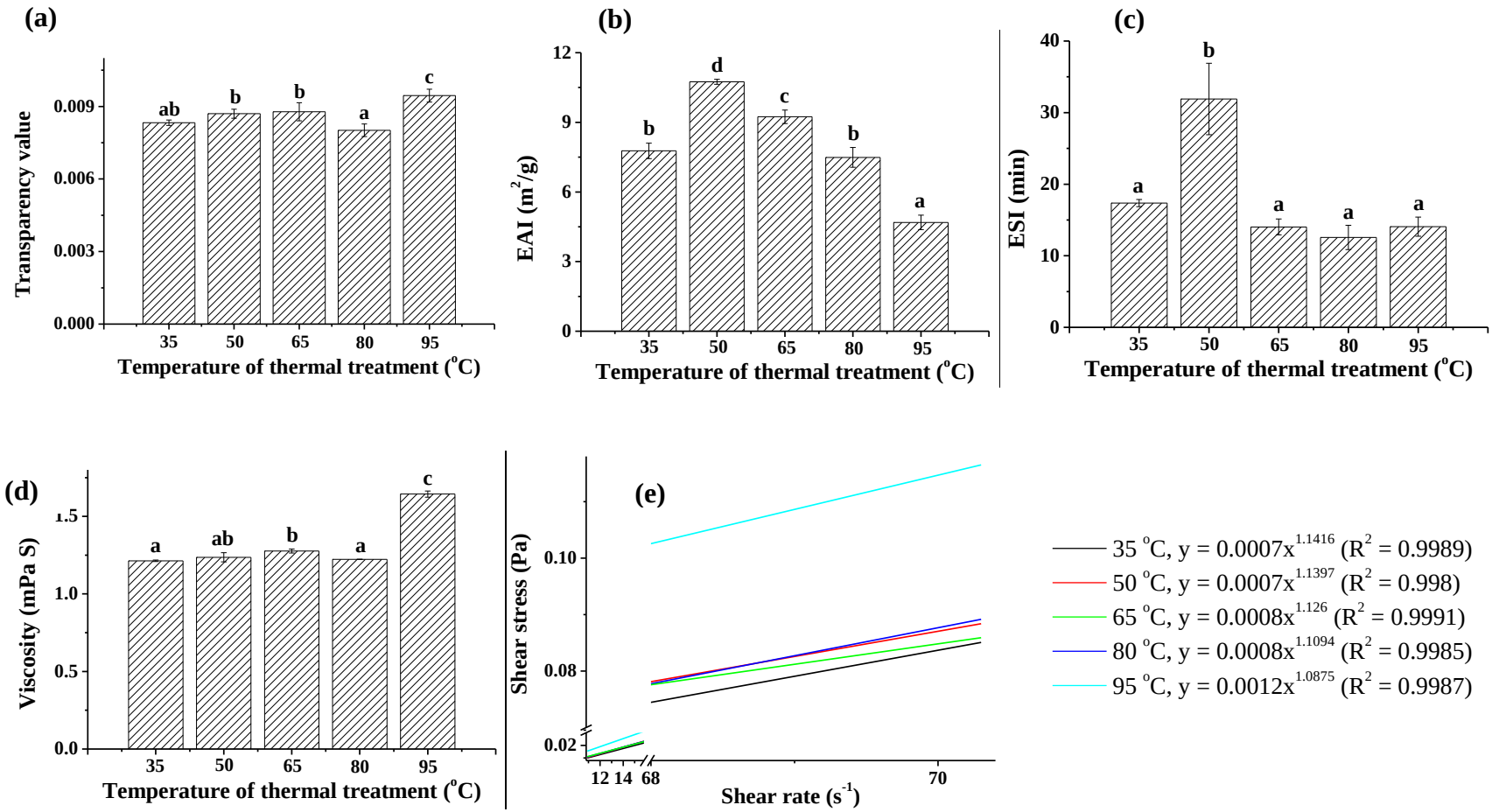

Figure 5.4. Functional properties: (a) Clarity; (b) EAI; (c) ESI; (d) Viscosity; (e) Rheology behavior of the novel gelatin hydrogel after thermal treatments at different temperatures. Different letters in the same panel indicate significant difference ($p < 0.05$).

Table 5.1

The experiment data for the α-chain percentage and α-chain yield of fish skin gelatin by alcalase-assisted production using face-centered central composite design.

Run	Independent variables				Responses	
	A: Alcalase amount, U/g	B: Alcalase treatment time, h	C: Water extraction temperature, °C	D: Water extraction time, h	Response 1: α-chain percentage, %	Response 2: α-chain yield, mg/g skin
1	0.2	0.5	40	2	8.0483	7.2488
2	4.8	0.5	40	2	10.0755	5.4109
3	0.2	5.5	40	2	13.4077	10.4713
4	4.8	5.5	40	2	12.6002	6.3293
5	0.2	0.5	80	2	26.5185	32.1773
6	4.8	0.5	80	2	20.8511	19.2087
7	0.2	5.5	80	2	18.4318	26.7431
8	4.8	5.5	80	2	12.4619	7.5514
9	0.2	0.5	40	10	16.7770	23.5350
10	4.8	0.5	40	10	26.7640	29.2795
11	0.2	5.5	40	10	19.0972	29.9323
12	4.8	5.5	40	10	15.1678	20.0590
13	0.2	0.5	80	10	21.5983	38.6365
14	4.8	0.5	80	10	23.7050	37.4468
15	0.2	5.5	80	10	12.8671	22.9670
16	4.8	5.5	80	10	1.8113	2.0542
17	0.2	3	60	6	28.3958	38.7584
18	4.8	3	60	6	28.5132	37.5338
19	2.5	0.5	60	6	30.4098	39.4372
20	2.5	5.5	60	6	25.4476	35.7835
21	2.5	3	40	6	22.7105	30.4940
22	2.5	3	80	6	25.1346	34.9432
23	2.5	3	60	2	27.2343	30.0218
24	2.5	3	60	10	24.2198	31.5424
25	2.5	3	60	6	31.7780	43.4814
26	2.5	3	60	6	32.5314	42.8451
27	2.5	3	60	6	31.2996	37.7618
28	2.5	3	60	6	35.3165	45.8222
29	2.5	3	60	6	29.4054	37.6018
30	2.5	3	60	6	31.5807	40.2038

Table 5.2

Statistical summary of the surface response analysis.

Source	Response 1			Response 2		
	Mean Square	*F* Value	*p* Value	Mean Square	*F* Value	*p* Value
Model	140.62	26.41	< 0.0001	326.46	20.99	< 0.0001
A	9.67	1.82	0.1978	239.05	15.37	0.0014
B	158.75	29.81	< 0.0001	276.04	17.75	0.0008
C	19.49	3.66	0.0750	193.18	12.42	0.0031
D	8.51	1.6	0.2254	452.90	29.12	< 0.0001
AB	57.06	10.72	0.0051	120.28	7.73	0.0140
AC	48.52	9.11	0.0086	121.85	7.83	0.0135
AD	3.54	0.66	0.4276	8.86	0.57	0.4620
BC	130.58	24.52	0.0002	301.64	19.40	0.0005
BD	61.27	11.51	0.0040	104.73	6.73	0.0203
CD	168.71	31.69	< 0.0001	209.68	13.48	0.0023
A^2	8.35	1.57	0.2297	9.01	0.58	0.4583
B^2	13.95	2.62	0.1263	14.93	0.96	0.3427
C^2	103.71	19.48	0.0005	137.79	8.86	0.0094
D^2	52.99	9.95	0.0005	220.68	14.19	0.0019
Residual	5.32			15.55		
Lack of fit	6.11	1.63	0.3067	17.83	1.62	0.3096
Pure error	3.75			11.00		

A is alcalase amount, B is alcalase treatment time, C is extraction temperature, and D is extraction time.

Response 1: R^2 = 0.9610, Adj R^2 = 0.9246, Pred R^2 = 0.7899, Adeq Precision = 17.66.

Response 2: R^2 = 0.9514, Adj R^2 = 0.9061, Pred R^2 = 0.7400, Adeq Precision = 13.83.

CONNECTING STATEMENT 4

The material presented in this part of the thesis is also on the use of the alcalase as processing aid to produce high molecular weight gelatin from fish skin; specifically, for the preparation of gelatin films with improved mechanical and barrier properties for food packaging and allied uses. In recent years, there has been growing interest in the development of biodegradable / compostable materials for use to curtail reliance on single use synthetic plastics produced from finite fossil fuels that pose severe hazards to environmental health. In this regard, natural biopolymers such as proteins, polysaccharides and fat, have been the preferred source materials for the manufacture of biodegradable/compostable films because of their biocompatibility and biodegradability. Nonetheless, these natural biopolymers tend to have poorer mechanical and barrier properties versus their non-biodegradable synthetic plastic counterparts; thus, the challenge is to develop innovative procedures to improve their mechanical and barrier properties. Hence, the rational for the studies entailed in this section was to investigate the efficacy of the high molecular weight gelatin to form improved mechanical and barrier properties of gelatin films.

This chapter constitutes the text of a manuscript published as:

Y Zhang, P Dutilleul, C Li, B K Simpson. Alcalase-assisted production of fish skin gelatin rich in high molecular weight (HMW) polypeptide chains and their characterization for film forming capacity. LWT - Food Science and Technology, 2019, 110: 117-125.

For this paper, PhD candidate Y Zhang designed and performed the experiments, analyzed the data, and drafted the manuscript. Professor P Dutilleul guided the statistics work and revised related manuscripts. Dr. C Li contributed academic discussion and some training. Professor B K Simpson supervised the research work, provided the research materials and facilities, guided the lab performance and data analysis, revised the manuscript.

CHAPTER VI. ALCALASE-ASSISTED PRODUCTION OF FISH SKIN GELATIN RICH IN HIGH MOLECULAR WEIGHT (HMW) POLYPEPTIDE CHAINS AND THEIR CHARACTERIZATION FOR FILM FORMING CAPACITY

6.1. Abstract

Gelatin rich in high molecular weight (HMW) polypeptide chains exhibit superior film forming capacity. Alcalase enzyme was used to produce gelatin rich in HMW polypeptide chains from shark (spiny dogfish) skin. The optimum conditions were established as 1.15 U/g alcalase pre-treatment for 2.1 h followed by water extraction at 50.4 ^{o}C for 4.6 h and produced gelatin with 33% HMW polypeptide chains of total protein. There was significant interaction ($p < 0.1$) between alcalase treatment and water extraction to control the HMW polypeptide chain content in gelatin. Optimized gelatin had 31.6% of glycine, 10% of proline and 7.9% of hydroxyproline. Gelatin rich in HMW polypeptide chains had strong capacity to form films from solutions with low gelatin concentrations (0.5 – 4%, w/v). Films formed by 3% gelatin solution (GF3) had low opacity and showed no difference with films formed by 4% gelatin solution (GF4), in terms of water solubility, water vapor permeability, as well as tensile strength and elongation at break ($p > 0.05$). FTIR spectrum of the GF3 film disclosed five characteristic amide bands, and the TGA trace showed GF3 film was stable up to 225 ^{o}C. Microstructure of GF3 using SEM displayed a smooth and compact film network.

6.2. Introduction

Gelatin consists of multiple polypeptide fractions, i.e., peptides, α-chain (~100 kDa), β-chain (~200 kDA, dimer of α-chain formed via covalent cross links) and γ-chain (~300 kDa, trimer of α-chain formed by covalent cross links) from acid, alkali, or enzymatic hydrolysis of collagen. The functions of gelatin are influenced by its polypeptide fraction distribution. Gelatin rich in low molecular weight (LMW) polypeptide fractions obtained by extensive hydrolysis exhibits diverse bioactive properties such as anti-oxidant, antihypertensive, and enzyme-inhibitory activities (Neves et al., 2017). Abundant high molecular weight (HMW) polypeptide chains, especially α-chain and β-chain, impart high gel strength, viscosity, melting point, and fast setting rate to gelatin (Boran and Regenstein, 2010; Elharfaoui et al., 2007; Eysturskarð et al., 2009), which are all important properties that underpin quality attributes and applications of gelatin. However, there has been little research investigating the efficient preparation of gelatin rich in HMW polypeptide chains.

Film forming capacity of gelatin is well acknowledged in preparing edible films or coatings for food preservation. This property is affected by the source material, polypeptide distribution of gelatin, film forming conditions, and the amount of plasticizer added (Benjakul et al., 2012). It has

been found that gelatin with HMW polypeptides, especially with predominance of β-chains, could strengthen the corresponding films (Gómez-Estaca et al., 2009; Jongjareonrak et al., 2006a). Normally, film forming solutions with 3 – 8% (w/v) gelatin are used. High gelatin concentrations tend to form solid film networks. Various cross-linkers such as transglutaminase, aldehydes and phenols may also be added to low gelatin concentration solutions to strengthen films. In this case, it is interesting to use different levels of gelatin that are rich in HMW polypeptide chains to form films.

Enzymatic hydrolysis is preferred to chemical hydrolysis for producing HMW components in gelatin. Collagen is composed of three α-chains coiled around a common axis to form a right handed triple helical rod that is stabilized by intra- and inter-chain cross-linkages formed via hydrogen bonds, and condensation reactions between NH_2- groups of lysine and aldehyde groups formed by enzymatic oxidation of lysine or hydroxy-lysine residues. Chemical hydrolysis usually involves harsh conditions in which not only the covalent cross-linkages but also the peptide bonds within the primary structure can be disrupted resulting in a high distribution of small subunits. Thus, production of HMW polypeptide chains needs milder reaction conditions. Enzymes are specific, effective in small amounts and under mild reaction conditions, and easy to inactivate. Various proteases such as pepsin, trypsin, bromelain, and collagenase have been used for producing gelatin. Alcalase is inexpensive and can act as an esterase to favor the formation of HMW polypeptide chains. Thus, it is useful to explore its usage to produce high-quality gelatin in addition to its current use to produce protein hydrolysates endowed with bioactivities.

The characterization of protein fractions in gelatin usually includes electrophoresis and gel filtration chromatography. In this study, the HMW polypeptide chains in gelatin were identified based on the molecular weights of standard proteins, and then quantified according to the band intensities. Some elasmobranchs such as dogfish shark (*Squalus acanthias*), bamboo shark (*Chiloscyllium punctatum*), the small-spotted catshark (*Scyliorhinus canicula*), and blue shark (*Prionace glauca*) are good source materials to produce gelatin rich in HMW polypeptide chains due to their high amounts of β and γ components (Blanco et al., 2017; Kittiphattanabawon et al., 2010). Other fish species such as giant catfish and skate fish are alternatives for producing HMW gelatin from skin (Jongjareonrak et al., 2010; Zhang et al., 2018c).

6.3. Materials and methods

6.3.1. Materials

Spiny dogfish fish (*Squalus acanthias*) were purchased from a local fish market in Montreal, Canada. Fish skins were frozen and stored at −80 ºC until needed. Alcalase (FoodPro alkaline protease) was obtained from Danisco, Co., Ltd (Copenhagen, Denmark). Bicinchoninic acid (BCA) assay kit was purchased from Pierce (Rockford, IL, USA). Pre-cast SDS-PAGE gels and Laemmli sample buffer were purchased from Bio-Rad Laboratories (Richmond, CA). High molecular weight calibration kits with standard protein markers (220 kDa, 170 kDa, 116 kDa, 76 kDa, and 53 kDa) were procured from GE Healthcare, Mississauga, ON, Canada. Coomassie brilliant blue, 2-mercaptoethanol, Folin's phenol reagent, casein, trichloroacetic acid, and phenylisothiocyanate were purchased from Sigma Chemical Co., Ltd (St Louis, MO, USA).

6.3.2. Alcalase activity analysis

Alcalase activity was measured by the Folin-casein method (Xie et al., 2010). Alcalase was inactivated by heating at 100 ºC for 30 sec. A standard curve was carried out using tyrosine solutions at concentrations of 0-80 µg/mL, and extinction coefficient of 100.1 was obtained to calculate alcalase activity. One unit of alcalase was defined as the amount that can hydrolyze casein to produce color equivalent to 1 µmole of tyrosine per min at pH 9.5 at 25 °C.

6.3.3. Gelatin production

The dogfish skins were separated manually and cut into pieces (0.5 cm × 0.5 cm). Production of gelatin was performed as per the method of Sae-leaw et al. (2016) with slight modification, by soaking in 0.1 M NaOH solution (1: 5, w/v) for 2 h at 4 ºC with continuous stirring and changes of the NaOH solution every 30 min. The NaOH-treated skins were washed with distilled water until pH 9.5. Alcalase at different levels (0.2, 1.4 and 2.6 U/g alkali-treated skin) in 0.05 M phosphate buffer (pH 9.5) was applied to swell the skins (1:1, v/v) for different times (0.5, 2.0 and 3.5 h) at 25 ºC. The alcalase-treated skins were washed with distilled water until pH 7.0, and then soaked in distilled water with a skin/water ratio of 1/2.5 (w/v). The mixture was first placed in 100 ºC boiling water for 30 sec, and then agitated in a water bath to produce gelatins at various temperatures (40, 55 and 70 ºC) for different times (1, 4.5 and 8 h). Finally, the gelatin solutions were filtered, and the filtrates were freeze dried.

6.3.4. Analysis of HMW polypeptide chains percentage

The protein chain distribution of gelatin was verified by SDS-PAGE using Mini-PROTEAN

Tetra Electrophoresis System (Bio-Rad Laboratories Inc.). Total soluble protein content of each gelatin sample (i.e., each run) was measured by the BCA assay, and gelatin samples at concentration of 1.5 mg protein/mL were loaded onto the gels. The same amount of HMW standard protein marker was electrophoresed against the gelatin samples on each gel, to increase accuracy and reliability for calculating the band intensities of each gelatin sample from the gels. The band intensities of the protein markers and HMW polypeptide chains (α- and β-chains) for each gelatin sample were quantified by using Quantity One software (Bio-Rad). Quantity One is commonly used for detecting protein band intensity with a sensitivity of 0.001. Before band detection and analysis, the gel background was subtracted to eliminate the different de-staining effects on gels. HMW polypeptide chains percentage was calculated using Equation (1):

$$\text{HMW polypeptide chains percentage in gelatin (\%)} = \frac{\text{HMW polypeptide chains intensities} \times 100}{\text{total protein intensities}} \quad (1)$$

6.3.5. Response surface methodology

Response surface methodology (RSM) is used to model and analyze the output / response that is influenced by various inputs / independent variables, and finally to optimize the levels of selected inputs / independent variables to obtain the maximum or minimum of output / response (Rai et al., 2016). Enzymatic treatment and water extraction were found to largely alter the protein fractions in gelatin production (Lassoued et al., 2014; Norziah et al., 2014), instead of NaOH treatment. Furthermore, four related variables were selected, i.e., alcalase amount (U/g), alcalase treatment time (h), water extraction temperature (^{o}C) and water extraction time (h) to study the effects on HMW polypeptide chains, and other parameters were fixed at their favorable and/or determined conditions such as alcalase treatment at 25 ^{o}C, pH 9.5, and skin/water ratio of 1/2.5 (w/v). Central composite design (CCD) is one of the most widely used designs that contains the high and low levels, axial points and center points of each input variable. Compared with other spherical CCD, face-centered central composite design (FCCCD) was considered as this design locates the axial points on the center of the faces of cube or hypercube, and requires only three levels for each factor as well as two or three centre points in practice (Montgomery, 2017). In this study, FCCCD was performed by examining four variables, and HMW polypeptide chains percentage (%) was the response, which allows examining the effect of individual and interactions of input variables on the output response. The three levels (-1, 0, +1) of four independent variables were chosen based on preliminary data (not shown). Based on the experimental results for the design which consisted of 30 experiments including 6 replicates of the center point (**Table 6.1**),

the following second-degree polynomial regression model was fitted to obtain the response surface (Equation 2):

$$Y = \beta_0 + \beta_1 A + \beta_2 B + \beta_3 C + \beta_4 D + \beta_{11} A^2 + \beta_{22} B^2 + \beta_{33} C^2 + \beta_{44} D^2 + \beta_{12} AB + \beta_{13} AC + \beta_{14} AD + \beta_{23} BC + \beta_{24} BD + \beta_{34} CD \quad (2)$$

where Y is the estimated response; A, B, C, D are four independent variables, i.e., alcalase amount, alcalase treatment time, water extraction temperature and time, respectively; β_0 is the intercept; β_1, β_2, β_3, β_4 are the 4 linear coefficients; β_{11}, β_{22}, β_{33}, β_{44} are the 4 quadratic coefficients; and β_{12}, β_{13}, β_{14}, β_{23}, β_{24}, β_{34} are the 6 bilinear interaction coefficients.

6.3.6. Determination of amino acid composition

Amino acid composition analysis was determined according to the method of Gallego et al. (2018) with slight modifications. Firstly, gelatin was hydrolyzed with 6 M HCl and 1% phenol at 110 °C for 24 h under nitrogen atmosphere. Excess HCl was removed by vacuum and the hydrolysates were derivatized with phenylisothiocyanate (PITC) solution at 25 °C for 30 min to form phenylthiocarbamoyl (PTC) derivatives, and then dried by vacuum. Derivatized amino acids were redissolved in 0.5 M sodium phosphate buffer (pH 7.4) with 5% acetonitrile and subjected to reverse phase HPLC separation with a C18 column (Waters, Milford, MA, USA). The PTC-amino acids eluted were monitored at 254 nm.

6.3.7. Gelatin film preparation

Gelatin produced at optimum conditions was used to prepare gelatin films. Film forming solutions with gelatin concentration of 0.5, 1, 2, 3 and 4% (w/v) were mixed with glycerol as plasticizer at a concentration of 20% (w/w) at 40 °C for 30 min. Then, 10 g of each solution were poured in leveled silicon resin plates (5 cm × 12 cm) and dried in an oven at 30 °C for 24 h. The corresponding formed films (GF0.5, GF1, GF2, GF3, and GF4) were conditioned at 25 °C, 50% relative humidity (HR) for 24 h (Sun et al., 2017a).

6.3.8. Determination of film properties

Thickness. The thickness of films was measured at eight random locations with a high precision digital micrometer (Shimana SHAYDC082, ON, Canada).

Color and opacity. Color of gelatin film was determined as *L** (lightness), *a** (red-green), *b** (yellow-blue) using a Minolta spectrophotometer CM-3500d colorimeter (Minolta Co., Ltd., Osaka, Japan) with Spectra Magic software. The instrument was calibrated using a standard black-and-white plate. Opacity of film was measured based on the method of Yu et al. (2017c), by

measuring absorbance at 600 nm (A_{600nm}) in a UV-Visible spectrophotometer (Beckman, USA) with an empty test cell as blank. The opacity values of films were calculated using Equation (3) where x is the film thickness (mm). Larger opacity value of films denotes lower film clarity.

$$Opacity\ value = \frac{A_{600nm}}{x} \quad (3)$$

Water solubility. Water solubility was determined following the method described by Antoniou et al. (2015) with slight modifications. Film pieces (2 cm × 2 cm) were dried in an oven at 105 °C for 24 h and weighed (W_0). Afterwards, films were immersed in 30 mL distilled water under constant agitation of 50 rpm at 25 °C for 24 h. The unsolubilized fractions were collected and dried at 105 °C for 24 h and weighed (W_1). Water solubility was calculated using Equation (4).

$$Water\ solubility\ (\%) = \frac{W_0 - W_1}{W_0} \times 100 \quad (4)$$

Water vapor permeability (WVP). WVP was determined gravimetrically according to the methods described by Sun et al. (2017a) with slight modifications. Films were mounted on test cups (diameter 2.5 cm and depth 4.0 cm) filled with 6 g anhydrous calcium chloride desiccant (0% RH) and placed in a desiccator containing distilled water (100% RH) at 25 °C. The weight gain of each text cup was measured every 4 h for a total of 24 h. WVP values were calculated using Equation (5).

$$WVP = wxt^{-1}A^{-1}\Delta P^{-1} \quad (5)$$

where w is the weight gain (g), x is the film thickness (mm), t is the time of gain (h), A is the area of the exposed film surface (cm^2) and ΔP is the difference of water vapor pressure between two sides of the film (3158 Pa at 25 °C).

Mechanical properties. Tensile strength (TS) and elongation at break (EB) of the films were measured using a Universal Testing Machine (Instron Model 4002, Canton, MA, USA) according to ASTM standard method D882 (2003). Film samples were cut in 1 cm × 4 cm rectangular shapes, and tested using a double clamp with 20 mm of initial grip separation and 30 mm/min of cross-head speed. The TS and EB values of the films were calculated using Equations (6) and (7), respectively.

$$TS = \frac{F}{W \times T} \quad (6)$$

where F is the maximum tensile force of film (N), W and T represent the film width (mm) and thickness (mm), respectively.

$$EB = \frac{L_1}{L_0} \times 100 \quad (7)$$

where L_1 is the increase of film length after stretching, L_0 is the original film length.

6.3.9. FTIR analysis

The FTIR spectrum of gelatin film was recorded on a Thermo Scientific Nicolet iS5 FTIR spectrometer (Thermo, Madison, WI) using an attenuated total reflectance diamond crystal. The spectra in the range of 400 – 4000 cm^{-1} with automatic signal gain were collected in 32 scans at a resolution of 8 cm^{-1} and were rationed against a background spectrum recorded from the empty cell at 25 ^oC.

6.3.10. Thermal gravimetric analysis (TGA)

The thermal property and stability of gelatin film were determined by using thermal gravimetric analysis (TGA, Q50, TA Instrument, New Castle, DE, USA). Gelatin film sample of 5 mg was heated from 20 ^oC to 600 ^oC at a rate of 10 ^oC/min. Nitrogen was used as the purge gas at a flow rate of 60 mL/min.

6.3.11. Microstructure observation

The surface and cross-section of gelatin film were determined by scanning electronic microscopy (SEM) using a TM 3000 Tabletop Microscope (Hitachi, Tokyo, Japan) with the TM 3000 program. Gelatin film was dehydrated in desiccator with silica gel, fractured, and then placed on double-sided carbon tape, which was then fixed to aluminium stub. The images were captured with voltage acceleration of 5 kV.

6.3.12. Statistical analysis

Design Expert version 7.0.0 (Stat-Ease Inc., Minneapolis, MN, USA) was used to perform surface response analysis, including the ANOVA decomposition and significance tests for model coefficients, the optimization of the response as a function of the independent variables and the plotting of the fitted surface (Mead, 1988). Studies for film properties were carried out in five measurements, and comparisons of means were based on the least significant difference (LSD) computed with SPSS software version 22.0 (IBM SPSS Inc., Chicago, IL, USA).

6.4. Results and discussion

6.4.1. HMW polypeptide chains percentage in gelatin

The SDS-PAGE pattern of each shark skin gelatin produced under various conditions designed by FCCCD are presented in **Figure 6.1**. The different protein patterns indicated that alcalase treatment and water extraction influenced the peptide chain distribution in the produced gelatins. The corresponding HMW polypeptide chains percentage, as shown in **Table 6.1**, were in a range

of 15% – 37%. **Table 6.2** showed that the model is significant ($p < 0.0001$, $F = 16.3$). It also can be seen that three (A, C and D) of the 4 linear effects are statistically significant (2: $p < 0.05$; 1: $p < 0.1$); four (AC, AD, BD and CD) of the 6 bilinear effects are statistically significant (3: $p < 0.05$; 1: $p < 0.1$), and the 4 quadratic effects (A^2, B^2, C^2 and D^2) are statistically significant (2: $p < 0.05$; 2: $p < 0.1$) for the fitted model, as seen in Equation (8). The lack of fit was not significant ($p = 0.6311$), which showed the model fitted the data well.

The interaction AC of the independent variables A and C (i.e., the combination of alcalase amount with water extraction temperature) significantly ($p = 0.0047$) matters for the optimization of HMW polypeptide chains, and this response is also dependent on the AD ($p = 0.0032$) and CD ($p = 0.0025$) interactions. **Figure 6.2** represents response surface plots of the second-degree polynomial function with two variables kept constant and the other two varying within the determined experimental ranges. As shown in **Figure 6.2a**, the response increased slightly with the increase of both A (alcalase amount) and C (water extraction temperature). Alcalase addition of 1.4 U/g and water extraction temperature of 55 ^{o}C gave the highest HMW polypeptide chains percentage. The independent variables A (alcalase amount) and D (water extraction time) also interacted significantly as shown in **Figure 6.2b**, when alcalase treatment time and water extraction temperature were fixed at 2 h and 55 ^{o}C; moreover, the alcalase amount had a larger influence on HMW polypeptide chains percentage than water extraction time (**Figure 6.2b**). This result indicated that factors in either enzyme treatment process or water extraction process need to be combined to optimize the HMW polypeptide chains in gelatin.

Furthermore, the linear effect of water extraction temperature (C) and time (D), as well as the quadratic effect of alcalase amount (A^2) and water extraction temperature (C^2) are more significant than other linear or quadratic factors, meaning that these three factors act as key points where little variation would alter the HMW chain percentage in gelatin. Addition of high level of alcalase can cause extensive hydrolysis of gelatin into low molecular weight peptides, resulting in less HMW polypeptide chains percentage. Hema et al. (2017) reported similar formation of LMW collagen peptides from fish skins by various proteases. Alcalase has broad specificity for protein hydrolysis and can cleave multiple sites on the peptide bonds in collagen, which justifies its common use to produce hydrolysates or peptides. Higher water temperatures and long water extraction can also result in denaturation and degradation of HMW polypeptides into LMW fractions.

$$\text{HMW polypeptide chains percentage } (\%) = 3.12254 - 0.69613A + 5.38739B +$$

$$0.98152C - 0.069176D - 0.24963AB + 0.093912AC + 0.42597AD + 0.00364727BC -$$

$$0.17093BD + 0.035241CD - 2.38216A^2 - 1.07414B^2 - 0.012503C^2 - 0.1995D^2 \quad (8)$$

6.4.2 Optimum conditions

The optimum conditions for producing gelatin rich in HMW polypeptide chains were pre-treatment using 1.15 U/g alcalase for 2.1 h, followed by water extraction at 50.4 ^{o}C for 4.6 h, with predicted 32.92% of HMW polypeptide chains. To verify the prediction, new gelatins were produced at the optimum conditions and contained 33.61±1.78% of HMW polypeptide chains, which was comparable with the optimum estimated response. However, the optimized conditions vary depending on the raw collagen materials and the enzyme used (Hema et al., 2017). The great importance of HMW polypeptide chains on the properties of gelatin films also is emphasized in the literature. Therefore, the new gelatin rich in HMW polypeptide chains was used for preparing the gelatin films by using different gelatin levels.

6.4.3 Amino acid composition of optimized gelatin

Table 6.3 shows the amino acid composition (%) of the new gelatin, expressed as 100 × (the number of an amino acid residue / number of total amino acid residues). The data presented in **Table 6.3** shows glycine as the predominant amino acid at 31.6%, followed by alanine (11.5%), proline (10%) and hydroxyproline (7.9%), in that order. The glycine content of about a third of all the amino acids present in the gelatin, suggesting that it originated from collagen. The combined content of the imino acids (i.e., proline and hydroxyproline) in the gelatin was 17.9% (**Table 6.3**) and represents the second most abundant after glycine. Hydroxyproline plays an important role in the stabilization of gelatin structure, via hydrogen bonds from their hydroxyl groups, to maintain the integrity of the triple helical structure (Haug and Draget, 2009). Thus, the gelatin reported here will be expected to be less stable than its mammalian counterparts that have about 22% imino acid content (Karim and Bhat, 2009); but was comparable to those reported for white-cheek shark skin gelatin (18.1%) and dog shark (*Scoliodon sorrakowah*) skin gelatin (19.75%). No cysteine and tryptophan were detected because these two amino acids were easily damaged by acid hydrolysis during determination, which is similar to findings made with fish gelatins from Amur sturgeon (Nikoo et al., 2013), and skipjack tuna, dog shark and rohu skins (Shyni et al., 2014).

6.4.4 Properties of gelatin films

The optimized shark skin gelatin rich in HMW polypeptide chains was used to prepare gelatin

films (GF0.5, GF1, GF2, GF3 and GF4) with corresponding gelatin concentrations of 0.5, 1, 2, 3 and 4% (w/v) in film forming solutions. Since the film sizes were the same, the weight/volume percent of gelatin contained in films increased from GF0.5 to GF4. Table 4 lists the film properties, from which it can be deduced that generally, the physical and mechanical properties steadily increased with increasing gelatin content. Previous studies reported high level of HMW polypeptides had strong film forming capacity (Gómez-Estaca et al., 2009; Jongjareonrak et al., 2006a). The results from **Table 6.4** further indicated that using relatively low content (such as 2 – 4%) of the optimized gelatin rich in HMW chains, was able to produce excellent films in terms of clarity, water solubility, and water vapor permeability, as discussed below.

Thickness. The thickness of gelatin films increased with the increase of gelatin content in films (**Table 6.4**) because more gelatin applied per unit volume led to thicker matrix. The thickness of GF0.5, GF1 and GF2 were comparable and not statistically different ($p > 0.05$), but there was significant increase when gelatin present was increased beyond 2%, i.e., in films GF3 (0.051 mm) and GF4 (0.063 mm) ($p < 0.05$). Film thickness is influenced by the concentration of the dry matter and total solids in the film forming solution and plays an important role in its mechanical and barrier properties (Benbettaïeb et al., 2014). As shown in Table 4, the thicker films formed with varying amounts of the same gelatin source material were stronger (higher TS) and more extensible (higher EB%) than the thinner films.

Color and opacity. The color and opacity of films are important considering the special interest for use as packaging material in the food industry. The addition of plasticizers, which are transparent compounds such as glycerol and sorbitol, could increase the clarity of gelatin films. Films of gelatin with HMW polypeptide chains may be superior in clarity compared with LMW gelatin films, because the greater number of free amino groups from extensive hydrolysis in LMW gelatin could undergo non-enzymatic browning reactions with other groups such as reducing sugars in the complex food matrix (Zhang et al., 2018a). Different gelatin films showed differences in color and opacity values (**Table 6.4**). The L^* and b^* values of gelatin films generally increased from GF0.5 to GF4, but a^* values were negative and decreased. The results suggested slight increase in lightness, greenness, and yellowness with the increase of the gelatin levels in films. There was no significant difference observed for GF1 and GF2 in terms of L^*, b^*, and a^* values ($p > 0.05$). GF3 had the highest value of L^* (lightness) ($p < 0.05$). Generally, all gelatin films were very transparent based on their opacity values, and GF3 and GF4 films exhibited significantly

lower opacity values than other studied films ($p < 0.05$). The better arrangement of HMW polypeptide molecules in the film matrix may contribute to its superior optical properties including clarity and lightness.

Water solubility. The preference of film solubility in water depends on the needs of use. Edible films with high water solubility favor ready decomposition in nature as well as digestion. On the other hand, edible films with low water solubility prevent foods from humidity and water loss (Arham et al., 2016). From GF0.5 to GF4, water solubility decreased from 41.22% to 29.08% (**Table 6.4**). GF3 (31.23%) and GF4 films had significant lower water solubility than others ($p < 0.05$). In general, films made by shark skin gelatin rich in HMW polypeptide chains had much lower water solubility compared with other fish gelatin films or fish gelatin-based composite films (Giménez et al., 2009b; Hosseini et al., 2013), and the studied films were comparable with bovine gelatin film (~30% of water solubility). The difference in amino acid composition, especially hydroxylysine could introduce new covalent cross-linking as well as electrostatic interactions, to impact the solubility of the films (Giménez et al., 2009b). Compared with films GF0.5 – GF2, films GF3 and GF4 had higher content of hydroxylysine residues, resulting in high degree of stable cross-linking and other interactions to make them less soluble in water (Giménez et al., 2009b).

Water vapor permeability (WVP). In food packaging, low WVP is preferred for edible films to minimize moisture transfer between food and its surrounding environment. It is well known that cold-water fish skin gelatin films have significantly lower WVP than warm-water fish gelatin films and mammalian gelatin films (Avena-Bustillos et al., 2006). Generally, low molecular weight peptide chains in gelatin could decrease the amount of intermolecular interactions in films to result in a loose film matrix and higher WVP (Nagarajan et al., 2012). Thus, gelatin rich in HMW polypeptide chains is preferred to form stronger and compact film network to reduce water vapor permeation into the food material. In this regard, various types of oils can be added to increase the hydrophobicity of films. From **Table 6.4**, WVP values of gelatin films gradually decreased with the increase of gelatin amounts contained in films. GF2, GF3 and GF4 had relatively low WVP values of 5.43, 5.35 and 5.90 $\times 10^{-8}$ g mm h^{-1} cm^{-2} Pa^{-1}, respectively. Similar WVP values were reported for cod skin gelatin films (4.87×10^{-8} g mm h^{-1} cm^{-2} Pa^{-1}) by Pérez-Mateos et al. (2009). GF3 had the lowest WVP value which could probably be due to the 3% of gelatin solution producing more compact structures to serve as barrier to water vapor.

Mechanical properties. Tensile strength (TS) and elongation at break (EB) of gelatin films

tended to increase with increasing gelatin concentration from 0.5 – 4% in the films (**Table 6.4**), and GF2, GF3, and GF4 showed significantly higher TS and EB values than GF0.5 and GF1 films ($p < 0.05$). As stated before, the LMW fragments in gelatin have negative effect in the formation of well-organized film network and thus lead to low TS and EB values. It is noticeable that GF3 and GF4 had similar TS values (30.19 and 30.30 MPa, respectively), as well as similar EB values (44.82 and 45.57%, respectively) ($p > 0.05$). The TS values of GF3 and GF4 were comparable with the those of gelatin films made from squid skin gelatin extracted at low temperatures (Nagarajan et al., 2012). GF3 and GF4 were higher in EB values than those reported for snapper and squid skin gelatin films (Jongjareonrak et al., 2006b; Nagarajan et al., 2012).

6.4.5 Characterization of GF3 film

The above findings indicated films GF3 and GF4 had low opacity, and comparably low water solubility and water vapor permeability ($p > 0.05$), as well as comparably high TS and EB values ($p > 0.05$). GF3 is considered cost-effective as it used less gelatin amount to achieve the excellent film properties. Therefore, GF3 was characterized for functional groups by FTIR, thermal stability by TGA, and microstructure via SEM (**Figure 3**).

The FTIR spectrum of GF3 is depicted in **Figure 6.3a**, and shows characteristic absorption regions of amide A (3305 cm^{-1}), amide B (2933 cm^{-1}), amide I (1633 cm^{-1}), amide II (1537 cm^{-1}) and amide III (1235 cm^{-1}) bands, as well as OH group (1040 cm^{-1}) corresponding to the interaction between gelatin film with the glycerol added as plasticizer (Ejaz et al., 2018). Specifically, amide A band is related to N-H stretching vibration; Amide I band is associated with C=O stretching vibration that may be associated with α-helical structure in gelatin (Li et al., 2018c); amide II band denotes the N-H bending and C-N stretching vibrations; amide III band represents the C-N and N-H vibrations as well as wagging vibrations of CH_2 groups from Gly backbone and Pro side chain. The assignment of absorption bands were in agreement with the findings reported for gelatin films by Ejaz et al. (2018) and Li et al. (2018c).

TGA trace of weight loss (%) and derivative weight (%/^oC) as a function of degradation temperature (^oC) for film GF3 is depicted in **Figure 6.3b**. The main thermal decomposition temperature of GF3 film starting from 225 ^oC and the derivative thermogravimetric curve was the highest at a temperature of 314.6 ^oC that suggested the maximum degradation of film. There were two stages of weight loss for GF3. The first stage was from 54.1 ^oC to 89.1 ^oC with weight loss of 1.7 – 4.9% that was probably associated with the free water loss in film. The second weight loss

(9.4 – 66.3%) was from 225.0 ºC to 376.9 ºC that may be related with the loss of the glycerol compound and bound water, as well as the degradation of gelatin chain and gelatin film matrix (Wu et al., 2013). This effect of temperature observed is consistent with the notion that high temperatures result in relatively less high molecular weight peptides (≥ β-chains) versus low molecular weight peptides (≤ α-chains); while the reverse is the case at low temperatures (Hanani et al., 2012; Muyonga et al., 2004; Shakila et al., 2012). These results are in agreement with those reported previously for plain gelatin films by Gómez-Estaca et al. (2017).

The microstructure of GF3 is described in **Figure 6.3c** in magnification of 2.0 k. The surface of the film was smooth and uniform, and the cross-section of the gelatin film was even and compact. High content of HMW chains in gelatin allowed well-organized arrangement of ordered helical structure from the disordered random coil during film formation, and thus the free space within gelatin molecules in the polymer reduced resulting in continuous microstructure and stronger mechanical properties. Previous research also found that LMW gelatin caused less interactions within molecules leading to rough surface with cracks and loose cross-section with voids (Nagarajan et al., 2012). Generally, superior microstructure of film is closely related with lower water solubility and WVP, as well as stronger mechanical properties of films.

6.5. Conclusions

This research explored enzymatic processing for producing fish skin gelatin rich in HMW polypeptide chains considered to impart superior quality attributes to gelatin for food applications. In this study, alcalase was used in a small amount to produce high molecular weight chain in gelatin, instead of its previous common usage to produce bioactive peptides or protein hydrolysates. The optimization study established the optimum conditions to produce a fish skin gelatin with 33% of HMW polypeptide chains. Low concentrations of gelatin solutions formed films with excellent physical and mechanical properties. The characterization studies ascertained its thermal stability, as well as smooth and compact microstructure.

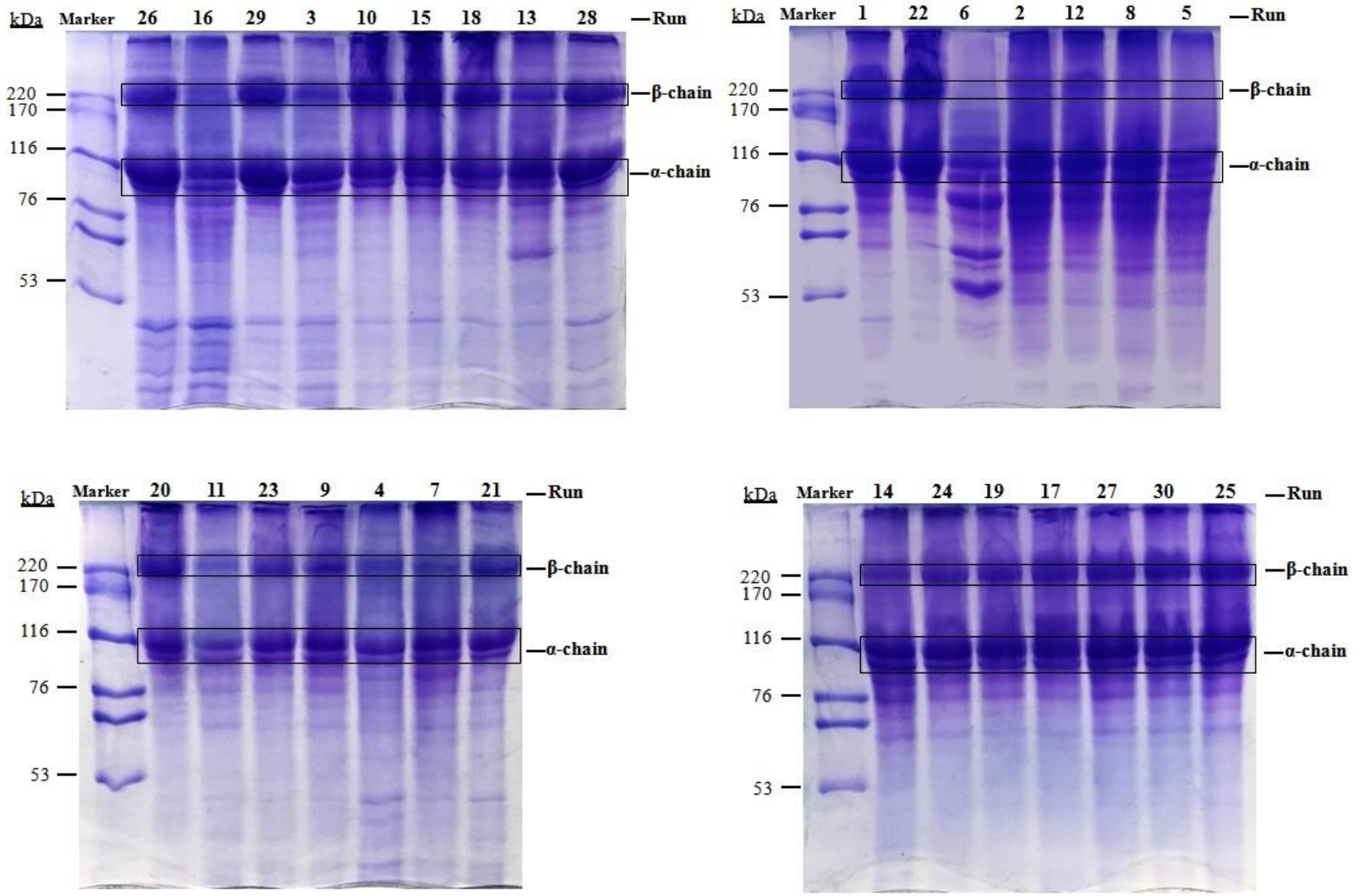

Figure 6.1. SDS-PAGE patterns of fish skin gelatin by alcalase-assisted production using face-centered central composite design.

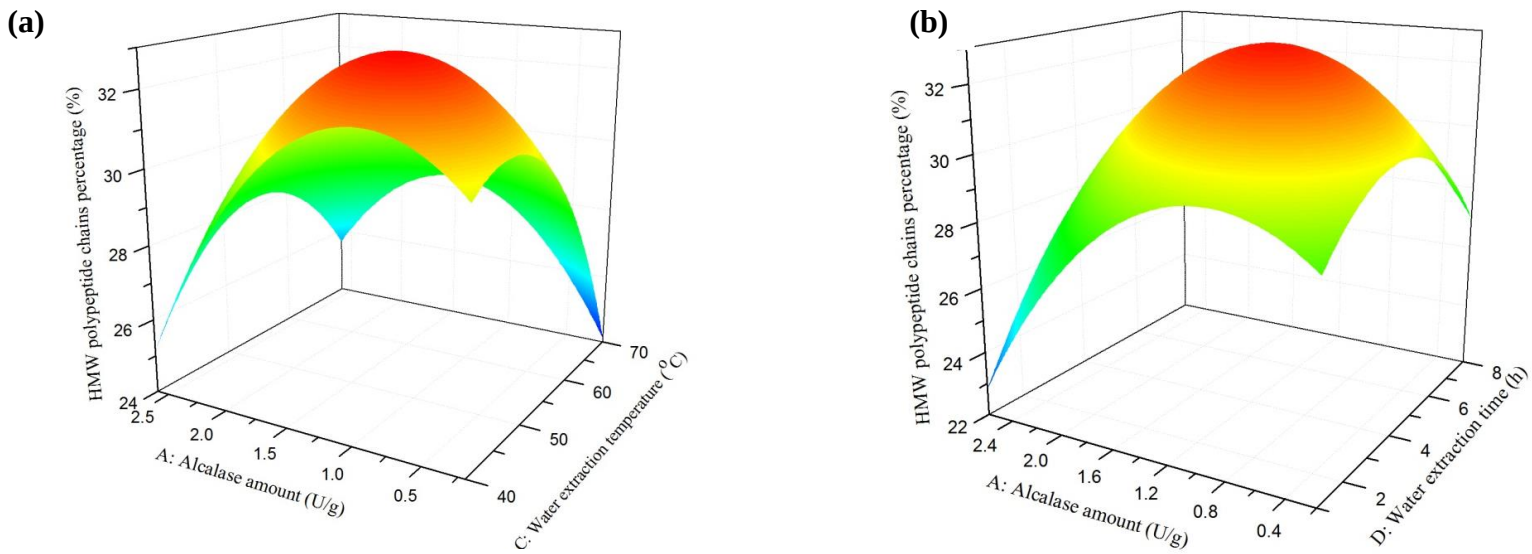

Figure 6.2. Three-dimensional (3D) response surface plots. (a) HMW polypeptide chains percentage (%) as a function of alcalase amount (U/g) × water extraction temperature (^{o}C); (b) HMW polypeptide chains percentage (%) as a function of alcalase amount (U/g) × water extraction time (h).

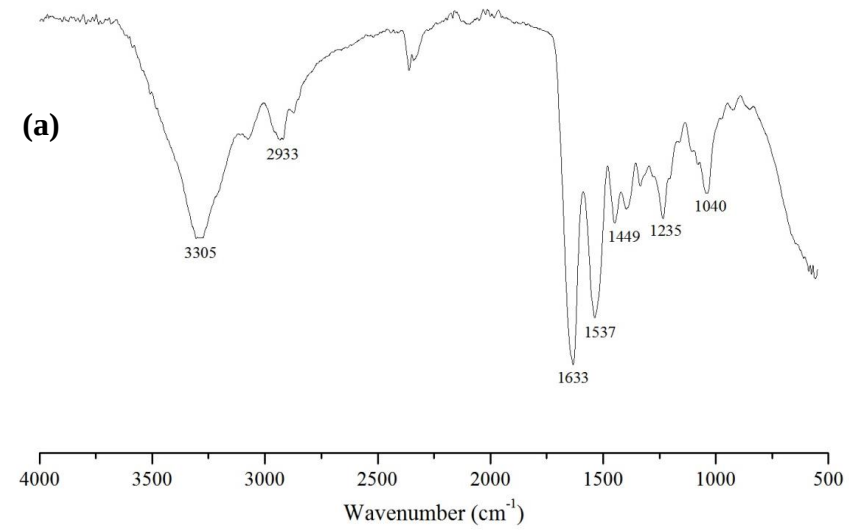

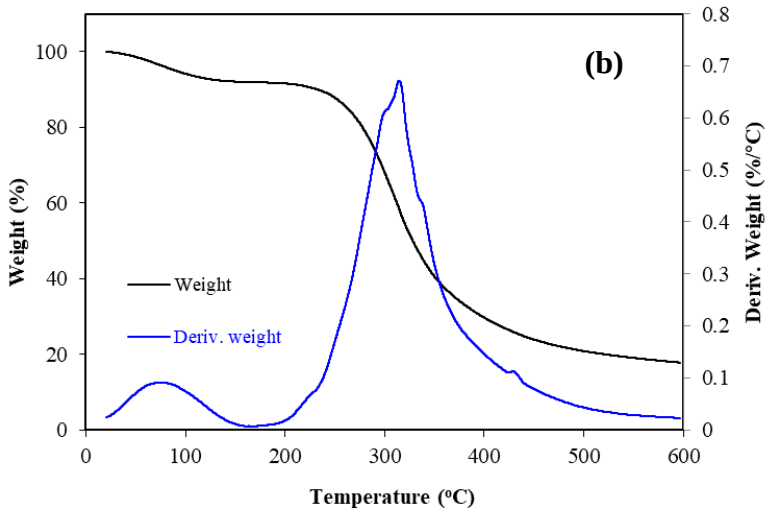

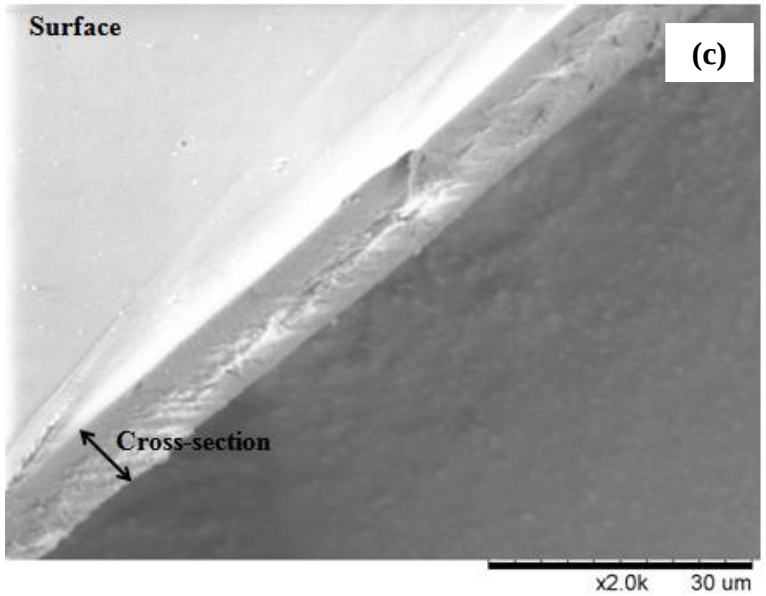

Figure 6.3. Characterization of GF3 film. (a) FTIR spectrum; (b) TGA trace; (c) Microstructure in magnification of 2.0 k.

Table 6.1

The experiment data for the HMW polypeptide chains percentage in fish skin gelatin by alcalase-assisted production using face-centered central composite design.

Run	Independent variables				Response
	A: Alcalase amount (U/g)	B: Alcalase treatment time (h)	C: Water extraction temperature (°C)	D: Water extraction time (h)	HMW polypeptide chains percentage (%)
1	0.2	0.5	40	1.0	27.018
2	2.6	0.5	40	1.0	17.183
3	0.2	3.5	40	1.0	29.974
4	2.6	3.5	40	1.0	21.210
5	0.2	0.5	70	1.0	16.551
6	2.6	0.5	70	1.0	15.781
7	0.2	3.5	70	1.0	18.971
8	2.6	3.5	70	1.0	17.121
9	0.2	0.5	40	8.0	22.610
10	2.6	0.5	40	8.0	24.287
11	0.2	3.5	40	8.0	23.165
12	2.6	3.5	40	8.0	19.657
13	0.2	0.5	70	8.0	20.167
14	2.6	0.5	70	8.0	25.783
15	0.2	3.5	70	8.0	21.395
16	2.6	3.5	70	8.0	25.016
17	0.2	2.0	55	4.5	29.452
18	2.6	2.0	55	4.5	26.343
19	1.4	0.5	55	4.5	30.143
20	1.4	3.5	55	4.5	27.678
21	1.4	2.0	40	4.5	29.383
22	1.4	2.0	70	4.5	27.646
23	1.4	2.0	55	1.0	27.684
24	1.4	2.0	55	8.0	30.083
25	1.4	2.0	55	4.5	35.762
26	1.4	2.0	55	4.5	33.174
27	1.4	2.0	55	4.5	31.014
28	1.4	2.0	55	4.5	32.929
29	1.4	2.0	55	4.5	36.993
30	1.4	2.0	55	4.5	32.971

Table 6.2

Statistical summary of the surface response analysis.

Source	Response		
	Mean Square	*F* Value	*p* Value
Model	67.91	16.3	< 0.0001
A	15.91	3.82	0.0696
B	1.21	0.29	0.5981
C	37.72	9.05	0.0088
D	23.74	5.7	0.0306
AB	3.23	0.78	0.3925
AC	45.72	10.97	0.0047
AD	51.21	12.29	0.0032
BC	0.11	0.026	0.8744
BD	12.89	3.09	0.0990
CD	54.77	13.14	0.0025
A^2	30.49	7.32	0.0163
B^2	15.13	3.63	0.0760
C^2	20.51	4.92	0.0424
D^2	15.47	3.71	0.0731
Residual	4.17		
Lack of fit	3.89	0.82	0.6311
Pure error	4.73		

Note: A is alcalase amount, B is alcalase treatment time, C is water extraction temperature, and D is water extraction time. For response, R^2 = 0.9383, Adj R^2 = 0.8807, Pred R^2 = 0.7955, Adeq Precision = 12.04.

Table 6.3

Amino acid composition of the optimized gelatin.

Amino acids	**Composition (%, or /100 residues)**
Alanine	11.5
Arginine	5.5
Aspartic acid	4.8
Glutamic acid	7.6
Glycine	31.6
Histidine	0.9
Hydroxylysine	0.7
Hydroxyproline †	7.9
Isoleucine	2.1
Leucine	3.2
Lysine	1.9
Methionine	1.5
Phenylalanine	1.5
Proline †	10
Serine	3.5
Threonine	2.1
Tyrosine	0.5
Valine	3.2
Total	**100**
Imino acids †	17.9

Table 6.4

Properties of fish gelatin films prepared by different film forming solution containing gelatin levels of 0.5% – 4% (w/v).

Films	Thickness (mm)	Color			Opacity value	Water Solubility (%)	WVP ($\times 10^{-8}$ g mm h^{-1} cm^{-2} Pa^{-1})	TS (MPa)	EB (%)
		*L**	*a**	*b**					
GF0.5	0.030 ± 0.005^{a}	31.86 ± 0.37^{a}	-0.23 ± 0.02^{d}	0.29 ± 0.04^{a}	2.83 ± 0.07^{e}	41.22 ± 0.94^{d}	7.07 ± 0.41^{d}	8.80 ± 2.29^{a}	23.45 ± 3.28^{a}
GF1	0.031 ± 0.006^{a}	32.37 ± 0.11^{b}	-0.48 ± 0.02^{c}	0.42 ± 0.07^{b}	2.38 ± 0.07^{d}	37.36 ± 1.50^{c}	6.20 ± 0.28^{c}	22.42 ± 1.78^{b}	32.04 ± 1.52^{b}
GF2	0.033 ± 0.005^{a}	32.62 ± 0.23^{b}	-0.50 ± 0.07^{c}	0.49 ± 0.07^{b}	2.22 ± 0.07^{c}	34.22 ± 1.21^{bc}	5.43 ± 0.45^{ac}	29.89 ± 2.80^{c}	39.87 ± 2.39^{c}
GF3	0.051 ± 0.004^{b}	33.22 ± 0.09^{c}	-0.66 ± 0.04^{b}	0.87 ± 0.04^{c}	1.73 ± 0.03^{b}	31.23 ± 0.72^{ab}	5.35 ± 0.12^{ab}	30.19 ± 1.27^{c}	44.82 ± 2.44^{c}
GF4	0.063 ± 0.008^{c}	32.47 ± 0.19^{b}	-0.74 ± 0.02^{a}	1.76 ± 0.08^{d}	1.37 ± 0.04^{a}	29.08 ± 1.95^{a}	5.90 ± 0.29^{bc}	30.30 ± 0.74^{c}	45.57 ± 1.06^{c}

Note: Values with the different superscript letters in one panel were significantly ($p < 0.05$) different.

CONNECTING STATEMENT 5

The material presented in this part of the thesis builds on the studies in the previous sections of gelatin preparation and were designed to improve their mechanical and barrier properties of biodegradable/compostable gelatin-based films using food wax, specifically beeswax and carnauba wax to improve the mechanical and barrier properties of the gelatin films.

This chapter constitutes the text of papers published as:

Y Zhang, B K Simpson, M J Dumont. Effect of beeswax and carnauba wax addition on properties of gelatin films: A comparative study. Food Bioscience, 2018, 26: 88-95.

For this paper, PhD candidate Y Zhang designed and performed the experiments, analyzed the data, and drafted the manuscript. Professors M J Dumont provided some research facilities for the experiments. Professor B K Simpson supervised the research work, provided the research materials and facilities, guided the lab performance and data analysis, revised the manuscript.

CHAPTER VII. EFFECT OF BEESWAX AND CARNAUBA WAX ADDITION ON PROPERTIES OF GELATIN FILMS: A COMPARATIVE STUDY

7.1. Abstract

Different levels of beeswax (B) or carnauba wax (C) were added into gelatin (G) at 5, 10, and 15% (w/w) to prepare films containing glycerol as a plasticizer. Although the wax addition increased the opacity and yellowness of gelatin films, both the UV/visible light and water vapor barriers were successfully improved gradually with increasing wax levels, and B was more effective than C. Addition of 10 and 15% wax significantly reduced the water solubility and WVP ($P \leq 0.05$). However, the mechanical properties of gelatin-wax films were not strengthened compared with control film G. As wax levels increased, the resulting films became more brittle, harder, and less stretchable. SEM showed GB films have more uniform surfaces and compact cross-sections compared with GC films. All films showed antioxidant activity against DPPH and hydroxyl radicals, and iron reducing; however, the effects obtained with the gelatin-wax films were not significantly different from the G films ($P > 0.05$). Based on FTIR analysis, all films showed amide absorption regions, but GB films showed higher intensity of absorption peaks for lipid functional groups than GC films. Wax addition improved thermal stability of films suggesting an interaction between wax and gelatin. The improved barrier properties and thermal stability of the gelatin-wax films suggest that they can be used to protect foods from deterioration, and B was found to be better than C when added in gelatin films.

7.2. Introduction

Oxidation and moisture migration in foods can have adverse effects on the properties of foods such as color, texture, flavor, safety and nutritional quality. Exposure to light, loss or gain of water vapor, and the presence of oxygen during food storage can lead to undesirable changes such as browning reactions, discolorations, autolysis, rancidity, microbial proliferation, protein denaturation, or disintegration of polymers. For example, photo oxidation damages photosensitive substances such as pigments, and/or degrades lipids and vitamins. Biodegradable films based on natural biopolymers such as polysaccharides, proteins and lipids that have barrier properties to moisture, oxygen and light, have been evaluated to resolve these problems.

Interest in gelatin-based films has increased (Etxabide et al., 2017). Gelatins with a more linear structure generally have better oxygen barrier properties compared with globular proteins, and this feature leads to higher cohesive energy density and lower free volume (Miller and Krochta, 1997). Cold-water fish gelatins (CWFG) have comparable amphiphilic properties to their mammalian counterparts; thus, they can act as stabilizers to form emulsions with other components (e.g., lipids

and bioactive peptides) at ambient temperatures to avoid degradation of the heat labile components at harsh conditions. Gelatin has several advantages over the other natural proteins in forming edible films. It is non-toxic and can be readily dissolved in warm water to minimize denaturation, which makes it distinct from zein and soy protein that need to be dissolved in ethanol and boiling water, respectively. Gelatin consists of unique amino acid sequences and it can set into hydrogels on cooling by forming hydrogen bonds to recover part of the triple-helix structure of its parent collagen molecules (Gorgieva and Kokol, 2011). Gelatin-based films with improved mechanical, thermal and bioactive properties are increasingly being studied. Examples include gelatin-nanoparticle films with improved barrier properties and a thermal insulation effect (Kundu et al., 2017), and smart gelatin-curcumin films able to sense pH changes of packaged foods (Musso et al., 2017). However, gelatin and the commonly added plasticizers (e.g., glycerol and sorbitol) are all hydrophilic molecules that cause poor water resistance in films. Thus, the addition of lipids in gelatin films is of particular interest to reinforce barrier properties. Various essential oils (e.g., clove and cinnamon oils), edible oils (e.g., soybean, corn, sunflower, olive, and palm oils), and fatty acids (e.g., stearic, oleic, and palmitic acids) were added in gelatin films to impart excellent water and oxygen barrier properties (Cao et al., 2009; Kavoosi et al., 2014).

Wax itself is a protective coating for some fruits in nature. Among all natural waxes, beeswax and carnauba wax are the most studied, and added into some protein-based films (e.g., whey protein, soy protein, casein, wheat gluten and zein) (Klangmuang and Sothornvit, 2016; Kowalczyk and Baraniak, 2014; Shih et al., 2011).

Beeswax is secreted from wax glands of honey bees. It is relatively soft, yellow in color and has a low melting temperature of 62–64 ºC. Its chemical components are esters, free fatty acids, and hydrocarbons; mainly palmitate, palmitoleate and oleate esters of long-chain alcohols. Beeswax has anti-inflammatory, anti-stress, wound healing, antimicrobial and antioxidant activities (Fratini et al., 2016). Klangmuang and Sothornvit (2016) reported that beeswax significantly reduced water vapor permeability (WVP) of hydroxypropyl methylcellulose-based films. Khanzadi et al. (2015) reported that addition of beeswax in whey protein-pullulan films reduced water solubility and WVP; but increased tensile strength of films.

Carnauba wax is produced from a Brazilian palm tree *Copernica cerifera*. It is hard, yellow in color, and has a high melting temperature of 82–86 ºC. Chemically, it mainly consists of aliphatic esters, *p*-hydroxycinnamic aliphatic diesters, ω-hydroxy aliphatic esters and monohydric alcohols,

and some of them showed antioxidant and antiprotozoal activities (de Almeida et al., 2016; Freitas et al., 2016). The incorporation of carnauba wax in chitosan films and cashew tree gum films increased opacity, but decreased WVP and water solubility of the films (Rodrigues et al., 2014; Santos et al., 2017). However, studies on adding wax into gelatin films are lacking.

7.3. Materials and methods

7.3.1. Materials

Gelatin from cold-water fish skins (Species unspecified, Cat. No. G7041; Lot No. SLBR6949V) and beeswax (Cat. No. 243248; Lot No. MKBV9971V) were purchased from Sigma-Aldrich Co. (St. Louis, MO, USA). Carnauba wax (Cat. No. 31117; Lot No. Z18D005) was obtained from Alta Aesar (Ward Hill, MA, USA). Calcium chloride ($CaCl_2$), ethylenediaminetetraacetic acid (EDTA), ethyl acetate, ferric chloride ($FeCl_3$), and ferrous sulfate ($FeSO_4$) were purchased from Fisher Scientific (Geel, Belgium). Trichloroacetic acid (TCA), 2,2-diphenyl-1-picrylhydrazyl (DPPH), 1,10-phenanthroline, hydrogen peroxide (H_2O_2), and potassium ferricyanide were purchased from Sigma-Aldrich Co.

7.3.2. Film preparation

A 5% (w/v) gelatin solution was prepared in warm distilled water at 40 ^oC using the uncharacterized gelatin as purchased. Glycerol was added as the plasticizer at a concentration of 40g/100 g gelatin, as reported by Rivero et al. (2010). Beeswax or carnauba wax was first melted on a hot plate at 65 and 85 ^oC, respectively, for 5 min, and the molten wax was added into the gelatin solution at a concentration of 5, 10 and 15% (w/w of gelatin). The resulting film forming solutions (**Table 7.1**) were placed in an ultrasonic mixer (Branson Ultrasonics Corp., Danbury, CT, USA) at 25 kHz for 1 min. Then, a vacuum pump was used to degas the emulsified film forming solution. Each film was prepared by placing film forming solution with a constant solids mass (1.5 g of gelatin, glycerol and wax) on a leveled casting plate (diameter of 9.5 cm) and dried at 25 ^oC and 50% relative humidity (RH) measured using a humidity meter (AccuTemp, Fort Wayne, IN, USA), peeled off and conditioned at 25 ^oC in a sealed desiccator that had been pre-treated with desiccant down to 40% RH for 48 h before analysis.

7.3.3. Determination of film properties

Thickness. The thickness of the films was measured at 8 random locations with a high precision (0.01 mm) digital micrometer (Shimana SHAYDC082, Brampton, ON, Canada).

Light transmission, clarity and color. Light transmission of films against ultraviolet (UV) and

visible light was measured as transmittance (%) value using a DU 800 UV/visible spectrophotometer (Beckman Coulter Inc., Brea, CA, USA) at selected wavelengths from 200 to 800 nm. Films were put in a holder designed in the laboratory with grooves on opposite sides to hold the films upright in the spectrophotometer, and air was used as blank. Clarity of films was measured based on the transparency value with the spectrophotometer, using the method of Hamdi et al. (2019). From Equation 1, a higher transparency value denotes lower film clarity.

$$\text{Transparency value} = \frac{-\log(T_{600})}{x} \quad (1)$$

where T600 is the fractional transmittance at 600 nm and 'x' is the average film thickness (mm).

Color of films was determined as *L** (lightness), *a** (red-green), *b** (yellow-blue) using a Minolta spectrophotometer CM-3500d colorimeter (Minolta Co., Ltd., Osaka, Japan) with Spectra Magic software version 2.11. The instrument was calibrated using a standard black-and-white plate. The film was placed directly on the target mask (aperture size 11 mm) of the instrument, and measurements were made as per the manufacturer's instructions.

Water solubility. Water solubility was defined as the percentage of dry film compounds dissolved in water using the method of Antoniou et al. (2015) with slight modifications. Film pieces (2 × 2 cm) were cut using scissors, dried in an oven at 105 °C for 24 h and weighed (W_0). Afterwards, films were immersed in 20 mL distilled water with constant agitation of 50 rpm at 25 °C for 24 h. The undissolved fractions were collected and dried at 105 °C for 24 h and weighed (W_1). Water solubility was calculated using Equation 2.

$$\text{Water solubility (\%)} = \frac{W_0 - W_1}{W_0} \times 100 \quad (2)$$

Water vapor permeability (WVP). WVP was determined gravimetrically using the method of Gómez-Guillén et al. (2007) with slight modifications. Films were mounted on test cups made from Nalgene jars (diameter 2.5 cm and depth 4.0 cm, Thermo Scientific, Madison, WI, USA) with an open cap that was fabricated in the university machine shop. The screw-in cap circumference and a silicon sealant were used to seal the films. Test cups were filled with 6 g anhydrous $CaCl_2$ as a desiccant (0% RH) and placed in a desiccator containing distilled water (100% RH) at 25 °C. The weight gain of each cup was measured every 4 h for a total of 24 h. WVP values were calculated using Equation 3.

$$WVP = wxt^{-1}A^{-1}\Delta P^{-1} \quad (3)$$

where w is the weight gain (g), x is the film thickness (mm), t is the time of gain (h), A is the area

of the exposed film surface (cm^2), and ΔP is the difference of water vapor pressure between two sides of the film (3158 Pa) (Cao et al., 2009).

Mechanical properties. Tensile strength (TS), elongation at break (EB), and Young's modulus (YM) of the films were measured with a Universal Testing Machine (Instron Model 4002, Canton, MA, USA) using American Society for Testing and Materials (ASTM) Standard Method D638-10. Film samples were first cut using scissors in dumbbell shape, and then were preconditioned at 25 °C and 40% RH for 48 h. The texture analyzer was set to an initial grip of 51 mm and an extension rate of 50 mm/min. YM was calculated using Series IX software (Instron Ltd.). The TS and EB values were calculated using Equations 4 and 5, respectively.

$$\text{TS (MPa)} = \frac{F}{W \times T} \qquad (4)$$

where F is the maximum tensile force of film (N), W and T represent the initial film width (mm) and average thickness (mm), respectively.

$$\text{EB (\%)} = \frac{L_1}{L_0} \times 100 \qquad (5)$$

where L_1 is the increase of film length after stretching, L_0 is the original film length.

Antioxidant activity. Films (100 mg) were first soaked in distilled water (10 mL) at 50 °C for 10 min, and then centrifuged (Marathon 21000R, Fisher Scientific, Pittsburgh, PA, USA) at 10,000 g for 10 min at 25 °C. The supernatants were used.

DPPH radical scavenging activity was determined using the method of Wu et al. (2013) with slight modifications. An aliquot of 0.5 mL of supernatant was mixed with 1 mL of 100 μM DPPH solution which was freshly prepared in 95% ethanol. After incubation in the dark for 30 min at 25 °C, absorbance was measured at 517 nm. DPPH radical scavenging activity (%) was calculated using Equation 6.

$$\text{DPPH radical scavenging activity (\%)} = 100 \times \frac{A_{control} - A_{sample}}{A_{control}} \qquad (6)$$

where $A_{control}$ was measured using distilled water instead of supernatant.

Hydroxyl radical scavenging activity was measured using the method of You et al. (2011) with slight modifications. An aliquot of 0.6 mL of 5 mM 1,10-phenanthroline, 0.6 mL of 5 mM $FeSO_4$ and 0.6 mL of 15 mM EDTA were mixed with 0.4 mL of 0.2 M sodium phosphate buffer (pH 7.5). Then, 0.6 mL of the supernatant and 0.8 mL of 0.01% H_2O_2 were added. The mixture was incubated at 37 °C for 60 min, and the absorbance was measured at 536 nm. The hydroxyl radical scavenging activity was calculated using Equation 7.

$$\text{Hydroxyl radical scavenging activity (\%)} = 100 \times \frac{A_{sample}-A_{control}}{A_{blank}-A_{control}} \quad (7)$$

where $A_{control}$ was measured using distilled water instead of supernatant, and A_{blank} was measured in the absence of H_2O_2.

Iron reducing activity was determined using the method of Wu et al. (2013). One mL aliquot of supernatant (sample) or distilled water (blank) was mixed with 2.5 mL of 0.2 M phosphate buffer (pH 6.6) and 2.5 mL of 1% potassium ferricyanide. After the mixture was incubated at 50 ^oC for 30 min, 2.5 mL of 10% TCA were added. The mixture was centrifuged at 1,650 g for 10 min, then 2.5 mL of supernatant were mixed with 2.5 mL of distilled water and 0.5 mL of 0.1% $FeCl_3$, and reacted for 10 min. The absorbance at 700 nm was measured against blank solution. Higher absorbance indicated higher reducing activity.

7.3.4. FTIR spectroscopy

The FTIR spectra of films were measured using a Nicolet iS5 FTIR spectrometer (Thermo Fisher Scientific, Madison, WI, USA) equipped with an attenuated total reflectance diamond crystal. Films were dried in a desiccator with silica gel for 2 wk. at 25 ^oC before analysis. The spectra in the range of 500–4000 cm^{-1} with automatic signal gain were collected in 32 scans at a resolution of 8 cm^{-1} and were ratioed against a background spectrum measured using the empty cell at 25 ^oC. The FTIR data was processed using OMNIC software version 8.0 (Thermo Fisher Scientific).

7.3.5. TGA analysis

The thermal properties of the films were determined using thermal gravimetric analysis (TGA, Q50, TA Instrument, New Castle, DE, USA). Films were first dried, and 10 mg were heated from 20 to 600 ^oC at a rate of 10 ^oC/min. Nitrogen was used as the purge gas at a flow rate of 60 mL/min. Temperature calibration was done using the Curie Temperature Standard Nickel in the same range of temperature and heating rate. The weight loss (%) and derivative weight (%/^oC) versus temperature for films was obtained.

7.3.6. SEM analysis

The surfaces and cross-sections of the films were observed using a scanning electron microscope (SEM) (TM 3000 Tabletop Microscope, Hitachi, Tokyo, Japan) with the TM 3000 program. Films were dehydrated in a desiccator with silica gel, cut into small pieces using knife, and then placed on double-sided carbon tape, which was then fixed to aluminum stub. The images were captured with voltage acceleration of 5 kV and magnification of 600.

7.3.7. Statistical analyses

Five replicates were done for the film properties determinations. The data were expressed as means ± SD (standard deviations). Statistical analyses were done using the SPSS 22.0 program (SPSS Inc., Chicago, IL, USA). One-way analysis of variance (ANOVA) was carried out. The differences between means were determined using the least significant difference (LSD) test. Level of significance was set for $P \leq 0.05$.

7.4. Results and discussion

7.4.1. Thickness

The thickness of films was comparable with each other, which was attributed to the fact that the mass of solids (i.e., gelatin, glycerol and wax, as shown in **Table 7.1**) used to prepare each film was the same. The measured thickness of films G, GB1, GB2, GB3, GC1, GC2, GC3 were 0.16 ± 0.01, 0.15 ± 0.01, 0.17 ± 0.01, 0.18 ± 0.01, 0.17 ± 0.01, 0.14 ± 0.01, 0.15 ± 0.01 mm, respectively. The film thickness might be correlated with the resistance to water and mechanical properties of films (Gutiérrez et al., 2015).

7.4.2. Color and clarity

The color and clarity of films are important considering the special interest in its use as packaging material in the food industry (Shah et al., 2016). As shown in **Table 7.2**, film G had the lowest L^* value (lightness), and films GB1 and GB2 were not significantly different from film G in terms of lightness ($P>0.05$). There was gradual increase in L^* values with increase of wax addition, and gelatin-carnauba wax films were lighter than gelatin-beeswax films. All the films showed slight greenness based on their a^* values. No significant differences in a^* values were observed ($P>0.05$) among GB1, GB2, GB3, as well as among GC1, GC2, GC3. Thus, the levels of wax addition did not significantly alter the redness/greenness of films. Carnauba wax addition gave a deeper greenness than beeswax. There was an increase in yellowness with increasing levels of wax, based on the increase in b^* values. The 15% wax addition led to significantly higher b^* values than 5 and 10% ($P \leq 0.05$). In general, carnauba wax gave more intense yellowness than beeswax. Besides, wax addition largely decreased the clarity of gelatin-based films. The transparency values significantly increased from 3.90 to 14.0 for gelatin-beeswax films ($P \leq 0.05$), and from 2.21 to 9.96 for gelatin-carnauba wax films ($P \leq 0.05$), which suggested that beeswax addition led to more opacity than carnauba wax.

7.4.3. Light barrier properties

Edible films can be designed to provide barrier to light transmission to avoid damage by photo-oxidation of various nutritive components (Jridi et al., 2014). From **Figure 7.1**, the light barrier properties of the films increased in this order: film G < film GC1 < film GB1 < film GC2 < film GB2 < film GC3 < film GB3. There was a different trend observed in the range from 200 to 300 nm, although the transmittance values of all films were extremely low (<5%). Films GB2 and GC3 had the lowest light transmission particularly from 200–300 nm, so they may be used to package foods high in active peptides, because some aromatic amino acids (e.g., tryptophan, tyrosine) absorb UV light below 310 nm resulting in peptide bond cleavage (Edwards and Silva, 2001). It is known that UV light (200–400 nm) promotes lipid oxidation that leads to rancidity and deterioration (Girotti, 2001). **Figure 7.1** shows that wax addition decreased the UV light transmission, and films GB3, GC3 and GB2 decreased UV light transmission values by about 50% as compared with the control film G. Moreover, food products usually contain photosensitive components such as riboflavin, myoglobin, and hemoglobin that absorb light at various wavelengths above 400 nm (Johnson and Decker, 2015). Visible light (400–800 nm) transmission of film G was 77–91%, but decreased light transmission was observed for wax added films. For instance, film GB3 showed only 13–20% visible light transmission (**Figure 7.1**). Similar results were reported by Talens and Krochta (2005). Thus, beeswax was more effective than carnauba wax in increasing the light barrier properties of the gelatin films, which was probably due to bioactive compounds in beeswax, and the uniform structure formed as shown in **Figure 7.5**. Thus, films with beeswax would be expected to reduce food spoilage caused by photodegradation.

7.4.4. Water solubility and WVP

Edible films with high water solubility readily disintegrate in nature and are easily digested in the human body. On the other hand, edible films with low water solubility prevent foods from humidity and water loss (Galus and Kadzińska, 2015). With the goal of preventing the functional and active components from breakdown, films with low water solubility are preferred. Gelatin films generally have high water solubility due to the hydrophilicity of gelatin (Kundu et al., 2017). From **Figure 7.2A**, film G (control) had the highest water solubility, and increasing wax addition decreased water solubility. Films GB2, GB3, GC2, GC3 showed significantly improved water resistance compared with film G ($P \leq 0.05$). It is suggested that the incorporation of wax in gelatin films help to maintain film integrity when immersed in water. Soazo et al. (2011) reported that

addition of beeswax into whey protein films reduced the water solubility. Chiumarelli and Hubinger (2014) also reported that carnauba wax added into cassava starch films produced low water solubility. The present study suggested that beeswax was more effective in reducing water solubility than carnauba wax. This was probably because the beeswax-based emulsions increased the hydrophobic character to a greater extent than carnauba wax-based emulsions, as suggested by Talens and Krochta (2005). Thus, beeswax addition into films will be expected to increase the stability of foods more than the corresponding films supplemented with carnauba wax through reduced moisture-induced disintegration of the films. Furthermore, addition of beeswax resulted in more uniform emulsion pellets than the addition of carnauba wax, as can be observed in **Figure 7.5** such that the film network of GB2 films were firm without any cracks, which is consistent with the findings of Chiumarelli and Hubinger (2014).

Edible films with low WVP are preferred to retard the moisture transfer between foods and their surrounding environment (Cao et al., 2009). **Figure 7.2B** shows that addition of carnauba wax slightly reduced WVP, and addition of beeswax significantly reduced WVP to approximately 5×10^{-8} g mm h^{-1} cm^{-2} Pa^{-1} compared with film G (control, WVP value of 13.2×10^{-8} g mm h^{-1} cm^{-2} Pa^{-1}) ($P\leq0.05$). Wax, a solid fat, has dense structure to prevent water vapor from passing through. Moreover, wax is efficient in reducing WVP due to its high hydrophobicity from high contents of long-chain fatty alcohols and alkanes (Zhang et al., 2014). Previous studies showed that addition of carnauba wax into zein (Weller et al., 1998) and addition of beeswax into carrageenan (Fabra et al., 2009) decreased WVP values of films. Furthermore, **Figure 7.2B** showed that the differences in wax levels had little effect on WVP, as films GB1, GB2 and GB3 had no significant difference ($P>0.05$), as well as for films GC2 and GC3 ($P>0.05$). In brief, beeswax reduced WVP more than carnauba wax when added into gelatin films ($P\leq0.05$), and beeswax can thus increase food stability better than carnauba wax.

7.4.5. Mechanical properties

Table 3 shows that addition of wax generally decreased the mechanical properties of gelatin-based films, which were probably due to the discontinuity in the gelatin matrix with wax addition, and similar results were reported previously (Chiumarelli and Hubinger, 2014; Fabra et al., 2009). Film G (control) had the highest TS value followed by film GB1 with no significant difference ($P>0.05$). With the increase of wax content, the TS values of films decreased slightly (**Table 7.3**). Films with higher wax content were more brittle, which can be explained by the disruption of the

flexible gelatin matrix, and the reduction of polymer chain-to-chain hydrogen bonding (Fabra et al., 2009; Talens and Krochta, 2005). Films GB2, GB3, GC1, GC2 and GC3 showed no significant differences for their TS values ($P>0.05$). At the same level of incorporation, carnauba wax had less effect on film TS than beeswax. The addition of wax also reduced the EB values of gelatin films. Films GB1, GB2, GB3 and GC1, had no significant difference when compared with film G (control) in EB values ($P>0.05$). But high levels of carnauba wax produced significant decreases in elongation compared with film G (control) ($P\leq0.05$). Film G had the highest EB value because the added glycerol is a common plasticizer added into gelatin to give flexible films. The EB values of gelatin-beeswax films were comparable with film G, which suggested the soft and viscous texture of beeswax contributes to the stretchable film network (Talens and Krochta, 2005). On the other hand, carnauba wax is hard and elastic, and that results in the resistant structure of the films. YM is a measure of the intrinsic stiffness of films. From **Table 7.3**, the YM values of the films generally increased with increasing wax addition. No significant difference was observed between gelatin-beeswax films (GB1, GB2, GB3) and film G (control) in terms of the YM values ($P>0.05$). Carnauba wax in films GC2 and GC3 significantly increased the film stiffness compared with film G ($P\leq0.05$). The data suggest that carnauba wax reduced the plasticizing effect of the glycerol to a greater extent than beeswax, and thereby produced relatively stiffer and stronger films. Previous research reported that beeswax added into chitosan films (Hromiš et al., 2015), as well as carnauba wax added into cassava starch films (Santos et al., 2014) decreased their mechanical properties. The present study showed that the addition of beeswax generated comparatively weaker, more flexible/stretchable gelatin-based films than carnauba wax, which is consistent with previous findings that beeswax had better plasticizing effects on whey protein than carnauba wax (Talens and Krochta, 2005).

7.4.6. Antioxidant activity

The antioxidant activity of the films is shown in **Table 7.4**. Although film GB2 showed the highest DPPH radical scavenging activity, the DPPH radical scavenging activity of all films showed no significant difference ($P>0.05$), suggesting wax addition statistically had no effect in improving the DPPH radical scavenging activity of films. The hydroxyl radical scavenging activity was improved by adding beeswax ($P>0.05$), or carnauba wax ($P\leq0.05$). Film GB2 had hydroxyl radical scavenging activity of 10.4%; for GC films, the hydroxyl radical scavenging activity increased as the wax addition level increased up to 14.9% (film GC3). Iron reducing activity

showed no significant difference among all films (P>0.05), although the addition of carnauba wax appeared to slightly increase iron reducing activity, especially film GC2 with a higher iron reducing activity than film G. Film G showed antioxidant properties, which was because gelatin, a protein with a range of polypeptide and peptides, is expected to have the capacity to scavenge free radicals by donating hydrogen. Jridi et al. (2013) reported that gelatin films had DPPH radical scavenging and iron reducing activities. Recently, a mixture of higher aliphatic primary alcohols isolated from beeswax, named D002, was found with antioxidant, and anti-inflammatory effects (Fratini et al., 2016; Ravelo et al., 2011). From carnauba wax, components such as *p*-methoxycinnamic diester showed antioxidant activity and *in vitro* bio-accessibility (Freitas et al., 2016). However, these bioactive compounds found in beeswax or carnauba wax may hardly function in the small amounts present in the films. A previous study on addition of beeswax into chitosan-caraway oil films found that beeswax had no obvious and concentration ordered effect on DPPH radical scavenging activity (Hromiš et al., 2015). The present results showed the addition of beeswax and carnauba wax had no distinct effect on the antioxidant activity of gelatin films.

7.4.7. FTIR spectra

The FTIR spectra of the gelatin and gelatin-wax films are shown in **Figure 7.3**. Differences were detected when beeswax or carnauba wax were added into gelatin films. The OH group showed a peak at 1038–1040 cm^{-1} in all films corresponding to the glycerol added as plasticizer. There were 5 characteristic absorption peaks identified for film G (control): amide A (3286 cm^{-1}) related to N-H stretching vibration, amide B (2933 cm^{-1}), amide I (1637 cm^{-1}) associated with C=O stretching vibration, amide II (1537 cm^{-1}) associated with the N-H bending and C-N stretching vibrations, and amide III (1239 cm^{-1}) bands representing the C-N and N-H vibrations as well as wagging vibrations of CH_2 groups from the glycine backbone and proline side chains. The gelatin films supplemented with beeswax and carnauba wax all showed lower intensities of the characteristic amide absorption regions than the wax-free gelatin films, and there were absorption regions related to functional groups of wax in the wax added films. The sharp peaks at 2916 and 2848 cm^{-1} found in gelatin-beeswax films (GB1, GB2 and GB3) showed the presence of fatty acid chains due to the asymmetric and symmetric stretching vibrations of aliphatic C-N groups, and the intensities grew gradually with increased levels of beeswax. There was a small peak at 1736 cm^{-1} originating from C=O stretching vibrations of the functional group ester carbonyl, and the peak intensity also increased with increasing beeswax. Gelatin-carnauba wax films showed less

intensities of absorptions at 2916, 2848 and 1736 cm^{-1} than beeswax films, similar to previous research that also found carnauba wax to have lower intensities than beeswax at these wavenumbers (Muscat et al., 2014). With the increase of carnauba wax level, the peak intensities increased at 2916 and 2848 cm^{-1} that originate from fatty acid chains, but peaks at 1736 cm^{-1} due to ester carbonyl functional groups were hardly observed in GC1 and GC2 films.

7.4.8. Thermal stability

TGA traces of weight loss (%) and derivative weight (%/^{o}C) as a function of degradation temperature (^{o}C) for film G, gelatin-beeswax film GB2 and gelatin-carnauba wax film GC2 are shown in **Figure 7.4**. For film G, there were 3 main stages of weight loss. The first stage was from 74.2 to 106 ^{o}C with weight loss of 1.85–3.71% that was probably associated with the free water loss. However, for films GB2 and GC2, this first stage for film G was not detected. It was probably due to low moisture contained in gelatin-wax films as both beeswax and carnauba wax are hydrophobic, and the observation is similar to the findings of Fratini et al. (2016) and Santos et al. (2017). It suggested that there was less water absorption by the gelatin-wax films versus the wax-free gelatin films, which corroborated the water solubility and WVP results (**Figure 7.2**). The second stage of weight loss at 19.9–38.4% for film G was from 232 to 272 ^{o}C and this might relate to loss of bound water, and the breakdown of the gelatin chain (Wu et al., 2013). For the same stage, higher temperatures in the range of 244–282 ^{o}C were found for GB2 films, and 238–281 ^{o}C for GC2 films, respectively. It suggests that some interactions existed in emulsions of wax, gelatin and glycerol, mainly hydrogen bonds contributed by electrostatic, van der Waals forces and steric repulsion (McClements, 2015). The third phase of weight loss (44.0–58.0%) for film G was found from 286 to 316 ^{o}C, and the corresponding stages for films GB2 and GC2 were 292–320 ^{o}C and 293–322 ^{o}C, respectively, which was related with the decomposition of gelatin and wax. A slight increase in the temperature was also found for gelatin-wax films, suggesting the interactions between polar side groups in gelatin (such as hydroxyl, carbonyl, and amino groups) and wax fraction (Halal et al., 2016). In summary, beeswax and carnauba wax had similar effects on the improvement of thermal stability of gelatin-based films.

7.4.9. Microstructure

The microstructure of the gelatin film (G), gelatin-beeswax film (GB2) and gelatin-carnauba wax film (GC2) are shown in **Figure 7.5** at magnification of 600. The surface of the G film was smooth and uniform, and its cross-section was compact. Film GB2 also had a compact cross-

section but its surface had a few spots suggesting that some of the added beeswax wax was unable to form uniform emulsions with gelatin. Film GC2 had clear spots on the surface and uneven cross-section with cracks. The results correlated with the mechanical properties (**Table 7.3**) that gelatin-beeswax films were more flexible than gelatin-carnauba wax films. Carnauba wax had a hard texture and high melting point (Talens and Krochta, 2005), which made it difficult to produce stable and uniform emulsions. Thus, gelatin-wax films prepared by emulsification tend to show both incorporated and layered forms.

7.5. Conclusion

Addition of natural wax, i.e., beeswax and carnauba wax, improved gelatin films' capacity to serve as barrier to light and moisture, which are key factors that lead to oxidation, degradation and deterioration of foods. Beeswax was better than carnauba wax in improving various properties for gelatin films. Both beeswax and carnauba wax are bioactive polymers that are beneficial to human health, thus the edible gelatin films could be widely used in food applications. Improvements can be done to optimize the emulsification of gelatin and wax to generate more uniform films. Bi-layer films are also of interest to study in future.

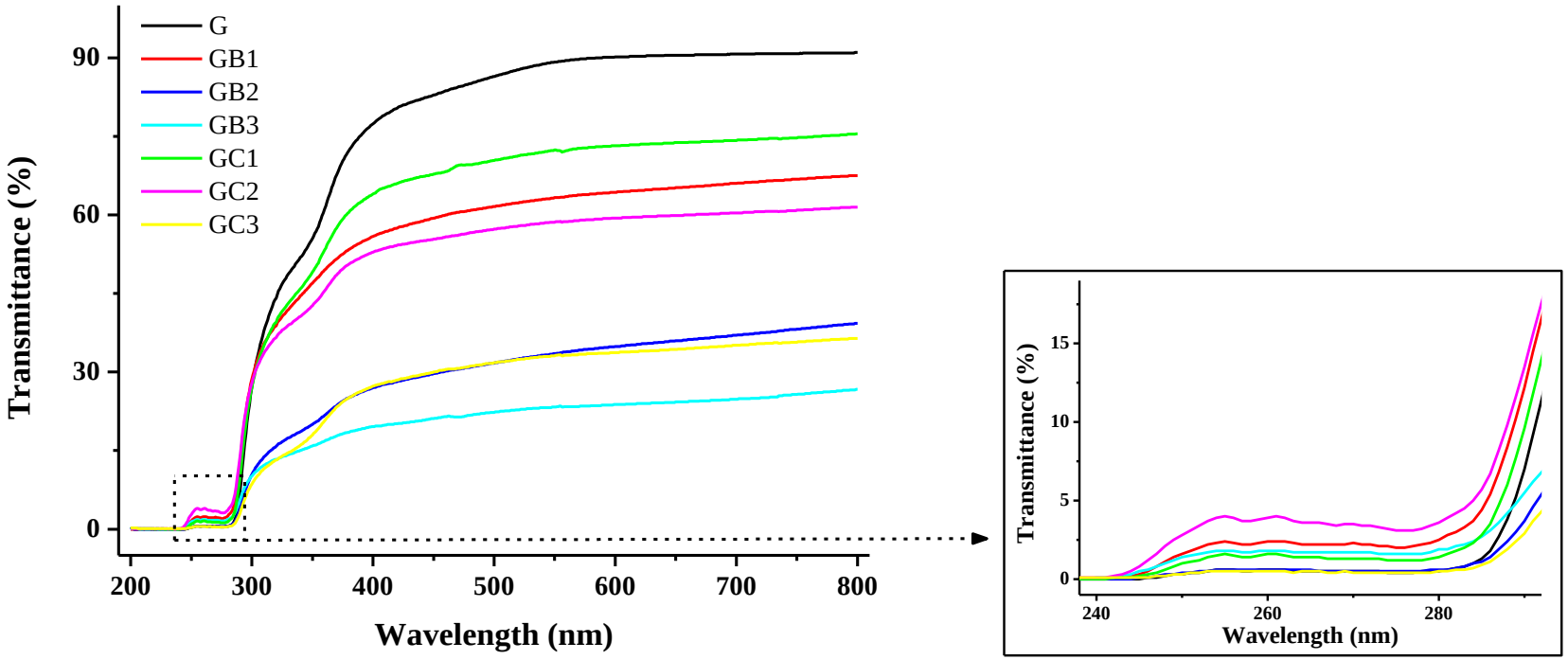

Figure 7.1. Light transmission (%) at 200–800 nm wavelength range of gelatin film (G), gelatin-beeswax films (GB1, GB2, GB3) and gelatin-carnauba wax films (GC1, GC2, GC3).

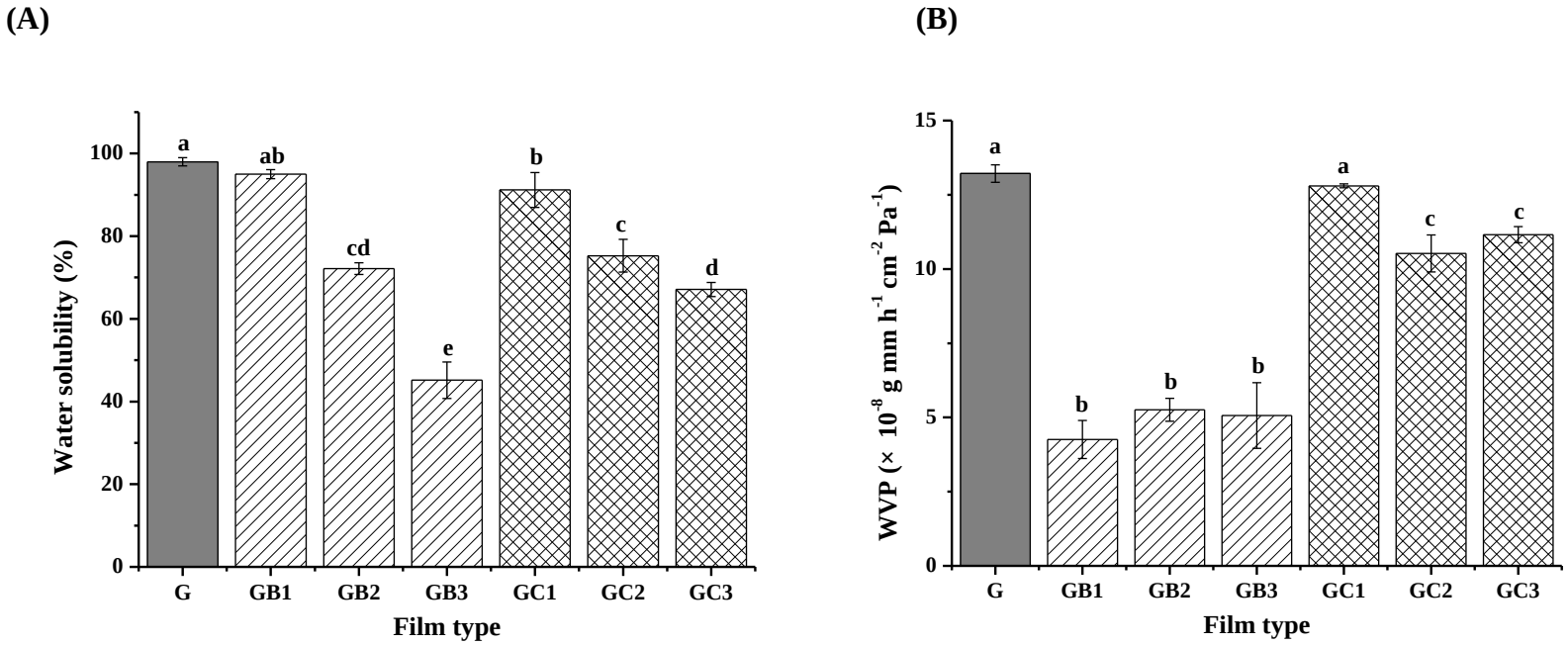

Figure 7.2. The (A) water solubility and (B) water vapor permeability of gelatin film (G), gelatin-beeswax films (GB1, GB2, GB3) and gelatin-carnauba wax films (GC1, GC2, GC3). Different letters in the same panel indicate significant difference among the different films ($P \leq 0.05$).

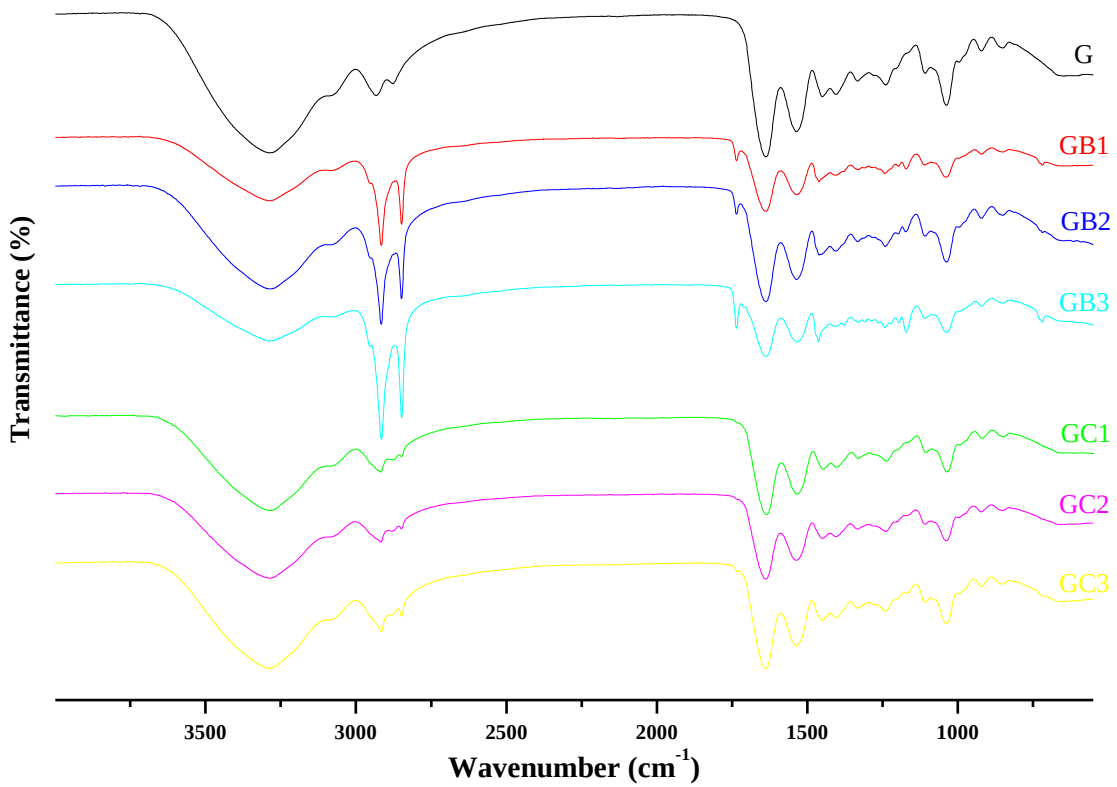

Figure 7.3. The FTIR spectra of gelatin film (G), gelatin-beeswax films (GB1, GB2, GB3) and gelatin-carnauba wax films (GC1, GC2, GC3).

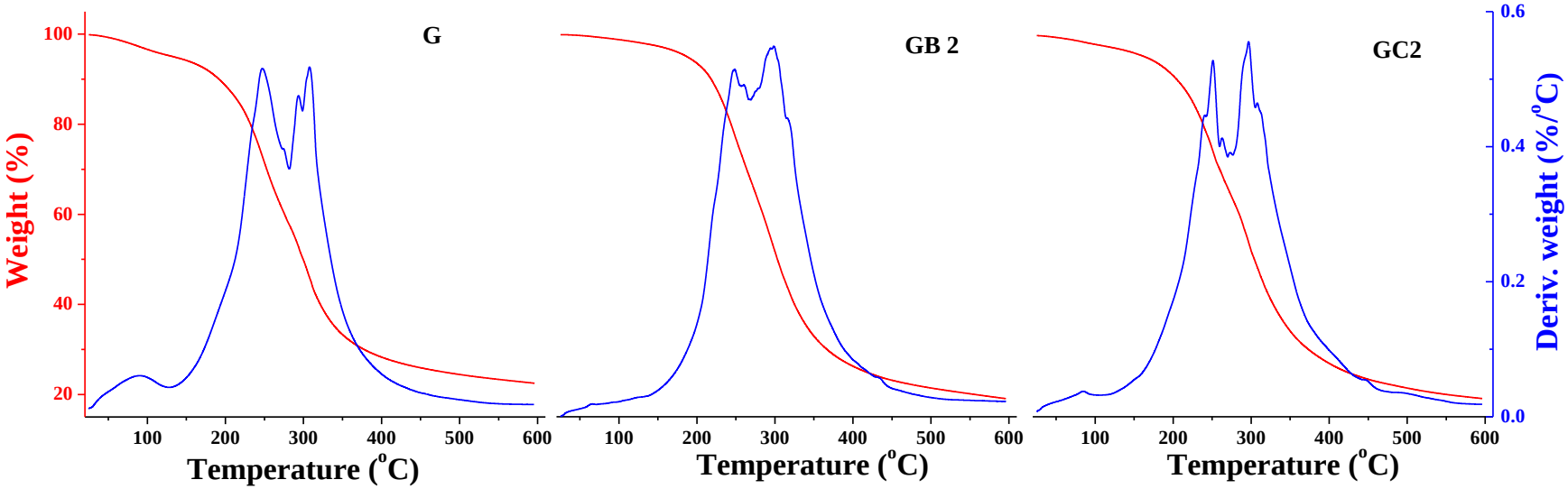

Figure 7.4. The TGA spectra of gelatin film G, gelatin-beeswax film GB2, and gelatin-carnauba wax film GC2.

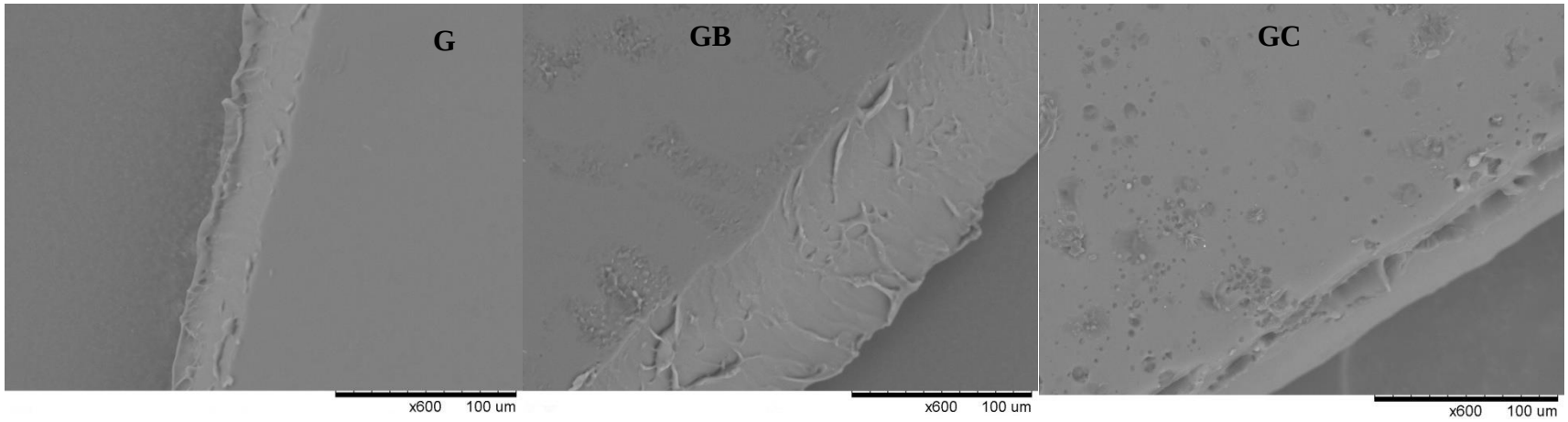

Figure 7.5. SEM graphs of the surface and cross-section of gelatin film G, gelatin-beeswax film GB2, and gelatin-carnauba wax film GC2.

Table 7.1

Composition of gelatin films, gelatin-beeswax films and gelatin-carnauba wax films used in current study.

Film symbol	Polymer amount in film forming solution (g / 100 ml)			
	Gelatin	Beeswax	Carnauba wax	Glycerol
G (control)	5	-	-	2
GB1	5	0.25	-	2
GB2	5	0.5	-	2
GB3	5	0.75	-	2
GC1	5	-	0.25	2
GC2	5	-	0.5	2
GC3	5	-	0.75	2

Table 7.2

Color (*L**, *a** and *b**) and transparency values of gelatin film (G), gelatin-beeswax films (GB1, GB2, GB3) and gelatin-carnauba wax films (GC1, GC2, GC3).

Film	*L**	*a**	*b**	Transparency value
G	33.25 ± 0.67^{a}	-0.38 ± 0.08^{ab}	0.93 ± 0.10^{a}	0.93 ± 0.03^{ab}
GB1	33.56 ± 0.70^{a}	-0.41 ± 0.06^{ab}	0.88 ± 0.28^{a}	3.90 ± 0.33^{cd}
GB2	33.97 ± 0.33^{a}	-0.37 ± 0.04^{ab}	1.28 ± 0.37^{ab}	10.51 ± 1.92^{e}
GB3	36.28 ± 0.63^{bc}	-0.33 ± 0.07^{a}	2.01 ± 0.40^{c}	13.91 ± 2.65^{f}
GC1	35.71 ± 0.79^{c}	-0.43 ± 0.08^{bc}	1.88 ± 0.29^{bc}	2.21 ± 0.30^{bd}
GC2	36.99 ± 1.46^{b}	-0.45 ± 0.09^{bc}	2.41 ± 1.02^{c}	4.41 ± 1.15^{c}
GC3	40.39 ± 0.92^{d}	-0.51 ± 0.02^{c}	3.72 ± 0.45^{d}	9.96 ± 1.40^{e}

Results are mean ± standard deviation. Different letters in the same column indicate significant difference among the different films ($P \leq 0.05$).

Table 7.3

Tensile strength (TS), elongation at break (EB), and Young's modulus (YM) of gelatin film (G), gelatin-beeswax films (GB1, GB2, GB3) and gelatin-carnauba wax films (GC1, GC2, GC3).

Film	Tensile strength (MPa)	Elongation at break (%)	Young's modulus (MPa)
G	2.55 ± 0.24^{a}	356.77 ± 10.55^{a}	3.26 ± 0.35^{abc}
GB1	2.28 ± 0.66^{a}	347.50 ± 34.32^{a}	3.20 ± 0.86^{cd}
GB2	0.92 ± 0.34^{b}	348.79 ± 14.28^{a}	3.76 ± 0.46^{abde}
GB3	0.84 ± 0.08^{b}	341.43 ± 17.57^{a}	5.09 ± 1.68^{bfg}
GC1	0.96 ± 0.14^{b}	347.93 ± 10.50^{a}	4.27 ± 1.13^{abce}
GC2	0.84 ± 0.23^{b}	307.83 ± 19.90^{b}	5.48 ± 1.81^{efg}
GC3	0.66 ± 0.34^{b}	218.30 ± 25.92^{c}	6.20 ± 0.61^{fg}

Results are mean ± standard deviation. Different letters in the same column indicate significant difference among the different films ($P \leq 0.05$).

Table 7.4

Antioxidant properties of gelatin film (G), gelatin-beeswax films (GB1, GB2, GB3) and gelatin-carnauba wax films (GC1, GC2, GC3).

Film	DPPH scavenging activity (%)	Hydroxyl scavenging activity (%)	Iron reducing activity ($\times 10^{-2}$)
G	6.91 ± 1.17^{a}	9.42 ± 1.11^{a}	4.69 ± 0.58^{a}
GB1	6.00 ± 0.49^{a}	10.27 ± 0.80^{abc}	5.02 ± 0.82^{a}
GB2	7.18 ± 0.55^{a}	10.44 ± 0.72^{abc}	4.54 ± 0.89^{a}
GB3	6.02 ± 1.07^{a}	9.57 ± 1.04^{ab}	4.34 ± 1.05^{a}
GC1	5.87 ± 0.30^{a}	11.11 ± 0.99^{bc}	5.49 ± 0.61^{a}
GC2	5.52 ± 1.33^{a}	11.42 ± 0.81^{c}	5.33 ± 0.69^{a}
GC3	5.57 ± 1.42^{a}	14.92 ± 0.89^{d}	5.15 ± 0.52^{a}

Results are mean ± standard deviation. Different letters in the same column indicate significant difference among the different films ($P \leq 0.05$).

CONNECTING STATEMENT 6

The following chapter (Chapter VIII) describes enzymatic process for the preparation of antioxidative peptides using alcalase versus trypsin as TGase substrates for subsequent application and characterization studies via techniques such as *de novo* sequencing of the peptides by LC-MS/MS and molecular docking of the peptides using myeloperoxidase (MPO) enzyme.

This chapter constitutes a paper submitted to Food Chemistry for consideration for publication as:

Y Zhang, S He, E Bonneil, B K Simpson. Generation of antioxidative hydrolysates from Atlantic sea cucumber using alcalase versus trypsin: *in vitro* activity, *de novo* sequencing, and *in silico* docking for *in vivo* function prediction. (Submitted)

PhD candidate Y Zhang designed and performed the experiments, analyzed the data, and drafted the manuscript. Dr. S He contributed software usage on the molecular docking studies. Dr. E Bonneil contributed the sequencing of peptides. Professor B K Simpson supervised the research work, provided the research materials and facilities, guided the lab performance and data analysis, revised the manuscript.

CHAPTER VIII. GENERATION OF ANTIOXIDATIVE HYDROLYSATES FROM ATLANTIC SEA CUCUMBER USING ALCALASE VERSUS TRYPSIN: *IN VITRO* ACTIVITY, *DE NOVO* SEQUENCING, AND *IN SILICO* DOCKING FOR *IN VIVO* FUNCTION PREDICTION

8.1. Abstract

The effect of alcalase and trypsin on generating antioxidative hydrolysates from Atlantic sea cucumber was compared. *In vitro* tests were used to select antioxidant hydrolysates/peptide fractions, and the identified sequences from *de novo* sequencing were analyzed using *in silico* methods for physicochemical properties and molecular interactions with myeloperoxidase (MPO), an enzyme implicated in *in vivo* antioxidative damage. Alcalase produced hydrolysates with higher antioxidant activity than trypsin. Ultrafiltrated peptide fractions (< 2 kDa) were found with high amount of leucine, a key amino acid in protein synthesis, and alcalase produced peptides with higher EAA/NEAA than trypsin using UPLC. Among all the peptide sequences identified by LC–MS/MS, alcalase and trypsin generated 35.4% and 30.3% peptide sequences, respectively, with both key antioxidative amino acids and potential MPO inhibition activity. Four weak interactions were predicted for sequences TEFHLL and EEELAALVLDNGSGMCK, to limit oxidative stress *in vivo* by binding and blocking MPO.

8.2. Introduction

Proper choice of proteases for preparing food protein hydrolysates is important in terms of efficacy and economics (Kristinsson and Rasco, 2000). The types of proteases used can partially determine the functional characteristics of the final hydrolysate products. On the other hand, the cost, hydrolytic conditions, specificity, stability and catalytic efficiency of different proteases vary to a large extent. Trypsin (EC 3.4.21.4), commercially available from bovine or porcine pancreas, is relatively expensive and specific for peptide bonds on the carboxylic side of lysine and arginine, with optimal pH ranging between 7.5–9.0, and optimal temperature from 35–55 ^{o}C. Alcalase, produced from *Bacillus licheniformis*, is non-specific with optimal pH ranging between 7–10 and optimal temperature from 30–65 ^{o}C. So far, there is no established standard or criterion regarding the selection of proteases for producing hydrolysates with specified bioactivities; thus, most research first carry out screening of proteases to decide on which enzyme(s) to use (He et al., 2019; Tripoteau et al., 2015; Yan et al., 2016). There are a few problems concerning the current rationale/procedures for protease selection: (i) the addition of the proteases have mostly been based on weight (g) or volume (mL) instead of normalized enzyme activity units (U); (ii) the process conditions were usually different according to the optimal conditions of each protease, making pH and temperature to be also variables that influence final products; (iii) the selection was generally made using data collected from degree of hydrolysis and *in vitro* activity of hydrolysates, without

further consideration of the peptide sequences and their *in vivo* functions. In this context, an in-depth understanding of the effects of different proteases on their generated bioactive hydrolysates is necessary, where all the other reaction conditions are kept the same.

Atlantic sea cucumber (*Cucumaria frondosa*) or orange-footed sea cucumber, is an abundantly available marine specie that dwells at great depths on ocean floors on both sides of the North Atlantic, with potential as an economically important species (Gianasi et al., 2018). The latest data reported that the landing of Atlantic sea cucumber in 2008 was approximately 4,500 metric tons in western Atlantic Oceans within New Brunswick, Newfoundland, Nova Scotia in Canada, and Maine in USA (Nelson et al., 2012). Recent research has disclosed a host of bioactive compounds from it, including triterpene glycosides, cerebrosides, fucosylated chondroitin sulfate, fucoidan, sphingolipid, saponins and other metabolites, which are responsible for various bioactivities such as anti-inflammatory, anti-tumor/anti-cancer, anti-hyperglycemic, anti-coagulant, anti-thrombotic and anti-adipogenic (Janakiram et al., 2015; Jia et al., 2016; Nguyen et al., 2017; Ustyuzhanina et al., 2017; Wang et al., 2016b). There are also a few studies on the bioactivities of its enzymatic hydrolysates, including antiviral and antioxidant activities examined in the viscera/byproducts hydrolysates (Tripoteau et al., 2015; Yan et al., 2016), as well as anti-aging activity determined in the peptides from protamex-produced hydrolysates form whole *C. frondosa* (Lin et al., 2018). However, compared with other well-commercialized sea cucumber species, Atlantic sea cucumber has low economic value and is relatively underutilized (Lin et al., 2018; Nelson et al., 2012). The information on the antioxidative activity of enzyme-produced hydrolysates from its whole body is also scarce.

Currently, the bioactivities of food protein hydrolysates are mostly determined by *in vitro* tests that are performed using isolated chemicals, cells, tissues, or organs; while *in vivo* tests are used to validate the bioactivity via a living animal model that is usually a rat, and to a lesser extent clinical trial. There is little literature combining *in vitro* and *in vivo* data to compare the bioactivity from protein hydrolysates. It is worth noting that numbers of conventional *in vitro* activity studies based on peptide purification and sequencing have discovered structure–bioactivity relationships. For example, antioxidative peptides are found with specific composition (e.g., high amount of tyrosine, tryptophan, methionine, cysteine and histidine), structure and hydrophobicity (Chalamaiah et al., 2012; Sarmadi and Ismail, 2010). To date, molecular docking, an *in silico* process to screen potent bioactive compounds for new drug design and discovery, has been

successfully applied to screen enzyme inhibitors in a high-throughput way and to predict the binding interactions between the ligand (inhibitor/drug) and the receptor (enzyme, etc.) (Davies et al., 2008). Several *in vivo* enzymes are involved in antioxidative damage in human body. MPO) is one of them and it is known to stimulate oxidative stress in several inflammatory diseases such as atherosclerosis, rheumatoid arthritis, glomerulonephritis, multiple sclerosis, asthma, cystic fibrosis, diabetes mellitus and certain cancers (Davies et al., 2008; Forbes et al., 2013). Various reversible inhibitors (e.g., hydroxamates, tryptamines) and irreversible inhibitors (e.g., acetaminophen, isoniazid) have been used with varying degrees of effectiveness to nullify the effects of MPO (Forbes et al., 2013), but some of them invariably have adverse sides effects such as depression and dizziness (Ramachandran and Jaeschke, 2018; Rollas and Küçükgüzel, 2007). Recently, a peptide hLF1-11 with specific inhibition of MPO activity was found to have immunomodulatory effects (van der Does et al., 2012), and another peptide from *Volutharpa ampullacea perryi* was similarly considered as potential inhibitor to MPO enzyme using molecular docking (He et al., 2019).

In the present work, the strategy for comparing the effect of alcalase and trypsin on the antioxidative hydrolysates are summarized in **Figure 8.1**. The overall objectives were to produce antioxidative hydrolysates/peptides from Atlantic sea cucumber (the red part in **Figure 8.1**), and to evaluate the effect of alcalase and trypsin (the blue part in **Figure 8.1**). The comparison was performed by combining *in vitro* activity, *de novo* sequencing, *in silico* docking, and *in vivo* function prediction.

8.3. Materials and methods

8.3.1. Materials

Fresh *C. frondosa* samples were kindly provided by Ubisee Natural Food Inc., Quebec, Canada. Alcalase (FoodPro alkaline protease) was purchased from Danisco (Dupont, USA). Porcine pancreas trypsin was procured from ICN Biomedicals, USA. Ethylenediaminetetraacetic acid (EDTA), ethyl acetate, ferric chloride ($FeCl_3$), ferrous chloride ($FeCl_2$), ferrous sulfate ($FeSO_4$), lecithin, and Triton X-100 were purchased from Fisher Scientific. Casein, Folin reagent, trichloroacetic acid (TCA), tyrosine, 2,4,6-trinitrobenzenesulfonic acid (TNBS), sodium sulfite (Na_2SO_3), 2,2-diphenyl-1-Picrylhydrazyl (DPPH), 1,10-phenanthroline, hydrogen peroxide (H_2O_2), pyrogallol, potassium ferricyanide, and ferrozine were purchased from Sigma, USA.

8.3.2. Determination of enzyme activity

Alcalase and trypsin activities were determined by Folin-Ciocalteu method. Briefly, enzyme and casein in phosphate buffer solutions (pH 7.5) were firstly incubated at 25 ^{o}C for hydrolysis before 10% TCA was added. The precipitate was removed by centrifugation at 8000 *g*, and the supernatant was placed with 0.4 M Na_2CO_3 and Folin reagent. A blank was performed by adding 10% TCA before adding casein substrate. Absorbance was recorded at 680 nm, and a tyrosine standard graph was used for measuring enzyme activity. One enzyme activity unit was defined as the amount of enzyme to hydrolyze casein to produce a colorimetric response ($\lambda_{680\ nm}$) equivalent to 1.0 µM of tyrosine per min at pH 7.5 and 25 °C.

8.3.3. Enzymatic hydrolysates preparation and fractionation

Fresh sea cucumbers were cleaned by washing with water, then homogenized by blending. Lipids were removed by adding 95% ethanol to a final concentration of 60% (v/w) for 12 h at 4 ^{o}C. The mixture was filtered, and the residue was collected for hydrolysis. Alcalase and trypsin were added at concentrations of 0, 500, 1000, 2000, 3000 and 5000 U/g to sea cucumber homogenates. Hydrolysis was carried out at 25 ^{o}C for 2 h, the mixture was boiled at 100 ^{o}C for 1 min to inactivate the enzymes, and then filtered using vacuum filtration with 0.22 µm membrane (Millipore, USA). According to the addition concentrations of alcalase (A) and trypsin (T), hydrolysates were labeled as A_0, A_{500}, A_{1000}, A_{2000}, A_{3000}, A_{5000}, and T_0, T_{500}, T_{1000}, T_{2000}, T_{3000}, T_{5000}, respectively. Hydrolysates were freeze-dried and re-dissolved before further analysis.

The hydrolysate with the highest antioxidant activity was subjected to fractionation using ultrafiltration membranes with MW cut off (MWCO) of 10 kDa, 5 kDa, 3 kDa and 2 kDa (Millipore, USA). The 7 fractions produced were labeled as $A_{<10}$, $A_{10–5}$, $A_{<5}$, $A_{5–3}$, $A_{<3}$, $A_{3–2}$, $A_{<2}$, and $T_{<10}$, $T_{10–5}$, $T_{<5}$, $T_{5–3}$, $T_{<3}$, $T_{3–2}$, $T_{<2}$, respectively. Peptide fractions were freeze-dried and re-dissolved in distilled water before subsequent analyses.

8.3.4. Determination of hydrolysis degree

Degree of hydrolysis was determined using method of Toopcham et al. (2017) with modifications. An aliquot of 0.1 mL of hydrolysates was mixed with 2.0 mL of 0.2 M phosphate buffer (pH 8.2) and 1 mL of 0.1% TNBS solution. The reaction was carried out at 50 °C for 30 min in darkness, and 2 mL of 0.1 M Na_2SO_3 were added to terminate the reaction. The mixture was cooled down at 25 ^{o}C for 10 min, and the absorbance was measured at 420 nm. The degree of hydrolysis was calculated using Equation (1), where $A_{420\ nm,\ blank}$ is for original protein solution

before hydrolysis, and $A_{420\ nm,\ maximum}$ is for 100% hydrolysis obtained from the hydrolysates by complete acid hydrolysis.

$$\text{Degree of hydrolysis } (\%) = 100 \times \frac{A_{420nm,\ sample} - A_{420nm,\ blank}}{A_{420nm,\ maximum} - A_{420\ nm,\ blank}} \quad (1)$$

8.3.5. Determinations of antioxidant activity

The DPPH radical scavenging activity was determined based on method of Pownall et al. (2010) with slight modifications. An aliquot of 0.1 mL of hydrolysates/peptide fractions was mixed with 1 mL of 100 μM DPPH solution freshly prepared in 95% ethanol and incubated in darkness for 30 min at 25 ^{o}C. Absorbance was recorded at 517 nm. DPPH radical scavenging activity (%) was calculated using Equation (2), where $A_{517\ nm,\ control}$ was measured using distilled water instead of hydrolysate.

$$\text{DPPH radical scavenging activity } (\%) = 100 \times \frac{A_{517\ nm,\ control} - A_{517\ nm,\ sample}}{A_{517\ nm,\ control}} \quad (2)$$

The hydroxyl radical scavenging activity was measured using the method described by You et al. (2011) with slight modifications. Briefly, 600 μL of 5 mM 1,10-phenanthroline, 600 μL of 5 mM $FeSO_4$ and 600 μL of 15 mM EDTA were mixed with 400 μL of 0.2 M sodium phosphate buffer (pH 7.5). Then, 600 μL of hydrolysates/peptide fractions and 800 μL of 0.01% H_2O_2 were added. The mixture was incubated at 37 °C for 60 min, and the absorbance was measured at 536 nm. The hydroxyl radical scavenging activity was calculated via Equation (3), where $A_{536\ nm,\ control}$ was recorded using distilled water instead of hydrolysate, and $A_{536\ nm,\ blank}$ was the absorbance of blank solution containing 1,10-phenanthroline, $FeSO_4$ and EDTA.

$$\text{Hydroxyl radical scavenging activity } (\%) = 100 \times \frac{A_{536\ nm,\ sample} - A_{536\ nm,\ control}}{A_{536\ nm,\ blank} - A_{536\ nm,\ control}} \quad (3)$$

Superoxide anion scavenging activity was conducted using method described by Li (2012) with slight modifications. Exactly 0.1 mL aliquot of 60 mM pyrogallol solution freshly prepared in 1 mM HCl was mixed with 2.6 mL of 50 mM Tris-HCl buffer (pH 7.4) containing 0.5 mM EDTA. An aliquot of 0.3 mL of hydrolysates/peptide fractions was added, and absorbance was measured at 325 nm at intervals of 30 s for 5 min at 25 ^{o}C. The superoxide anion scavenging activity was calculated using Equation (4), where $\Delta A_{325\ nm,\ control}$ is the increment of absorbance measured using distilled water instead of hydrolysate, and T is 5 min.

$$\text{Superoxide anion scavenging activity } (\%) = 100 \times \frac{\frac{\Delta A_{325\ nm,\ control}}{T} - \frac{\Delta A_{325\ nm,\ sample}}{T}}{\frac{\Delta A_{325\ nm,\ control}}{T}} \quad (4)$$

Fe (III) reducing power was determined using method of Kumar et al. (2012). An aliquot of 1

mL of hydrolysates/peptide fractions was mixed with 2.5 mL of 0.2 M phosphate buffer (pH 6.6) and 2.5 mL of 1% potassium ferricyanide. The mixture was incubated at 50 ^{o}C for 30 min, and then 2.5 mL of 10% TCA were added. The mixture was centrifuged at 1650 g for 10 min at 25 ^{o}C, then 2.5 mL of the supernatant were mixed with 2.5 mL distilled water and 0.5 mL of 0.1% $FeCl_3$, and reacted for 10 min at 25 ^{o}C. The absorbance at 700 nm was measured as index of the reducing power.

The Fe(II) chelating activity was determined by monitoring the formation of Fe^{2+}-ferrozine complex using a modified method of Pownall et al. (2010). An aliquot of 1 mL of hydrolysate/peptide fraction was mixed with 0.05 mL of 2 mM $FeCl_2$, 0.5 mL distilled water, and 0.1 mL 5 mM ferrozine solution. The mixture was incubated in darkness for 10 min at 25 ^{o}C, and the absorbance at 562 nm was measured. Fe (II) chelating activity was calculated as Equation (5), where $A_{562\ nm,\ control}$ was measured using distilled water instead of hydrolysate.

$$\text{Fe (II) chelating activity (\%)} = 100 \times \frac{A_{562\ nm,\ control} - A_{562\ nm,\ sample}}{A_{562\ nm,\ control}} \quad (5)$$

8.3.6. Determination of amino acids composition

To analyze amino acids in high sensitivity, ACQUITY ultra-performance liquid chromatography (UPLC) system (Waters, MA, USA) equipped with Pico-Tag system and ACQUITY BEH C18 column (2.1 mm × 10 cm, Waters, MA, USA) was used. Peptide powders were subjected to vapor phase hydrolysis by 6 M HCl with 1% phenol at 110 °C for 24 h under N_2 atmosphere. Samples for cysteine analyses were firstly subjected to performic acid oxidation, and then acid hydrolysis. Samples for tryptophan analyses were subjected to hydrolysis by 4.2 M NaOH at 110 °C for 24 h. The hydrolysates were washed, re-dried, and derivatized with phenylisothiocyanate (PITC, Waters, MA, USA). The formed phenylthiocarbamoyl (PTC)-amino acids were dissolved in phosphate buffer (pH 7.4) and measured at 254 nm. Pierce amino acid standard H was used as calibration standard. The elution conditions were: column temperature 48 ^{o}C; eluent A contained 0.14 M sodium acetate (pH 6.0), 0.05% triethylamine, 6% acetonitrile (Waters, MA, USA); eluent B contained 60% acetonitrile in water (Waters, MA, USA). A gradient elution with eluent B increasing was employed. Data was collected and analyzed using Empower 2 software (Waters, MA, USA).

8.3.7. *De novo* sequencing of peptides using LC–MS/MS

Hydrolysates were solubilized in 5% acetonitrile (ACN)-0.2% formic acid (FA). The samples were loaded on a C_{18} precolumn (0.3 mm inside diameter [i.d.] by 5 mm) connected directly to the

switching valve. They were separated on a reversed-phase column (150-μm i.d. by 150 mm) with a 56 min gradient from 10 to 30% ACN-0.2% FA and a 600 nL/min flow rate on a Nano-LC-Ultra-2D (Eksigent, Dublin, CA) connected to a Q-Exactive Plus (Thermo Fisher Scientific, San Jose, CA). Each full MS spectrum acquired at a resolution of 70,000 was followed by 12 tandem MS spectra on the most abundant multiply charged precursor ions. Tandem MS experiments were performed using collision-induced dissociation (CID) at a collision energy of 25%. The data were processed using PEAKS 8.5 (Bioinformatics Solutions, Waterloo, ON). Mass tolerances on precursor and fragment ions were 10 ppm and 0.01 Da, respectively. Variable selected posttranslational modifications were carbamidomethyl (C), oxidation (M), deamidation (NQ), and phosphorylation (STY). The data were visualized with Scaffold 4.3.0 (protein threshold, 99%, with at least 2 peptides identified and a false-discovery rate [FDR] of 0.1% for peptides).

8.3.8. Physicochemical property analyses of peptides

The peptide sequences identified using LC–MS/MS were submitted to web-based peptide sequence analyses tool ExPASy ProtParam (http://web.expasy.org/protparam/). The amino acid composition and "grand average of hydropathy" (GRAVY) score for each peptide sequence was collected, where a higher GRAVY value indicates more hydrophobicity of the peptide.

8.3.9. Molecular docking of peptides on MPO enzyme

Human MPO enzyme with characterized crystal structure (Carpena et al., 2009) (PDB ID: 3F9P) was used as receptor for the molecular docking for each peptide (ligand) identified using LC-MS/MS. Discovery Studio software (Accelrys, San Diego, CA, USA) was used to perform the molecular docking. The 3D structure of MPO was optimized at first using Prepare Protein program to minimize the energy, protonize and remove water molecules. CDOCKER docking program, using a molecular dynamics simulated-annealing-based algorithm, was applied to determine the interaction of peptide and MPO. The setting of the performance parameters followed our previous study (He et al., 2019), and a peptide hLF1-11 (GRRRRSVQWCA) derived from the N terminus of human lactoferrin that has shown inhibition activity on MPO (van der Does et al., 2012), was used as reference to select the potential peptide sequences that have inhibitory interaction with MPO.

8.3.10. Statistical analysis

Triplicate measurements were performed for the anti-oxidant property determinations, and the results were given as mean ± SD. The significance was analyzed using SPSS 12.0 (SPSS Inc, IL,

USA) with significance level of * $p<0.05$, ** $p<0.01$, and *** $p<0.001$.

8.4. Results and discussion

8.4.1. Hydrolysis of Atlantic sea cucumber

Alcalase and trypsin are proteases that catalyze the hydrolysis of proteins into peptides and amino acids. As shown in **Figure 8.2a**, alcalase-produced hydrolysates involved higher degree of hydrolysis than trypsin-produced ones, especially when enzyme addition was above 1000 U/g ($p<0.05$). Alcalase is a non-specific protease that randomly cleaves peptide bonds to produce various peptides and amino acids. On the contrary, trypsin is specific to basic amino acids residues, so the amount of basic amino acids composed in Atlantic sea cucumber could limit its hydrolytic efficiency. With the increase of enzyme addition from 500 to 3000 U/g, the degree of hydrolysis increased significantly ($p<0.05$), for both alcalase and trypsin-produced hydrolysates. There was no significant difference between the enzyme addition of 3000 and 5000 U/g, which produced hydrolysis degree of 81.37 ± 1.32% and 80.92 ± 1.10% for A_{3000} and A_{5000}, respectively, as well as 53.31 ± 1.17% and 55.92 ± 1.61% for T_{3000} and T_{5000}, respectively.

8.4.2. Effect of enzyme addition on antioxidant activity of hydrolysates

Five antioxidant activities were determined on alcalase and trypsin-produced hydrolysates (A_0, A_{500}, A_{1000}, A_{2000}, A_{3000}, A_{5000}, and T_0, T_{500}, T_{1000}, T_{2000}, T_{3000}, T_{5000}). There was constant trend shown in **Figures 8.2b–f** that the activities increased from no enzyme addition to the enzyme addition of 2000 or 3000 U/g, and then decreased with further enzyme addition up to 5000 U/g. The water extract of Atlantic sea cucumber, i.e., A_0 and T_0 hydrolysate samples showed lower antioxidant activities than the enzymatic hydrolysates ($p>0.05$). This bioactivity may come from the component profile of sea cucumber water extract including vitamin B, minerals, triterpene glycosides, peptides, etc., as well as some water-insoluble compounds such as sterols and phospholipids released via water extraction (Bordbar et al., 2011). For Atlantic sea cucumber species, the water/organic extract was previously determined with flavonoids that exhibited antioxidant activity (Mamelona et al., 2007).

Generally, alcalase-produced hydrolysates had higher antioxidant activity than trypsin-produced hydrolysates, when enzymes were added at the same activity levels (**Figures 8.2 b**, **d** & **f**). The exception was observed on the hydroxyl scavenging activity and Fe (III) reducing power of hydrolysates that varied randomly with the enzyme type and enzyme addition (**Figures 8.2 c** & **e**). When enzyme addition was high as 3000 and 5000 U/g, the effect of enzyme type, i.e., adding

alcalase or trypsin, significantly influenced the antioxidant activity of produced hydrolysates (p<0.05, 0.01 or 0.001) as shown in **Figures 8.2 b**, **d**, **e** & **f**. Alcalase was found superior to trypsin on generating antioxidant hydrolysates from Atlantic sea cucumber viscera when the enzymes were added based on their optimum conditions (Yan et al., 2016). In this study, alcalase and trypsin were added with the same activity (U), and it was found that alcalase is a better choice to produce antioxidative hydrolysates from Atlantic sea cucumber.

Among the alcalase-produced hydrolysates, A_{3000} had the highest DPPH radical scavenging activity (p<0.05; **Figure 8.2b**), hydroxyl radical scavenging activity (**Figure 8.2c**), superoxide anion scavenging activity (p<0.05; **Figure 8.2d**) and Fe (II) chelating activity (p<0.05; **Figure 8.2f**); while A_{1000} and A_{2000} had relatively high Fe (III) reducing power (p<0.05; **Figure 8.2e**). For trypsin-produced hydrolysates, the highest DPPH radical scavenging activity (Figure 2b), hydroxyl radical scavenging activity (p<0.05; **Figure 8.2c**), superoxide anion scavenging activity (p<0.05; **Figure 8.2d**) were found in T_{2000}; the highest Fe (III) reducing power (p<0.05; **Figure 8.2e**) and Fe (II) chelating activity (p<0.05; **Figure 8.2f**) were found in T_{3000}. Increasing the addition of enzymes increased the degree of hydrolysis, and it contributed to the improvement of the antioxidant property of hydrolysates; however, extensive hydrolysis could have negative effect on antioxidant property, which suggested that the antioxidant property of hydrolysates also depend on other factors such as peptide sequence and structure. Based on the results, A_{3000} and T_{2000} hydrolysates were selected for the fractionation using ultrafiltration.

8.4.3. Effect of peptide MW on antioxidant activity

The antioxidant activity of the peptide fractions ($A_{<10}$, $A_{10–5}$, $A_{<5}$, $A_{5–3}$, $A_{<3}$, $A_{3–2}$, $A_{<2}$, and $T_{<10}$, $T_{10–5}$, $T_{<5}$, $T_{5–3}$, $T_{<3}$, $T_{3–2}$, $T_{<2}$, 0.5 mg/mL) are shown in **Figures 8.3 a–e**. Compared with the crude hydrolysates (1.0 mg/mL) before ultrafiltration in **Figures 8.2 b–f**, the peptide fractions showed comparable or even higher antioxidant activity, which agreed with previous studies that lower MW hydrolysates produced higher antioxidant activity (Chalamaiah et al., 2012). From **Figure 8.3**, there seemed to be no constant relation between the antioxidant activity and MW of peptides; however, a few alcalase-produced peptide fractions showed significantly higher antioxidant activities than trypsin-produced counterparts regarding free radical scavenging activities (**Figures 8.3 a**, **b** and **c**). Fe (III) reducing power of trypsin-produced peptide fractions T_{5-3}, $T_{<3}$ and T_{3-2} were significantly (p<0.05) higher than their corresponding alcalase-produced fractions; moreover, no significant difference was found for Fe (II) chelating activity. Peptides with lower MW could

interact more efficiently with free radicals and are easier to pass through intestinal barrier to exert antioxidant capacity *in vivo* (Sarmadi and Ismail, 2010). For the $A_{<2}$ and $T_{<2}$ peptide fractions, the DPPH radical scavenging activity, hydroxyl radical scavenging activity, superoxide anion scavenging activity, Fe (III) reducing power and Fe (II) chelating activity, were 88% and 65% (p<0.01), 52% and 42% (p<0.05), 59% and 48% (p<0.01), 0.063 and 0.066, 58% and 57%, respectively, suggesting $A_{<2}$ fraction had higher antioxidant activity than $T_{<2}$.

8.4.4. Essential versus non-essential amino acids

To evaluate peptide fractions $A_{<2}$ and $T_{<2}$, total amino acid profiles are provided in **Table 8.1** which lists the amino acids compositions of $A_{<2}$ and $T_{<2}$ peptide fractions in terms of numbers (per 1000 amino acids) and concentration (g/100 g protein). A high content of leucine (110/1000, 11.44 g), serine (108/1000, 8.64 g), valine and alanine (98/1000, 8.99 g, and 98/1000, 6.40 g, respectively) were found in $A_{<2}$ fraction; while $T_{<2}$ peptide fraction had a high content of arginine (123/1000, 16.79 g) followed by leucine (95/1000, 9.42 g). The apparently high content of arginine in $T_{<2}$ when compared to $A_{<2}$ is attributed to the specificity of trypsin on peptide bonds involving arginine and lysine. Some amino acids such as tryptophan, histidine and cysteine showed relatively low content in both $A_{<2}$ and $T_{<2}$ peptide fractions.

In general, both $A_{<2}$ and $T_{<2}$ were rich in leucine, which is a key amino acid that stimulates protein synthesis *in vivo* (Columbus et al., 2015). Leucine, along with isoleucine and valine, are branched–chain amino acids (BCAA) that have showed impact on human health such as regulating blood sugar levels and reducing physical and mental fatigue (Zhang et al., 2017a). $A_{<2}$ fraction contained higher number of BCAA (265/1000, 26.42 g), compared with $T_{<2}$ fraction that had BCAA of 192/1000 and 18.30 g. Different from this present result, previous studies on Atlantic sea cucumber found a high content of glutamic acid and glycine for body wall (Zhong et al., 2007), and a high content of glutamic acid and aspartic acid for the viscera (Mamelona et al., 2010); however, those were all non-essential amino acids (NEAA). Thus, the present research suggested that enzymatic hydrolysis combined with ultrafiltration may be useful to increase the essential amino acids (EAA) composition in final peptide products. The EAA and NEAA ratio, reflecting the quality of protein products, was found higher in $A_{<2}$ than $T_{<2}$ (**Table 8.1**), indicating that $A_{<2}$ had higher nutritional value than $T_{<2}$. Moreover, both $A_{<2}$ and $T_{<2}$ contain amino acid residues, such as tyrosine, methionine, histidine, cysteine, etc., that contribute to antioxidant activity (Chalamaiah et al., 2012).

8.4.5. Peptide sequences

The $A_{<2}$ and $T_{<2}$ peptide fractions were subjected to LC–MS/MS and their total ion chromatograms (**Figure 8.4**) showed that their retention time scales of the peptides were different. The peptide sequence were determined by *de novo* sequencing, and all the sequences with the average local confidence (ALC; the average of the local confidence of all amino acids in the sequence) ≥ 75% are listed in **Table 8.2**, as high ALC values indicate high confidence considering a peptide as correctly sequenced (Song et al., 2017). In total, there were 48 and 254 peptide sequences selected for $A_{<2}$ and $T_{<2}$ fractions, respectively, and they were labelled as $A_{<2}$ #1–48 and $T_{<2}$ #1–254 based on their ALC scores. Several factors can decrease the reliability of peptide sequencing such as isobaric amino acids existed in sequence and side-chain reactions (Medzihradszky and Chalkley, 2015). The MS/MS spectra of $A_{<2}$ #1 and $T_{<2}$ #1 peptides with the highest ALC values of 97, respectively, are depicted in **Figure 8.5** where *m*/*z* 393.681 corresponds to sequence YDWRF in $A_{<2}$ peptide fraction, and *m*/*z* 351.699 corresponds to sequence VELWR in $T_{<2}$ peptide fraction.

Table 8.2 showed that the molecular masses of the sequences ranged from 636 to 1388 Da for $A_{<2}$ peptide fraction, and from 698 to 2286 Da for $T_{<2}$ peptide fraction; moreover, the sequences in $A_{<2}$ were made of 5–12 amino acid residues while the sequences in $T_{<2}$ contained 5–21 amino acid residues. Results suggested that alcalase produced overall smaller and shorter peptides than trypsin, which might be due to the non-specificity of alcalase that allows more random and extensive cleavages of peptide bonds in Atlantic sea cucumber protein matrix. Peptides with smaller MW or shorter lengths exhibited higher antioxidant properties (Chalamaiah et al., 2012), which could explain their *in vitro* antioxidant activity results in **Figure 8.3** that $A_{<2}$ peptide fraction generally had stronger antioxidant activity than $T_{<2}$. In addition, the amino acid residues on the C–terminals of $A_{<2}$ peptides were diverse; while the sequences in $T_{<2}$ fraction had only arginine (R) or lysine (K) residues on their C–terminals. Specifically, 171 sequences had R on their C–terminals and 83 sequences had K on their C–terminals, respectively, which was probably because of the more arginine residues (123/1000) composed in $T_{<2}$ fraction compared with lysine residues (34/1000) from **Table 8.1**.

8.4.6. Comprehensive evaluation on the antioxidative peptides

8.4.6.1. Based on physiochemical property

A few amino acid residues, especially cysteine (C), histidine (H), methionine (M), tryptophan

(W) and tyrosine (Y) have been intensively investigated for their contributions to the antioxidant property of proteins/peptides (Matsui et al., 2018). The composition of these 5 amino acids in each peptide sequence are listed in **Table 8.2**. There were 24 sequences selected for $A_{<2}$ and 115 sequences for $T_{<2}$ with a proportion of 50.0% and 45.3%, respectively (**Figure 8.6**). It indicated that alcalase-produced hydrolysates from Atlantic sea cucumber contained more potential antioxidative peptides than the trypsin-produced hydrolysates, which agreed with results in **Figure 8.3** that $A_{<2}$ peptide fraction generally had higher *in vitro* antioxidant activity than $T_{<2}$ peptide fraction. Cysteine residue is capable of scavenging free radicals and binding metal ions due to its unique ionizable thiol group (Poole, 2015), but it was found the least abundant key antioxidative amino acids in $A_{<2}$ and $T_{<2}$. Only 2 and 5 peptide sequences contained cysteine residues in $A_{<2}$ and $T_{<2}$, respectively. Sequences containing histidine were also few, i.e., 6 sequences in $A_{<2}$ and 7 sequences in $T_{<2}$. Histidine can interact with metal ions and reactive oxygen species (ROS) with its imidazole ring (Ihara et al., 2019). Methionine has reactivity towards specific oxidants due to its unique thioether group but it has lower nucleophilicity compared to cysteine (Manta and Gladyshev, 2017). Among the 8 sequences containing methionine in $A_{<2}$ fraction, #12 peptide had the highest percentage of 33.33%; and there were 51 sequences containing methionine in $T_{<2}$ fraction. Tryptophan, a non-polar aromatic amino acid, was found in 11 sequences in $A_{<2}$ from which the #17 & #38 peptides had the highest content of 40%; and in 41 sequences in $T_{<2}$ where some peptides had the highest content of 20%. Tryptophan has side chain indole, that can scavenge radicals via electron donation (Estevão et al., 2010). Another aromatic amino acid, tyrosine, exhibits ability to scavenge ROS by losing the hydrogen atom from its phenolic hydroxyl group (Torkova et al., 2015). There were 5 sequences with tyrosine residue in $A_{<2}$ fraction and 32 sequences in $T_{<2}$ fraction. By putting these 5 key antioxidative amino acids together, reference peptide had 18.2% of cysteine and tryptophan; $A_{<2}$ fraction contained more sequences with high content of the key amino acids, e.g., #1, #17, #38 & #41 peptides with amount of 40%, #34 peptide with 42.86%, #36 peptide with 44.44%, and #12 with 50%; however, $T_{<2}$ fraction had only #180 & #214 peptides with amount of 40%. Besides, a high hydrophobicity was usually found with antioxidative peptides. $A_{<2}$ #12 peptide and $T_{<2}$ #114 peptide had the highest GRAVY values of 1.233 and 1.708, respectively, exhibiting the largest hydrophobicity; while reference peptide had a GRAVY value of –1.373. Hydrophobic peptides are believed to enhance *in vivo* antioxidant effect by getting through cell membrane to target organs, as well as to enhance their interaction

with hydrophobic radicals (Liu et al., 2018).

8.4.6.2. Based on molecular docking

There were 41 peptide sequences in $A_{<2}$ fraction and 211 peptide sequences in $T_{<2}$ fraction successfully docked with MPO enzyme, while the sequences that failed the docking were labelled as "F". The (−)CDOCKER energy is negative, and thus higher (−)CDOCKER energy value indicates easier binding. The 41 and 211 sequences in $A_{<2}$ and $T_{<2}$ peptide fractions totally produced 332 and 1712 docking poses, respectively (data not shown), and the pose with the highest (−)CDOCKER energy value for each peptide sequence are listed in **Table 8.2**.

Reference peptide GRRRRSVQWCA had value of 10.2023 for (−)CDOCKER energy. All peptides with (−)CDOCKER energy higher than 10.2023 were considered as potential inhibitors to MPO enzyme. After screening based on this, there were 38 sequences and 187 sequences in $A_{<2}$ and $T_{<2}$ fractions selected, which made up 79.2% and 73.6% of total identified sequences for $A_{<2}$ and $T_{<2}$, respectively (**Figure 8.6**). Results indicated that alcalase produced higher percentage of peptides with potential *in vivo* antioxidant activity by inhibiting MPO compared with trypsin. **Figure 8.6** shows the collection relation of 3 sets, i.e., the peptide sequences by *de novo* sequencing, the peptide sequences with key antioxidant amino acids, and peptide sequences as potential MPO inhibitors. The overlapped circles exhibiting sequences with key amino acids, as potential MPO inhibitors, or both, were observed larger in size for of $A_{<2}$ fraction (35.4%) than $T_{<2}$ fraction (30.3%), suggesting that alcalase-produced peptide within 2 kDa had higher percentage of peptides with antioxidant activity compared with alcalase-produced peptide.

8.4.6.3. Based on interactions with MPO

One peptide sequence each was selected from $A_{<2}$ and $T_{<2}$ for the interaction study with MPO molecule. From **Table 8.2**, $A_{<2}$ #9 peptide, Thr–Glu–Phe–His–Leu–Leu, had the least docking energy among all other peptides in $A_{<2}$, with (−)CDOCKER energy value of 133.559 and contained 16.67% of histidine; while $T_{<2}$ #127 peptide, Glu–Glu–Glu–Leu–Ala–Ala–Leu–Val–Leu–Asp–Asn–Gly–Ser–Gly–Met–Cys–Lys, had the least docking energy in $T_{<2}$ with a (−)CDOCKER energy value of 221.295 and contained 5.88% of cysteine and 5.88% of methionine. These 2 peptides were potentially good ligands for binding MPO, and it could be inferred from the docking energy that $T_{<2}$ #127 peptide was a stronger inhibitor to MPO, and thus may have better *in vivo* antioxidative function than $A_{<2}$ #9 peptide. The interactions between peptides and the active site of MPO are shown in **Figure 8.7**. Both peptides could block the active site cavity of MPO (figure

not shown), which can result in the inhibition of MPO by preventing the approach of substrates. As seen from the 3D interactions, $T_{<2}$ #127 peptide had a relatively relaxing pose (**Figure 8.7b**, left) in the docking pocket compared with $A_{<2}$ #9 peptide (**Figure 8.7a**, left). A high internal strain energy of peptide ligand, along with a high ligand–receptor interaction energy would negatively affect the docking.

There are 4 weak interactions observed from the docking, i.e., van der Waals, hydrogen bonds, hydrophobic and electrostatic interactions between the peptides and the active site located on A, B, C, D chains of MPO. For $A_{<2}$ #9 peptide (**Figure 8.7a**, right), there were 14 van der Waals (with PHE29, TRP32, LEU33 on A chain, PHE29, VAL30 on B chain, THR159, ARG161, ASP321 on C chain, CYS153, ILE160, ASN162, THR159, PHE439, LYS505 on D chain); 9 hydrophobic alkyl/pi-alkyl interactions (with ALA28, ARG31, PRO34, ALA35 on A chain, ALA28 on B chain, ILE160 on C chain, ALA152 on D chain); 8 hydrogen bonds (with ARG31 on A chain, ARG31, TRP32, LEU33, PRO34 on B chain, ARG323 on D chain); and 5 electrostatic interactions (ARG323, LYS505 on C chain, ASP321, ARG323 on D chain). A few amino acid residues were involved in more than one interaction type. For example, $A_{<2}$ #9 peptide formed hydrogen bond from its O15 atom on –C=O group with the –NH group of ARG31 on A chain, but also formed 2 hydrophobic alkyl interactions with ARG31 on A chain of MPO. For $T_{<2}$ #127 peptide (**Figure 8.7b**, right), there were 26 van der Waals (with VAL 30, TRP32, LEU33 on A chain, PHE29, TRP32, LEU33, ALA35, PHE41, PRO103 on B chain, CYS153, THR159, ASN162, ARG438, CYS440, GLY441, THR501, LYS505 on C chain, PRO123, PRO124, ARG148, PRO154, GLY155, SER156, THR159, ARG323, PHE439 on D chain); 12 hydrophobic alkyl/pi-alkyl interactions (with ARG31, PRO34 on A chain, ALA28, VAL30, ARG31, PRO34 on B chain, ILE160, TYR300, PHE439, CYS497 on C chain, PRO151 on D chain); 16 hydrogen bonds (with ARG31, SER42 on B chain, ALA152, CYS153, THR159, ILE160, ARG161, ASN162 on D chain); and 4 electrostatic interactions (LYS308, ARG323 on C chain). Similarly, the $T_{<2}$ #127 peptide formed 2 hydrophobic and 2 hydrogen bonds with ARG31 residue on B chain of MPO. Residue CYS153 on D chain formed 2 conventional hydrogen bonds via its –NH group with the O166 and O173 atoms on peptide, as well as 1 carbon hydrogen bond via its –C=O group with H180 on peptide. Thus, $T_{<2}$ #127 peptide formed more interactions with the active site of MPO molecule than $A_{<2}$ #9 peptide.

8.5. Conclusion

Alcalase and trypsin were used to hydrolyze Atlantic sea cucumber based on equivalent activity units. Atlantic sea cucumber is a good source for functional food development and its value can be enhanced via enzymatic treatment. Alcalase-produced hydrolysates showed generally higher antioxidant activity than the trypsin produced ones, but the concentration of trypsin addition is lower compared with that of alcalase to achieve the highest antioxidant activity. The peptide fractions produced after ultrafiltration showed comparable or even higher antioxidant activity than the crude hydrolysates. $A_{<2}$ and $T_{<2}$ peptide fractions contained high content of leucine, and $A_{<2}$ fraction had higher nutritional value than $T_{<2}$ based on the EAA/NEAA ratio. For the identified peptide sequences, alcalase-produced $A_{<2}$ fraction generated larger proportion of peptides with key antioxidative amino acids, as well as potential inhibition effect on MPO, compared with trypsin-produced $T_{<2}$ fraction. According to molecular docking prediction, weak interactions including van der Waals, hydrogen bonds, hydrophobic and electrostatic interactions were found with each chain of MPO enzyme that are responsible for inhibition effect on MPO.

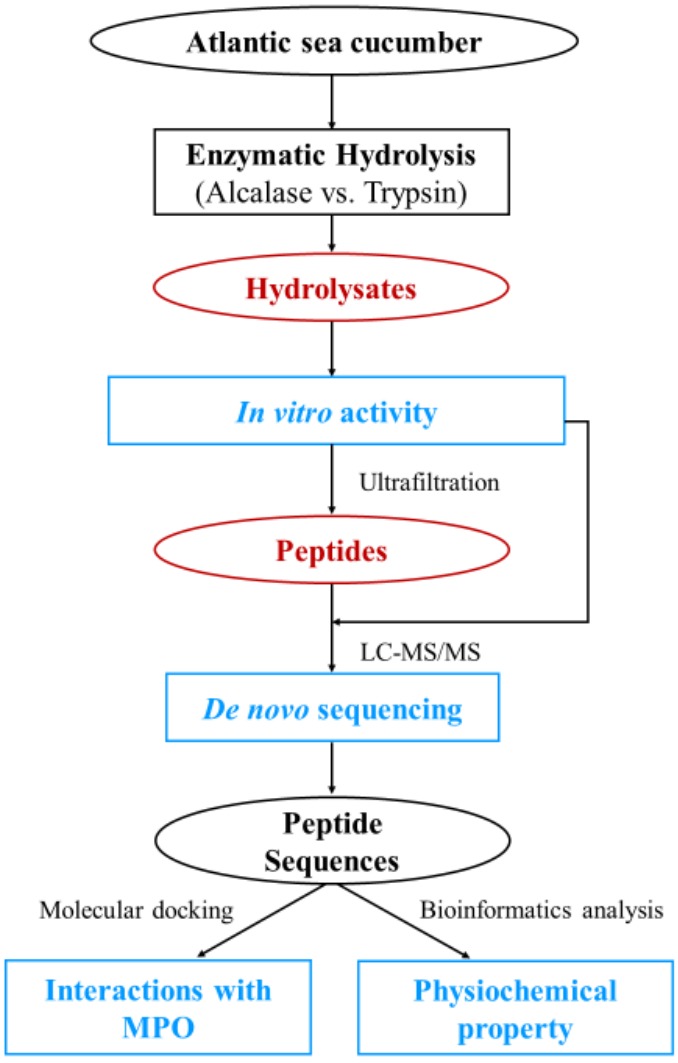

Figure 8.1. The strategy of the present work.

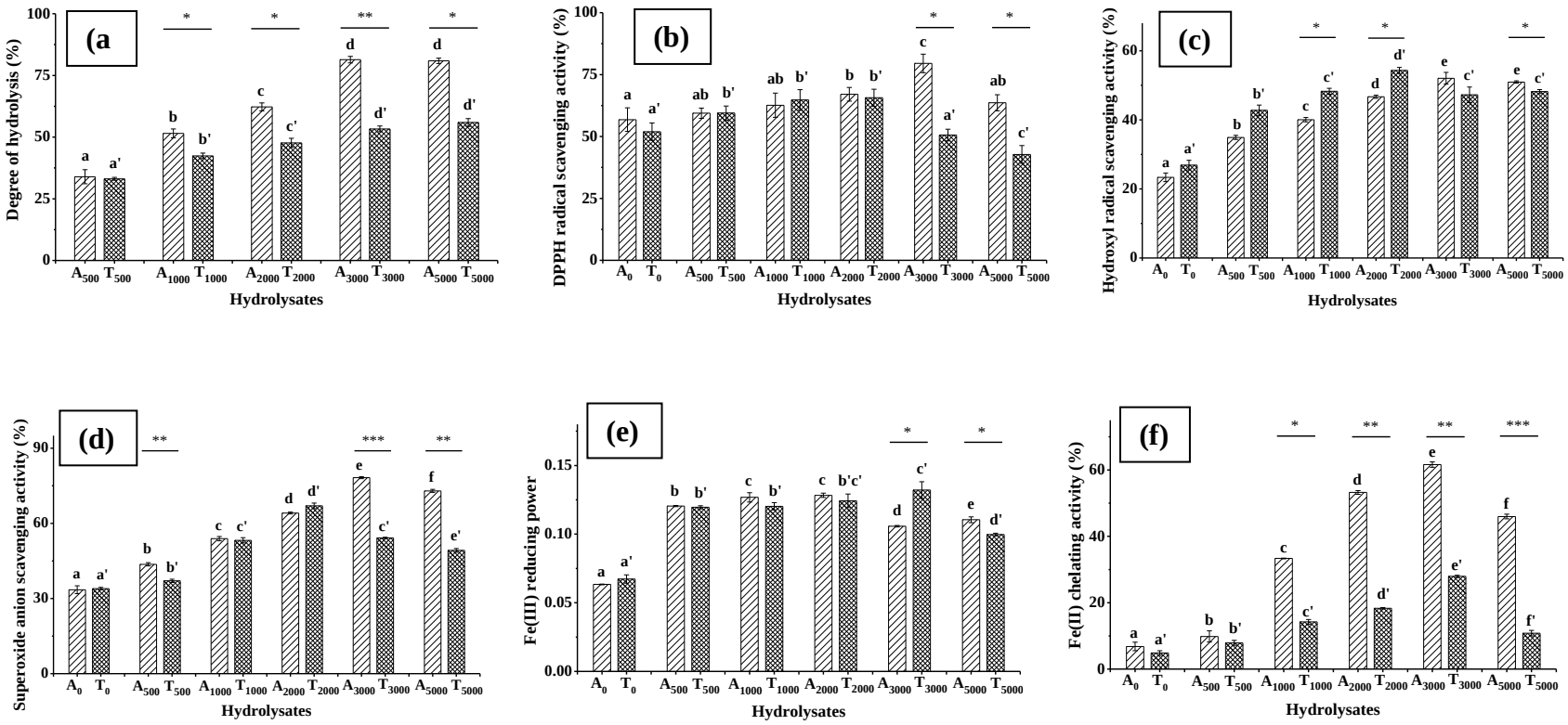

Figure 8.2. The **(a)** degree of hydrolysis, **(b)** DPPH radical scavenging activity, **(c)** hydroxyl radical scavenging activity, **(d)** superoxide anion scavenging activity, **(e)** Fe (III) reducing power, **(f)** Fe (II) chelating activity of hydrolysates produced from alcalase (A) and trypsin (T), respectively, at concentrations of 0, 500, 1000, 2000, 3000 and 5000 U/g, respectively.

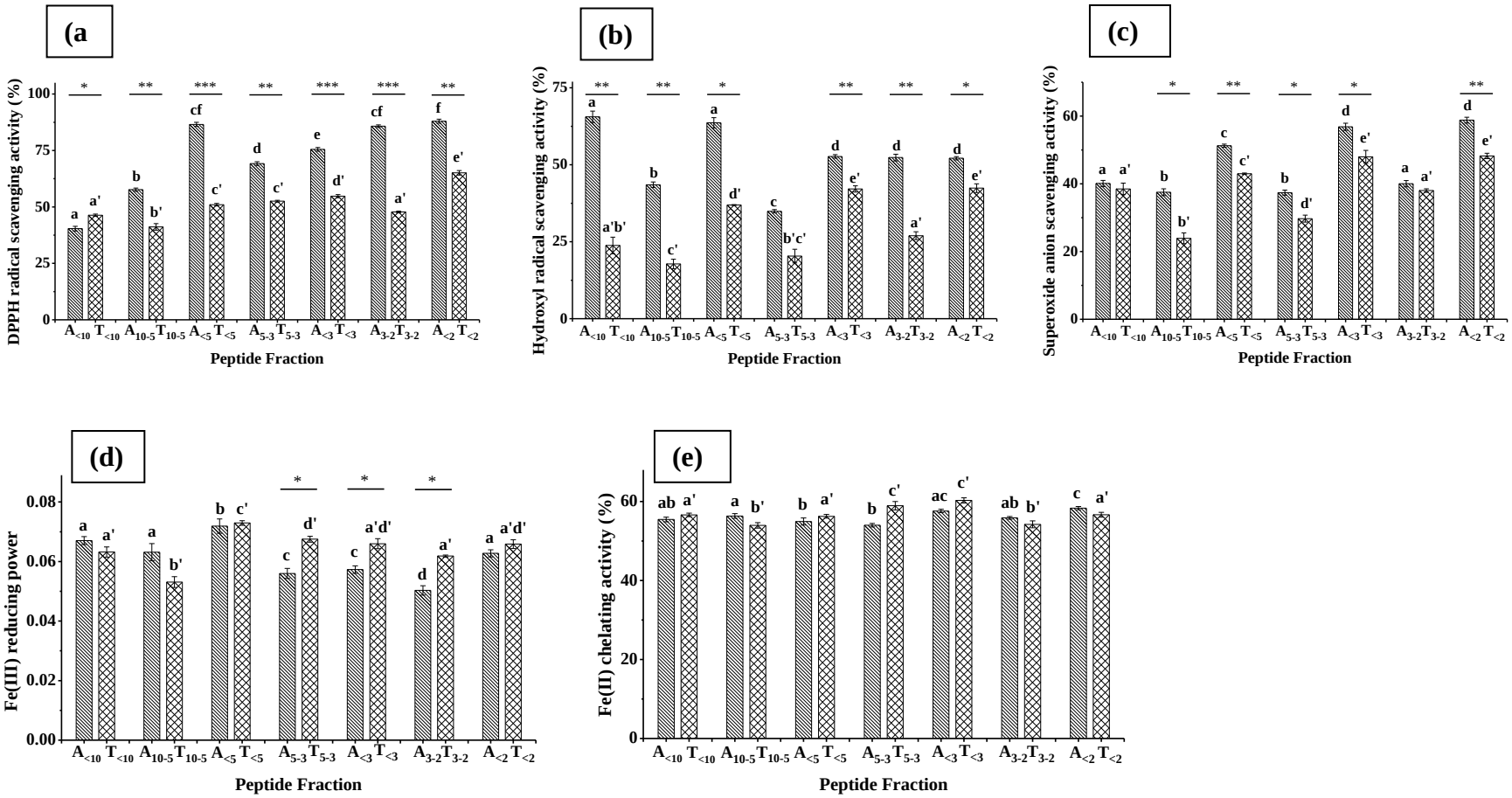

Figure 8.3. The **(a)** DPPH radical scavenging activity, **(b)** hydroxyl radical scavenging activity, **(c)** superoxide anion scavenging activity, **(d)** Fe (III) reducing power and **(e)** Fe (II) chelating activity of peptide fractions generated by alcalase (A) and trypsin (T), respectively, with MW < 10, 10–5, < 5, 5–3, < 3, 3–2 and < 2 kDa.

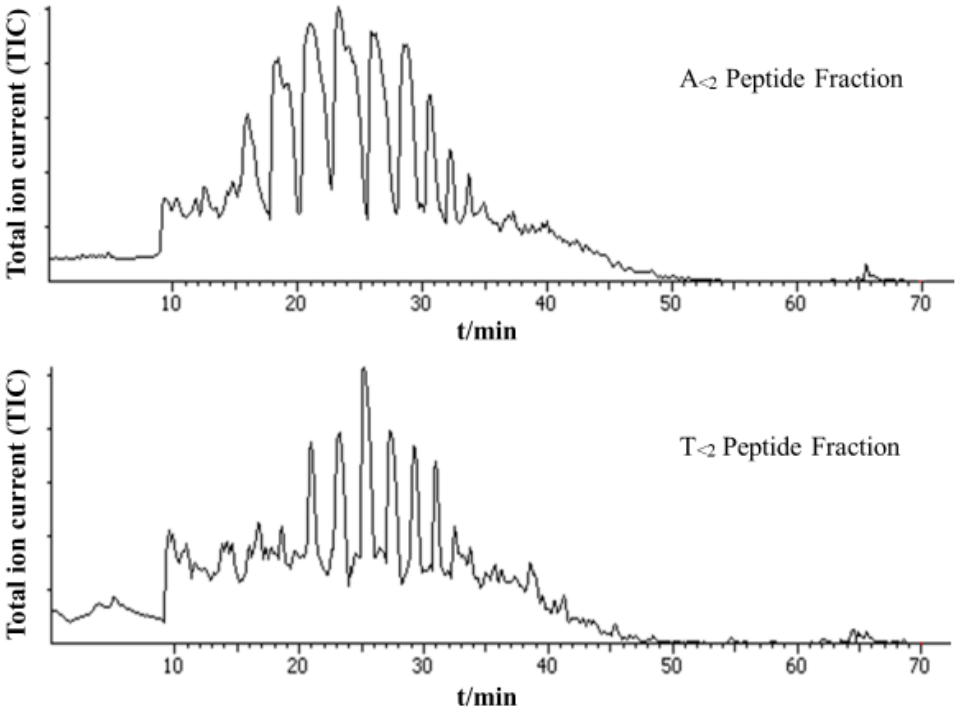

Figure 8.4. Total ion current (TIC) chromatograms of $A_{<2}$ and $T_{<2}$ peptide fractions, respectively.

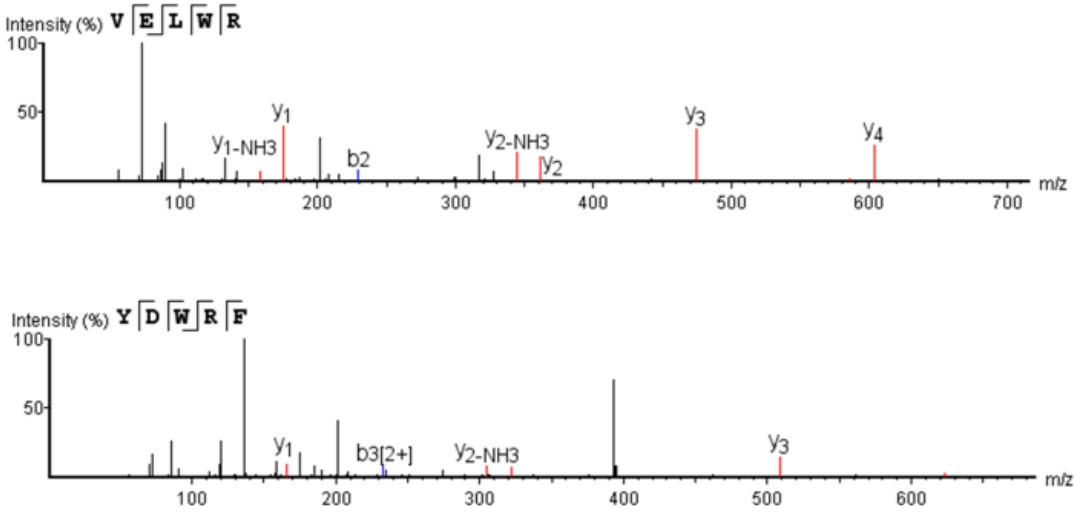

Figure 8.5. MS/MS spectra of the peptide with the highest average local confidence (ALC), i.e., YDWRF in $A_{<2}$ peptide fraction, and VELWR in $T_{<2}$ peptide fraction.

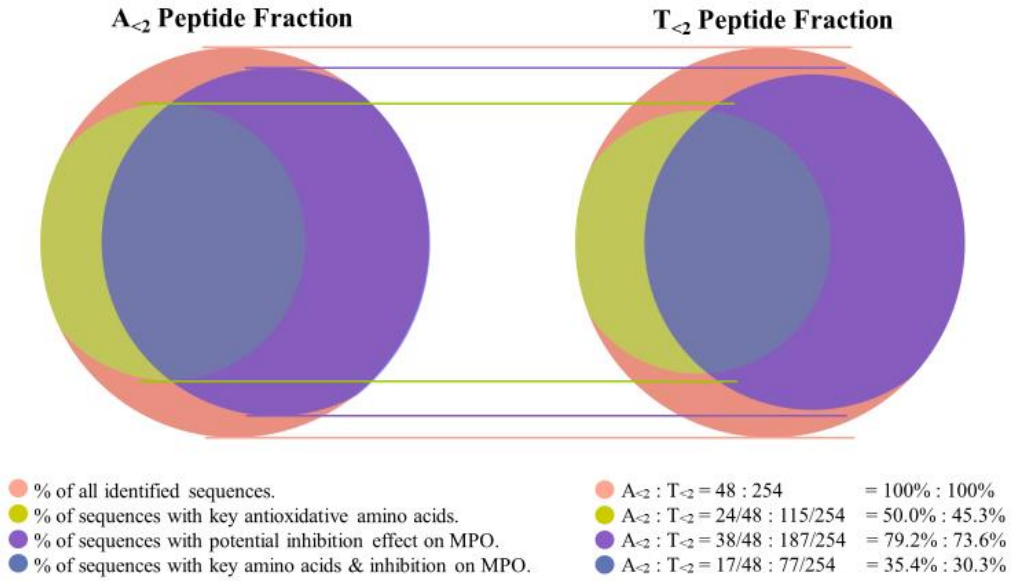

Figure 8.6. Venn diagrams displaying the proportion of peptide sequences with key antioxidative amino acid residues, inhibition potential on myeloperoxidase (MPO) and the overlaps, in $A_{<2}$ and $T_{<2}$ peptide fractions, respectively.

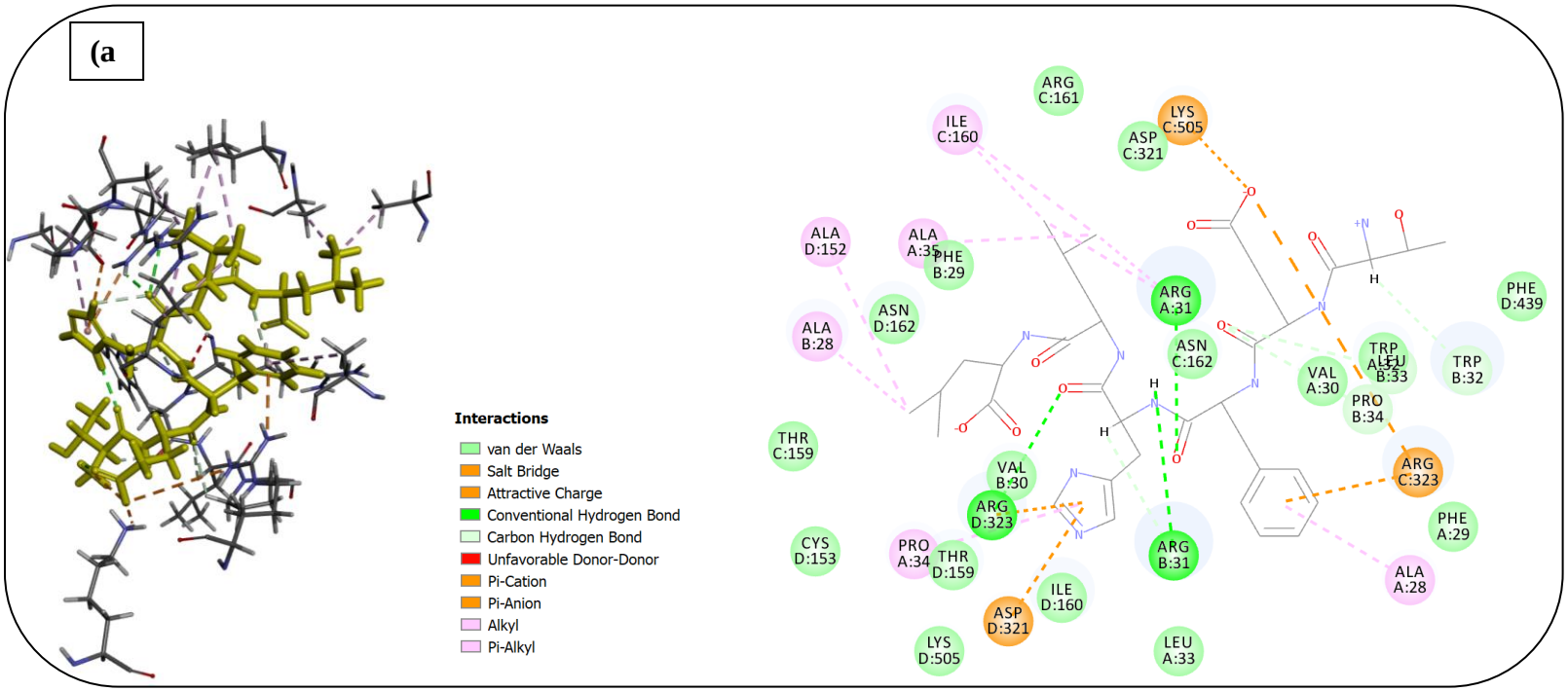
(a
Interactions
van der Waals
Salt Bridge
Attractive Charge
Conventional Hydrogen Bond
Carbon Hydrogen Bond
Unfavorable Donor-Donor
Pi-Cation
Pi-Anion
Alkyl
Pi-Alkyl
ARG C:161
ILE C:160
LYS C:505
ASP C:321
ALA D:152
ALA A:35
PHE B:29
ARG A:31
PHE D:439
ASN D:162
ALA B:28
ASN C:162
TRP B:32
VAL A:30
PRO B:34
THR C:159
VAL B:30
ARG C:323
ARG D:323
PHE A:29
CYS D:153
PRO A:34
THR D:159
ARG B:31
ILE D:160
ALA A:28
ASP D:321
LYS D:505
LEU A:33

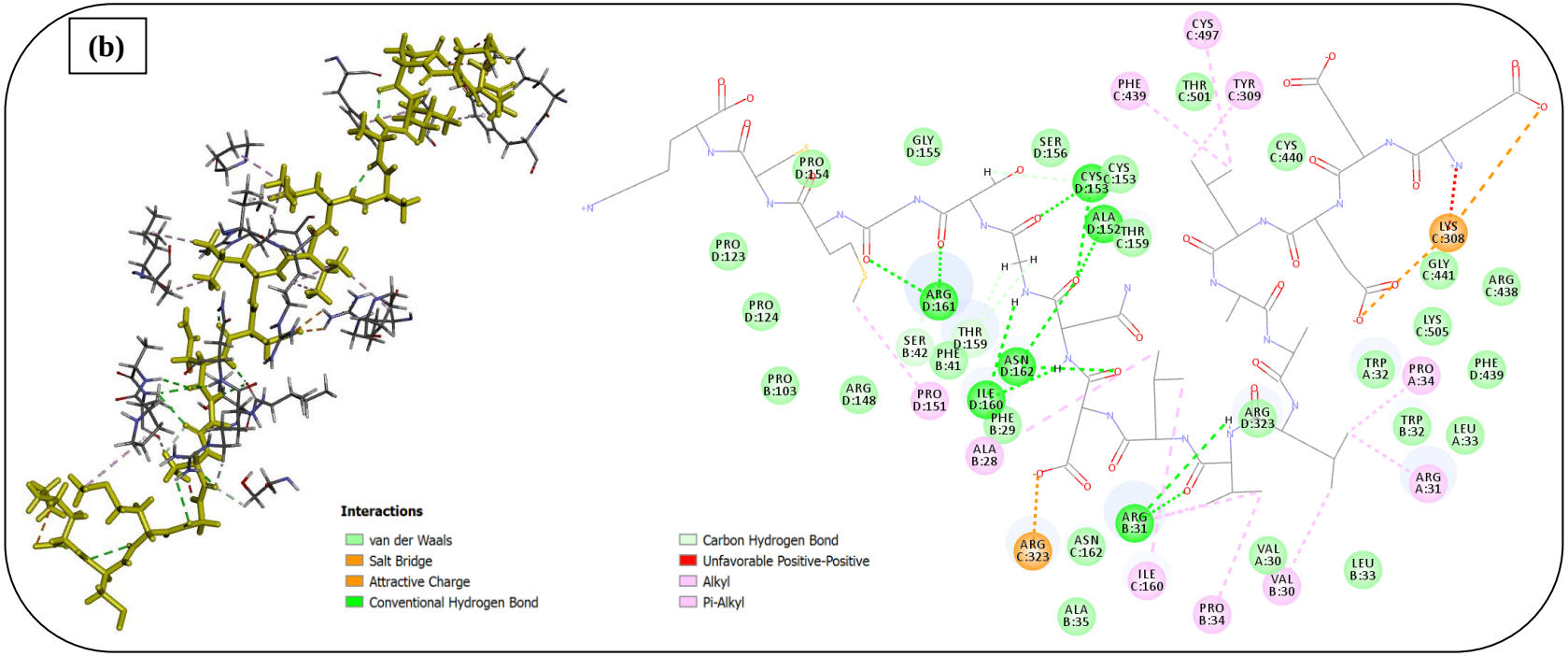

Figure 8.7. Molecular interaction of peptides with myeloperoxidase (MPO). (a) 3D (left) and 2D (right) diagrams of the interactions between $A_{<2}$ #127 peptide TEFHLL and the amino acid residues around MPO active site. The structure of TEFHLL is shown in yellow stick representation in 3D, and black in 2D. (b) 3D (left) and 2D (right) diagrams of the interactions between $T_{<2}$ #127 peptide EEELAALVLDNGSGMCK and the amino acid residues around MPO active site. The structure of EEELAALVLDNGSGMCK is shown in yellow stick representation in 3D, and black in 2D.

Table 8.1

Amino acid composition of $A_{<2}$ and $T_{<2}$ peptide fractions, respectively.

Amino acids	Numbers (per 1000 amino acids)		Content (g/100 g protein)	
	$A_{<2}$	**$T_{<2}$**	**$A_{<2}$**	**$T_{<2}$**
Essential amino acids (EAA)				
Histidine (H)	15	11	1.84	1.28
Isoleucine (I)	57	38	5.99	3.75
Leucine (L)	110	95	11.44	9.42
Lysine (K)	22	34	2.58	3.86
Methionine (M)	35	29	4.22	3.38
Phenylalanine (F)	52	57	7.08	7.40
Threonine (T)	79	51	7.40	4.53
Tryptophan (W)	11	1	1.94	0.20
Valine (V)	98	59	8.99	5.13
Total EAA	479	375	51.48	38.95
Non-essential amino acids (NEAA)				
Alanine (A)	98	84	6.40	5.22
Arginine (R)	64	123	9.19	16.79
Asparagine + Aspartic acid (N+D)	51	71	5.46	7.14
Cysteine (C)	13	15	1.26	1.37
Glutamine + Glutamic acid (Q+E)	30	81	3.53	9.16
Glycine (G)	86	79	4.55	3.93
Proline (P)	21	34	1.89	2.88
Serine (S)	108	76	8.64	5.76
Tyrosine (Y)	50	62	7.60	8.80
Total NEAA	521	625	48.52	61.05
EAA/NEAA	0.92	0.60	1.06	0.64

Table 8.2

Information of reference peptide, as well as all the peptides identified from *de novo* sequencing in $A_{<2}$ and $T_{<2}$ peptide fractions, respectively, including *m*/*z*, mass, percentage of key oxidative amino acid residues, GRAVY, and docking energy.

#	Sequence	ALC (%)	RT (min)	*m/z*	Mass	Cys (%)	His (%)	Met (%)	Trp (%)	Tyr (%)	GRAVY	(-) CDOCKER Energy
Ref	**GRRRRSVQWCA**	**--**	**--**	**--**	**--**	**9.1**	**0**	**0**	**9.1**	**0**	**-1.373**	**10.2023**
$A_{<2}$ Peptide Fraction												
1	YDWRF	97	35.18	393.6808	785.3497	0	0	0	20	20	-1.48	118.713
2	VVLLPLR	95	30.2	405.2818	808.5534	0	0	0	0	0	1.957	79.9687
3	LDLPLR	95	39.24	363.7268	725.4435	0	0	0	0	0	0.3	108.213
4	WDLFR	94	38.57	368.6906	735.3704	0	0	0	20	0	-0.46	112.258
5	ELPPHFL	93	38.61	426.7323	851.4541	0	14.29	0	0	0	0.071	93.011
6	A(+42.01)PFPLR	92	40	371.7144	741.4173	0	0	0	0	0	0.117	74.9514
7	VPFLPR	92	37.54	364.7245	727.438	0	0	0	0	0	0.517	73.5015
8	PLQLRP	91	32.61	362.2259	722.4439	0	0	0	0	0	-0.6	75.1329
9	TEFHLL	91	39.07	380.2046	758.3963	0	16.67	0	0	0	0.5	133.559
10	PVFPLR	90	34.76	364.7241	727.438	0	0	0	0	0	0.517	68.6938
11	EVPLRFW	90	50.2	473.76	945.5072	0	0	0	14.29	0	0.043	89.833
12	M(+15.99)M(+15.99)SLHL	89	30.2	382.1739	762.3405	0	16.67	33.33	0	0	1.233	110.632
13	LVPLQLRP	89	32.88	468.3028	934.5964	0	0	0	0	0	0.55	49.6711
14	TLLWLNK	89	39.72	444.269	886.5276	0	0	0	14.29	0	0.343	108.768
15	TFLFVP	88	33.08	362.206	722.4003	0	0	0	0	0	1.883	94.1057
16	DLFPLR	86	40.38	380.7193	759.4279	0	0	0	0	0	0.133	108.716
17	WN(+.98)WKV	86	40.71	367.1861	732.3595	0	0	0	40	0	-1	105.752
18	MLLLLEVLSGER	85	61.8	686.8959	1371.7795	0	0	8.33	0	0	1.033	F
19	P(+42.01)QPRSP	85	9.11	362.1913	722.3711	0	0	0	0	0	-2.267	47.255
20	WAVPLR	85	40.25	371.2259	740.4333	0	0	0	16.67	0	0.467	-0.0689853
21	LSLPGPAAF	85	40.82	436.7439	871.4803	0	0	0	0	0	1.067	66.5192
22	TFLFVP	84	36.21	362.2054	722.4003	0	0	0	0	0	1.883	93.3919
23	SN(+.98)PLLPLFK	84	47.45	515.3024	1028.5906	0	0	0	0	0	0.311	F
24	R(+42.01)PAFTTPKAMK	83	37.37	645.3605	1288.696	0	0	9.09	0	0	-0.782	F
25	EVLPLR	82	38.73	363.727	725.4435	0	0	0	0	0	0.367	108.66
26	LM(+15.99)LLLEVLSEGR	82	53.22	694.8932	1387.7744	0	0	8.33	0	0	1.033	61.9322

27	FAFPLH	82	35.81	366.1995	730.3802	0	16.67	0	0	0	1.067	90.9405
28	EVFPLRF	81	49.95	454.2545	906.4963	0	0	0	0	0	0.571	83.6052
29	FLLPLR	81	38.2	379.7469	757.485	0	0	0	0	0	1.35	93.5055
30	HN(+.98)N(+.98)VVPSH	80	45.07	453.205	904.4039	0	25	0	0	0	-0.925	114.643
31	D(+42.01)TLLLFAL	80	52.02	474.274	946.5375	0	0	0	0	0	1.95	F
32	LMLLLEVLASDR	80	62.31	686.8953	1371.7795	0	0	8.33	0	0	1.217	90.0772
33	EVPLRSF	80	35.99	424.2356	846.4599	0	0	0	0	0	0.057	120.543
34	WPPNYQW	79	48.05	495.7265	989.4395	0	0	0	28.57	14.29	-1.9	F
35	EFM(+15.99)LYK	79	32.65	423.7027	845.3993	0	0	16.67	0	16.67	-0.033	122.62
36	R(+42.01)MCCCSPLK	79	9.75	541.7368	1081.4541	33.33	0	11.11	0	0	0.267	58.4927
37	GPLLGPR	78	12.79	355.2198	708.4282	0	0	0	0	0	-0.129	79.5549
38	WN(+.98)WKL	78	46.61	374.1929	746.3752	0	0	0	40	0	-1.08	10.7659
39	FGPGLF	78	48.45	637.3336	636.3271	0	0	0	0	0	1.167	98.1639
40	FGPVDFR	78	32.87	419.2139	836.418	0	0	0	0	0	-0.029	102.115
41	TFLM(+15.99)VP	77	31.06	362.19	722.3673	0	0	16.67	0	0	1.733	89.7135
42	HLN(+.98)FW	77	43.28	359.1696	716.3282	0	20	0	20	0	-0.2	107.846
43	FLFLYN(+.98)Q	76	46.8	473.2372	944.4644	0	0	0	0	14.29	0.7	-6.15607
44	A(+42.01)KPFGPEVWP	75	25.42	585.3034	1168.5916	0	0	0	10	0	-0.47	-146.812
45	NLPFLGV	75	33.14	380.2226	758.4327	0	0	0	0	0	1.3	104.682
46	E(+42.01)RC(+57.02)KFWYT	75	53.74	616.2827	1230.5491	12.5	0	0	12.5	12.5	-1.188	F
47	K(+42.01)LPLLK	75	37.71	377.263	752.516	0	0	0	0	0	0.333	88.8286
48	K(+42.01)FPSLLAQP	75	36.59	521.8033	1041.5859	0	0	0	0	0	0.089	F
$T_{<2}$ Peptide Fraction												
1	VELWR	97	25.44	351.6987	701.386	0	0	0	20	0	-0.18	114.432
2	W(+42.01)ALLVDAPR	96	24.39	541.7986	1081.592	0	0	0	11.11	0	0.544	F
3	LLVNFR	96	33.4	381.2346	760.4595	0	0	0	0	0	1.1	102.583
4	VVNLWR	96	32.41	393.7322	785.4548	0	0	0	16.67	0	0.55	105.21
5	QAPVKPR	96	9.27	398.2441	794.4763	0	0	0	0	0	-1.3	100.613
6	LQLWR	96	29.95	358.2154	714.4177	0	0	0	20	0	-0.26	98.0203
7	VELWR	95	24.94	351.6976	701.386	0	0	0	20	0	-0.18	117.819
8	VELWR	95	25.94	351.6991	701.386	0	0	0	20	0	-0.18	117.819
9	FPSLVGR	95	36.17	388.2246	774.4388	0	0	0	0	0	0.5	88.184
10	LEEQSR	95	9.26	381.1913	760.3715	0	0	0	0	0	-2	151.106
11	WLDVLR	95	39.06	401.2327	800.4545	0	0	0	16.67	0	0.483	131.75
12	LLMELR	95	29.23	387.7284	773.447	0	0	16.67	0	0	0.883	128.606

13	LLLEMEK	94	29.04	438.2484	874.4833	0	0	14.29	0	0	0.343	125.026
14	LLELLK	94	38.11	364.7474	727.4843	0	0	0	0	0	1.3	139.186
15	FENLLEELK	93	43.71	567.8018	1133.5967	0	0	0	0	0	-0.411	F
16	MNLPFR	93	35.3	389.2108	776.4003	0	0	16.67	0	0	-0.183	93.5629
17	FPSLVGRPR	93	31.27	514.8006	1027.5927	0	0	0	0	0	-0.289	F
18	FVLELR	93	37.28	388.7346	775.4592	0	0	0	0	0	1.1	126.664
19	EYVFR	93	20.2	357.1823	712.3544	0	0	0	0	20	-0.46	119.571
20	LNLDLLR	93	40.21	428.7646	855.5178	0	0	0	0	0	0.529	126.482
21	SN(+.98)NVLFR	93	23.35	425.7229	849.4344	0	0	0	0	0	-0.214	117.803
22	LENVLR	93	16.18	372.2213	742.4337	0	0	0	0	0	0.05	136.086
23	VMQDQVLR	93	16.43	494.7633	987.5172	0	0	12.5	0	0	-0.113	88.8101
24	K(+42.01)VSWR	92	27.24	359.2043	716.397	0	0	0	20	0	-1.18	91.646
25	SYN(+.98)ELLTK	92	21.5	484.7476	967.4862	0	0	0	0	12.5	-0.762	F
26	LLQLAR	92	20.3	357.2355	712.4595	0	0	0	0	0	0.867	107.425
27	FNTDSALER	92	18.02	526.7512	1051.4934	0	0	0	0	0	-0.9	121.798
28	LNFEPR	91	24.63	388.2061	774.4024	0	0	0	0	0	-1.083	117.786
29	TTDVLR	91	12.14	352.6988	703.3864	0	0	0	0	0	-0.233	125.1
30	FEQ(+.98)FFK	91	36.16	423.7026	845.3959	0	0	0	0	0	-0.417	141.664
31	FVTVLR	90	24.57	367.7295	733.4487	0	0	0	0	0	1.633	109.62
32	MANLQR	90	10.96	366.6929	731.3748	0	0	16.67	0	0	-0.667	105.832
33	WTVVLR	90	35.21	387.2349	772.4595	0	0	0	16.67	0	1.017	100.686
34	WDLFR	90	40.07	368.691	735.3704	0	0	0	20	0	-0.46	10.1431
35	ELFDPR	90	23.56	388.6997	775.3864	0	0	0	0	0	-1.083	132.757
36	EVPLFR	90	41.77	380.7197	759.4279	0	0	0	0	0	0.2	108.465
37	ALSDLLEWLR	90	51.65	608.3386	1214.6658	0	0	0	10	0	0.38	-693.274
38	EDSGPSLVHR	90	12.58	548.7704	1095.5308	0	10	0	0	0	-1.03	-164.596
39	C(+42.01)PQLENVSVALEFLDR	89	61.29	937.9691	1873.9243	6.25	0	0	0	0	0.156	-28.6563
40	N(+42.01)DLWR	89	23.45	373.1852	744.3555	0	0	0	20	0	-1.72	113.56
41	TLLEER	89	15.12	380.7115	759.4127	0	0	0	0	0	-0.767	147.499
42	TWTPPLR	89	28.95	435.7428	869.4759	0	0	0	14.29	0	-0.886	71.3843
43	ELNLLK	89	24.61	365.226	728.4432	0	0	0	0	0	0.083	141.407
44	EVMLWMEDVLR	88	61.3	710.85	1419.689	0	0	18.18	9.09	0	0.355	F
45	LLETLDQLYLEYAK	88	50.59	856.4633	1710.908	0	0	0	0	14.29	-0.029	F
46	APLEVDVLQGR	88	32.9	598.8327	1195.656	0	0	0	0	0	0.073	F
47	EVVN(+.98)WLDK	88	37.23	502.2553	1002.5022	0	0	0	12.5	0	-0.388	96.0642

48	AHGNLSK	88	0.01	363.6974	725.382	0	14.29	0	0	0	-0.886	115.51
49	DFVNLGR	88	27.43	410.7175	819.4239	0	0	0	0	0	-0.157	138.496
50	LEFETR	88	19.82	397.7033	793.397	0	0	0	0	0	-0.933	156.775
51	VPQ(+.98)YGFQNALLVR	88	43.61	753.4054	1504.8037	0	0	0	0	7.69	0.177	F
52	VEDFLER	88	28.4	454.2263	906.4446	0	0	0	0	0	-0.6	156.82
53	WTFDR	88	26.43	362.6718	723.334	0	0	0	20	0	-1.36	109.621
54	LFYLR	88	32.46	356.2122	710.4115	0	0	0	0	20	0.92	98.8894
55	LMLLLEVLSGER	88	64.35	686.8962	1371.7795	0	0	8.33	0	0	1.033	162.412
56	LTLETQVK	88	20.85	466.2738	930.5386	0	0	0	0	0	-0.063	124.369
57	FLLGEK	88	24.16	353.7083	705.4061	0	0	0	0	0	0.433	0.420103
58	YPPPLLR	88	29.42	428.2573	854.5014	0	0	0	0	14.29	-0.429	11.7848
59	WLLTLNK	87	40.96	444.2679	886.5276	0	0	0	14.29	0	0.343	90.3202
60	GPLLGPR	87	16.23	355.2194	708.4282	0	0	0	0	0	-0.129	77.5318
61	LMLLLEVLSEGR	87	61.17	686.8962	1371.7795	0	0	8.33	0	0	1.033	F
62	LMLLLEVLSDAR	87	61.69	686.8967	1371.7795	0	0	8.33	0	0	1.217	61.5373
63	A(+42.01)AFSLLMDMLEK	87	59.1	705.8531	1409.6934	0	0	16.67	0	0	0.825	F
64	VSAVGGPLNK	87	14.51	471.2719	940.5341	0	0	0	0	0	0.34	F
65	MSEAEMLQLQEELAAAER	87	52.38	1024.9854	2047.9553	0	0	11.11	0	0	-0.411	-154.973
66	TLQ(+.98)WR	87	21.14	352.6876	703.3653	0	0	0	20	0	-1.16	96.2433
67	K(+42.01)FPSLVVAR	87	43.26	529.8187	1057.6284	0	0	0	0	0	0.667	52.0143
68	ESQTSATVR	87	10.43	489.7439	977.4778	0	0	0	0	0	-0.944	138.664
69	EGFLGSFLYEYSR	87	51.5	784.376	1566.7354	0	0	0	0	15.38	-0.254	32.2838
70	LGLGLELK	87	39.03	421.7687	841.5273	0	0	0	0	0	0.875	131.326
71	MSPFEK	87	17.89	369.6755	737.3418	0	0	16.67	0	0	-0.85	109.532
72	EYN(+.98)ESGPSLVHR	87	16.8	694.8223	1387.6367	0	8.33	0	0	8.33	-1.258	-213.6
73	FPSLVGRPR	87	31.77	514.8031	1027.5927	0	0	0	0	0	-0.289	-29.2797
74	K(+42.01)LDLLR	87	46.84	400.2539	798.4963	0	0	0	0	0	-0.083	128.518
75	DFEPLR	86	25.03	388.6978	775.3864	0	0	0	0	0	-1.083	136.201
76	FPSLVGR	86	29.04	388.2257	774.4388	0	0	0	0	0	0.5	95.7323
77	DFEPLR	86	25.53	388.6993	775.3864	0	0	0	0	0	-1.083	129.882
78	SN(+.98)LVDLR	86	26.82	409.2211	816.4341	0	0	0	0	0	-0.071	140.013
79	MLLLLEVLSEGR	86	62.21	686.895	1371.7795	0	0	8.33	0	0	1.033	84.9254
80	WREQLLTTLAR	86	55.33	693.8893	1385.7778	0	0	0	9.09	0	-0.464	F
81	MLLLLEVLSADR	86	63.26	686.8962	1371.7795	0	0	8.33	0	0	1.217	113.587
82	EAADLGR	86	10.22	366.1862	730.3609	0	0	0	0	0	-0.643	152.028

83	TVDPMR	86	14.51	359.6791	717.348	0	0	16.67	0	0	-0.7	109.104
84	MSPFEK	86	17.38	369.6762	737.3418	0	0	16.67	0	0	-0.85	109.532
85	TLQDYR	86	12.45	398.2011	794.3923	0	0	0	0	16.67	-1.617	131.911
86	WNLQLK	86	35.92	401.2332	800.4545	0	0	0	16.67	0	-0.7	120.051
87	VGMPFR	86	26.01	353.6888	705.3632	0	0	16.67	0	0	0.4	78.5162
88	DSAFLR	85	19.37	354.6859	707.3602	0	0	0	0	0	-0.067	1.799
89	LSPLFK	85	28.59	352.7189	703.4268	0	0	0	0	0	0.683	91.2402
90	MLLLLEVLSGER	85	62.75	686.8958	1371.7795	0	0	8.33	0	0	1.033	161.141
91	K(+42.01)FPSLVGR	85	36.49	473.2771	944.5443	0	0	0	0	0	-0.05	76.7917
92	FN(+.98)LWK	85	38.32	354.6875	707.3643	0	0	0	20	0	-0.34	103.984
93	EQFWR	85	26	383.1855	764.3605	0	0	0	20	0	-1.92	124.56
94	ANLLVDAPR	85	24.04	484.7773	967.545	0	0	0	0	0	0.256	96.97
95	DFTEVGR	85	17.95	412.1986	822.3871	0	0	0	0	0	-0.8	155.46
96	LMLLLEVLSGER	85	63.81	686.8956	1371.7795	0	0	8.33	0	0	1.033	F
97	FVPPLK	85	23.95	350.7226	699.4319	0	0	0	0	0	0.617	80.4463
98	WGELEK	85	20.11	381.1926	760.3755	0	0	0	16.67	0	-1.4	152.674
99	LLAPPER	85	14.41	398.2378	794.465	0	0	0	0	0	-0.257	90.7893
100	A(+42.01)ALVRGPR	85	31.68	441.2684	880.5242	0	0	0	0	0	0.075	93.3406
101	QTSASLR	85	9.51	381.7068	761.4031	0	0	0	0	0	-0.671	111.919
102	FFPVFR	85	44.48	406.7247	811.438	0	0	0	0	0	1.083	91.6435
103	V(+42.01)MLLLEVLSADR	84	64.71	700.8922	1399.7744	0	0	8.33	0	0	1.25	161.352
104	K(+42.01)ENAGVK	84	11.33	394.2173	786.4235	0	0	0	0	0	-1.314	145.158
105	DNAYWR	84	20.01	412.6854	823.3613	0	0	0	16.67	16.67	-1.983	142.525
106	LLMELR	84	29.73	387.7298	773.447	0	0	16.67	0	0	0.883	124.263
107	TLSLLR	84	29.88	351.7269	701.4435	0	0	0	0	0	0.9	107.118
108	LGAQLVR	84	17.04	378.7381	755.4653	0	0	0	0	0	0.743	109.962
109	LSDEFSR	84	16.42	427.204	852.3977	0	0	0	0	0	-0.929	153.518
110	FN(+.98)VNLGR	84	27.93	410.7166	819.4239	0	0	0	0	0	-0.157	114.986
111	YLPAFEK	84	27.52	434.2326	866.4537	0	0	0	0	14.29	-0.271	93.6524
112	SN(+.98)QTLR	84	9.44	360.1854	718.361	0	0	0	0	0	-1.533	116.069
113	EALVFR	84	26.4	367.7115	733.4122	0	0	0	0	0	0.767	125.207
114	V(+42.01)M(+15.99)LGMLWTLLLR	83	64.61	752.4243	1502.8352	0	0	16.67	8.33	0	1.708	F
115	N(+.98)PLPLR	83	22.27	355.7113	709.4122	0	0	0	0	0	-0.6	79.2847
116	C(+42.01)PQLENVSVALEFLDR	83	61.83	937.9681	1873.9243	6.25	0	0	0	0	0.156	F
117	LEQASR	83	9.3	352.1884	702.366	0	0	0	0	0	-1.117	130.877

118	LVAVLGPK	83	27.92	398.7666	795.5218	0	0	0	0	0	1.488	95.613
119	T(+42.01)AGVVLLLPR	83	41.06	540.8395	1079.6702	0	0	0	0	0	1.44	F
120	TFQVLR	83	18.98	382.225	762.4388	0	0	0	0	0	0.35	113.907
121	M(+15.99)SEAEMLQLQEELAAAER	83	43.75	1032.9779	2063.9502	0	0	11.11	0	0	-0.411	F
122	TSN(+.98)FLK	83	18.46	355.687	709.3646	0	0	0	0	0	-0.383	116.344
123	EGVVTYVELLMDAEGK	83	50.29	876.9393	1751.865	0	0	6.25	0	6.25	0.2	F
124	N(+42.01)AHLTR	83	10.61	377.2012	752.3929	0	16.67	0	0	0	-1.05	110.581
125	NLADFLR	82	40.89	424.7326	847.4551	0	0	0	0	0	0.1	127.912
126	VLEYLK	82	24.56	382.7293	763.4479	0	0	0	0	16.67	0.517	139.722
127	E(+42.01)EELAALVLDNGSGMCK	82	52.87	910.9282	1819.8333	5.88	0	5.88	0	0	0.035	221.295
128	SFVDLVK	82	32.33	404.2336	806.4538	0	0	0	0	0	0.971	137.325
129	LLTATVN(+.98)NANLLLQLDNAR	82	45.76	1034.5708	2067.1323	0	0	0	0	0	0.289	-261.825
130	WHAMLGQAEEVVQER	82	64.33	891.9285	1781.8518	0	6.67	6.67	6.67	0	-0.587	125.316
131	QYDSALR	82	13.12	426.7119	851.4137	0	0	0	0	14.29	-1.143	135.043
132	SQVVPTK	82	10.7	379.7227	757.4334	0	0	0	0	0	-0.3	100.979
133	K(+42.01)N(+.98)LLLK	82	39.68	386.2503	770.4902	0	0	0	0	0	0.017	105.408
134	VPFVLR	82	39.06	365.7315	729.4537	0	0	0	0	0	1.483	88.7871
135	NTVSELEEALNDAR	81	44.99	780.8752	1559.7427	0	0	0	0	0	-0.829	F
136	YVPTVEGR	81	15.64	460.743	919.4763	0	0	0	0	12.5	-0.45	80.7981
137	C(+57.02)(+42.01)PSLENVSVALEFLDR	81	56.65	945.9666	1889.9192	6.25	0	0	0	0	0.325	-101.656
138	A(+42.01)NGPAQR	81	9.26	378.1922	754.3722	0	0	0	0	0	-1.414	100.159
139	DVSYVPTVEGR	81	26.3	611.3062	1220.6038	0	0	0	0	9.09	-0.336	-49.124
140	EVQLDHANR	81	10.67	541.2714	1080.5312	0	11.11	0	0	0	-1.322	134.471
141	ELPNSDLGLK	81	16.39	543.2928	1084.5764	0	0	0	0	0	-0.58	F
142	ELC(+57.02)QVR	81	10.25	402.7032	803.3959	16.67	0	0	0	0	-0.167	132.491
143	Q(+42.01)PYENAGTVEFLVDR	81	44.52	890.4224	1778.8474	0	0	0	0	6.67	-0.613	83.9386
144	LDEFVR	81	20.62	389.7061	777.402	0	0	0	0	0	-0.117	148.216
145	LFSMENWGQTFDVAMR	81	51.68	966.4382	1930.8706	0	0	12.5	6.25	0	-0.131	-115.259
146	LPPQLR	80	35.81	362.2278	722.4439	0	0	0	0	0	-0.6	77.0969
147	LEDLQAMEEALLLDNK	80	50.35	922.9689	1843.9236	0	0	6.25	0	0	-0.244	26.8242
148	WLPPGVNK	80	36.28	455.7579	909.5072	0	0	0	12.5	0	-0.487	F
149	GNLEVLLFTLQSK	80	52.2	731.4196	1460.8237	0	0	0	0	0	0.454	F
150	EATGGLGLR	80	16.39	437.2392	872.4716	0	0	0	0	0	-0.056	141.415
151	FLPLLR	80	42.81	379.7492	757.485	0	0	0	0	0	1.35	78.3818
152	FN(+.98)LGLR	80	36.14	360.7036	719.3966	0	0	0	0	0	0.333	106.404

153	DATEVTR	80	13.95	396.1967	790.3821	0	0	0	0	0	-0.986	153.454
154	ELVADLR	80	22.19	408.2325	814.4548	0	0	0	0	0	0.3	151.635
155	QNMFVLVLYDELK	80	59.75	806.4265	1610.8379	0	0	7.69	0	7.69	0.408	F
156	YLEFK	80	24.59	350.187	698.3639	0	0	0	0	20	-0.42	128.007
157	WLLANPR	80	29.96	435.2557	868.4919	0	0	0	14.29	0	-0.157	93.0968
158	QLLDFAK	80	34.14	417.7371	833.4647	0	0	0	0	0	0.186	137.78
159	LLPLFEER	80	40.54	508.7911	1015.5702	0	0	0	0	0	0.138	F
160	A(+42.01)VMLAVEGVLAELK	80	64.6	742.9212	1483.832	0	0	7.14	0	0	1.429	77.1959
161	VTPLLSK	80	20.48	379.2424	756.4745	0	0	0	0	0	0.686	-0.379943
162	LLLPLR	80	35.85	362.7555	723.5007	0	0	0	0	0	1.517	86.9609
163	TVAGQDAVLVLLSAR	80	46.18	756.9393	1511.8672	0	0	0	0	0	1.067	F
164	ELGLLVAK	80	27.09	421.7682	841.5273	0	0	0	0	0	1.2	113.1
165	WN(+.98)PDAR	79	18.33	380.174	758.3347	0	0	0	16.67	0	-2.033	106.869
166	LMSLVGR	79	36.37	388.2317	774.4422	0	0	14.29	0	0	1.143	108.291
167	L(+42.01)SFDPVLDER	79	38.59	616.8146	1231.6084	0	0	0	0	0	-0.28	F
168	NLPWAK	79	24.12	364.7057	727.4017	0	0	0	16.67	0	-0.717	96.2829
169	RALQLDN(+.98)VTGLLSQSDSK	79	44.16	973.5042	1945.0115	0	0	0	0	0	-0.456	48.5738
170	N(+42.01)N(+.98)LNENMR	79	12.88	524.2321	1046.4451	0	0	12.5	0	0	-2.037	103.325
171	NN(+.98)LEFFLAVAGR	79	52.39	676.3528	1350.6931	0	0	0	0	0	0.467	-51.1875
172	K(+42.01)LALQPALR	79	37.56	526.3318	1050.655	0	0	0	0	0	0.167	F
173	TMLGMLWTLLLR	79	64.37	724.4055	1446.8091	0	0	16.67	8.33	0	1.3	F
174	VALDFEQEMATAASSSSLEK	79	63.9	1057.5006	2112.9885	0	0	5	0	0	-0.08	193.939
175	EVPLFR	79	41.1	380.719	759.4279	0	0	0	0	0	0.2	105.035
176	VSLLGEFLEK	79	44.05	567.8226	1133.6331	0	0	0	0	0	0.63	F
177	LVSYDK	79	10.81	362.6958	723.3803	0	0	0	0	16.67	-0.25	133.28
178	LLLEVTYEALVDGGLNPDVTR	79	64.38	1144.1122	2286.2107	0	0	0	0	4.76	0.3	-404.767
179	VFPSLVGR	79	32.31	437.7603	873.5072	0	0	0	0	0	0.963	99.7897
180	EMEWR	79	16.25	375.6636	749.3167	0	0	20	20	0	-2.1	136.82
181	SYWGSK	79	15.75	364.1722	726.3337	0	0	0	16.67	16.67	-1.35	107.383
182	LLLAPEPR	79	26.65	454.7804	907.5491	0	0	0	0	0	0.25	83.314
183	R(+42.01)RAETDFSLADALNTEFK	78	53.78	1063.537	2125.0439	0	0	0	0	0	-0.778	136.142
184	TLLVELAK	78	41.37	443.7821	885.5535	0	0	0	0	0	1.162	106.004
185	QLAEFK	78	16.89	368.2035	734.3962	0	0	0	0	0	-0.417	130.575
186	K(+42.01)N(+.98)N(+.98)FLLSLDGTANK	78	46.9	789.9036	1577.7937	0	0	0	0	0	-0.55	129.039
187	LFSMENWGQTFDVAMR	78	51.15	966.4425	1930.8706	0	0	12.5	6.25	0	-0.131	F

188	DNFEFR	78	25.98	414.1869	826.3609	0	0	0	0	0	-1.567	162.427
189	LLPLLVNK	78	36.14	455.3059	908.6058	0	0	0	0	0	1.3	57.6731
190	KM(+15.99)PVFK	78	34.59	383.2163	764.4255	0	0	16.67	0	0	-0.083	87.5954
191	R(+42.01)DEFSR	78	16.49	426.2034	850.3933	0	0	0	0	0	-2.333	138.754
192	DLLTALTNLR	78	47.8	565.3312	1128.6501	0	0	0	0	0	0.41	-47.4306
193	AM(+15.99)VQLR	78	11.35	367.2033	732.3953	0	0	16.67	0	0	0.617	111.498
194	EEATALDLLVDALK	78	58.1	750.9093	1499.8083	0	0	0	0	0	0.443	-18.3082
195	L(+42.01)SLNFEELLK	78	52.2	624.3469	1246.6809	0	0	0	0	0	0.28	F
196	LFNELK	78	23.19	382.2195	762.4276	0	0	0	0	0	-0.083	134.067
197	VNLGAGDPR	78	13.66	449.7386	897.4668	0	0	0	0	0	-0.456	88.0135
198	LLDYSK	78	16.22	369.7033	737.3959	0	0	0	0	16.67	-0.317	133.014
199	VEDGVVLLLPR	78	41.48	605.3613	1208.7129	0	0	0	0	0	0.955	48.6963
200	G(+42.01)KPFLR	77	37.02	380.2289	758.4438	0	0	0	0	0	-0.633	83.1081
201	MQLFVK	77	28.67	383.2177	764.4255	0	0	16.67	0	0	0.883	115.67
202	TLN(+.98)LLGK	77	24.38	380.2325	758.4538	0	0	0	0	0	0.414	118.707
203	K(+42.01)NLEGLVGPGPSR	77	37.46	683.3752	1364.7412	0	0	0	0	0	-0.677	F
204	ASLVNWDDMEK	77	21	654.2972	1306.5864	0	0	9.09	9.09	0	-0.718	-605.199
205	TN(+.98)WLDGK	77	26.91	417.7011	833.3919	0	0	0	14.29	0	-1.3	139.007
206	M(+15.99)YPGLADR	77	17.06	469.7216	937.4327	0	0	12.5	0	12.5	-0.475	95.7067
207	QLFPVGR	77	29.72	408.7389	815.4653	0	0	0	0	0	0.114	117.839
208	TVYAPTLK	77	29.17	446.7579	891.5065	0	0	0	0	12.5	0.2	104.091
209	M(+15.99)LLLLEVLSEGR	77	53.9	694.8942	1387.7744	0	0	8.33	0	0	1.033	F
210	FN(+.98)N(+.98)LLK	77	28.61	375.7033	749.3959	0	0	0	0	0	-0.083	122.425
211	LLLPDR	77	24.83	363.7266	725.4435	0	0	0	0	0	0.3	102.655
212	TLLFLQK	77	33.38	431.7719	861.5323	0	0	0	0	0	0.871	F
213	KLELTLETQVK	77	20.9	651.3836	1300.7603	0	0	0	0	0	-0.373	F
214	KM(+15.99)LWK	77	32.4	361.205	720.3992	0	0	20	20	0	-0.6	92.2648
215	ESELLDFFLQSLK	77	60.11	784.9144	1567.8132	0	0	0	0	0	0.1	F
216	YALPLLK	77	36.01	409.2607	816.5109	0	0	0	0	14.29	0.914	90.8825
217	K(+42.01)NLWK	77	34.79	365.714	729.4174	0	0	0	20	0	-1.68	105.332
218	LM(+15.99)LLLEVLN(+.98)TGR	76	53.39	694.894	1387.7744	0	0	8.33	0	0	1.042	-242.777
219	ALAPPTMK	76	19.58	414.7334	827.4575	0	0	12.5	0	0	0.187	-5.43515
220	LVAPPER	76	12.63	391.2299	780.4493	0	0	0	0	0	-0.2	93.7233
221	QLTGLLR	76	25.96	400.7516	799.4916	0	0	0	0	0	0.329	83.6548
222	K(+42.01)SLFLESPMK	76	20.76	611.3268	1220.6475	0	0	10	0	0	-0.22	F

223	LLLTVMDQNEVAFNNTNVR	76	60.87	1096.0559	2190.1101	0	0	5.26	0	0	0.005	-738.134
224	QNPVQLR	76	14.47	427.7437	853.477	0	0	0	0	0	-1.229	113.967
225	YSLQYYMGLAEELVR	76	60.98	917.9557	1833.897	0	0	6.67	0	20	-0.053	-407.649
226	GVPLYR	76	18.07	352.7062	703.4017	0	0	0	0	16.67	0.033	87.4445
227	LLQDSVN(+.98)FSLADALNTEFK	76	54.29	1063.5377	2125.0579	0	0	0	0	0	0.074	117.445
228	LVPLQLR	76	30.44	419.7782	837.5436	0	0	0	0	0	0.857	88.6381
229	EVLPLR	76	40.29	363.7263	725.4435	0	0	0	0	0	0.367	110.652
230	EVPDVQVR	76	18.63	471.254	940.4977	0	0	0	0	0	-0.5	132.307
231	QFPVGR	76	16.63	352.1959	702.3813	0	0	0	0	0	-0.5	84.4753
232	DNLQGLTKLAPR	76	21.51	663.3786	1324.7463	0	0	0	0	0	-0.7	F
233	EVLVDVGLR	76	33.4	500.2919	998.576	0	0	0	0	0	0.922	105.918
234	FSSPLR	76	14.51	353.696	705.3809	0	0	0	0	0	-0.183	88.7273
235	QGPQGATNR	76	9.25	464.7327	927.4522	0	0	0	0	0	-1.811	89.3529
236	LQEDLYR	76	20.47	468.7405	935.4712	0	0	0	0	14.29	-1.243	151.05
237	K(+42.01)VTNWDDMEK	76	36.25	654.2944	1306.5864	0	0	10	10	0	-1.73	F
238	TN(+.98)HLAR	75	8.64	356.6886	711.3664	0	16.67	0	0	0	-1.05	110.118
239	K(+42.01)AQLFLELTLK	75	50.3	673.4095	1344.8018	0	0	0	0	0	0.391	F
240	TVDLTR	75	17.57	352.6992	703.3864	0	0	0	0	0	-0.233	129.99
241	F(+42.01)AM(+15.99)EVLVLYDQ(+.98)LK	75	54.29	814.4243	1626.8215	0	0	7.69	0	7.69	0.815	F
242	A(+42.01)TAVLPALTSR	75	37.46	571.329	1140.6501	0	0	0	0	0	0.809	60.122
243	K(+42.01)NYVGAKEEFLMDSK	75	45.55	900.9419	1799.8762	0	0	6.67	0	6.67	-0.913	171.82
244	VSPNWLK	75	34.6	422.239	842.465	0	0	0	14.29	0	-0.386	-5.85184
245	DFYPLLVGK	75	41.07	526.2914	1050.575	0	0	0	0	11.11	0.433	F
246	QN(+.98)DAPR	75	8.06	351.1632	700.314	0	0	0	0	0	-2.467	116.245
247	G(+42.01)FSLVGR	75	36.13	389.216	776.418	0	0	0	0	0	0.671	104.347
248	FN(+.98)DPALK	75	28.38	403.2055	804.4017	0	0	0	0	0	-0.586	124.439
249	QNDLLFK	75	31.56	439.2416	876.4705	0	0	0	0	0	-0.571	136.089
250	TVASFLK	75	35.53	383.2281	764.4432	0	0	0	0	0	1.029	117.304
251	LFASVSTVLTSK	75	67.98	626.86	1251.7075	0	0	0	0	0	1.075	50.9352
252	AQTLLLEVLSDAR	75	65.11	714.9097	1427.7983	0	0	0	0	0	0.5	80.5501
253	NNLLPR	75	15.89	363.7145	725.4184	0	0	0	0	0	-0.917	93.4364
254	K(+42.01)AQFPVGR	75	33.36	472.7663	943.5239	0	0	0	0	0	-0.638	F

CONNECTING STATEMENT 7

Chapter IX describes the heterologous expression of the krill TGase, for a large-scale production for industrial use. The recombinant TGase thus produced, was characterized for its cold-activity and applied to construct antioxidative hydrogels of gelatin and peptides derived from the studies in Chapters V and VIII, respectively.

This chapter constitutes a paper to be submitted to Food Chemistry journal for consideration for publication:

Y Zhang, C Li, T Geary, A Jardim, B K Simpson. Expression of cold-active krill transglutaminase and its utilization in preparing antioxidative peptides-gelatin hydrogel.

PhD candidate Y Zhang designed and performed the experiments, analyzed the data, and drafted the manuscript. Dr. C Li provide training and research discussion. Profs T Geary and A Jardim provided lab space and facilities and training. Professor B K Simpson supervised the research work, revised the manuscript.

CHAPTER IX. RECOMBINANT EXPRESSION OF COLD-ACTIVE TRANSGLUTAMINASE AND APPLICATION IN PEPTIDES/GELATIN HYDROGEL

9.1. Abstract

The DNA encoding a cold-active TGase from Antarctic krill was synthesized *in vitro* based on the sequence of codon optimization. Recombinant expression plasmid TGase inserted in pET-15b was constructed from agarose gel and transformed into *E. coli* cells. Expressed TGase showed ~78 kDa from SDS-PAGE gel but as inclusion body. Pure TGase was obtained from Ni-Sepharose column with 300 mM imidazole, and a yield of 6.18 mg/L was obtained. The activity of the recombinant TGase was recovered from step-wise dialysis with a specific activity of 1.63 U/mg for the refolded TGase. Cold-activity of the recombinant TGase was comparable with the wild-type, with residual activity of 90–95% at 0–10 ^{o}C. The recombinant TGase was added into hydrogels consisted of oxidative peptides and gelatin. During 10 days of cold-setting, the antioxidant activity of hydrogels prepared with TGase showed significant improvement than hydrogels without TGase ($p < 0.05$), indicating that recombinant TGase stabilized the peptides onto gelatin matrix or formed new isopeptide bonds within the gel matrix.

9.2. Introduction

A transglutaminase (TGase, EC 2.3.2.13.) enzyme active at low temperatures of 0–10 ^{o}C has been purified and characterized from Antarctic krill (*Euphausia superba*) (Zhang et al., 2017b). Another TGase obtained from crayfish also presented cold activity (Sirikharin et al., 2018). Those TGases are derived from fish species that inhabit at cold environments, leading to adaptations that facilitate endogenous TGase function in the live animal at low temperatures. TGase catalyzes acyl transfer reactions between the γ-carboxamide groups of peptides bound glutamine residues (acyl donors), and primary amines or water molecules (acyl acceptors), which can modify protein-based foods for improved functionality. Particularly, the TGases with cold-activity have potential to be used in food products that are processed or stored at low temperatures. Recently microbial TGases have been tested their effect in such food applications including yoghurt, ice cream, surimi, restructured meat and cold-set gels (An et al., 2018; Cai et al., 2018; Gharibzahedi and Chronakis, 2018; Gharibzahedi et al., 2018). However, microbial TGases currently available for commercial use (e.g., commercial TGases (Activa™) from *S. mobaraensis*) are not endowed with high catalytic activity at cold temperature. Studies on heterologous expression of TGases from microorganisms, plants such as maize (Li et al., 2019), and animals such as shrimp (Zheng et al., 2018) have been focused on improvements for high yield recoveries, activities and solubility (Wang et al., 2018), which are important for industrial and commercial production. However, there

is a dearth of research on the recombinant expression of TGase with cold-activity.

TGases have been widely studied to enhance quality attributes of food products, including texture (hardness, elasticity, chewiness, cohesiveness), rheology, gelling, water holding capacity, microstructure, emulsifying, foaming, thermal stability as well as sensory characteristics, nutritional values and health benefits (Amirdivani et al., 2018; Zhang et al., 2018b). However, the effect of TGase on the bioactivity of foods is relatively less studied. Peptides are capable of bioactivity and can serve as acyl donors, enabling them to be bioactive substrates for TGase. A few peptide-polymer conjugates facilitated by TGase have shown bioactivity, but most of them used polysaccharides as acyl acceptors. For instance, a research team has studied to use fish gelatin peptides, gluten hydrolysates, meat hydrolysates to be glycated with glucosamine using TGase, and the coagulates showed high antioxidant and high antimicrobial activities, as well as enhanced flavor (Gottardi et al., 2014; Hong et al., 2014; Hong et al., 2016). Furthermore, chitosan modified with silk peptides or collagen peptides using TGase also showed improved antioxidant properties (Liu et al., 2017a; Xiao et al., 2017). Thus far, there have been only few research studies in terms of peptide/peptide interactions, or peptide/protein interactions catalyzed by TGase. Emulsifying properties of a crosslinked peanut protein and fish protein hydrolysate product, as well as a crosslinked product of wheat gluten hydrolysates were improved by TGase catalysis (Agyare et al., 2009; Hu et al., 2011). In this context, there is the need to explore further the bioactivities of crosslinked product of peptides and protein matrices catalyzed by TGase; and producing recombinant TGase to supplement the traditional supply would enhance such investigations.

9.3. Materials and methods

9.3.1. Gene, strain, culture medium and chemicals

The gene encoding cold-active TGase from Antarctic krill (*Euphausia superba*) has been identified and characterized from our previously transcriptome study (Chapter IV). Before gene synthesis (Sangon Inc., Shanghai, China), condo optimization was performed to increase protein expression. The synthetic gene contained two digestion sites, Nde I and Bam HI, and ligated into cloning vector pUC57 and labelled as "pUC-TGase". The gene sequence was verified by DNA sequencing.

Expression vector pET-15b with Nde I and Bam HI digestion sites were obtained from our lab with an insertion of unknown 1000 bp gene, labelled as "pET15b-unknown". *E. coli* DH5α and *E. coli* T7 express PlysE competent cells were used in this study (Intrivogen). *E. coli* was grown in

lysogeny broth containing 10 g peptone, 5 g yeast extract, and 10 g NaCl per liter of distilled water, adjusted to pH 7.3 using NaOH. LB agar plates were prepared with 15 g agar addition to reagents listed above. Ampicillin (50 µg/mL) was added to medium as required.

The chemicals including Tris, NaCl, urea, glutathione (GSH), oxidized glutathione (GSSG), and glycerol were purchased from Sigma Aldrich (St. Louis, MO, USA). The antioxidative peptides and gelatin components in the hydrogel were prepared in our lab (chapter VIII). The antioxidative peptides with MW < 2kDa were prepared using alcalase from Atlantic sea cucumber. High molecular weight (MW) gelatin was prepared in our lab (chapter V) using alcalase (Zhang et al., 2019).

9.3.2. Expression plasmid construction and transformation

The "pUC-TGase" plasmid and "pET15b-unknown" plasmid in *E. coli* DH5α were extracted and purified using Bio Basic EZ-10 Spin Column Plasmid DNA Minipreps kit (Bio Basic Inc., Markham, Canada) following the manufacturer's instructions. The concentration and purity of extracted plasmid DNA were measured using a NanoDrop spectrophotometer (NanoDrop Technologies, Wilmington, DE, USA). The purified "pUC-TGase" plasmid and "pET15b-unknown" plasmid were double digested using Nde I and Bam HI enzymes (New England Biolabs, Frankfurt, Germany) according to the manufacturer's instructions. The digests were separated in a 1.0% agarose gel in Tris-acetate-EDTA (TAE) buffer at 120 V for 30 min. The appropriately sized bands regarding the insert (TGase gene) and vector (pET-15b) were recovered using a PureLink Quick Gel Extraction kit (Invitrogen). The vector ends were dephosphorylated using Antarctic phosphatase (New England Biolabs) as per the manufacturer's instructions. Ligation was conducted using a reaction mixture containing dephosphorylated vector, insert, T4 ligase (Fermentas, St. Leon-Rot, Germany) and buffer at 16 ^{o}C overnight, to generate "pET15b-TGase" expression plasmid. A control reaction without insert was conducted under the same conditions.

The constructed "pET15b-TGase" plasmid and the control were transformed into *E. coli* T7 express PlysE competent cells using hot shake at 42 ^{o}C for 90 s, respectively. The transformed cells were first grown in LB broth without ampicillin at 37 ^{o}C for 1 h, and subsequently grown on LB agar plates with ampicillin (50 µg/mL) at 37 ^{o}C for 24h. The construction of expression plasmid was evaluated by comparing the colonies grown on agar plates. Single clones were randomly picked and incubated in 5 ml of LB broth containing ampicillin at 37 ^{o}C for 12 h. Plasmid DNA was extracted and purified, and single/double enzymatic digestion were performed before

analyzing the resulting digests on 1.0% agarose gel. A 1kb DNA ladder was used (Thermo Scientific).

9.3.3. Expression and protein determination

The transformant that was verified with express plasmid "pET15b-TGase" was incubated in LB-ampicillin medium at 37 ^{o}C. To induce the expression, IPTG was added at 0.6 mM when the OD = 0.6. A control without addition of IPTG was conducted. After overexpression at 37 ^{o}C for 4 h, both induced and control cells were collected using centrifugation at 4000 rpm, 4 ^{o}C for 20 min, washed using 50 mM Tris buffer (pH 7.3), and disrupted on ice using sonication (Ultrasonic processor, Cole-Parmer, Vernon Hills, IL, USA). The proteins in both induced and control were determined by sodium dodecyl sulfate polyacrylamide gel electrophoresis (SDS-PAGE) using 10% resolving gel on Mini-PROTEAN Tetra Electrophoresis System (Bio-Rad Laboratories Inc.). High MW calibration kit with standard protein markers (GE Healthcare, Mississauga, ON, Canada) was used. The induced cells after sonication was further centrifuged at 12000 rpm, 4 ^{o}C for 20 min. The supernatant was collected and applied onto SDS-PAGE. The precipitates were washed with 50 mM Tris buffer (pH 7.3) containing 1% Triton X-100, 100 mM NaCl and 1 mM EDTA, and then suspended with 50 mM Tris buffer (pH 7.3) containing 8 M urea before being subjected to SDS-PAGE.

9.3.4. Purification of the expressed TGase

The protein in inclusion bodies was dissolved in 20 mM Tris buffer (pH 7.5) containing 8 M urea, 0.5 M NaCl, 10 mM imidazole, centrifuged (12000 rpm, 20 min) and the supernatant was collected. Ni-Sepharose^{TM} 6 fast flow (GE Healthcare) was packed in a 1 × 5 cm column and equilibrated with 20 mM Tris buffer (pH 7.5) containing 8 M urea, 0.5 M NaCl, 10 mM imidazole. The protein sample was loaded onto the equilibrated column, followed by washing of the column with the equilibrium buffer. The bound proteins were eluted with 20 mM Tris buffer (pH 7.5) containing 8 M urea, 0.5 M NaCl, and imidazole with a linear range from 10 mM to 500 mM imidazole. The purification fractions were analyzed at 280 nm on a UV spectrophotometer (Beckman, USA) and on SDS-PAGE gel. The fractions containing the target protein were pooled and concentrated using an ultrafiltration with a 30 kDa cut-off membrane (Amicon Ultra, Millipore). Protein concentration was measured with bicinchoninic acid (BCA) assay kit (Pierce, Appleton, WI, USA) using bovine serum albumin (BSA) as standard.

9.3.5. TGase refolding using dialysis

The fraction of TGase in 20 mM Tris buffer (pH 7.5) containing 8 M urea, 0.5 M NaCl, 300 mM imidazole, was further added with 5 mM $CaCl_2$, 20 mM β-mercaptoethanol, 3 mM GSH, 1 mM GSSG, 5% glycerol, and then placed in cellulose dialysis bag (Sigma-Aldrich Co., USA) at a concentration of 0.1 mg/mL. Solubilized inclusion body proteins were refolded by removal of solubilization agent. Dialysis of the solubilized TGase in presence of refolding buffer was used to recover the functionally active proteins. Considering the existence of disulfide bonds due to the 11 cysteine residues found in TGase sequence, step-wise dialysis was applied with 6 continuous refolding buffer solutions (**Table 9.1**), allowing a gentle removal of denaturant agents for correct refolding (Gabrielczyk et al., 2017). The solubilized TGase proteins was first brought to equilibrium with refolding buffer A, then B, C, D, E and F for 8 hr each, at 4 ^{o}C, and buffer to sample volume ratio of 100:1. After the last dialysis step, the protein in the dialysis bag was centrifuged at 12000 rpm at 4 ^{o}C for 10 min to eliminate the insoluble protein aggregates. The protein concentration and TGase activity were measured.

Table 9.1

The recipe of 6 refolding buffer solutions used in the dialysis of solubilized TGase.

	Urea (M)	Tris (mM)	NaCl (mM)	$CaCl_2$ (mM)	β-Mercaptoethanol (mM)	GSH (mM)	GSSG (mM)	Glycerol (%)
A	4	20	150	5	20	3	1	5
B	3	20	150	5	15	3	1	5
C	2	20	150	5	10	3	1	5
D	1	20	150	5	5	3	1	5
E	0.5	20	150	5	2.5	3	1	5
F	0	20	150	5	0	0	0	0

9.3.6. TGase activity assay

The TGase activity was measured according to the method of Zhang et al. (2017b). The reaction mixture comprised of 1 mg/mL DMC, 15 µM MDC, 3 mM DTT, 5 mM $CaCl_2$, 50 mM Tris-HCl (pH 7.5), and 100 µL TGase. The reaction was performed at 25 °C for 10 min and stopped by adding EDTA solution to a final concentration of 20 mM. Fluorescence intensity (FI) of MDC incorporated into DMC was measured with F2000 fluorescence spectrophotometer (Hitachi, Ltd, Tokyo, Japan) at excitation and emission wavelengths of 350 and 480 nm, respectively. FI values of blanks (FI_0) were measured in a similar procedure but deionized water was used to replace

TGase. Enhancing factor (EF) was determined to be 1.877 in this study. One unit of TGase enzyme activity was defined as the amount of enzyme that catalyzed the incorporation of 1 nmole of MDC into DMC during 1 min at 25 °C. TGase activity was calculated by Equation (1). Protein content was determined with a Pierce BCA protein assay kit (Thermo Scientific, USA), and specific activity was determined using Equations (2).

$$\text{TGase activity (1 U)} = \frac{(FI\text{-}FI_0)\times 15{,}000\ \text{nmol}\times 2\ \text{mL}\times 10^{-3}}{FI_0\times 10\ \text{min}\times 1.877} \quad (1)$$

$$\text{Specific activity (U/mg protein)} = \frac{\text{Total TGase activity}}{\text{Total protein}} \quad (2)$$

9.3.7. Cold-activity determination of expressed TGase

TGase activity was studied over a wide temperature range (0, 4, 10, 20, 30, 45, 55 and 65 ^{o}C). The reaction mixture comprising of 1 mg/mL DMC, 15 μM MDC, 3 mM DTT, 5 mM $CaCl_2$, 50 mM Tris (pH 7.5), were incubated at the corresponding temperatures for 5 min before adding 100 μL TGase. The relative TGase activity (%) was calculated using the highest TGase activity obtained as 100%.

9.3.8. Preparation cold-set peptides/gelatin hydrogel using recombinant TGase

High MW gelatin was first dissolved in distilled water at 40 ^{o}C to obtain a concentration of 6% (w/v) and stirred for 15 min at 25 ^{o}C. Antioxidative peptide mixture was added to a concentration of 0.5 mg/mL to the gelatin solution. Recombinant TGase was then added at 1 U/g gelatin with continuous stirring for another 10 min at 25 ^{o}C, and then cooled at 4 ^{o}C for 30 min to form hydrogel. The control group was performed with inactive recombinant TGase (obtained by heating at 100 ^{o}C for 1 min) and followed the same procedure to form hydrogel. The hydrogels were stored for another 2, 4, 6, 8 and 10 days at 4 ^{o}C. Antioxidant activity of the cold-set peptides/gelatin hydrogels with and without recombinant TGase were determined at each storage time interval.

9.3.9. Determination of antioxidant activity for peptides/gelatin hydrogel

Four antioxidant activity assays were used on peptides/gelatin hydrogels after different storage times (0, 2, 4, 6, 8 and 10 days) at 4 ^{o}C. The cold-set hydrogels were warmed at 40 ^{o}C for 15 min to obtain aqueous form before antioxidant analyses. The assays including DPPH radical scavenging activity, hydroxyl radical scavenging activity, Fe(III) reducing power and Fe(II) chelating activity were determined based on method of Zhang et al. (2018d) with slight modifications.

DPPH radical scavenging activity. Hydrogel sample (1 mL) was mixed with 100 μM DPPH (1

mL) which was freshly prepared in 95% ethanol. The mixture was incubated in darkness for 30 min at 25 °C. Absorbance was recorded at 517 nm. In Equation (3), the $A_{517\ nm,\ control}$ was measured using distilled water instead of hydrogel sample.

$$\text{DPPH radical scavenging activity (\%)} = 100 \times \frac{A_{517\ nm,\ control} - A_{517\ nm,\ sample}}{A_{517\ nm,\ control}} \quad (3)$$

Hydroxyl radical scavenging activity. Reagent of 5 mM 1,10-phenanthroline (0.6 mL), 5 mM $FeSO_4$ (0.6 mL), 15 mM EDTA (0.6 mL) and 0.2 M sodium phosphate buffer (pH 7.5, 0.4 mL) were added to hydrogel sample (0.6 mL) and 0.01% H_2O_2 (0.8 mL). The mixture was incubated at 37 °C for 60 min, and the absorbance was measured at 536 nm. In Equation (4), the $A_{536\ nm,\ control}$ was recorded using distilled water instead of hydrogel sample, and $A_{536\ nm,\ blank}$ was the absorbance of blank solution containing reagent solution.

$$\text{Hydroxyl radical scavenging activity (\%)} = 100 \times \frac{A_{536\ nm,\ sample} - A_{536\ nm,\ control}}{A_{536\ nm,\ blank} - A_{536\ nm,\ control}} \quad (4)$$

Fe (III) reducing activity. Hydrogel sample (1 mL) was mixed with 0.2 M phosphate buffer (pH 6.6, 2.5 mL) and 1% potassium ferricyanide (2.5 mL). After the mixture was incubated at 50 °C for 30 min, 10% TCA (2.5 mL) was added. The mixture was centrifuged at 1650g for 10 min, then 2.5 mL of supernatant (2.5 mL) was mixed with distilled water (2.5 mL) and 0.1% $FeCl_3$ (0.5 mL), and reacted for 10 min. The absorbance at 700 nm was measured against blank using distilled water instead of hydrogel sample. Higher absorbance indicated higher reducing activity.

Fe (II) chelating activity. Hydrogel sample (1 mL) was mixed with 2 mM $FeCl_2$ (0.05 mL), distilled water (0.5 mL), and 5 mM ferrozine (0.1 mL). The mixture was incubated in darkness for 10 min at 25 °C, and the absorbance at 562 nm was measured. In Equation (5), the $A_{562\ nm,\ control}$ was measured using distilled water instead of hydrogel sample.

$$\text{Fe(II) chelating activity (\%)} = 100 \times \frac{A_{562\ nm,\ control} - A_{562\ nm,\ sample}}{A_{562\ nm,\ control}} \quad (5)$$

9.3.10. Statistical analysis

Three replicates were done for the activity assay of recombinant TGase, as well as the antioxidant activity determinations. The data were expressed as means ± SD (standard deviations). Statistical analyses were done using the SPSS 22.0 program (SPSS Inc., Chicago, IL, USA). One-way analysis of variance (ANOVA) was carried out. The differences between means were determined using the least significant difference (LSD) test. Level of significance was set for $p < 0.05$.

9.4. Results and discussion

9.4.1. Synthesis of TGase gene

The TGase DNA sequence with Nde I and Bam HI digestion sites, i.e., CAT, GGATCC, respectively, was optimized with preferred codons of *E. coli*. It was synthesized and inserted into pUC57 vector. **Figure 9.1** showed the optimized DNA sequence of TGase confirmed by DNA sequencing, and the deduced amino acid sequence.

9.4.2. Recombinant expression plasmid

Single and double enzymatic digestion were performed to the "pUC-TGase" and "pET15b-unknown" plasmids, respectively, and the digests TGase and pET-15b fragments were recovered for further construction of recombinant expression plasmid. In **Figure 9.2A**, lane 1 showed pUC-TGase plasmid after single digestion (~4900 bp); lane 2 showed pUC-TGase plasmid after double digestion with TGase gene (~2300 bp) and pUC57 fragment (~2600 bp); lane 3 showed the recovered TGase gene (~2300 bp); lane 4 showed pET15b-unknown plasmid after single digestion (~6600 bp); lane 5 showed pET15b-unknown plasmid after double digestion with "unknown" gene (~1000 bp) and pET-15b fragment (~5700 bp); lane 6 showed the recovered and pET-15b fragment (~5700 bp). The results indicated that the target TGase gene and express vector pET-15b fragments were successfully recovered. After ligation, the enzymatic digests are shown in **Figure 9.2B**. Lane 1 showed the pET15b-TGase plasmid after single digestion (~8000 bp); lane 2 showed pET15b-TGase plasmid after double digestion with TGase gene (~2300 bp) and pET-15b fragment (~5700 bp). The electrophoresis gels in **Figure 9.2** indicated the successful construction of recombinant expression plasmid "pET15b-TGase". After transformation, the *E. coli* T7 express PlysE competent cells were cultured on medium plates. As shown in **Figure 9.3**, there were *E. coli* colonies grew on the agar plate I and no colony grew on plate II, suggesting that expression plasmid "pET15b-TGase" was successfully transformed into *E. coli* express competent cells.

9.4.3. Expression

To confirm the overexpression of the recombinant TGase, the expressed proteins were analyzed on SDS-PAGE as shown in **Figure 9.4**. Compared with the product of control without induction using IPTG (lane 1), there was an obvious band around 78 kDa detected in the proteins expressed from induced express cells (lane 2). Our previous study on purification of TGase from Antarctic krill (*Euphausia superba*) showed the apparent MW of Antarctic krill TGase to be 78 kDa using SDS-PAGE (Zhang et al., 2017b). In this study, the gene sequence encoding TGase was obtained

from Antarctic krill, thus the protein band with ~78 kDa in lane 2 was designated as TGase molecule. The theoretical MW from the deduced amino acids (**Figure 9.1**) was 85.139 kDa, exhibiting a lager MW than its apparent MW with a 7 kDa difference. It is common that there is slight discrepancy between the theoretical and apparent MW values (Bartels et al., 2011). The results suggested that the synthesized Antarctic krill TGase gene was successfully expressed in *E. coli* T7 express PlysE competent cells.

For the expressed protein induced with IPTG, the precipitates showed clear and intense target protein band with ~78 kDa MW (lane 3 in **Figure 9.4**), whereas the protein patterns of the supernatant hardly contained target protein bands (lane 4). It indicated that the recombinant TGase protein mainly presented in inclusion bodies. Apart from codon optimization, a few other strategies were applied to increase the expression in soluble form and enhance the expression level, which included change of expression temperature, change of IPTG concentration, use of various competent cells (e.g., *E. coli* BL21) but the target proteins were expressed in inclusion bodies (data not shown). The currently used method was the one that produce a high-level expression of TGase. Thus, the expressed TGase in inclusion bodies need to be recovered after purification.

9.4.4. Purification of TGase

The expressed TGase carrying His-tag was captured directly by Ni-Sepharose resin and eluted by a linear gradient of imidazole (50 – 500 mM). The elution profile shown in **Figure 9.5A**, indicates that there were three fractions containing proteins. Peak 1' was observed with equilibrium buffer containing 10 mM imidazole, which was contributed by the proteins without His-tag. Peak 2' had a relatively low protein content, and no obvious protein band was observed (**Figure 9.5B**). Peak 3' was eluted at imidazole concentration of 300 mM with absorbance of 0.6 at 280 nm, and only one band of 78 kDa was exhibited that corresponded to TGase. Peak 3' was concentrated and its protein concentration determined by BCA method showed the yield of TGase was 6.18 mg/L with a high pure form. A few other shrimp TGases have been successfully expressed but no yield was reported (Chang et al., 2016; Zheng et al., 2018).

9.4.5. Recovery of TGase activity

The recombinant TGase expressed in *E. coli* was inactive and insoluble due to misfolding. The recovery process included solubilization of the protein aggregates using denaturants, and then refolding of them to an active and soluble conformation. Dialysis using sequential refolding buffer was used to refold the TGase protein. The recipe of refolding buffer used in this study has been

optimized based on previous trials (data not shown). Urea could lower the protein hydration, weaken the hydrophobic effect, and also disrupt the peptide backbone, thus denature the protein (Steinke et al., 2016). Gradual decreasing of the urea concentration in refolding buffer could re-order the unfolded proteins. Antarctic krill TGase needs calcium ions as activators (Zhang et al., 2017b), and thus $CaCl_2$ was added into the recovery of TGase instead of the EDTA that is usually added in refolding buffer in other cases. Antarctic krill TGase contains cysteine residues; thus, β-mercaptoethanol, a reducing agent, was added in solubilization buffer to keep sulfhydryl groups in reduced state and cleave disulfide bonds formed during the expression. In the refolding buffer, a decrease of β-mercaptoethanol concentration from 20 to 0 mM would allow proper disulfide bonds formation that favor the activity recovery and correct conformation formation(Lukesh III et al., 2012). Similarly, a combination of reduced and oxidized thiols (e.g. GSH, GSSG), are redox shuffling reagents used to promote disulfide exchange, i.e., any incorrect disulfide bond formed during the refolding can be reduced and the refolding can proceed further toward achieving the proper fold (Singh et al., 2015). Glycerol, a commonly-used stabilizing osmolyte, has been demonstrated to have high recovery of protein in refolding process (Gabrielczyk et al., 2017). Moreover, it was not necessary to enhance the activity and solubility of recombinant TGase in *E. coli* since the TGase activity has been reported to be harmful to host cells (Ohtake et al., 2018).

By using the refolding buffer solutions listed in **Table 9.1**, the recombinant Antarctic krill TGase was recovered with functional activity and solubility in Tris buffer. The specific activity of the refolded TGase was 1.63 U/mg, and the yield was 10.07 U/L. However, this the recombinant TGase's specific activity was lower compared with the specific activity of wild TGase purified from the raw material Antarctic krill, which was 53 U/mg. TGase had relatively a high MW and 11 cysteine residues, that might bring difficult to the correct refolding. The recombinant Antarctic krill TGase showed higher specific activity than a maize TGase in *Pichia pastoris* with 0.4 U/mg (Li et al., 2019), but lower than a microbial *Streptomyces mobaraensis* TGase expressed in *E. coli* with 55 U/mg (Mu et al., 2018). To increase the recovery of activity, optimization including choice of host, induction and refolding buffer recipe can be done.

9.4.6. Cold-activity characterization

The TGase from Antarctic krill is active at cold temperatures; thus, the cold-activity of recombinant TGase needed to be verified. **Figure 9.6** presents the effect of different temperatures on the activity of purified and refolded recombinant Antarctic krill TGase. Its relative activities of

0, 4 and 10 °C were 94.85 ± 0.78%, 95.60 ± 0.42% and 91.35 ± 0.92%, respectively, which were higher than those of other temperatures, e.g., 76.55 ± 1.48%, 62.05 ± 0.49%, 45.30 ± 0.71%, 39.70 ± 0.57% and 37.60 ± 0.42% for 20, 30, 45, 55 and 65 °C. From 20 to 65 °C, a smooth decreasing trend of relative activity was observed for recombinant TGase, which was similar with the wild-type TGase from Antarctic krill (Zhang et al., 2017b). However, the relative activity of the recombinant TGase was generally lower than its wild counterpart for each temperature, with difference of 2–5% in value. Even though the recombinant TGase was still considered as cold-active or psychrophilic enzymes, the active and soluble TGase after refolding with dialysis might have slightly different conformation from the wild-type one. As cold-activity at low temperatures is closely related with high protein structure flexibility, it could be inferred that the recombinant TGase after activity recovery had a relatively rigid structure. The strategies that aim to enhance the cold-active performance for enzyme are actually to promote its proper folding. Previous studies found that using low incubation temperatures of the cell culture after induction may increase the expression of cold-active enzymes. Some other strategies such as the use of molecular chaperones, cold-active promoters, fusion partners, psychrophilic hosts, and low incubation temperatures after induction have also been successfully used for the expression of cold-active enzymes (Duarte et al., 2018; Santiago et al., 2016). Thus, such strategies can be considered in future studies to enhance the expression and cold-activity of the recombinant TGase.

9.4.7. Antioxidant activity of peptides/gelatin hydrogels

Recombinant TGase was added to facilitate the cold-setting of antioxidative peptides/gelatin hydrogels, to verify the cold-activity of the recombinant TGase at low temperatures (**Figure 9.6**). The antioxidant activities including DPPH radical scavenging activity, hydroxyl radical scavenging activity, Fe (III) reducing power and Fe (II) chelating activity of the peptides/gelatin hydrogel were determined after different storage times at 4 °C. From the results shown in **Figure 9.7**, with the addition of recombinant TGase, the antioxidant activity exhibited by the peptides/gelatin hydrogels were found to be more stable than the hydrogels without recombinant TGase.

The DPPH radical scavenging activity in **Figure 9.7A** showed that no significant difference on the 2nd, 4th and 6th day for the peptides/gelatin hydrogel with addition of TGase ($p > 0.05$), while for the hydrogel without TGase (control), the DPPH radical scavenging activity decreased significantly with the increase of storage time from 0 to 10 days ($p < 0.05$). The initial DPPH

radical scavenging activity was ~93% and decreased to be 82% and 73% for hydrogel with TGase and control hydrogel, respectively. Hydrogel with TGase had significantly higher DPPH radical scavenging activity than the control on the 8th and 10th days ($p < 0.01$ and $p < 0.05$, respectively). A microbial TGase has been used to modify carboxymethyl chitosan with silk peptide, and the resulting polymer showed enhanced DPPH scavenging activity (Liu et al., 2017a). The DPPH scavenging involved hydrogen atom and electron transfer reactions, and peptides composed of aromatic amino acid residues were found responsible for scavenging DPPH radicals (Lorenzo et al., 2018). Peptides with higher hydrophobicity showed better DPPH radical scavenging activity as the assay used methanol as solvent, but TGase has been demonstrated to decrease the hydrophobicity of protein hydrolysates (Agyare et al., 2009). In this context, the main reason might be that crosslinking of peptides/gelatin gels catalyzed by TGase may have protected and stabilized the antioxidative peptides.

The hydroxyl radical scavenging activity in **Figure 9.7B** also improved for the peptide/gelatin hydrogel with TGase addition. For TGase group, the hydroxyl radical scavenging activity decreased to 46% after 10 days from initial value of 56%, while the control group showed significant decrease each 2 days ($p < 0.05$) and decreased up to 39% after 10 days from 56%. Even though the hydroxyl radical scavenging activity for both TGase supplemented sample and the control exhibited a decreasing trend with increasing of the storage time, the TGase addition contributed to a less decrease than control, especially on the 10th day ($p < 0.01$). A collagen peptide grafted with *N*-succinyl chitosan using microbial TGase showed improved hydroxyl scavenging activity due to the existence of characteristic amino acid residues such as Pro in the polymer after TGase treatment (Xiao et al., 2017). In this study, the characteristic peptides that perform hydroxyl radical scavenging activity could also be stabilized in the cold-set hydrogel during the storage at 4 ^{o}C, which contribute a relatively stable antioxidant activity of the hydrogel against hydroxyl radicals.

As shown in **Figure 9.7C**, the Fe (III) reducing power for the peptides/gelatin hydrogel catalyzed with TGase showed no significant difference between 4th and 6th days, as well as 8th and 10th days ($p > 0.05$); however, for the control hydrogel, the Fe (III) reducing power reduced significantly after 6 days ($p < 0.05$). The results suggested that TGase addition effectively delayed the decrease of Fe (III) reducing power by the peptides/gelatin hydrogel, especially after 8 days' storage when the TGase addition significantly improved the Fe (III) reducing power, compared

with the hydrogel without TGase ($p < 0.05$). Previous research has shown that crosslinked whey protein hydrolysates using TGase had better Fe (III) reducing power than non-crosslinked hydrolysates (Bagheri et al., 2014); whereas another study on the sodium caseinate hydrolysates treated with commercial microbial TGase showed improved Fe (III) reducing power but no significant difference with the non-TGase treated hydrolysates (Cermeño et al., 2016). In this study, crosslinking catalyzed by recombinant TGase had improved effect on the Fe (III) reducing power, which might be due to the increased feasibility of neutralization of the multiplex peptide molecules from the crosslinking of reductive peptides (Bagheri et al., 2014), or the improved stability of peptides crosslinked onto gelatin matrix. The Fe (II) chelating activity in **Figure 9.7D** had a slightly different trend from the other antioxidant assays, as there was significant decrease observed for both TGase addition and Control hydrogels from 0 to 10 days ($p < 0.05$). With TGase addition, the decrease in Fe (II) chelating activity was found to be less and slower compared with the hydrogel without TGase.

9.5. Conclusion

The TGase gene was synthesized *in vitro* based on the gene sequence obtained from previous transcriptome data, and the codon optimization improved the expression level. Based on the construction process used in present work, a recombinant expression plasmid using pET-15b was successfully constructed. In terms of the expressed TGase in inclusion body form, a simple and efficient purification and refolding process was developed, including Ni-Sepharose purification with 300 mM imidazole elution and a multi-step dialysis using 6 different refolding buffers. The recovered TGase showed similar cold-activity with the wild counterpart, and thus, a cold-active TGase can be made available via microbial manipulations. This work also found that the recombinant TGase could stabilize oxidative peptides onto gelatin matrices during cold-setting at 4 ^{o}C, and such crosslinked antioxidative hydrogels could be added as ingredients in foods processed or stored at low temperatures.

cat atg gca ctg aat ttt ggt aat ttc ttt gat ttt gat ttc ttt gat aac ctg ttt aat aat ctg cgt gat gaa aat acc ggc cgc cgt 90
M A L N F G N F F D F D F F D N L F N N L R D E N T G R R 30
cgt gaa gat ggc cgt gaa ctg acc ttt atg gaa gaa gct gat gca aat aac gat att gat gct ggt gaa gaa cgt ccg cgt gtt aca tca 180
R E D G R E L T F M E E A D A N N D I D A G E E R P R V T S 60
gtt gat atg cag gct cgc tct aat gca ctg aaa tgt aat tgt gaa aaa ttt gaa ctg gtt gaa cgt cgt gat ggt cgt tca gtg att att 270
V D M Q A R S N A L K C N C E K F E L V E R R D G R S V I I 90
cgt cgc ggc gcc aca ctg acg ctg gat gtt acg ttt aat agt cag att gat ctg acg agc ggc cag aaa ctg ggc ctg acc ttt agt ttc 360
R R G A T L T L D V T F N S Q I D L T S G Q K L G L T F S F 120
ggt cgc tca gcg aat att ccg aat ggt acc cag gca aaa ctg gat gtt acc ggt aaa cag acc ttt gat gat gat acc gcc ctt tgg gat 450
G R S A N I P N G T Q A K L D V T G K Q T F D D D T A L W D 150
gta cgt tta gtg acc cag gcc gaa aat aca ctg acg tta gaa gtt cat gtt cct gtg cat gtg atg gtt ggc atc tgg cag ctg aca att 540
V R L V T Q A E N T L T L E V H V P V H V M V G I W Q L T I 180
gaa gtg agt ccg cag agc aac ccg tct gcg aaa cat gtt ttt cgc ccg gaa gaa acc ctg tat atc ctg ttt aat cct tgg aat aaa gaa 630
E V S P Q S N P S A K H V F R P E E T L Y I L F N P W N K E 210
gat gat gtg tat atg gaa gaa gat gaa ctg cgt gaa gaa tat att ctg aac gat gtt ggt aaa atc tgg gtg ggt aat tgg cgt agc aat 720
D D V Y M E E D E L R E E Y I L N D V G K I W V G N W R S N 240
ttt ggc cgt tcc tgg aat tat ggc cag ttt gat gat gca gtt ctg ccg gca tgc atg tat ctg atg gaa aat gca cgg ctg cgt ccg gaa 810
F G R S W N Y G Q F D D A V L P A C M Y L M E N A R L R P E 270
gaa cgc ggt gat gtg gtg aaa gtt tct cgc gcg att agt aaa atg atg aat gtt aat gat gaa ggc ggc gtt gtg tgg ggt cgt tgg gat 900
E R G D V V K V S R A I S K M M N V N D E G G V V W G R W D 300
ggt gaa tat cag gat ggc cag ggc ccg agc tat tgg acg ggc agc ata agt att ctg gaa cag tat atg tct acg aaa cgt ggt gtt aaa 990
G E Y Q D G Q G P S Y W T G S I S I L E Q Y M S T K R G V K 330
tat ggt cag tgc tgg gtt ttt gca ggc gtg gtt aac acc gtg tgt cgt gcg ctg ggt att cct tgt cgt ccg gtg agc aat ctg cgc tct 1080
Y G Q C W V F A G V V N T V C R A L G I P C R P V S N L R S 360
gca cat gat acc aat cag agt ctg agc atc gat cag ttt ctg aca gaa gat ggg acc gat cgt ctg agc gca aat gaa gtt act cgt cgt 1170
A H D T N Q S L S I D Q F L T E D G T D R L S A N E V T R R 390
gtt ttt aat tgg ggt ttt agt gat tct att tgg aat ttt cat gtg tgg aat gat gcc tgg atg gcg cgt aaa gat ctg ccg gat ggt tat 1260
V F N W G F S D S I W N F H V W N D A W M A R K D L P D G Y 420
ggt ggc tgg cag gca att gat agt acg ccg cag gaa cag tca ggc ggc ctg ttt cag tgt ggc ccg gcg agc cat acc gca att ctg ctg 1350
G G W Q A I D S T P Q E Q S G G L F Q C G P A S H T A I L L 450
ggc aaa aca gaa tta aat tat gat att aat ttt ctg gtg ggt gaa gtt aat gct gat gtg atc acc tgg att gtt gat ccg aaa gcc aaa 1440
G K T E L N Y D I N F L V G E V N A D V I T W I V D P K A K 480
tta ggc ttt agt aaa gtg cgt gca gat aaa ttt gat gtg ggc cgt gaa ctg att aca aaa gca cct ggt tat aac gcg ttt ggc gat cgc 1530
L G F S K V R A D K F D V G R E L I T K A P G Y N A F G D R 510
gat aaa gtg atc att aat gat ata tat aaa agt ccg gaa ggt tca gat gcg aac cgt tta atg ctg aat agt gcg gca tca cgt tct cgc 1620
D K V I I N D I Y K S P E G S D A N R L M L N S A A S R S R 540
acc ggt cgc ctg gcc ttt gaa ttt agc gaa ccg att gat gat gtt aaa ttt aca att gaa gat gtg gtg cag gtt ccg atg ggt gat gat 1710
T G R L A F E F S E P I D D V K F T I E D V V Q V P M G D D 570
ttc agc gtg acc gcc acc gca aaa aat gaa tct gat agt acg cgc aca gtt tgg atg aaa att tgc tgt gct tct gaa tat tat aca ggt 1800
F S V T A T A K N E S D S T R T V W M K I C C A S E Y Y T G 600
gtt cgt gcc aat cgc att aaa tgg gtt gat acc acc aaa aat agc gaa tat tat gat aat ctg gtc gaa tat ggt atg att aaa ctg atg 1890
V R A N R I K W V D T T K N S E Y Y D N L V E Y G M I K L M 630
gca ctg tgt cat gtg gag gaa acg acc cag tca tgg att ggt gaa gat tca ttt cag gtg att aaa ccg cgt att aaa att gaa ctg ccg 1980
A L C H V E E T T Q S W I G E D S F Q V I K P R I K I E L P 660
gaa acc gcc acc gtg ggt aaa gca att gtg gtg aaa ctg tca ttt aat aat cca ctg gaa acc att ctg aaa cag tgt agc ctg gtg gtt 2070
E T A T V G K A I V V K L S F N N P L E T I L K Q C S L V V 690
gat ggt ccg ggt ctg ctg cgt ccg aaa acc att ccg att cgt gat gtt gaa gca aaa ggc gaa atg tct tat gaa ctg aaa gtt tat ccg 2160
D G P G L L R P K T I P I R D V E A K G E M S Y E L K V Y P 720
aaa cgc ggt ggc cgc cgt acc att att gcg acg ttt aac agc cgt cag ctc gtg gat ctg acc ggt tct aaa aat att gat gtt gtt gaa 2250
K R G G R R T I I A T F N S R Q L V D L T G S K N I D V V E 750
cag gat gtt taa ggatcc 2268
Q D V stop 753

Figure 9.1. Optimized coding sequence of TGase and its deduced amino acid sequence. The enzymatic digestion sites were highlighted in blue shade.

A

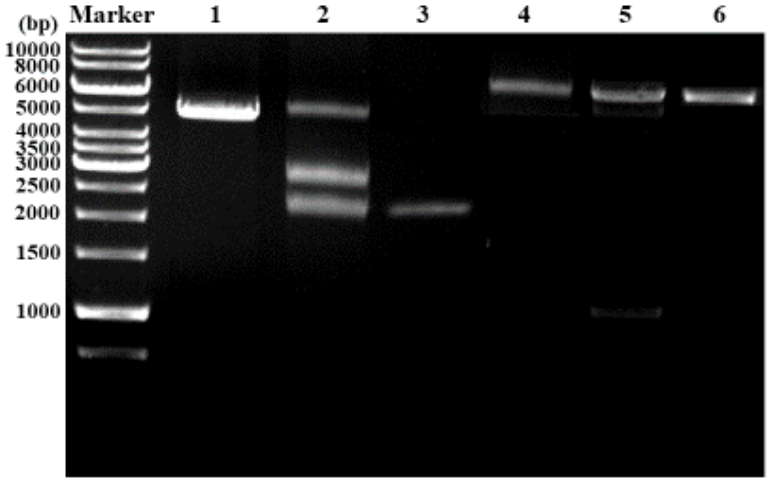

B

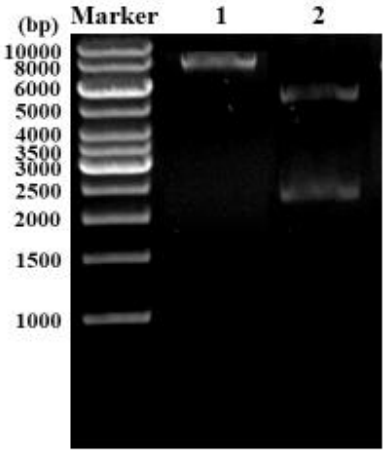

Figure 9.2. Electrophoresis on 1% agarose gel. **(A)** The single and double enzymatic digest fragments of "pUC-TGase" plasmid (lanes 1 & 2) and "pET15b-unknown" plasmid (lanes 4 & 5), respectively, as well as recovered target fragments TGase and pET-15b (lane 3 & 6). **(B)** The single and double enzymatic digest fragments of recombinant "pET15b-TGase" plasmid.

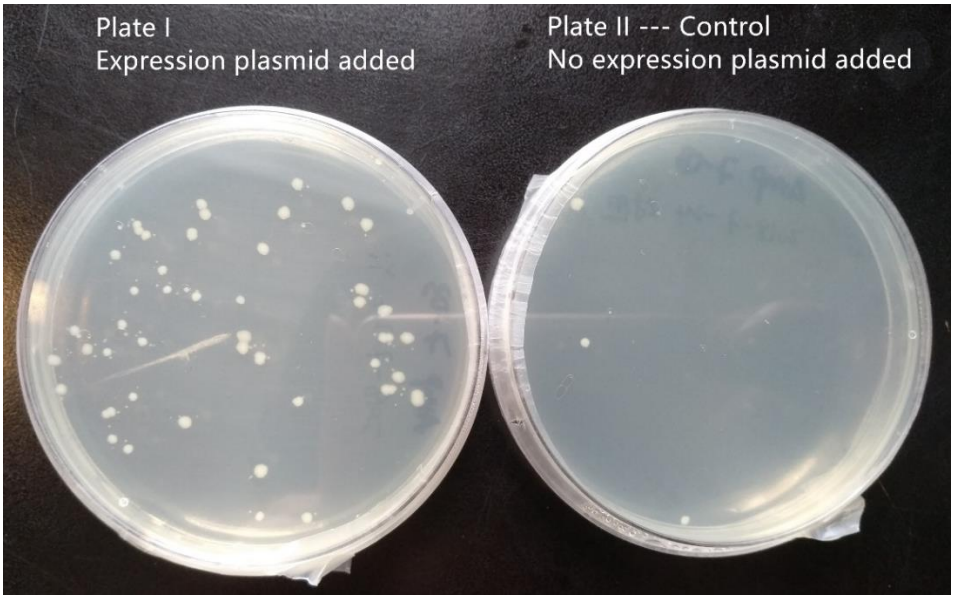

Figure 9.3. The LB agar plates with ampicillin. Plate I showed *E. coli* colonies transformed with expression plasmid PET15b-TGase. Plate II showed control - *E. coli* without expression plasmid.

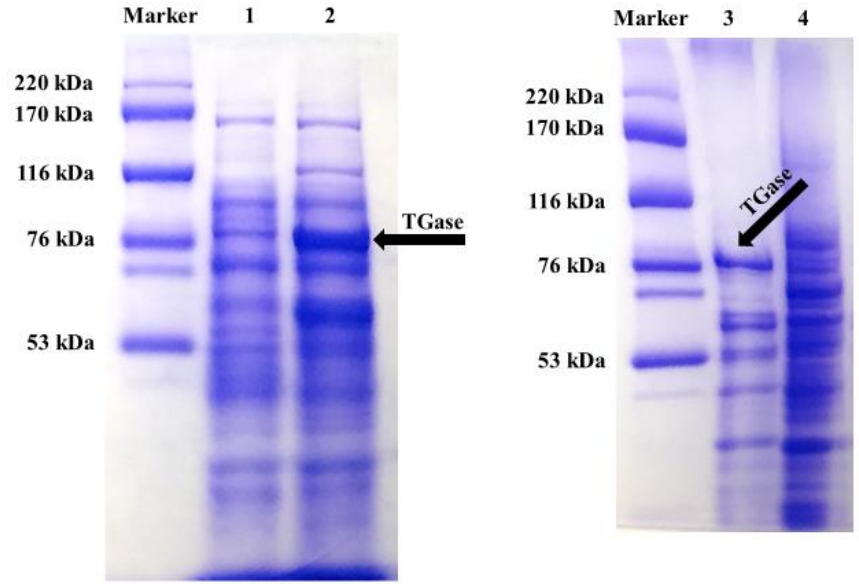

Figure 9.4. Protein patterns on SDS-PAGE gel. Lane 1: Protein expressed without induction. Lane 2: Protein expressed with induction using IPTG. Lane 3: Protein in inclusion bodies from induced *E. coli*. Lane 4: Protein in supernatant from induced *E. coli*.

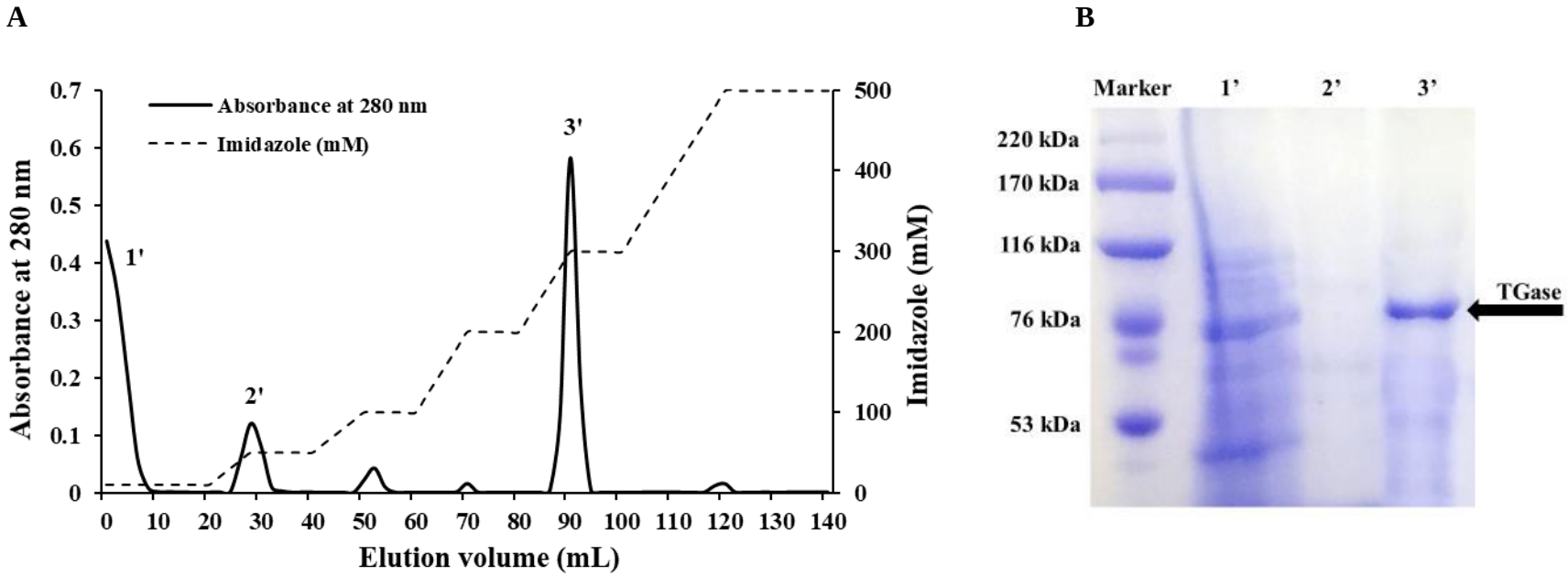

Figure 9.5. Purification of the expressed recombinant TGase. **(A)** The elution profile using imidazole. **(B)** SDS-PAGE profile of the eluted peaks.

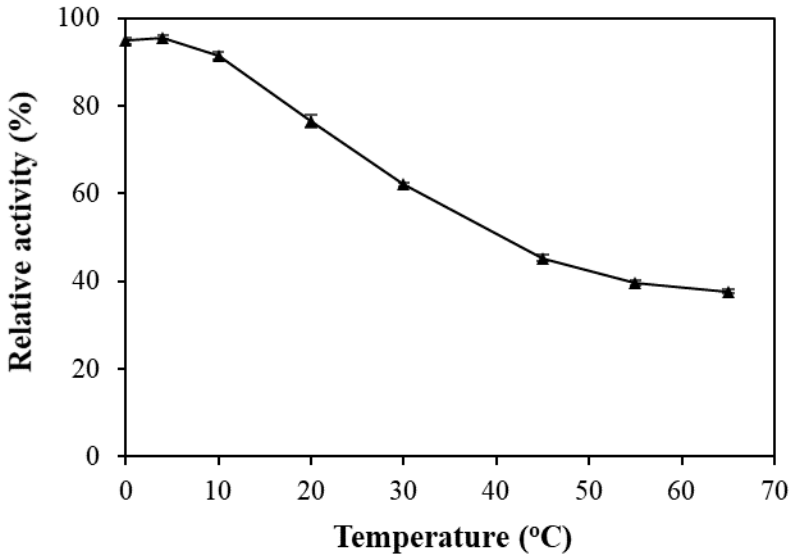

Figure 9.6. Cold-activity of recombinant Antarctic krill TGase expressed in *E. coli*. The relative activity (%) versus temperature at 0, 4, 10, 20, 30, 45, 55 and 65 ºC.

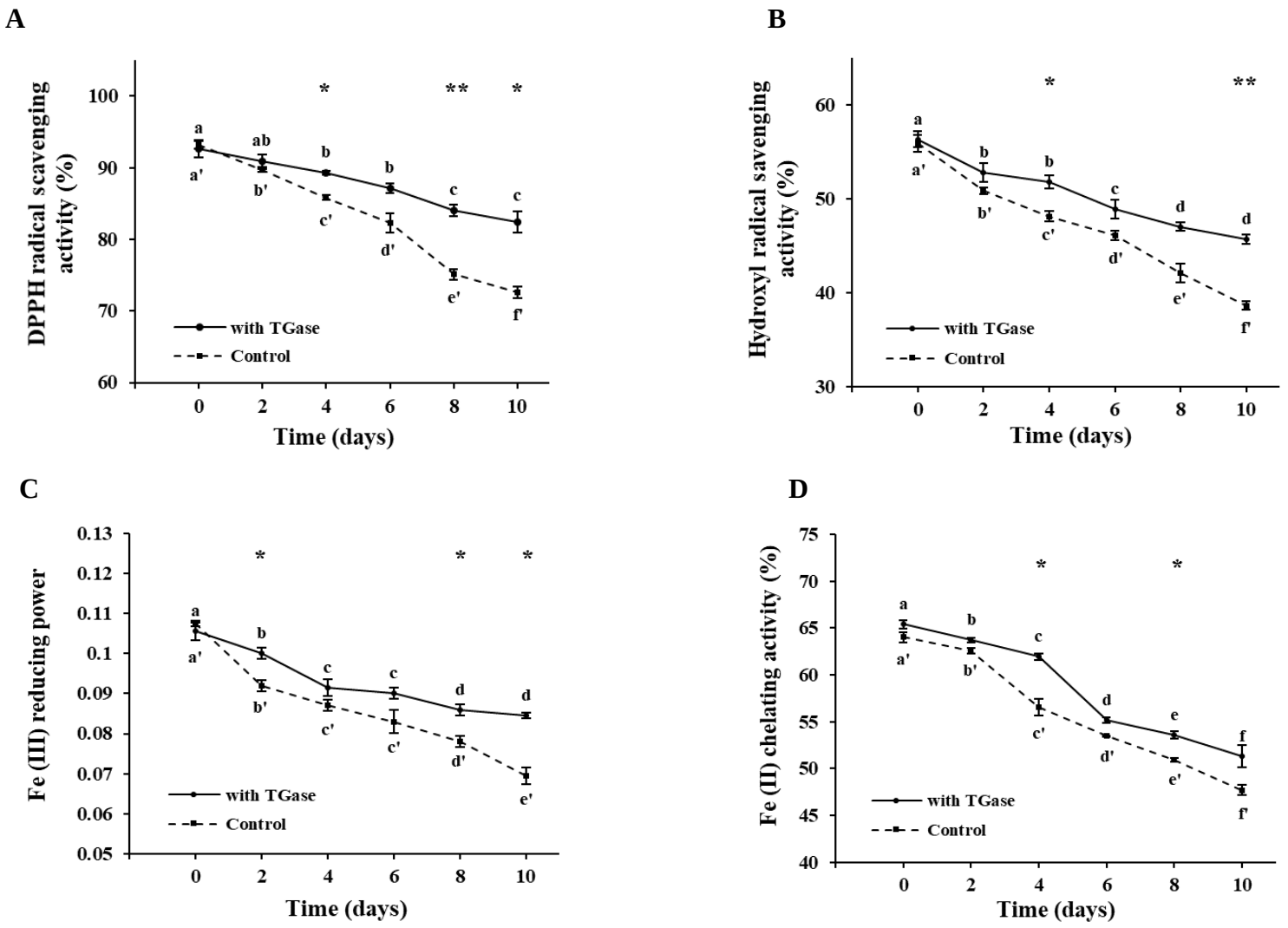

Figure 9.7. Antioxidant activity of the hydrogel crosslinked with recombinant TGase and added without TGase. **(A)** DPPH scavenging activity. **(B)** Hydroxyl scavenging activity. **(C)** Fe (III) reducing power. **(D)** Fe (II) chelating activity.

CHAPTER IX. GENERAL CONCLUSIONS, CONTRIBUTIONS TO KNOWLEDGE AND RECOMMENDATIONS FOR FUTURE WORK

10.1. General conclusions

Transglutaminase (TGase) purified from Antarctic krill exhibited unique properties, with optimal activity at weakly alkaline pH (pH 8.0–9.0) and low temperature (0–10^{o}C). The enzyme activity was enhanced by Ca^{2+} and Na^{+}. The Antarctic krill TGase was strongly inhibited by PCMB, IAA, NEM and Zn^{2+}, Cu^{2+} suggesting that the purified enzyme probably has cysteine in its catalytic site. The high activity at cold temperatures enabled the TGase to be used in cold reaction conditions, such as formation of cold-set gelatin hydrogels at 4 ^{o}C with enhanced mechanical properties.

The cold-active TGase from Antarctic krill showed relatively thermostable properties especially at temperatures 0–60 ^{o}C. Fluorescence spectroscopy was applied to characterize structural change when TGase was incubated at different temperatures. It suggested the existence of an intermediate molten globular state during unfolding, and peptide bond change occurring at 60 ^{o}C. Transcriptomics was used to obtain the gene sequence and a homologous structure was constructed. The domains and catalytic triad were identified, as well as the possible molecular interactions around the domains. Such structural interpretation explained the reason for the thermostability of this cold-active TGase.

Gelatin high in α-chain content was produced with the aid of alcalase enzyme under mild pH 7.5 and room temperatures reaction conditions. The amino acid composition, functional groups and thermal properties of the gelatin were characterized, from which it is inferred that this high α-chain fish gelatin will favor stable network formation in hydrogels. The functional properties data also suggest that the hydrogels made from the gelatin could withstand thermal treatments over a wide temperature range from 35–80 ^{o}C, thus can suit various applications that require thermal treatments.

Atlantic sea cucumber is good source for developing functional foods such as antioxidative peptides, and its value can be enhanced via enzymatic treatment. Alcalase-produced hydrolysates showed generally higher antioxidant activity than the trypsin produced ones. $A_{<2}$ and $T_{<2}$ peptide fractions contained high content of leucine, and $A_{<2}$ fraction had higher nutritional value than $T_{<2}$ based on the EAA/NEAA ratio. $A_{<2}$ fraction generated larger proportion of peptides with key antioxidative amino acids, as well as potential inhibition effect on MPO, compared with trypsin-produced $T_{<2}$ fraction. According to molecular docking prediction, weak interactions including van der Waals, hydrogen bonds, hydrophobic and electrostatic interactions were found with each chain of MPO enzyme that are responsible for inhibition effect on MPO.

TGase gene was difficult to obtain from Antarctic krill due to the long-term transportation from Antarctica. The TGase gene was synthesized *in vitro*, and the codon optimization improved the expression level. A recombinant expression plasmid using pET-15b was successfully constructed. In terms of the expressed TGase in inclusion body form, a simple and efficient purification and refolding process was proposed, including Ni-Sepharose purification with 300 mM imidazole elution and a multi-step dialysis using 6 different refolding buffers. The recovered TGase showed cold-activity. This work also found that the recombinant TGase could stabilize antioxidative peptides onto gelatin matrix during cold-setting at 4 ^{o}C, and such crosslinked antioxidative hydrogel could be added as ingredients in foods processed or storage at low temperatures.

10.2. Contribution to knowledge

1. Discovery and first reporting of a novel cold-active transglutaminase and observed its successful usage in improvement of the texture of cold-set gelatin hydrogels.

2. Thermal inactivation kinetics characterization of the TGase enzyme to provide an in-depth understanding of the relationships between structure and function.

3. Enzymatic production of a high-quality high content α-chain gelatins capable of forming strong hydrogels.

4. Enzymatic production of antioxidative peptides from Atlantic sea cucumber and their identification as well as *in vivo* function prediction using *in silico* methods

5. Reported the gene sequence encoding the cold-active TGase for the first time. Developed an efficient process of expression, purification and refolding to obtain active recombinant TGase.

6. Usage of the recombinant cold-active TGase in forming anti-oxidant cold-set gelatin hydrogels incorporated with bioactive peptides.

10.3. Recommendations for future work

1. Improvement of the activity and yield of recombinant TGase.

2. Structural characterization of the cold-active TGase using X-ray diffraction or modern electron microscope.

3. Exploring novel applications with the cold-active TGase in food or non-food industries.

REFERENCES

Aam B. B., Heggset E. B., Norberg A. L., Sørlie M., Vårum K. M., and Eijsink V. G. (2010). Production of chitooligosaccharides and their potential applications in medicine. *Marine drugs*. 8: 1482-1517.

Abe T., Chun S. I., DiAugustine R. P., and Folk J. (1977). Rabbit liver transglutaminase: physical, chemical, and catalytic properties. *Biochemistry*. 16: 5495-5501.

Achyuthan K., and Greenberg C. (1987). Identification of a guanosine triphosphate-binding site on guinea pig liver transglutaminase. Role of GTP and calcium ions in modulating activity. *Journal of Biological Chemistry*. 262: 1901-1906.

Agarwal A., Sharma R., Durairajanayagam D., Cui Z., Ayaz A., Gupta S., Willard B., Gopalan B., and Sabanegh E. (2016). Spermatozoa protein alterations in infertile men with bilateral varicocele. *Asian journal of andrology*. 18: 43.

Agyare K. K., Addo K., and Xiong Y. L. (2009). Emulsifying and foaming properties of transglutaminase-treated wheat gluten hydrolysate as influenced by pH, temperature and salt. *Food Hydrocolloids*. 23: 72-81.

Ahvazi B., Boeshans K. M., Idler W., Baxa U., Steinert P. M., and Rastinejad F. (2004). Structural basis for the coordinated regulation of transglutaminase 3 by guanine nucleotides and calcium/magnesium. *Journal of Biological Chemistry*. 279: 7180-7192.

Ahvazi B., Kim H. C., Kee S. H., Nemes Z., and Steinert P. M. (2002). Three - dimensional structure of the human transglutaminase 3 enzyme: binding of calcium ions changes structure for activation. *The EMBO Journal*. 21: 2055-2067.

Akanbi T. O., and Barrow C. J. (2017). Candida antarctica lipase A effectively concentrates DHA from fish and thraustochytrid oils. *Food Chemistry*. 229: 509-516.

Alemán A., Giménez B., Gómez-Guillén M. C., and Montero P. (2011). Enzymatic hydrolysis of fish gelatin under high pressure treatment. *International Journal of Food Science & Technology*. 46: 1129-1136.

Amirdivani S., Khorshidian N., Fidelis M., Granato D., Koushki M. R., Mohammadi M., Khoshtinat K., and Mortazavian A. M. (2018). Effects of transglutaminase on health properties of food products. *Current Opinion in Food Science*. 22: 74-80.

An Y., You J., Xiong S., and Yin T. (2018). Short-term frozen storage enhances cross-linking that

was induced by transglutaminase in surimi gels from silver carp (*Hypophthalmichthys molitrix*). *Food Chemistry*. 257: 216-222.

Ando H., Adachi M., Umeda K., Matsuura A., Nonaka M., Uchio R., Tanaka H., and Motoki M. (1989). Purification and characteristics of a novel transglutaminase derived from microorganisms. *Agricultural and Biological Chemistry*. 53: 2613-2617.

Ando Y., Imamura S., Murachi T., and Kannagi R. (1988). Calpain activates two transglutaminases from porcine skin. *Archives of Dermatological Research*. 280: 380-384.

Anthon G. E., and Barrett D. M. (2002). Kinetic parameters for the thermal inactivation of quality-related enzymes in carrots and potatoes. *Journal of Agricultural and Food Chemistry*. 50: 4119-4125.

Antoniou J., Liu F., Majeed H., and Zhong F. (2015). Characterization of tara gum edible films incorporated with bulk chitosan and chitosan nanoparticles: A comparative study. *Food Hydrocolloids*. 44: 309-319.

Apostolov A., Fakirov S., Vassileva E., Patil R., and Mark J. (1999). DSC and TGA studies of the behavior of water in native and crosslinked gelatin. *Journal of applied polymer science*. 71: 465-470.

Arham R., Mulyati M., Metusalach M., and Salengke S. (2016). Physical and mechanical properties of agar based edible film with glycerol plasticizer. *International Food Research Journal*. 23.

Aribaud M., Carré M., and Martin-Tanguy J. (1995). Transglutaminase-like activity in chrysanthemum leaf explants cultivated *in vitro* in relation to cell growth and hormone treatment. *Plant Growth Regulation*. 16: 11-17.

Ariëns R. A., Lai T.-S., Weisel J. W., Greenberg C. S., and Grant P. J. (2002). Role of factor XIII in fibrin clot formation and effects of genetic polymorphisms. *Blood*. 100: 743-754.

Arockiaraj J., Gnanam A. J., Palanisamy R., Kumaresan V., Bhatt P., Thirumalai M. K., Roy A., Pasupuleti M., Kasi M., and Sathyamoorthi A. (2013). A prawn transglutaminase: molecular characterization and biochemical properties. *Biochimie*. 95: 2354-2364.

Arroyo C., Kennedy T. M., Lyng J. G., and O'Sullivan M. (2017). Comparison of conventional heat treatment with selected non-thermal technologies for the inactivation of the commercial protease Protamex™. *Food and Bioproducts Processing*. 105: 95-103.

Ashie I., and Lanier T. C. (2000). Transglutaminases in seafood processing. In: Seafood enzymes:

utilization and influence on postharvest seafood quality, pp. 147-166. Haard N., and B.K. S. (Eds.), Marcel Dekker, Inc., New York, NY, USA.

Assisi L., Autuori F., Botte V., Farrace M. G., and Piacentini M. (1999). Hormonal control of "tissue" transglutaminase induction during programmed cell death in frog liver. *Experimental cell research*. 247: 339-346.

ASTM (2003). Annual book of ASTM standards. *Pennsylvania: American Society for Testing and Materials.*

Avena-Bustillos R., Olsen C., Olson D., Chiou B., Yee E., Bechtel P., and McHugh T. (2006). Water vapor permeability of mammalian and fish gelatin films. *Journal of Food Science*. 71: 202-207.

Aymard C., and Belarbi A. (2000). Kinetics of thermal deactivation of enzymes: a simple three parameters phenomenological model can describe the decay of enzyme activity, irrespectively of the mechanism. *Enzyme and Microbial Technology*. 27: 612-618.

Baba Y., Sumitani J.-i., Tanaka K., Tani S., and Kawaguchi T. (2016). Site-saturation mutagenesis for β-glucosidase 1 from *Aspergillus aculeatus* to accelerate the saccharification of alkaline-pretreated bagasse. *Applied Microbiology and Biotechnology*. 100: 10495-10507.

Babin H., and Dickinson E. (2001). Influence of transglutaminase treatment on the thermoreversible gelation of gelatin. *Food Hydrocolloids*. 15: 271-276.

Bagheri L., Madadlou A., Yarmand M., and Mousavi M. E. (2014). Potentially bioactive and caffeine-loaded peptidic sub-micron and nanoscalar particles. *Journal of Functional Foods*. 6: 462-469.

Bahrim G., Iancu C., Buţu N., and Negoiţă T. G. (2010). Production of a novel microbial transglutaminase using *Streptomyces* sp. polar strains. *Romanian Biotechnological Letters*. 15: 5197-5203.

Balti R., Jridi M., Sila A., Souissi N., Nedjar-Arroume N., Guillochon D., and Nasri M. (2011). Extraction and functional properties of gelatin from the skin of cuttlefish (*Sepia officinalis*) using smooth hound crude acid protease-aided process. *Food Hydrocolloids*. 25: 943-950.

Bartels T., Choi J. G., and Selkoe D. J. (2011). α-Synuclein occurs physiologically as a helically folded tetramer that resists aggregation. *Nature*. 477: 107.

Batista I., Salteiro A. T., and Mateus M. J. (2002). Preliminary characterization of European sardine transglutaminase. *Journal of Aquatic Food Product Technology*. 11: 57-64.

Benbettaïeb N., Kurek M., Bornaz S., and Debeaufort F. (2014). Barrier, structural and mechanical properties of bovine gelatin–chitosan blend films related to biopolymer interactions. *Journal of the Science of Food and Agriculture*. 94: 2409-2419.

Beninati S., and Piacentini M. (2004). The transglutaminase family: an overview: minireview article. *Amino Acids*. 26: 367-372.

Benjakul S., Kittiphattanabawon P., and Regenstein J. M. (2012). Fish gelatin. *Food Biochemistry and Food Processing, Second Edition*: 388-405.

Benjakul S., Visessanguan W., and Pecharat S. (2004). Suwari gel properties as affected by transglutaminase activator and inhibitors. *Food Chemistry*. 85: 91-99.

Bernet E., Claparols I., Dondini L., Santos M. A., Serafini-Fracassini D., and Torné J. M. (1999). Changes in polyamine content, arginine and ornithine decarboxylases and transglutaminase activities during light/dark phases (of initial differentiation) in maize calluses and their chloroplasts. *Plant Physiology and Biochemistry*. 37: 899-909.

Binsi P., and Shamasundar B. (2012). Purification and characterisation of transglutaminase from four fish species: effect of added transglutaminase on the viscoelastic behaviour of fish mince. *Food Chemistry*. 132: 1922-1929.

Bishop P. D., Teller D., Smith R., Lasser G., Gilbert T., and Seale R. (1990). Expression, purification, and characterization of human factor XIII in Saccharomyces cerevisiae. *Biochemistry*. 29: 1861-1869.

Bkhairia I., Khaled H. B., Ktari N., Miled N., Nasri M., and Ghorbel S. (2016). Biochemical and molecular characterisation of a new alkaline trypsin from *Liza aurata*: Structural features explaining thermal stability. *Food Chemistry*. 196: 1346-1354.

Blanco M., Vázquez J. A., Pérez-Martín R. I., and Sotelo C. G. (2017). Hydrolysates of fish skin collagen: An opportunity for valorizing fish industry byproducts. *Marine drugs*. 15: 131.

Boran G., and Regenstein J. M. (2010). Fish gelatin. *Advances in food and nutrition research*. 60: 119-143.

Bordbar S., Anwar F., and Saari N. (2011). High-value components and bioactives from sea cucumbers for functional foods—A review. *Marine drugs*. 9: 1761-1805.

Bourneow C., Benjakul S., and H-Kittikun A. (2011). Purification and characterization of microbial transglutaminase from *Enterobacter* sp. C2361. *Thai Journal of Agricultural Science*. 44: 496-504.

Brochier B., Mercali G. D., and Marczak L. D. F. (2016). Influence of moderate electric field on inactivation kinetics of peroxidase and polyphenol oxidase and on phenolic compounds of sugarcane juice treated by ohmic heating. *LWT-Food Science and Technology*. 74: 396-403.

Brookhart P. P., McMahon P. L., and Takahashi M. (1983). Purification of guinea pig liver transglutaminase using a phenylalanine-Sepharose 4B affinity column. *Analytical Biochemistry*. 128: 202-205.

BSI755 (1975). British Standards Institution Specification for Gelatin.: Pentonville Rd, London, UK.

Budnik L. T., Scheer E., Burge P. S., and Baur X. (2017). Sensitising effects of genetically modified enzymes used in flavour, fragrance, detergence and pharmaceutical production: cross-sectional study. *Occup Environ Med*. 74: 39-45.

Buettner K., Hertel T. C., and Pietzsch M. (2012). Increased thermostability of microbial transglutaminase by combination of several hot spots evolved by random and saturation mutagenesis. *Amino Acids*. 42: 987-996.

Buxman M. M., and Wuepper K. D. (1976). Isolation, purification and characterization of bovine epidermal transglutaminase. *Biochimica et Biophysica Acta (BBA)-Enzymology*. 452: 356-369.

Cai L., Feng J., Cao A., Tian H., Wang J., Liu Y., Gong L., and Li J. (2018). Effect of Partial Substitutes of NaCl on the Cold-Set Gelation of Grass Carp Myofibrillar Protein Mediated by Microbial Transglutaminase. *Food and Bioprocess Technology*. 11: 1876-1886.

Campos N., Castañón S., Urreta I., Santos M., and Torné J. (2013). Rice transglutaminase gene: identification, protein expression, functionality, light dependence and specific cell location. *Plant Science*. 205: 97-110.

Cao N., Yang X., and Fu Y. (2009). Effects of various plasticizers on mechanical and water vapor barrier properties of gelatin films. *Food Hydrocolloids*. 23: 729-735.

Cappannella E., Benucci I., Lombardelli C., Liburdi K., Bavaro T., and Esti M. (2016). Immobilized lysozyme for the continuous lysis of lactic bacteria in wine: Bench-scale fluidized-bed reactor study. *Food Chemistry*. 210: 49-55.

Carpena X., Vidossich P., Schroettner K., Calisto B. M., Banerjee S., Stampler J., Soudi M., Furtmüller P. G., Rovira C., and Fita I. (2009). Essential role of proximal histidine-asparagine interaction in mammalian peroxidases. *Journal of Biological Chemistry*. 284:

25929-25937.

Cates E. S., Dinwiddie J. A., Aux G., Batie C., and Crabb G. (2010). Process for starch liquefaction and fermentation. Google Patents.

Cavicchioli R., Siddiqui K. S., Andrews D., and Sowers K. R. (2002). Low-temperature extremophiles and their applications. *Current Opinion in Biotechnology*. 13: 253-261.

Ceresino E. B., de Melo R. R., Kuktaite R., Hedenqvist M. S., Zucchi T. D., Johansson E., and Sato H. H. (2018). Transglutaminase from newly isolated *Streptomyces* sp. CBMAI 1617: Production optimization, characterization and evaluation in wheat protein and dough systems. *Food Chemistry*. 241: 403-410.

Cermeño M., FitzGerald R. J., and O'Brien N. M. (2016). *In vitro* antioxidant and immunomodulatory activity of transglutaminase-treated sodium caseinate hydrolysates. *International Dairy Journal*. 63: 107-114.

Chalamaiah M., Hemalatha R., and Jyothirmayi T. (2012). Fish protein hydrolysates: Proximate composition, amino acid composition, antioxidant activities and applications: A review. *Food Chemistry*. 135: 3020-3038.

Chandrashekar R., Tsuji N., Morales T., Ozols V., and Mehta K. (1998). An ERp60-like protein from the filarial parasite <*Dirofilaria immitis*> has both transglutaminase and protein disulfide isomerase activity. *Proceedings of the National Academy of Sciences*. 95: 531-536.

Chang C.-C., Chang H.-C., Liu K.-F., and Cheng W. (2016). The known two types of transglutaminases regulate immune and stress responses in white shrimp, *Litopenaeus vannamei*. *Developmental & Comparative Immunology*. 59: 164-176.

Chang S.-W., Huang M., Hsieh Y.-H., Luo Y.-T., Wu T.-T., Tsai C.-W., Chen C.-S., and Shaw J.-F. (2014). Simultaneous production of fatty acid methyl esters and diglycerides by four recombinant *Candida rugosa* lipase's isozymes. *Food Chemistry*. 155: 140-145.

Chen M.-Y., Hu K.-Y., Huang C.-C., and Song Y.-L. (2005a). More than one type of transglutaminase in invertebrates? A second type of transglutaminase is involved in shrimp coagulation. *Developmental & Comparative Immunology*. 29: 1003-1016.

Chen M. Y., Hu K. Y., Huang C. C., and Song Y. L. (2005b). More than one type of transglutaminase in invertebrates? A second type of transglutaminase is involved in shrimp coagulation. *Developmental & Comparative Immunology*. 29: 1003-1016.

Chen S., Tang L., Su W., Weng W., Osako K., and Tanaka M. (2015). Separation and

characterization of alpha-chain subunits from tilapia (*Tilapia zillii*) skin gelatin using ultrafiltration. *Food Chemistry*. 188: 350-356.

Chen Y.-n., Chen W.-C., and Cheng W. (2014a). The second type of transglutaminase regulates immune and stress responses in white shrimp, *Litopenaeus vannamei*. *Fish & Shellfish Immunology*. 37: 30-37.

Chen Y., Chen W., and Cheng W. (2014b). The second type of transglutaminase regulates immune and stress responses in white shrimp, *Litopenaeus vannamei*. *Fish & Shellfish Immunology*. 37: 30-37.

Chiumarelli M., and Hubinger M. D. (2014). Evaluation of edible films and coatings formulated with cassava starch, glycerol, carnauba wax and stearic acid. *Food Hydrocolloids*. 38: 20-27.

Choi J. H., Kim K. J., Kim S. J., and Kim S. (2017). Novel protease from the leaves of edible medicinal plant *Aster koraiensis* Nakai with antithrombotic activity: Purification and partial characterization. *Journal of Food Biochemistry*. 41.

Chomarat N., Robert L., Seris J., and Kern P. (1994). Comparative efficiency of pepsin and proctase for the preparation of bovine skin gelatin. *Enzyme and Microbial Technology*. 16: 756-760.

Chou H.-H., Chang S.-W., Lee G.-C., Chen Y.-S., Yeh T., Akoh C. C., and Shaw J.-F. (2010). Site-directed mutagenesis improves the thermostability of a recombinant *Picrophilus torridus* trehalose synthase and efficiency for the production of trehalose from sweet potato starch. *Food Chemistry*. 119: 1017-1022.

Clarke D., Mycek M., Neidle A., and Waelsch H. (1959). The incorporation of amines into protein. *Archives of Biochemistry and Biophysics*. 79: 338-354.

Coker J. A. (2016). Extremophiles and biotechnology: current uses and prospects. *F1000Research*. 5.

Colgrave M. L., Byrne K., and Howitt C. A. (2017). Food for thought: Selecting the right enzyme for the digestion of gluten. *Food Chemistry*. 234: 389-397.

Columbus D. A., Fiorotto M. L., and Davis T. A. (2015). Leucine is a major regulator of muscle protein synthesis in neonates. *Amino Acids*. 47: 259-270.

Connellan J. M., Chung S., Whetzel N. K., Bradley L. M., and Folk J. (1971). Structural properties of guinea pig liver transglutaminase. *Journal of Biological Chemistry*. 246: 1093-1098.

Croall D. E., and DeMartino G. N. (1986). Calcium-dependent affinity purification of transclutaminase from rat liver cytosol. *Cell Calcium*. 7: 29-39.

Cubiro J. M. T., Lozano M. A. S., Baro D. T., Amador E. V., and Lloveras J. R. (2007). Maize nucleotide sequence coding for a protein with transglutaminase activity and use thereof. U.S. Patent No. 7,262,057.

Cui L., Du G., Zhang D., and Chen J. (2008). Thermal stability and conformational changes of transglutaminase from a newly isolated *Streptomyces hygroscopicus*. *Bioresource technology*. 99: 3794-3800.

Cui L., Du G., Zhang D., Liu H., and Chen J. (2007). Purification and characterization of transglutaminase from a newly isolated *Streptomyces hygroscopicus*. *Food Chemistry*. 105: 612-618.

Dadshahi Z., Homaei A., Zeinali F., Sajedi R. H., and Khajeh K. (2016). Extraction and purification of a highly thermostable alkaline caseinolytic protease from wastes *Penaeus vannamei* suitable for food and detergent industries. *Food Chemistry*. 202: 110-115.

Damodaran S. (2005). Protein stabilization of emulsions and foams. *Journal of Food Science*. 70: 54-66.

Dash R., Foston M., and Ragauskas A. J. (2013). Improving the mechanical and thermal properties of gelatin hydrogels cross-linked by cellulose nanowhiskers. *Carbohydrate polymers*. 91: 638-645.

Datta S., Christena L. R., and Rajaram Y. R. S. (2013). Enzyme immobilization: an overview on techniques and support materials. *3 Biotech*. 3: 1-9.

Davies M. J., Hawkins C. L., Pattison D. I., and Rees M. D. (2008). Mammalian heme peroxidases: From molecular mechanisms to health implications. *Antioxidants & Redox Signaling*. 10: 1199-1234.

de Almeida B. C., Araújo B. Q., Carvalho A. A., Freitas S. D. L., Maciel D. d. S. A., Ferreira A. J. S., Tempone A. G., Martins L. F., Alexandre T. R., and Chaves M. H. (2016). Antiprotozoal activity of extracts and isolated triterpenoids of 'carnauba' (*Copernicia prunifera*) wax from Brazil. *Pharmaceutical Biology*. 54: 3280-3284.

de Camargo A. C., Regitano-d'Arce M. A. B., Biasoto A. C. T., and Shahidi F. (2016). Enzyme-assisted extraction of phenolics from winemaking by-products: Antioxidant potential and inhibition of alpha-glucosidase and lipase activities. *Food Chemistry*. 212: 395-402.

de Miguel Bouzas T., Barros-Velázquez J., and Gonzalez Villa T. (2006). Industrial applications of hyperthermophilic enzymes: a review. *Protein and peptide letters*. 13: 645-651.

De Santis B., Stockhofe N., Wal J.-M., Weesendorp E., Lallès J.-P., van Dijk J., Kok E., De Giacomo M., Einspanier R., and Onori R. (2018). Case studies on genetically modified organisms (GMOs): Potential risk scenarios and associated health indicators. *Food and Chemical Toxicology*. 117: 36-65.

De Souza C. F., Flôres S. H., and Ayub M. A. Z. (2006). Optimization of medium composition for the production of transglutaminase by *Bacillus circulans* BL32 using statistical experimental methods. *Process Biochemistry*. 41: 1186-1192.

Deasey S., Grichenko O., Du S., and Nurminskaya M. (2012). Characterization of the transglutaminase gene family in zebrafish and *in vivo* analysis of transglutaminase-dependent bone mineralization. *Amino Acids*. 42: 1065-1075.

Dediu D. (2015). An introduction to genetics for language scientists. Cambridge University Press, Cambridge, UK.

Del Duca S., Bregoli A. M., Bergamini C., and Serafini-Fracassini D. (1997). Transglutaminase-catalyzed modification of cytoskeletal proteins by polyamines during the germination of *Malus domestica* pollen. *Sexual Plant Reproduction*. 10: 89-95.

Del Duca S., Serafini-Fracassini D., and Cai G. (2014). Senescence and programmed cell death in plants: polyamine action mediated by transglutaminase. *Frontiers in plant science*. 5: 120.

del Pilar Sánchez-Camargo A., Montero L., Stiger-Pouvreau V., Tanniou A., Cifuentes A., Herrero M., and Ibáñez E. (2016). Considerations on the use of enzyme-assisted extraction in combination with pressurized liquids to recover bioactive compounds from algae. *Food Chemistry*. 192: 67-74.

Della Mea M., Di Sandro A., Dondini L., Del Duca S., Vantini F., Bergamini C., Bassi R., and Serafini-Fracassini D. (2004). A Zea mays 39-kDa thylakoid transglutaminase catalyses the modification by polyamines of light-harvesting complex II in a light-dependent way. *Planta*. 219: 754-764.

Demirbay B., Akaoğlu C., Ulusaraç İ., and Acar F. G. (2017). Thermal and UV radiation effects on dynamic viscosity of gelatin-based riboflavin solutions. *Journal of Molecular Liquids*. 225: 147-150.

Devarajan E., Mishra P. K., Thirugnanam S., Mehta K., Chandrashekar R., and Perumal K. (2004).

Molecular characterization of a *Brugia malayi* transglutaminase. *Parasitol Res*. 93: 145-150.

Dixon M., Webb E., Thorne C., and Tipton K. (1979). Enzymes. 3rd Edition. Longmans, Green & Co., London, and Academic Press, New York.

Do D. H. T., Kong F., Penet C., Winetzky D., and Gregory K. (2016). Using a dynamic stomach model to study efficacy of supplemental enzymes during simulated digestion. *LWT-Food Science and Technology*. 65: 580-588.

Doyle B. B., Bendit E., and Blout E. R. (1975). Infrared spectroscopy of collagen and collagen-like polypeptides. *Biopolymers*. 14: 937-957.

Duarte A. W. F., dos Santos J. A., Vianna M. V., Vieira J. M. F., Mallagutti V. H., Inforsato F. J., Wentzel L. C. P., Lario L. D., Rodrigues A., and Pagnocca F. C. (2018). Cold-adapted enzymes produced by fungi from terrestrial and marine Antarctic environments. *Critical reviews in biotechnology*. 38: 600-619.

Edwards A. M., and Silva E. (2001). Effect of visible light on selected enzymes, vitamins and amino acids. *Journal of Photochemistry and Photobiology B: Biology*. 63: 126-131.

Ejaz M., Arfat Y. A., Mulla M., and Ahmed J. (2018). Zinc oxide nanorods/clove essential oil incorporated Type B gelatin composite films and its applicability for shrimp packaging. *Food Packaging and Shelf Life*. 15: 113-121.

El-Hofi M., Ismail A., Nour M., and Ibrahim O. (2014). Isolation, purifi cation and characterisation of transglutaminase from rosemary (*Rosmarinus officinalis* L.) leaves. *Acta Scientiarum Polonorum Technologia Alimentaria*. 13: 267-278.

El Abed H., Khemakhem B., Fendri I., Chakroun M., Triki M., Drira N., and Mejdoub H. (2017). Extraction, partial purification and characterization of amylase from parthenocarpic date (*Phoenix dactylifera*): effect on cake quality. *Journal of the Science of Food and Agriculture*. 97: 3445-3452.

Elharfaoui N., Djabourov M., and Babel W. (2007). Molecular weight influence on gelatin gels: structure, enthalpy and rheology. In: Macromolecular Symposia, pp. 149-157.

Ermis E. (2017). Halal status of enzymes used in food industry. *Trends in Food Science & Technology*. 64: 69-73.

Estevão M. S., Carvalho L. C., Ribeiro D., Couto D., Freitas M., Gomes A., Ferreira L., Fernandes E., and Marques M. M. B. (2010). Antioxidant activity of unexplored indole derivatives: Synthesis and screening. *European Journal of Medicinal Chemistry*. 45: 4869-4878.

Etxabide A., Uranga J., Guerrero P., and de la Caba K. (2017). Development of active gelatin films by means of valorisation of food processing waste: A review. *Food Hydrocolloids*. 68: 192-198.

Eysturskarð J., Haug I. J., Ulset A. S., and Draget K. I. (2009). Mechanical properties of mammalian and fish gelatins based on their weight average molecular weight and molecular weight distribution. *Food Hydrocolloids*. 23: 2315-2321.

Fabra M. J., Hambleton A., Talens P., Debeaufort F., Chiralt A., and Voilley A. (2009). Influence of interactions on water and aroma permeabilities of ι-carrageenan–oleic acid–beeswax films used for flavour encapsulation. *Carbohydrate polymers*. 76: 325-332.

Færgemand M., Otte J., and Qvist K. B. (1997). Enzymatic cross-linking of whey proteins by a Ca^{2+}-independent microbial transglutaminase from *Streptomyces lydicus*. *Food Hydrocolloids*. 11: 19-25.

Falcone P., Serafini-Fracassini D., and Del Duca S. (1993). Comparative studies of transglutaminase activity and substrates in different organs of *Helianthus tuberosus*. *Journal of plant physiology*. 142: 265-273.

Faryar R., Linares-Pastén J. A., Immerzeel P., Mamo G., Andersson M., Stålbrand H., Mattiasson B., and Karlsson E. N. (2015). Production of prebiotic xylooligosaccharides from alkaline extracted wheat straw using the K80R-variant of a thermostable alkali-tolerant xylanase. *Food and Bioproducts Processing*. 93: 1-10.

Faye C., Inforzato A., Bignon M., Hartmann D. J., Muller L., Ballut L., Olsen B. R., Day A. J., and Ricard-Blum S. (2010). Transglutaminase-2: a new endostatin partner in the extracellular matrix of endothelial cells. *Biochemical Journal*. 427: 467-475.

Fedøy A.-E., Yang N., Martinez A., Leiros H.-K. S., and Steen I. H. (2007). Structural and functional properties of isocitrate dehydrogenase from the psychrophilic bacterium *Desulfotalea psychrophila* reveal a cold-active enzyme with an unusual high thermal stability. *Journal of molecular biology*. 372: 130-149.

Fernandes P. (2016). Enzymes in fish and seafood processing. *Frontiers in bioengineering and biotechnology*. 4: 59.

Ferrer M., Martínez-Martínez M., Bargiela R., Streit W. R., Golyshina O. V., and Golyshin P. N. (2016). Estimating the success of enzyme bioprospecting through metagenomics: current status and future trends. *Microbial biotechnology*. 9: 22-34.

Fesus L., and Piacentini M. (2002). Transglutaminase 2: an enigmatic enzyme with diverse functions. *Trends in biochemical sciences*. 27: 534-539.

Fleckenstein B., Qiao S. W., Larsen M. R., Jung G., Roepstorff P., and Sollid L. M. (2004). Molecular characterization of covalent complexes between tissue transglutaminase and gliadin peptides. *Journal of Biological Chemistry*. 279: 17607-17616.

Fleischer D. M., Venter C., and Vandenplas Y. (2016). Hydrolyzed Formula for Every Infant? In: Protein in Neonatal and Infant Nutrition: Recent Updates, pp. 51-65. Bhatia J., Shamir R., and Vandenplas Y. (Eds.), Karger Publishers.

Foegeding E. A., and Mleko S. W. (2002). Whey protein products. U.S. Patent No. 6,383,551.

Folk J., and Cole P. (1965). Structural requirements of specific substrates for guinea pig liver transglutaminase. *Journal of Biological Chemistry*. 240: 2951-2960.

Fontana A., Spolaore B., Mero A., and Veronese F. M. (2008). Site-specific modification and PEGylation of pharmaceutical proteins mediated by transglutaminase. *Advanced drug delivery reviews*. 60: 13-28.

Forbes L. V., Sjögren T., Auchère F., Jenkins D. W., Thong B., Laughton D., Hemsley P., Pairaudeau G., Turner R., and Eriksson H. (2013). Potent reversible inhibition of myeloperoxidase by aromatic hydroxamates. *Journal of Biological Chemistry*. 288: 36636-36647.

Fratini F., Cilia G., Turchi B., and Felicioli A. (2016). Beeswax: A minireview of its antimicrobial activity and its application in medicine. *Asian Pacific Journal of Tropical Medicine*. 9: 839-843.

Freitas C. A. S., Vieira Í. G. P., Sousa P. H. M., Muniz C. R., da Costa Gonzaga M. L., and Guedes M. I. F. (2016). Carnauba wax *p*-methoxycinnamic diesters: Characterisation, antioxidant activity and simulated gastrointestinal digestion followed by *in vitro* bioaccessibility. *Food Chemistry*. 196: 1293-1300.

Gabrielczyk J., Kluitmann J., Dammeyer T., and Jördening H.-J. (2017). Effects of ionic strength on inclusion body refolding at high concentration. *Protein expression and purification*. 130: 100-106.

Gallego M., Mora L., Escudero E., and Toldrá F. (2018). Bioactive peptides and free amino acids profiles in different types of European dry-fermented sausages. *International journal of food microbiology*. 276: 71-78.

Galus S., and Kadzińska J. (2015). Food applications of emulsion-based edible films and coatings. *Trends in Food Science & Technology*. 45: 273-283.

Gao C., Lan D., Liu L., Zhang H., Yang B., and Wang Y. (2014). Site-directed mutagenesis studies of the aromatic residues at the active site of a lipase from *Malassezia globosa*. *Biochimie*. 102: 29-36.

Gao R., Shi T., Liu X., Zhao M., Cui H., and Yuan L. (2017). Purification and characterisation of a salt-stable protease from the halophilic archaeon *Halogranum rubrum*. *Journal of the Science of Food and Agriculture*. 97: 1412-1419.

García-Saldaña J. S., Campas-Baypoli O. N., López-Cervantes J., Sánchez-Machado D. I., Cantú-Soto E. U., and Rodríguez-Ramírez R. (2016). Microencapsulation of sulforaphane from broccoli seed extracts by gelatin/gum arabic and gelatin/pectin complexes. *Food Chemistry*. 201: 94-100.

Gentile A., Antognoni F., Iorio R. A., Distefano G., Las Casas G., La Malfa S., Serafini-Fracassini D., and Del Duca S. (2012). Polyamines and transglutaminase activity are involved in compatible and self-incompatible pollination of *Citrus grandis*. *Amino Acids*. 42: 1025-1035.

Georlette D., Blaise V., Collins T., D'Amico S., Gratia E., Hoyoux A., Marx J.-C., Sonan G., Feller G., and Gerday C. (2004). Some like it cold: biocatalysis at low temperatures. *FEMS Microbiology Reviews*. 28: 25-42.

Gharibzahedi S. M. T., and Chronakis I. S. (2018). Crosslinking of milk proteins by microbial transglutaminase: utilization in functional yogurt products. *Food Chemistry*. 245: 620-632.

Gharibzahedi S. M. T., Koubaa M., Barba F. J., Greiner R., George S., and Roohinejad S. (2018). Recent advances in the application of microbial transglutaminase crosslinking in cheese and ice cream products: A review. *International journal of biological macromolecules*. 107: 2364-2374.

Gianasi B. L., Hamel J.-F., and Mercier A. (2018). Morphometric and behavioural changes in the early life stages of the sea cucumber *Cucumaria frondosa*. *Aquaculture*. 490: 5-18.

Giménez B., Alemán A., Montero P., and Gómez-Guillén M. (2009a). Antioxidant and functional properties of gelatin hydrolysates obtained from skin of sole and squid. *Food Chemistry*. 114: 976-983.

Giménez B., Gómez-Estaca J., Alemán A., Gómez-Guillén M., and Montero M. (2009b). Physico-chemical and film forming properties of giant squid (*Dosidicus gigas*) gelatin. *Food*

Hydrocolloids. 23: 585-592.

Girotti A. W. (2001). Photosensitized oxidation of membrane lipids: Reaction pathways, cytotoxic effects, and cytoprotective mechanisms. *Journal of Photochemistry and Photobiology B: Biology*. 63: 103-113.

GMIA (2006). Standard methods for the testing of edible gelatin. Gelatin Manufacturers Institute of America, Inc.

Gómez-Estaca J., Balaguer M., López-Carballo G., Gavara R., and Hernández-Muñoz P. (2017). Improving antioxidant and antimicrobial properties of curcumin by means of encapsulation in gelatin through electrohydrodynamic atomization. *Food Hydrocolloids*. 70: 313-320.

Gómez-Estaca J., Montero P., Fernández-Martín F., and Gómez-Guillén M. (2009). Physico-chemical and film-forming properties of bovine-hide and tuna-skin gelatin: a comparative study. *Journal of Food Engineering*. 90: 480-486.

Gómez-Guillén M., Ihl M., Bifani V., Silva A., and Montero P. (2007). Edible films made from tuna-fish gelatin with antioxidant extracts of two different murta ecotypes leaves (*Ugni molinae* Turcz). *Food Hydrocolloids*. 21: 1133-1143.

Gómez-Guillén M., Turnay J., Fernández-Dıaz M., Ulmo N., Lizarbe M., and Montero P. (2002). Structural and physical properties of gelatin extracted from different marine species: a comparative study. *Food Hydrocolloids*. 16: 25-34.

Gong B.-L., Mao R.-Q., Xiao Y., Jia M.-L., Zhong X.-L., Liu Y., Xu P.-L., and Li G. (2017). Improvement of enzyme activity and soluble expression of an alkaline protease isolated from oil-polluted mud flat metagenome by random mutagenesis. *Enzyme and Microbial Technology*. 106: 97-105.

Gorgieva S., and Kokol V. (2011). Collagen-vs. gelatine-based biomaterials and their biocompatibility: review and perspectives. In: Biomaterials Applications for Nanomedicine, pp. 17-52. Pignatello R. (Ed.), InTech, Rijeka, Croatia.

Gottardi D., Hong P. K., Ndagijimana M., and Betti M. (2014). Conjugation of gluten hydrolysates with glucosamine at mild temperatures enhances antioxidant and antimicrobial properties. *LWT-Food Science and Technology*. 57: 181-187.

Grootjans J. J., Groenen P. J., and de Jong W. W. (1995). Substrate Requirements for Transglutaminases. Influence of the amino acid residue preceding the amine donor lysine in a native protein. *Journal of Biological Chemistry*. 270: 22855-22858.

Gudmundsson M. (2002). Rheological properties of fish gelatins. *Journal of Food Science*. 67: 2172-2176.

Gundersen M. T., Keillor J. W., and Pelletier J. N. (2014). Microbial transglutaminase displays broad acyl-acceptor substrate specificity. *Applied Microbiology and Biotechnology*. 98: 219-230.

Gutiérrez T. J., Tapia M. S., Pérez E., and Famá L. (2015). Structural and mechanical properties of edible films made from native and modified cush-cush yam and cassava starch. *Food Hydrocolloids*. 45: 211-217.

Halal S. L. M. E., Zavareze E. d. R., Rocha M. d., Pinto V. Z., Nunes M. R., Luvielmo M. d. M., and Prentice C. (2016). Films based on protein isolated from croaker (*Micropogonias furnieri*) and palm oil. *Journal of the Science of Food and Agriculture*. 96: 2478-2485.

Hamdi M., Nasri R., Hajji S., Nigen M., Li S., and Nasri M. (2019). Acetylation degree, a key parameter modulating chitosan rheological, thermal and film-forming properties. *Food Hydrocolloids*. 87: 48-60.

Han B.-G., Cho J.-W., Cho Y. D., Jeong K.-C., Kim S.-Y., and Lee B. I. (2010). Crystal structure of human transglutaminase 2 in complex with adenosine triphosphate. *International journal of biological macromolecules*. 47: 190-195.

Hanani Z. N., Roos Y., and Kerry J. P. (2012). Use of beef, pork and fish gelatin sources in the manufacture of films and assessment of their composition and mechanical properties. *Food Hydrocolloids*. 29: 144-151.

Hansson T., Dahlbom I., Rogberg S., Dannæus A., Höpfl P., Gut H., Kraaz W., and Klareskog L. (2002). Recombinant human tissue transglutaminase for diagnosis and follow-up of childhood coeliac disease. *Pediatric research*. 51: 700-705.

Hasegawa G., Motoi S., Ichikawa Y., Ohtsuka T., Kumagai S., Kikuchi M., Yoshitaka S., and Saito Y. (2003). A novel function of tissue-type transglutaminase: protein disulphide isomerase. *Biochemical Journal*. 373: 793-803.

Haug I., and Draget K. (2009). Gelatin. In: Handbook of Hydrocolloids, pp. 142-163. Phillips G. O., and Williams P. A. (Eds.), Woodhead Publishing Ltd, Cambridge.

Hbaieb R. H., Kotti F., Valli E., Bendini A., Toschi T. G., and Gargouri M. (2017). Effect of Tunisian olive ripeness on endogenous enzymes and virgin olive oil phenolic composition. *Journal of Food Composition and Analysis*. 62: 43-50.

He M., Li Y., Pi F., Ji J., He X., Zhang Y., and Sun X. (2016). A novel detoxifying agent: Using rice husk carriers to immobilize zearalenone-degrading enzyme from *Aspergillus niger* FS10. *Food Control*. 68: 271-279.

He S., Zhang Y., Sun H., Du M., Qiu J., Tang M., Sun X., and Zhu B. (2019). Antioxidative peptides from proteolytic hydrolysates of False abalone (*Volutharpa ampullacea perryi*): Characterization, identification, and molecular docking. *Marine drugs*. 17: 116.

Hema G., Joshy C., Shyni K., Chatterjee N. S., Ninan G., and Mathew S. (2017). Optimization of process parameters for the production of collagen peptides from fish skin (*Epinephelus malabaricus*) using response surface methodology and its characterization. *Journal of Food Science and Technology*. 54: 488-496.

Hemung B.-O., and Yongsawatdigul J. (2008a). Partial purification and characterization of transglutaminase from threadfin bream (*Nemipterus* sp.) liver. *Journal of Food Biochemistry*. 32: 182-200.

Hemung B. O., and Yongsawatdigul J. (2008b). Partial purification and characterization of transglutaminase from threadfin bream (*Nemipterus sp.*) liver. *Journal of Food Biochemistry*. 32: 182-200.

Henriques A. O., and Moran J., Charles P (2007). Structure, assembly, and function of the spore surface layers. *Annu. Rev. Microbiol.* 61: 555-588.

Hitomi K., Kitamura M., and Sugimura Y. (2009). Preferred substrate sequences for transglutaminase 2: screening using a phage-displayed peptide library. *Amino Acids*. 36: 619-624.

Hitomi K., Kojima S., and Fesus L. (2016). Transglutaminases: Multiple functional modifiers and targets for new drug discovery. Springer.

Ho M.-L., Leu S.-Z., Hsieh J.-F., and Jiang S.-T. (2000). Technical approach to simplify the purification method and characterization of microbial transglutaminase produced from *Streptoverticillium ladakanum*. *Journal of Food Science*. 65: 76-80.

Holmes C. P., Casey J., and Cook D. J. (2017). Mashing with unmalted sorghum using a novel low temperature enzyme system: Impacts of sorghum grain composition and microstructure. *Food Chemistry*. 221: 324-334.

Hong G. P., and Chin K. B. (2010). Effects of microbial transglutaminase and sodium alginate on cold-set gelation of porcine myofibrillar protein with various salt levels. *Food Hydrocolloids*.

24: 444-451.

Hong P. K., Gottardi D., Ndagijimana M., and Betti M. (2014). Glycation and transglutaminase mediated glycosylation of fish gelatin peptides with glucosamine enhance bioactivity. *Food Chemistry*. 142: 285-293.

Hong P. K., Ndagijimana M., and Betti M. (2016). Glucosamine-induced glycation of hydrolysed meat proteins in the presence or absence of transglutaminase: chemical modifications and taste-enhancing activity. *Food chemistry*. 197: 1143-1152.

Hong S., Lee C., and Jang S. H. (2012). Purification and properties of an extracellular esterase from a cold-adapted *Pseudomonas mandelii*. *Biotechnology Letters*. 34: 1051-1055.

Hoque M. S., Benjakul S., and Prodpran T. (2010). Effect of heat treatment of film-forming solution on the properties of film from cuttlefish (*Sepia pharaonis*) skin gelatin. *Journal of Food Engineering*. 96: 66-73.

Hosseini-Parvar S. H., Keramat J., Kadivar M., Khanipour E., and Motamedzadegan A. (2009). Optimising conditions for enzymatic extraction of edible gelatin from the cattle bones using response surface methodology. *International Journal of Food Science & Technology*. 44: 467-475.

Hosseini S. F., Rezaei M., Zandi M., and Ghavi F. F. (2013). Preparation and functional properties of fish gelatin–chitosan blend edible films. *Food Chemistry*. 136: 1490-1495.

Hoyoux A., Blaise V., Collins T., D'Amico S., Gratia E., Huston A. L., Marx J.-C., Sonan G., Zeng Y., and Feller G. (2004). Extreme catalysts from low-temperature environments. *Journal of Bioscience and Bioengineering*. 98: 317-330.

Hromiš N. M., Lazić V. L., Markov S. L., Vaštag Ž. G., Popović S. Z., Šuput D. Z., Džinić N. R., Velićanski A. S., and Popović L. M. (2015). Optimization of chitosan biofilm properties by addition of caraway essential oil and beeswax. *Journal of Food Engineering*. 158: 86-93.

Hu X., Ren J., Zhao M., Cui C., and He P. (2011). Emulsifying properties of the transglutaminase-treated crosslinked product between peanut protein and fish (*Decapterus maruadsi*) protein hydrolysates. *Journal of the Science of Food and Agriculture*. 91: 578-585.

Hua W., El Sheikha A. F., and Xu J. (2018). Molecular techniques for making recombinant enzymes used in food processing. *Molecular Techniques in Food Biology: Safety, Biotechnology, Authenticity and Traceability*: 95.

Hwang J.-H., Mizuta S., Yokoyama Y., and Yoshinaka R. (2007). Purification and characterization

of molecular species of collagen in the skin of skate (*Raja kenojei*). *Food Chemistry*. 100: 921-925.

Icekson I., and Apelbaum A. (1987). Evidence for transglutaminase activity in plant tissue. *Plant Physiology*. 84: 972-974.

Ihara H., Kakihana Y., Yamakage A., Kai K., Shibata T., Nishida M., Yamada K.-i., and Uchida K. (2019). 2-Oxo-histidine–containing dipeptides are functional oxidation products. *Journal of Biological Chemistry*. 294: 1279-1289.

Iismaa S. E., Holman S., Wouters M. A., Lorand L., Graham R. M., and Husain A. (2003). Evolutionary specialization of a tryptophan indole group for transition-state stabilization by eukaryotic transglutaminases. *Proceedings of the National Academy of Sciences*. 100: 12636-12641.

Ikura K., Kokubu T., Natsuka S., Ichikawa A., Adachi M., Nishihara K., Yanagi H., and Utsumi S. (2002). Co-overexpression of folding modulators improves the solubility of the recombinant guinea pig liver transglutaminase expressed in *Escherichia coli*. *Preparative Biochemistry and Biotechnology*. 32: 189-205.

Ioniţă E., Aprodu I., Stănciuc N., Râpeanu G., and Bahrim G. (2014). Advances in structure–function relationships of tyrosinase from Agaricus bisporus–Investigation on heat-induced conformational changes. *Food Chemistry*. 156: 129-136.

Jackson M., Watson P. H., Halliday W. C., and Mantsch H. H. (1995). Beware of connective tissue proteins: assignment and implications of collagen absorptions in infrared spectra of human tissues. *Biochimica et Biophysica Acta (BBA)-Molecular Basis of Disease*. 1270: 1-6.

Janakiram N., Mohammed A., and Rao C. (2015). Sea cucumbers metabolites as potent anti-cancer agents. *Marine drugs*. 13: 2909-2923.

Jeon H.-Y., Kim N.-R., Lee H.-W., Choi H.-J., Choung W.-J., Koo Y.-S., Ko D.-S., and Shim J.-H. (2016). Characterization of a novel maltose-forming α-Amylase from *Lactobacillus plantarum* subsp. *plantarum* ST-III. *Journal of Agricultural and Food Chemistry*. 64: 2307-2314.

Jeon J., Kim J. K., Kim H., Kim Y. J., Park Y. J., Kim S. J., Kim C., and Park S. U. (2018). Transcriptome analysis and metabolic profiling of green and red kale (*Brassica oleracea* var. *acephala*) seedlings. *Food Chemistry*. 241: 7-13.

Jia Z., Song Y., Tao S., Cong P., Wang X., Xue C., and Xu J. (2016). Structure of sphingolipids

from sea cucumber *Cucumaria frondosa* and structure-specific cytotoxicity against human HepG2 cells. *Lipids*. 51: 321-334.

Jin X., Stamnaes J., Klöck C., DiRaimondo T. R., Sollid L. M., and Khosla C. (2011). Activation of extracellular transglutaminase 2 by thioredoxin. *Journal of Biological Chemistry*. 286: 37866-37873.

Johnson D. R., and Decker E. A. (2015). The role of oxygen in lipid oxidation reactions: a review. *Annual Review of Food Science and Technology*. 6: 171-190.

Jongjareonrak A., Benjakul S., Visessanguan W., Prodpran T., and Tanaka M. (2006a). Characterization of edible films from skin gelatin of brownstripe red snapper and bigeye snapper. *Food Hydrocolloids*. 20: 492-501.

Jongjareonrak A., Benjakul S., Visessanguan W., and Tanaka M. (2006b). Effects of plasticizers on the properties of edible films from skin gelatin of bigeye snapper and brownstripe red snapper. *European Food Research and Technology*. 222: 229-235.

Jongjareonrak A., Rawdkuen S., Chaijan M., Benjakul S., Osako K., and Tanaka M. (2010). Chemical compositions and characterisation of skin gelatin from farmed giant catfish (*Pangasianodon gigas*). *LWT-Food Science and Technology*. 43: 161-165.

Jridi M., Hajji S., Ayed H. B., Lassoued I., Mbarek A., Kammoun M., Souissi N., and Nasri M. (2014). Physical, structural, antioxidant and antimicrobial properties of gelatin–chitosan composite edible films. *International journal of biological macromolecules*. 67: 373-379.

Jridi M., Souissi N., Mbarek A., Chadeyron G., Kammoun M., and Nasri M. (2013). Comparative study of physico-mechanical and antioxidant properties of edible gelatin films from the skin of cuttlefish. *International journal of biological macromolecules*. 61: 17-25.

Kaewudom P., Benjakul S., and Kijroongrojana K. (2012). Effect of bovine and fish gelatin in combination with microbial transglutaminase on gel properties of threadfin bream surimi. *International Aquatic Research*. 4: 1-13.

Kang H., and Cho Y. D. (1996). Purification and properties of transglutaminase from soybean (*Glycine max*) leaves. *Biochemical and biophysical research communications*. 223: 288-292.

Karim A., and Bhat R. (2009). Fish gelatin: properties, challenges, and prospects as an alternative to mammalian gelatins. *Food Hydrocolloids*. 23: 563-576.

Karzan T., Nawal H., and Ashna T. (2016). The effect of microbial transglutaminase enzyme on some physicochemical and sensory properties of goat's whey cheese. *International Food*

Research Journal. 23: 688-693.

Kashiwagi T., Yokoyama K.-i., Ishikawa K., Ono K., Ejima D., Matsui H., and Suzuki E.-i. (2002). Crystal structure of microbial transglutaminase from *Streptoverticillium mobaraense*. *Journal of Biological Chemistry*. 277: 44252-44260.

Kavoosi G., Rahmatollahi A., Dadfar S. M. M., and Purfard A. M. (2014). Effects of essential oil on the water binding capacity, physico-mechanical properties, antioxidant and antibacterial activity of gelatin films. *LWT - Food Science and Technology*. 57: 556-561.

Kazuoka T., Oikawa T., Muraoka I., Kuroda S. i., and Soda K. (2007). A cold-active and thermostable alcohol dehydrogenase of a psychrotorelant from Antarctic seawater, *Flavobacterium frigidimaris* KUC-1. *Extremophiles*. 11: 257-267.

Ke Y., Huang W.-Q., Li J.-z., Xie M.-q., and Luo X.-c. (2012). Enzymatic characteristics of a recombinant neutral protease I (rNpI) from *Aspergillus oryzae* expressed in Pichia pastoris. *Journal of Agricultural and Food Chemistry*. 60: 12164-12169.

Keillor J. W., Clouthier C. M., Apperley K. Y., Akbar A., and Mulani A. (2014). Acyl transfer mechanisms of tissue transglutaminase. *Bioorganic chemistry*. 57: 186-197.

Khanzadi M., Jafari S. M., Mirzaei H., Chegini F. K., Maghsoudlou Y., and Dehnad D. (2015). Physical and mechanical properties in biodegradable films of whey protein concentrate–pullulan by application of beeswax. *Carbohydrate polymers*. 118: 24-29.

Kieliszek M., and Błażejak S. (2017). Microbial transglutaminase and applications in food industry. In: Microbial enzyme technology in food applications, pp. 180-194. Ray R. C., and Rosell C. M. (Eds.), CRC Press, Boca Raton, FL, USA.

Kieliszek M., and Misiewicz A. (2014). Microbial transglutaminase and its application in the food industry. A review. *Folia microbiologica*. 59: 241-250.

Kittiphattanabawon P., Benjakul S., Sinthusamran S., and Kishimura H. (2016). Gelatin from clown featherback skin: Extraction conditions. *LWT-Food Science and Technology*. 66: 186-192.

Kittiphattanabawon P., Benjakul S., Visessanguan W., Kishimura H., and Shahidi F. (2010). Isolation and characterisation of collagen from the skin of brownbanded bamboo shark (*Chiloscyllium punctatum*). *Food Chemistry*. 119: 1519-1526.

Klangmuang P., and Sothornvit R. (2016). Combination of beeswax and nanoclay on barriers, sorption isotherm and mechanical properties of hydroxypropyl methylcellulose-based

composite films. *LWT - Food Science and Technology*. 65: 222-227.

Klein J. D., Guzman E., and Kuehn G. D. (1992). Purification and partial characterization of transglutaminase from *Physarum polycephalum*. *Journal of Bacteriology*. 174: 2599-2605.

Kobayashi K., Hashiguchi K.-i., Yokozeki K., and YAMANAKA S. (1998). Molecular cloning of the transglutaminase gene from *Bacillus subtilis* and its expression in *Escherichia coli*. *Bioscience, biotechnology, and biochemistry*. 62: 1109-1114.

Koob T. J., and Hernandez D. J. (2003). Mechanical and thermal properties of novel polymerized NDGA–gelatin hydrogels. *Biomaterials*. 24: 1285-1292.

Kowalczyk D., and Baraniak B. (2014). Effect of candelilla wax on functional properties of biopolymer emulsion films–a comparative study. *Food Hydrocolloids*. 41: 195-209.

Kraehenbuehl K., Page-Zoerkler N., Mauroux O., Gartenmann K., Blank I., and Bel-Rhlid R. (2017). Selective enzymatic hydrolysis of chlorogenic acid lactones in a model system and in a coffee extract. Application to reduction of coffee bitterness. *Food Chemistry*. 218: 9-14.

Kristinsson H. G., and Rasco B. A. (2000). Fish protein hydrolysates: Production, biochemical, and functional properties. *Critical reviews in food science and nutrition*. 40: 43-81.

Kumar N. S., Nazeer R., and Jaiganesh R. (2012). Purification and identification of antioxidant peptides from the skin protein hydrolysate of two marine fishes, horse mackerel (*Magalaspis cordyla*) and croaker (*Otolithes ruber*). *Amino Acids*. 42: 1641-1649.

Kumazawa Y., Nakanishi K., Yasueda H., and Motoki M. (1996). Purification and characterization of transglutaminase from walleye pollack liver. *Fisheries science*. 62: 959-964.

Kumazawa Y., Sano K.-i., Seguro K., Yasueda H., Nio N., and Motoki M. (1997). Purification and characterization of transglutaminase from Japanese oyster (*Crassostrea gigas*). *Journal of Agricultural and Food Chemistry*. 45: 604-610.

Kundu S., Das A., Basu A., Abdullah M. F., and Mukherjee A. (2017). Guar gum benzoate nanoparticle reinforced gelatin films for enhanced thermal insulation, mechanical and antimicrobial properties. *Carbohydrate polymers*. 170: 89-98.

Kuo T.-C., Shaw J.-F., and Lee G.-C. (2015). Conversion of crude *Jatropha curcas* seed oil into biodiesel using liquid recombinant *Candida rugosa* lipase isozymes. *Bioresource technology*. 192: 54-59.

Kurtovic I., Marshall S. N., Cleaver H. L., and Miller M. R. (2016). The use of immobilised digestive lipase from Chinook salmon (*Oncorhynchus tshawytscha*) to generate flavour

compounds in milk. *Food Chemistry*. 199: 323-329.

Kuznetsova I. M., Turoverov K. K., and Uversky V. N. (2004). Use of the phase diagram method to analyze the protein unfolding-refolding reactions: fishing out the "invisible" intermediates. *Journal of proteome research*. 3: 485-494.

Kwon S. J., Park J.-W., Choi W.-K., Kim I. H., and Kim K. (1994). Inhibition of metal-catalyzed oxidation systems by a yeast protector protein in the presence of thioredoxin. *Biochemical and biophysical research communications*. 201: 8-15.

Labrou N. E. (2010). Random mutagenesis methods for *in vitro* directed enzyme evolution. *Current Protein and Peptide Science*. 11: 91-100.

Laki K., and Lorand L. (1948). On the solubility of fibrin clots. *Science*. 108: 280-280.

Laokuldilok T., Potivas T., Kanha N., Surawang S., Seesuriyachan P., Wangtueai S., Phimolsiripol Y., and Regenstein J. M. (2017). Physicochemical, antioxidant, and antimicrobial properties of chitooligosaccharides produced using three different enzyme treatments. *Food Bioscience*. 18: 28-33.

Larre C., Chiarello M., Blanloeil Y., Chenu M., and Gueguen J. (1993). Gliadin modifications catalyzed by guinea pig liver transglutaminase. *Journal of Food Biochemistry*. 17: 267-282.

Lassoued I., Jridi M., Nasri R., Dammak A., Hajji M., Nasri M., and Barkia A. (2014). Characteristics and functional properties of gelatin from thornback ray skin obtained by pepsin-aided process in comparison with commercial halal bovine gelatin. *Food Hydrocolloids*. 41: 309-318.

Lau M., Tang J., and Paulson A. (2000). Texture profile and turbidity of gellan/gelatin mixed gels. *Food Research International*. 33: 665-671.

Lee C. C., Kibblewhite Accinelli R. E., Wagschal K., Robertson G. H., and Wong D. W. (2006). Cloning and characterization of a cold-active xylanase enzyme from an environmental DNA library. *Extremophiles*. 10: 295-300.

Lee J. K., Jeon J.-K., and Byun H.-G. (2011). Effect of angiotensin I converting enzyme inhibitory peptide purified from skate skin hydrolysate. *Food Chemistry*. 125: 495-499.

Lee J. M., Moon S. Y., Kim Y.-R., Kim K. W., Lee B.-J., and Kong I.-S. (2017). Improvement of thermostability and halostability of β-1, 3-1, 4-glucanase by substituting hydrophobic residue for Lys48. *International journal of biological macromolecules*. 94: 594-602.

Lee S. M., Chiang C. F., and Pan B. (1998). Occurrence of transglutaminase in grey mullet (*Mugil*

cephalus) muscle and it's effect on minced fish product. *Journal of Food Biochemistry*. 22: 475-487.

Lemes A. C., Pavón Y., Lazzaroni S., Rozycki S., Brandelli A., and Kalil S. J. (2016). A new milk-clotting enzyme produced by *Bacillus* sp. P45 applied in cream cheese development. *LWT-Food Science and Technology*. 66: 217-224.

Leys S., Pauly A., Delcour J. A., and Courtin C. M. (2016). Modification of the secondary binding site of xylanases illustrates the impact of substrate selectivity on bread making. *Journal of Agricultural and Food Chemistry*. 64: 5400-5409.

Li H., Zhang L., Cui Y., Luo X., Xue C., and Wang S. (2013). Expression of soluble recombinant transglutaminase from Zea mays in *Pichia pastoris*. *World Journal of Microbiology and Biotechnology*. 29: 939-947.

Li H., Zhang T., Li J., Li H., Xu Y., and Yu J. (2019). Expression of *Zea mays* transglutaminase in *Pichia pastoris* under different promoters and its impact on properties of acidified milk protein concentration (MPC) gel. *Journal of the Science of Food and Agriculture*.

Li L. J., Wu Z. Y., Yu Y., Zhang L. J., Zhu Y. B., Ni H., and Chen F. (2018a). Development and characterization of an α-l-rhamnosidase mutant with improved thermostability and a higher efficiency for debittering orange juice. *Food Chemistry*. 245: 1070-1078.

Li S., Yang Q., Tang B., and Chen A. (2018b). Improvement of enzymatic properties of *Rhizopus oryzae* α-amylase by site-saturation mutagenesis of histidine 286. *Enzyme and Microbial Technology*. 117: 96-102.

Li X. (2012). Improved pyrogallol autoxidation method: A reliable and cheap superoxide-scavenging assay suitable for all antioxidants. *Journal of Agricultural and Food Chemistry*. 60: 6418-6424.

Li Y., Zhang X., Zhao Y., Ding J., and Lin S. (2018c). Investigation on complex coacervation between fish skin gelatin from cold-water fish and gum arabic: Phase behavior, thermodynamic, and structural properties. *Food Research International*. 107: 596-604.

Lilley G. R., Skill J., Griffin M., and Bonner P. L. (1998). Detection of Ca^{2+}-dependent transglutaminase activity in root and leaf tissue of monocotyledonous and dicotyledonous plants. *Plant Physiology*. 117: 1115-1123.

Lin L., Yang K., Zheng L., Zhao M., Sun W., Zhu Q., and Liu S. (2018). Anti-aging effect of sea cucumber (*Cucumaria frondosa*) hydrolysate on fruit flies and d-galactose-induced aging

mice. *Journal of Functional Foods*. 47: 11-18.

Lin Y.-S., Chao M.-L., Liu C.-H., Tseng M., and Chu W.-S. (2006). Cloning of the gene coding for transglutaminase from Streptomyces platensis and its expression in Streptomyces lividans. *Process Biochemistry*. 41: 519-524.

Littlechild J. A. (2015). Enzymes from extreme environments and their industrial applications. *Frontiers in bioengineering and biotechnology*. 3: 161.

Liu C., Ren D., Li J., Fang L., Wang J., Liu J., and Min W. (2018). Cytoprotective effect and purification of novel antioxidant peptides from hazelnut (*C. heterophylla* Fisch) protein hydrolysates. *Journal of Functional Foods*. 42: 203-215.

Liu H., Zhang H., and Jin B. (2013). Fluorescence of tryptophan in aqueous solution. *Spectrochimica Acta Part A: Molecular and Biomolecular Spectroscopy*. 106: 54-59.

Liu M., Min L., Zhu C., Rao Z., Liu L., Xu W., Luo P., and Fan L. (2017a). Preparation, characterization and antioxidant activity of silk peptides grafted carboxymethyl chitosan. *International journal of biological macromolecules*. 104: 732-738.

Liu S., Zhang D., Wang M., Cui W., Chen K., Du G., Chen J., and Zhou Z. (2011). The order of expression is a key factor in the production of active transglutaminase in *Escherichia coli* by co-expression with its pro-peptide. *Microbial cell factories*. 10: 1.

Liu Y.-C., Li F.-H., Wang B., Dong B., Zhang Q.-L., Luan W., Zhang X.-J., and Xiang J.-H. (2007). A transglutaminase from Chinese shrimp (*Fenneropenaeus chinensis*), full-length cDNA cloning, tissue localization and expression profile after challenge. *Fish & Shellfish Immunology*. 22: 576-588.

Liu Y., Ban X., Li C., Gu Z., Cheng L., Hong Y., and Li Z. (2017b). Met349 mutations enhance the activity of 1, 4-α-glucan branching enzyme from *Geobacillus thermoglucosidans* STB02. *Journal of Agricultural and Food Chemistry*. 65: 5674-5680.

Liu Y., Fan S., Liu X., Zhang Z., Wang J., Wang Z., and Lu F. (2014a). A highly active alpha amylase from *Bacillus licheniformis*: directed evolution, enzyme characterization and structural analysis. *Journal of M icrobiology and Biotechnology*. 24: 898-904.

Liu Y., Huang L., Jia L., Gui S., Fu Y., Zheng D., Guo W., and Lu F. (2017c). Improvement of the acid stability of *Bacillus licheniformis* alpha amylase by site-directed mutagenesis. *Process Biochemistry*. 58: 174-180.

Liu Y., Zhang T., Zhang Z., Sun T., Wang J., and Lu F. (2014b). Improvement of cold adaptation

of *Bacillus alcalophilus* alkaline protease by directed evolution. *Journal of Molecular Catalysis B: Enzymatic*. 106: 117-123.

Liu Z.-Q., Zhang X.-H., Xue Y.-P., Xu M., and Zheng Y.-G. (2014c). Improvement of *Alcaligenes faecalis* nitrilase by gene site saturation mutagenesis and its application in stereospecific biosynthesis of (R)-(−)-mandelic acid. *Journal of Agricultural and Food Chemistry*. 62: 4685-4694.

Lorenzo J. M., Munekata P. E., Gomez B., Barba F. J., Mora L., Perez-Santaescolastica C., and Toldra F. (2018). Bioactive peptides as natural antioxidants in food products–A review. *Trends in Food Science & Technology*.

Lu S., Zhou N., Tian Y., Li H., and Chen J. (2003). Purification and properties of transglutaminase from *Streptoverticillium mobaraense*. *Journal of food biochemistry*. 27: 109-125.

Luciano F. B., and Arntfield S. (2012). Use of transglutaminases in foods and potential utilization of plants as a transglutaminase source–Review. *Biotemas*. 25: 1-11.

Lukasik K. V., and Ludescher R. D. (2006). Molecular mobility in water and glycerol plasticized cold-and hot-cast gelatin films. *Food Hydrocolloids*. 20: 96-105.

Lukesh III J. C., Palte M. J., and Raines R. T. (2012). A potent, versatile disulfide-reducing agent from aspartic acid. *Journal of the American Chemical Society*. 134: 4057-4059.

Lustigman S., Brotman B., Huima T., Castelhano A. L., Singh R. N., Mehta K., and Prince A. M. (1995). Transglutaminase-catalyzed reaction is important for molting of *Onchocerca volvulus* third-stage larvae. *Antimicrob Agents Chemother*. 39: 1913-1919.

Mageswari A., Subramanian P., Chandrasekaran S., Karthikeyan S., and Gothandam K. M. (2017). Systematic functional analysis and application of a cold-active serine protease from a novel *Chryseobacterium* sp. *Food Chemistry*. 217: 18-27.

Malinowska-Pańczyk E., and Kołodziejska I. (2018). Changes in enzymatic activity of fish and slaughter animals meat after high pressure treatment at subzero temperatures. *Polish Journal of Food and Nutrition Sciences*. 68: 125-131.

Mamelona J., Pelletier E., Girard-Lalancette K., Legault J., Karboune S., and Kermasha S. (2007). Quantification of phenolic contents and antioxidant capacity of Atlantic sea cucumber, *Cucumaria frondosa*. *Food Chemistry*. 104: 1040-1047.

Mamelona J., Saint-Louis R., and Pelletier É. (2010). Proximate composition and nutritional profile of by‐products from green urchin and Atlantic sea cucumber processing plants.

International Journal of Food Science & Technology. 45: 2119-2126.

Maningas M. B. B., Kondo H., Hirono I., Saito-Taki T., and Aoki T. (2008). Essential function of transglutaminase and clotting protein in shrimp immunity. *Molecular immunology*. 45: 1269-1275.

Manta B., and Gladyshev V. N. (2017). Regulated methionine oxidation by monooxygenases. *Free Radical Biology and Medicine*. 109: 141-155.

Marathe S. J., Jadhav S. B., Bankar S. B., and Singhal R. S. (2017). Enzyme-Assisted Extraction of Bioactives. In: Food Bioactives, pp. 171-201. Springer.

Marín-Navarro J., Talens-Perales D., and Polaina J. (2015). One-pot production of fructooligosaccharides by a *Saccharomyces cerevisiae* strain expressing an engineered invertase. *Applied Microbiology and Biotechnology*. 99: 2549-2555.

Maso K., Grigoletto A., and Pasut G. (2018). Transglutaminase and sialyltransferase enzymatic approaches for polymer conjugation to proteins. In: Advances in protein chemistry and structural biology, pp. 123-142. Donev R. (Ed.), Elsevier.

Matsui R., Honda R., Kanome M., Hagiwara A., Matsuda Y., Togitani T., Ikemoto N., and Terashima M. (2018). Designing antioxidant peptides based on the antioxidant properties of the amino acid side-chains. *Food Chemistry*. 245: 750-755.

Mattock P., Barford D., Basford J., and Jones J. (1970). The effect of substrate concentration and pH on the enzymic sulphation of l-tyrosyl derivatives. *Biochemical Journal*. 116: 805-810.

McClements D. J. (2004). Protein-stabilized emulsions. *Current opinion in colloid & interface science*. 9: 305-313.

McClements D. J. (2015). Molecular Characteristics. In: Food Emulsions: Principles, Practices, and Techniques, pp. 48-49. CRC press, Boca Raton, FL, USA.

Mead R. (1988). The design of experiments: statistical principles for practical applications. Cambridge University Press.

Medzihradszky K. F., and Chalkley R. J. (2015). Lessons in *de novo* peptide sequencing by tandem mass spectrometry. *Mass Spectrometry Reviews*. 34: 43-63.

Mehta K., and Eckert R. L. (2005). Transglutaminases: family of enzymes with diverse functions, Vol 38. Karger Medical and Scientific Publishers.

Memarpoor-Yazdi M., Karbalaei-Heidari H. R., and Khajeh K. (2017). Production of the renewable extremophile lipase: Valuable biocatalyst with potential usage in food industry.

Food and Bioproducts Processing. 102: 153-166.

Menéndez O., Rawel H., Schwarzenbolz U., and Henle T. (2006). Structural changes of microbial transglutaminase during thermal and high-pressure treatment. *Journal of Agricultural and Food Chemistry*. 54: 1716-1721.

Merlino A., Krauss I. R., Castellano I., De Vendittis E., Rossi B., Conte M., Vergara A., and Sica F. (2010). Structure and flexibility in cold-adapted iron superoxide dismutases: the case of the enzyme isolated from *Pseudoalteromonas haloplanktis*. *Journal of structural biology*. 172: 343-352.

Mierczyńska J., Cybulska J., Pieczywek P. M., and Zdunek A. (2015). Effect of storage on rheology of water-soluble, chelate-soluble and diluted alkali-soluble pectin in carrot cell walls. *Food and Bioprocess Technology*. 8: 171-180.

Miller K. S., and Krochta J. (1997). Oxygen and aroma barrier properties of edible films: A review. *Trends in Food Science & Technology*. 8: 228-237.

Mishra S., and Murphy L. J. (2006). The p53 oncoprotein is a substrate for tissue transglutaminase kinase activity. *Biochemical and biophysical research communications*. 339: 726-730.

Mohandesi N., Haghbeen K., Ranaei O., Arab S. S., and Hassani S. (2017). Catalytic efficiency and thermostability improvement of Suc2 invertase through rational site-directed mutagenesis. *Enzyme and Microbial Technology*. 96: 14-22.

Montgomery D. C. (2017). Design and analysis of experiments. John wiley & sons.

Moraes I. C., Carvalho R. A., Bittante A. M. Q., Solorza-Feria J., and Sobral P. J. (2009). Film forming solutions based on gelatin and poly (vinyl alcohol) blends: Thermal and rheological characterizations. *Journal of Food Engineering*. 95: 588-596.

Morales-Medina R., Munio M., Guadix A., Guadix E., and Camacho F. (2018). A lumped model of the lipase catalyzed hydrolysis of sardine oil to maximize polyunsaturated fatty acids content in acylglycerols. *Food Chemistry*. 240: 286-294.

Motoki M., and Seguro K. (1998). Transglutaminase and its use for food processing. *Trends in Food Science & Technology*. 9: 204-210.

Mrabet A., Rodríguez-Gutiérrez G., Rubio-Senent F., Hamza H., Rodríguez-Arcos R., Guillén-Bejarano R., Sindic M., and Jiménez-Araujo A. (2017). Enzymatic conversion of date fruit fiber concentrates into a new product enriched in antioxidant soluble fiber. *LWT-Food Science and Technology*. 75: 727-734.

Mu D., Lu J., Shu C., Li H., Li X., Cai J., Luo S., Yang P., Jiang S., and Zheng Z. (2018). Improvement of the activity and thermostability of microbial transglutaminase by multiple-site mutagenesis. *Bioscience, biotechnology, and biochemistry*. 82: 106-109.

Murthy P. S., and Kusumoto K.-I. (2015). Acid protease production by *Aspergillus oryzae* on potato pulp powder with emphasis on glycine releasing activity: A benefit to the food industry. *Food and Bioproducts Processing*. 96: 180-188.

Muscat D., Tobin M. J., Guo Q., and Adhikari B. (2014). Understanding the distribution of natural wax in starch–wax films using synchrotron-based FTIR (S-FTIR). *Carbohydrate polymers*. 102: 125-135.

Musso Y. S., Salgado P. R., and Mauri A. N. (2017). Smart edible films based on gelatin and curcumin. *Food Hydrocolloids*. 66: 8-15.

Muyonga J., Cole C., and Duodu K. (2004). Extraction and physico-chemical characterisation of Nile perch (*Lates niloticus*) skin and bone gelatin. *Food hydrocolloids*. 18: 581-592.

Myhrman R., and Bruner-Lorand J. (1970). Lobster muscle transpeptidase. *Methods in Enzymology*. 19: 765-770.

Nagarajan M., Benjakul S., Prodpran T., and Songtipya P. (2012). Properties of film from splendid squid (*Loligo formosana*) skin gelatin with various extraction temperatures. *International journal of biological macromolecules*. 51: 489-496.

Nalinanon S., Benjakul S., Visessanguan W., and Kishimura H. (2008). Improvement of gelatin extraction from bigeye snapper skin using pepsin-aided process in combination with protease inhibitor. *Food Hydrocolloids*. 22: 615-622.

Nandakumar R., and Wakayama M. (2015). Enzymes in flavors and food additives. In: Enzymes in food and beverage processing, pp. 311-330. Chandrasekaran M. (Ed.), CRC Press, Boca Raton, FL, USA.

Nasr A. I., Mohamed Ahmed I. A., and Hamid O. I. (2016). Characterization of partially purified milk‐clotting enzyme from sunflower (*Helianthus annuus*) seeds. *Food science & nutrition*. 4: 733-741.

Nelson E. J., MacDonald B. A., and Robinson S. M. (2012). A review of the Northern sea cucumber *Cucumaria frondosa* (Gunnerus, 1767) as a potential aquaculture species. *Reviews in Fisheries Science*. 20: 212-219.

Nemes Z., Csosz E., Petrovski G., and Fesus L. (2005). Structure-function relationships of

transglutaminases--a contemporary view. *Progress in experimental tumor research*. 38: 19-36.

Neves A. C., Harnedy P. A., O'Keeffe M. B., Alashi M. A., Aluko R. E., and FitzGerald R. J. (2017). Peptide identification in a salmon gelatin hydrolysate with antihypertensive, dipeptidyl peptidase IV inhibitory and antioxidant activities. *Food Research International*. 100: 112-120.

Nguyen B. C. Q., Yoshimura K., Kumazawa S., Tawata S., and Maruta H. (2017). Frondoside A from sea cucumber and nymphaeols from Okinawa propolis: Natural anti-cancer agents that selectively inhibit PAK1 *in vitro*. *Drug Discoveries & Therapeutics*. 11: 110-114.

Nicol S., Foster J., and Kawaguchi S. (2012). The fishery for Antarctic krill - recent developments. *Fish and Fisheries*. 13: 30-40.

Nikoo M., Benjakul S., Ocen D., Yang N., Xu B., Zhang L., and Xu X. (2013). Physical and chemical properties of gelatin from the skin of cultured A mur sturgeon (*Acipenser schrenckii*). *Journal of Applied Ichthyology*. 29: 943-950.

Nistor O. V., Stănciuc N., Aprodu I., and Botez E. (2014). New insights into heat induced structural changes of pectin methylesterase on fluorescence spectroscopy and molecular modeling basis. *Spectrochimica Acta Part A: Molecular and Biomolecular Spectroscopy*. 128: 15-21.

Niu C., Yang P., Luo H., Huang H., Wang Y., and Yao B. (2017). Engineering of *Yersinia* phytases to improve pepsin and trypsin resistance and thermostability and application potential in the food and feed industry. *Journal of Agricultural and Food Chemistry*. 65: 7337-7344.

Niu C., Zhu L., Zhu P., and Li Q. (2015). Lysine-based site-directed mutagenesis increased rigid *β*-sheet structure and thermostability of mesophilic 1, 3–1, 4-*β*-glucanase. *Journal of Agricultural and Food Chemistry*. 63: 5249-5256.

Noguchi K., Ishikawa K., Yokoyama K.-i., Ohtsuka T., Nio N., and Suzuki E.-i. (2001). Crystal structure of red sea bream transglutaminase. *Journal of Biological Chemistry*. 276: 12055-12059.

Norziah M., Al Hassan A., Khairulnizam A., Mordi M., and Norita M. (2009). Characterization of fish gelatin from surimi processing wastes: Thermal analysis and effect of transglutaminase on gel properties. *Food Hydrocolloids*. 23: 1610-1616.

Norziah M., Kee H., and Norita M. (2014). Response surface optimization of bromelain-assisted gelatin extraction from surimi processing wastes. *Food Bioscience*. 5: 9-18.

Novelli P. K., Barros M. M., and Fleuri L. F. (2016). Novel inexpensive fungi proteases: Production by solid state fermentation and characterization. *Food Chemistry*. 198: 119-124.

Nozawa H., Cho S. Y., and Seki N. (2001a). Purification and characterization of transglutaminase from squid gill. *Fisheries science*. 67: 912-919.

Nozawa H., Mamegoshi S.-i., and Seki N. (1997a). Partial purification and characterization of six transglutaminases from ordinary muscles of various fishes and marine invertebrates. *Comparative Biochemistry and Physiology Part B: Biochemistry and Molecular Biology*. 118: 313-317.

Nozawa H., Mamegoshi S., and Seki N. (1997b). Partial purification and characterization of six transglutaminases from ordinary muscles of various fishes and marine invertebrates. *Comparative Biochemistry and Physiology Part B: Biochemistry and Molecular Biology*. 118: 313-317.

Nozawa H., Mori T., Kimura M., and Seki N. (2005). Characterization of a transglutaminase from scallop hemocyte and identification of its intracellular substrates. *Comparative Biochemistry and Physiology Part B: Biochemistry and Molecular Biology*. 140: 395-402.

Nozawa H., Mori T., and Seki N. (2001b). Different effects of NaCl on activities of transglutaminases from marine and freshwater shellfish muscles. *Fisheries science*. 67: 383-385.

Nozawa H., and Seki N. (2002). Biochemical properties of transglutaminases from fish and shellfish. *Fisheries science*. 68: 1571-1574.

Nurminskaya M. V., and Belkin A. M. (2012). Cellular functions of tissue transglutaminase. In: International review of cell and molecular biology, pp. 1-97. Elsevier.

Nury S., Meunier J. C., and Mouranche A. (1989). The kinetics of the thermal deactivation of transglutaminase from guinea-pig liver. *The FEBS Journal*. 180: 161-166.

Oancea D., Stuparu A., Nita M., Puiu M., and Raducan A. (2008). Estimation of the overall kinetic parameters of enzyme inactivation using an isoconversional method. *Biophysical chemistry*. 138: 50-54.

Ohashi H., Itoh Y., Birckbichler P. J., and Takeuchi Y. (1995). Purification and characterization of rat brain transglutaminase. *Journal of biochemistry*. 118: 1271-1278.

Ohtake K., Mukai T., Iraha F., Takahashi M., Haruna K.-i., Date M., Yokoyama K., and Sakamoto K. (2018). Engineering an automaturing transglutaminase with enhanced thermostability by

genetic code expansion with two codon reassignments. *ACS synthetic biology*. 7: 2170-2176.

Ohtsuka T., Sawa A., Kawabata R., Nio N., and Motoki M. (2000). Substrate specificities of microbial transglutaminase for primary amines. *Journal of Agricultural and Food Chemistry*. 48: 6230-6233.

Ohtsuka T., Umezawa Y., Nio N., and Kubota K. (2001). Comparison of deamidation activity of transglutaminases. *Journal of Food Science*. 66: 25-29.

Oliviero T., Verkerk R., Van Boekel M., and Dekker M. (2014). Effect of water content and temperature on inactivation kinetics of myrosinase in broccoli (*Brassica oleracea* var. *italica*). *Food Chemistry*. 163: 197-201.

Ortega G., Laín A., Tadeo X., López-Méndez B., Castano D., and Millet O. (2011). Halophilic enzyme activation induced by salts. *Scientific Report*. 1.

Özgün G. P., Ordu E. B., Tütüncü H. E., Yelboğa E., Sessions R. B., and Gül Karagüler N. (2016). Site saturation mutagenesis applications on *Candida methylica* formate dehydrogenase. *Scientifica*. 2016.

Paciello L., Landi C., Orilio P., Di Matteo M., Zueco J., and Parascandola P. (2015). Bread making with *Saccharomyces cerevisiae* CEN. PK113‐5D expressing lipase A from *Bacillus subtilis*: leavening characterisation and aroma enhancement. *International Journal of Food Science & Technology*. 50: 2120-2128.

Packer M. S., and Liu D. R. (2015). Methods for the directed evolution of proteins. *Nature Reviews Genetics*. 16: 379.

Palanski B. A., and Khosla C. (2018). Cystamine and disulfiram inhibit human transglutaminase 2 via an oxidative mechanism. *Biochemistry*. 57: 3359-3363.

Panner Selvam M. K., and Agarwal A. (2018). Update on the proteomics of male infertility: A systematic review. *Arab journal of urology*. 16: 103-112.

Pellicer J. A., and Gómez-López V. M. (2017). Pulsed light inactivation of horseradish peroxidase and associated structural changes. *Food Chemistry*. 237: 632-637.

Pérez-Mateos M., Montero P., and Gómez-Guillén M. (2009). Formulation and stability of biodegradable films made from cod gelatin and sunflower oil blends. *Food Hydrocolloids*. 23: 53-61.

Petersen B. R., and Yates J. R. (1977). Gelatin extraction. U.S. Patent No. 4,064,008.

Pinkas D. M., Strop P., Brunger A. T., and Khosla C. (2007). Transglutaminase 2 undergoes a

large conformational change upon activation. *PLoS biology*. 5: e327.

Poole L. B. (2015). The basics of thiols and cysteines in redox biology and chemistry. *Free Radical Biology and Medicine*. 80: 148-157.

Porcelli B., Ferretti F., Vindigni C., and Terzuoli L. (2016). Assessment of a Test for the Screening and Diagnosis of Celiac Disease. *Journal of clinical laboratory analysis*. 30: 65-70.

Pownall T. L., Udenigwe C. C., and Aluko R. E. (2010). Amino acid composition and antioxidant properties of pea seed (*Pisum sativum* L.) enzymatic protein hydrolysate fractions. *Journal of Agricultural and Food Chemistry*. 58: 4712-4718.

Puszkin E., and Raghuraman V. (1985). Catalytic properties of a calmodulin-regulated transglutaminase from human platelet and chicken gizzard. *Journal of Biological Chemistry*. 260: 16012-16020.

Radek J., Jeong J., Wilson J., and Lorand L. (1993). Association of the A subunits of recombinant placental factor XIII with the native carrier B subunits from human plasma. *Biochemistry*. 32: 3527-3534.

Rahman M. S., Al-Saidi G., Guizani N., and Abdullah A. (2010). Development of state diagram of bovine gelatin by measuring thermal characteristics using differential scanning calorimetry (DSC) and cooling curve method. *Thermochimica Acta*. 509: 111-119.

Rai A., Mohanty B., and Bhargava R. (2016). Supercritical extraction of sunflower oil: A central composite design for extraction variables. *Food Chemistry*. 192: 647-659.

Ramachandran A., and Jaeschke H. (2018). Acetaminophen toxicity: Novel insights into mechanisms and future perspectives. *Gene Expression*. 18: 19-30.

Ramírez E., Brenes M., García P., Medina E., and Romero C. (2016). Oleuropein hydrolysis in natural green olives: Importance of the endogenous enzymes. *Food Chemistry*. 206: 204-209.

Rao M. A. (2007). Rheology of food gum and starch dispersions. In: Rheology of fluid, semisolid, and solid foods, pp. 161-229. Springer.

Ravelo Y., Molina V., Carbajal D., Fernández L., Fernández J. C., Arruzazabala M. L., and Más R. (2011). Evaluation of anti-inflammatory and antinociceptive effects of D-002 (beeswax alcohols). *Journal of Natural Medicines*. 65: 330-335.

Rbii K., Surel O., Brambati N., Buchert A.-M., and Violleau F. (2011). Study of gelatin renaturation in aqueous solution by AFlFFF–MALS: Influence of a thermal pre-treatment

applied on gelatin. *Food Hydrocolloids*. 25: 511-514.

Rentschler E., Schwarz T., Stressler T., and Fischer L. (2016). Development and validation of a screening system for a *β*-galactosidase with increased specific activity produced by directed evolution. *European Food Research and Technology*. 242: 2129-2138.

Rigoldi F., Donini S., Redaelli A., Parisini E., and Gautieri A. (2018). Engineering of thermostable enzymes for industrial applications. *APL bioengineering*. 2: 011501.

Rivero S., García M., and Pinotti A. (2010). Correlations between structural, barrier, thermal and mechanical properties of plasticized gelatin films. *Innovative Food Science & Emerging Technologies*. 11: 369-375.

Rodrigues D. C., Caceres C. A., Ribeiro H. L., de Abreu R. F., Cunha A. P., and Azeredo H. M. (2014). Influence of cassava starch and carnauba wax on physical properties of cashew tree gum-based films. *Food Hydrocolloids*. 38: 147-151.

Rollas S., and Küçükgüzel S. (2007). Biological activities of hydrazone derivatives. *Molecules*. 12: 1910-1939.

Rosano G. L., and Ceccarelli E. A. (2014). Recombinant protein expression in *Escherichia coli*: advances and challenges. *Frontiers in microbiology*. 5: 172.

Rossa P. N., Burin V. M., and Bordignon-Luiz M. T. (2012). Effect of microbial transglutaminase on functional and rheological properties of ice cream with different fat contents. *LWT-Food Science and Technology*. 48: 224-230.

Sae-Leaw T., and Benjakul S. (2018). Lipase from liver of seabass (*Lates calcarifer*): Characteristics and the use for defatting of fish skin. *Food Chemistry*. 240: 9-15.

Sae-leaw T., Benjakul S., O'brien N. M., and Kishimura H. (2016). Characteristics and functional properties of gelatin from seabass skin as influenced by defatting. *International Journal of Food Science & Technology*. 51: 1204-1211.

Şahin-Ercan S., Bozkurt H., and Soysal Ç. (2016). Reduction of cadaverine and tyramine formation by proteolytic enzymes in model system. *International Journal of Food Properties*. 19: 1465-1474.

Sai-Ut S., Jongjareonrak A., and Rawdkuen S. (2012). Re-extraction, recovery, and characteristics of skin gelatin from farmed giant catfish. *Food and Bioprocess Technology*. 5: 1197-1205.

Şakiroğlu H., Birdal C., Başlar M., and Öztürk A. E. (2016). Inactivation kinetics of polyphenol oxidase in an aqueous model system under stand-alone and combined ultrasound and

ultraviolet treatments. *International Journal of Food Properties*. 19: 1535-1543.

Salis B., Spinetti G., Scaramuzza S., Bossi M., Jotti G. S., Tonon G., Crobu D., and Schrepfer R. (2015). High-level expression of a recombinant active microbial transglutaminase in *Escherichia coli*. *BMC biotechnology*. 15: 84.

Sano K.-i., Nakanishi K., Nakamura N., Motoki M., and Yasueda H. (1996). Cloning and sequence analysis of a cDNA encoding salmon (*Onchorhynchus keta*) liver transglutaminase. *Bioscience, biotechnology, and biochemistry*. 60: 1790-1794.

Santhi D., Kalaikannan A., Malairaj P., and Arun Prabhu S. (2015). Application of microbial transglutaminase in meat foods: A review. *Critical reviews in food science and nutrition*: 00-00.

Santiago M., Ramírez-Sarmiento C. A., Zamora R. A., and Parra L. P. (2016). Discovery, molecular mechanisms, and industrial applications of cold-active enzymes. *Frontiers in microbiology*. 7: 1408.

Santos F. K. G. D., Silva K. N. d. O., Xavier T. D. N., Leite R. H. d. L., and Aroucha E. M. M. (2017). Effect of the addition of carnauba wax on physicochemical properties of chitosan films. *Materials Research*: 479-484.

Santos T. M., Pinto A., Oliveira A. V., Ribeiro H. L., Caceres C. A., Ito E. N., and Azeredo H. (2014). Physical properties of cassava starch–carnauba wax emulsion films as affected by component proportions. *International Journal of Food Science & Technology*. 49: 2045-2051.

Sarmadi B. H., and Ismail A. (2010). Antioxidative peptides from food proteins: A review. *Peptides*. 31: 1949-1956.

Sarmiento F., Peralta R., and Blamey J. M. (2015). Cold and hot extremozymes: industrial relevance and current trends. *Frontiers in bioengineering and biotechnology*. 3: 148.

Savoca M., Tonoli E., Atobatele A., and Verderio E. (2018). Biocatalysis by Transglutaminases: A Review of Biotechnological Applications. *Micromachines*. 9: 562.

Scherf K. A., Wieser H., and Koehler P. (2016). Novel approaches for enzymatic gluten degradation to create high-quality gluten-free products. *Food Research International*.

Schmidt M., Toplak A., Quaedflieg P. J., and Nuijens T. (2017). Enzyme-mediated ligation technologies for peptides and proteins. *Current opinion in chemical biology*. 38: 1-7.

Serafini-Fracassini D., and Del Duca S. (2008). Transglutaminases: widespread cross-linking

enzymes in plants. *Annals of botany*. 102: 145-152.

Serafini-Fracassini D., Del Duca S., and Beninati S. (1995). Plant transglutaminases. *Phytochemistry*. 40: 355-365.

Serafini-Fracassini D., Del Duca S., Monti F., Poli F., Sacchetti G., Bregoli A. M., Biondi S., and Della Mea M. (2002). Transglutaminase activity during senescence and programmed cell death in the corolla of tobacco (*Nicotiana tabacum*) flowers. *Cell death and differentiation*. 9: 309-321.

Shah U., Naqash F., Gani A., and Masoodi F. (2016). Art and science behind modified starch edible films and coatings: A review. *Comprehensive Reviews in Food Science and Food Safety*. 15: 568-580.

Shakila R. J., Jeevithan E., Varatharajakumar A., Jeyasekaran G., and Sukumar D. (2012). Comparison of the properties of multi-composite fish gelatin films with that of mammalian gelatin films. *Food Chemistry*. 135: 2260-2267.

Shen Q., Zhang Y., Yang R., Pan S., Dong J., Fan Y., and Han L. (2016). Enhancement of isomerization activity and lactulose production of cellobiose 2-epimerase from *Caldicellulosiruptor saccharolyticus*. *Food Chemistry*. 207: 60-67.

Shih F., Daigle K., and Champagne E. (2011). Effect of rice wax on water vapour permeability and sorption properties of edible pullulan films. *Food Chemistry*. 127: 118-121.

Shoulders M. D., and Raines R. T. (2009). Collagen structure and stability. *Annual Review of Biochemistry*. 78: 929-958.

Shyni K., Hema G., Ninan G., Mathew S., Joshy C., and Lakshmanan P. (2014). Isolation and characterization of gelatin from the skins of skipjack tuna (*Katsuwonus pelamis*), dog shark (*Scoliodon sorrakowah*), and rohu (*Labeo rohita*). *Food Hydrocolloids*. 39: 68-76.

Siegel M., and Khosla C. (2007). Transglutaminase 2 inhibitors and their therapeutic role in disease states. *Pharmacology & therapeutics*. 115: 232-245.

Siepaio M. P., and Meunier J.-C. F. (1995). Diamine oxidase and transglutaminase activities in white lupine seedlings with respect to crosslinking of proteins. *Journal of Agricultural and Food Chemistry*. 43: 1151-1156.

Signorini M., Beninati S., and Bergamini C. M. (1991). Identification of transglutaminase activity in the leaves of silver beet (*Beta vulgaris* L.). *Journal of plant physiology*. 137: 547-552.

Singh A., Upadhyay V., and Panda A. K. (2015). Solubilization and refolding of inclusion body

proteins. In: Insoluble Proteins, pp. 283-291. Springer.

Sirikharin R., Söderhäll I., and Söderhäll K. (2018). Characterization of a cold-active transglutaminase from a crayfish, *Pacifastacus leniusculus*. *Fish & shellfish immunology*. 80: 546-549.

Sjödahl J., Emmer Å., Vincent J., and Roeraade J. (2002). Characterization of proteinases from Antarctic krill (*Euphausia superba*). *Protein expression and purification*. 26: 153-161.

Soazo M., Rubiolo A., and Verdini R. (2011). Effect of drying temperature and beeswax content on physical properties of whey protein emulsion films. *Food Hydrocolloids*. 25: 1251-1255.

Sobral P., and Habitante A. (2001). Phase transitions of pigskin gelatin. *Food Hydrocolloids*. 15: 377-382.

Song R., Shi Q., Yang P., and Wei R. (2017). Identification of antibacterial peptides from Maillard reaction products of half-fin anchovy hydrolysates/glucose via LC-ESI-QTOF-MS analysis. *Journal of Functional Foods*. 36: 387-395.

Souza P. M., Werneck G., Aliakbarian B., Siqueira F., Ferreira Filho E. X., Perego P., Converti A., Magalhães P. O., and Junior A. P. (2017). Production, purification and characterization of an aspartic protease from *Aspergillus foetidus*. *Food and Chemical Toxicology*.

Sow L. C., and Yang H. (2015). Effects of salt and sugar addition on the physicochemical properties and nanostructure of fish gelatin. *Food Hydrocolloids*. 45: 72-82.

Srivastava N. (2019). Production of food-processing enzymes from recombinant microorganisms. In: Enzymes in Food Biotechnology, pp. 739-767. Elsevier.

Stănciuc N., Aprodu I., Ioniță E., Bahrim G., and Râpeanu G. (2015). Exploring the process–structure–function relationship of horseradish peroxidase through investigation of pH-and heat induced conformational changes. *Spectrochimica Acta Part A: Molecular and Biomolecular Spectroscopy*. 147: 43-50.

Steinke N., Gillams R. J., Pardo L. C., Lorenz C. D., and McLain S. E. (2016). Atomic scale insights into urea–peptide interactions in solution. *Physical Chemistry Chemical Physics*. 18: 3862-3870.

Stephany M., Eckert P., Bader-Mittermaier S., Schweiggert-Weisz U., and Carle R. (2016). Lipoxygenase inactivation kinetics and quality-related enzyme activities of narrow-leafed lupin seeds and flakes. *LWT-Food Science and Technology*. 68: 36-43.

Stieler M., Weber J., Hils M., Kolb P., Heine A., Büchold C., Pasternack R., and Klebe G. (2013).

Structure of active coagulation factor XIII triggered by calcium binding: basis for the design of next‐generation anticoagulants. *Angewandte Chemie International Edition*. 52: 11930-11934.

Sugimura Y., Hosono M., Wada F., Yoshimura T., Maki M., and Hitomi K. (2006). Screening for the preferred substrate sequence of transglutaminase using a phage-displayed peptide library identification of peptide substrates for TGASE 2 and factor XIIIA. *Journal of Biological Chemistry*. 281: 17699-17706.

Sun H., Xue Y., and Lin Y. (2014). Enhanced catalytic efficiency in quercetin-4′-glucoside hydrolysis of *Thermotoga maritima* β-glucosidase A by site-directed mutagenesis. *Journal of Agricultural and Food Chemistry*. 62: 6763-6770.

Sun L., Sun J., Chen L., Niu P., Yang X., and Guo Y. (2017a). Preparation and characterization of chitosan film incorporated with thinned young apple polyphenols as an active packaging material. *Carbohydrate polymers*. 163: 81-91.

Sun Q., Chen F., Geng F., Luo Y., Gong S., and Jiang Z. (2017b). A novel aspartic protease from *Rhizomucor miehei* expressed in *Pichia pastoris* and its application on meat tenderization and preparation of turtle peptides. *Food Chemistry*. 245: 570-577.

Surh J., Decker E. A., and McClements D. J. (2006). Properties and stability of oil-in-water emulsions stabilized by fish gelatin. *Food Hydrocolloids*. 20: 596-606.

Takagi J., Saito Y., Kikuchi T., and Inada Y. (1986). Modification of transglutaminase assay: use of ammonium sulfate to stop the reaction. *Analytical Biochemistry*. 153: 295-298.

Talens-Perales D., Polaina J., and Marín-Navarro J. (2016). Structural dissection of the active site of *Thermotoga maritima β*-Galactosidase identifies key residues for transglycosylating activity. *Journal of Agricultural and Food Chemistry*. 64: 2917-2924.

Talens P., and Krochta J. M. (2005). Plasticizing effects of beeswax and carnauba wax on tensile and water vapor permeability properties of whey protein films. *Journal of Food Science*. 70: 239-243.

Tang Q., Lan D., Yang B., Khan F. I., and Wang Y. (2017). Site‐directed mutagenesis studies of hydrophobic residues in the lid region of T1 lipase. *European Journal of Lipid Science and Technology*. 119: 1600107.

Tao X., Wang T., Su L., and Wu J. (2018). Enhanced 2-O-α-d-glucopyranosyl-l-ascorbic acid

synthesis through iterative saturation mutagenesis of acceptor subsite residues in *Bacillus stearothermophilus* NO2 cyclodextrin glycosyltransferase. *Journal of Agricultural and Food Chemistry*. 66: 9052-9060.

Thangaraju K., Király R., Demény M. A., Mótyán J. A., Fuxreiter M., and Fésüs L. (2017). Genomic variants reveal differential evolutionary constraints on human transglutaminases and point towards unrecognized significance of transglutaminase 2. *PloS one*. 12: e0172189.

Thies S., Rausch S. C., Kovacic F., Schmidt-Thaler A., Wilhelm S., Rosenau F., Daniel R., Streit W., Pietruszka J., and Jaeger K.-E. (2016). Metagenomic discovery of novel enzymes and biosurfactants in a slaughterhouse biofilm microbial community. *Scientific reports*. 6: 27035.

Thomas D., and Dieckmann G. (2002). Antarctic sea ice - a habitat for extremophiles. *Science*. 295: 641-644.

Tian K., Tai K., Chua B. J. W., and Li Z. (2017). Directed evolution of *Thermomyces lanuginosus* lipase to enhance methanol tolerance for efficient production of biodiesel from waste grease. *Bioresource technology*. 245: 1491-1497.

Tian Y., Chen H., Zhang X., Zhan J., Jin Z., and Wang J. (2016). Highly branched dextrin prepared from high-amylose maize starch using waxy rice branching enzyme (WRBE). *Food Chemistry*. 203: 530-535.

Toopcham T., Mes J. J., Wichers H. J., Roytrakul S., and Yongsawatdigul J. (2017). Bioavailability of angiotensin I-converting enzyme (ACE) inhibitory peptides derived from *Virgibacillus halodenitrificans* SK1-3-7 proteinases hydrolyzed tilapia muscle proteins. *Food Chemistry*. 220: 190-197.

Torkova A., Koroleva O., Khrameeva E., Fedorova T., and Tsentalovich M. (2015). Structure-functional study of tyrosine and methionine dipeptides: An approach to antioxidant activity prediction. *International Journal of Molecular Sciences*. 16: 25353-25376.

Tripoteau L., Bedoux G., Gagnon J., and Bourgougnon N. (2015). *In vitro* antiviral activities of enzymatic hydrolysates extracted from byproducts of the Atlantic holothurian *Cucumaria frondosa*. *Process Biochemistry*. 50: 867-875.

Tsai G. J., Lin S. M., and Jiang S. T. (1996). Transglutaminase from *Streptoverticillium ladakanum* and application to minced fish product. *Journal of Food Science*. 61: 1234-1238.

Tseng H.-C., Lin H.-J., Gandhi P. S., Wang C.-Y., and Chen Y.-H. (2008). Purification and identification of transglutaminase from mouse coagulating gland and its cross-linking

activity among seminal vesicle secretion proteins. *Journal of Chromatography B*. 876: 198-202.

Uresti R. M., Velazquez G., Vázquez M., Ramírez J. A., and Torres J. A. (2006). Effects of combining microbial transglutaminase and high pressure processing treatments on the mechanical properties of heat-induced gels prepared from arrowtooth flounder (*Atheresthes stomias*). *Food Chemistry*. 94: 202-209.

Ustyuzhanina N. E., Bilan M. I., Dmitrenok A. S., Shashkov A. S., Nifantiev N. E., and Usov A. I. (2017). The structure of a fucosylated chondroitin sulfate from the sea cucumber *Cucumaria frondosa*. *Carbohydrate polymers*. 165: 7-12.

Van Den Bulcke A. I., Bogdanov B., De Rooze N., Schacht E. H., Cornelissen M., and Berghmans H. (2000). Structural and rheological properties of methacrylamide modified gelatin hydrogels. *Biomacromolecules*. 1: 31-38.

van der Does A. M., Hensbergen P. J., Bogaards S. J., Cansoy M., Deelder A. M., van Leeuwen H. C., Drijfhout J. W., van Dissel J. T., and Nibbering P. H. (2012). The human lactoferrin-derived peptide hLF1-11 exerts immunomodulatory effects by specific inhibition of myeloperoxidase activity. *The Journal of Immunology*. 188: 5012-5019.

Van Oort M. (2010). Enzymes in food technology - introduction. *Enzymes in food technology*: 14.

Van Vlierberghe S., Dubruel P., and Schacht E. (2010). Effect of cryogenic treatment on the rheological properties of gelatin hydrogels. *Journal of bioactive and compatible polymers*. 25: 498-512.

Wang H., Wang H., Xing T., Wu N., Xu X., and Zhou G. (2016a). Removal of *Salmonella* biofilm formed under meat processing environment by surfactant in combination with bio-enzyme. *LWT-Food Science and Technology*. 66: 298-304.

Wang L., Yu B., Wang R., and Xie J. (2018). Biotechnological routes for transglutaminase production: Recent achievements, perspectives and limits. *Trends in Food Science & Technology*.

Wang R., Liang Z., Hall M., and Söderhäll K. (2001). A transglutaminase involved in the coagulation system of the freshwater crayfish, *Pacifastacus leniusculus*. Tissue localisation and cDNA cloning. *Fish & Shellfish Immunology*. 11: 623-637.

Wang Y., Wang J., Zhao Y., Hu S., Shi D., and Xue C. (2016b). Fucoidan from sea cucumber *Cucumaria frondosa* exhibits anti-hyperglycemic effects in insulin resistant mice via

activating the PI3K/PKB pathway and GLUT4. *Journal of Bioscience and Bioengineering*. 121: 36-42.

Weller C. L., Gennadios A., and Saraiva R. A. (1998). Edible bilayer films from zein and grain sorghum wax or carnauba wax. *LWT - Food Science and Technology*. 31: 279-285.

Weng M., Deng X., Bao W., Zhu L., Wu J., Cai Y., Jia Y., Zheng Z., and Zou G. (2015). Improving the activity of the subtilisin nattokinase by site-directed mutagenesis and molecular dynamics simulation. *Biochemical and biophysical research communications*. 465: 580-586.

White J. S., and White D. C. (1997). Hydrolases. In: Source book of enzymes (pp. 569). CRC Press. Taylor & Francis Group.

Wilhelm B., Meinhardt A., and Seitz J. (1996). Transglutaminases: purification and actuivity assays. *Journal of Chromatography B: Biomedical Sciences and Applications*. 684: 163-177.

Worratao A., and Yongsawatdigul J. (2003). Cross-linking of actomyosin by crude tilapia (*Oreochromis Niloticus*) transglutaminase. *Journal of Food Biochemistry*. 27: 35-51.

Worratao A., and Yongsawatdigul J. (2005). Purification and characterization of transglutaminase from Tropical tilapia (*Oreochromis niloticus*). *Food Chemistry*. 93: 651-658.

Wróblewska B., Kołakowski P., Pawlikowska K., Troszyńska A., and Kaliszewska A. (2009). Influence of the addition of transglutaminase on the immunoreactivity of milk proteins and sensory quality of kefir. *Food Hydrocolloids*. 23: 2434-2445.

Wu J., Chen S., Ge S., Miao J., Li J., and Zhang Q. (2013). Preparation, properties and antioxidant activity of an active film from silver carp (*Hypophthalmichthys molitrix*) skin gelatin incorporated with green tea extract. *Food Hydrocolloids*. 32: 42-51.

Xiao Y., Ge H., Zou S., Wen H., Li Y., Fan L., and Xiao L. (2017). Enzymatic synthesis of *N*-succinyl chitosan-collagen peptide copolymer and its characterization. *Carbohydrate polymers*. 166: 45-54.

Xie F., Chao Y., Yang X., Yang J., Xue Z., Luo Y., and Qian S. (2010). Purification and characterization of four keratinases produced by *Streptomyces* sp. strain 16 in native human foot skin medium. *Bioresource technology*. 101: 344-350.

Xu F., Oruna-Concha M.-J., and Elmore J. S. (2016). The use of asparaginase to reduce acrylamide levels in cooked food. *Food Chemistry*. 210: 163-171.

Yan M., Tao H., and Qin S. (2016). Effect of enzyme type on the antioxidant activities and functional properties of enzymatic hydrolysates from sea cucumber (*Cucumaria frondosa*)

viscera. *Journal of Aquatic Food Product Technology*. 25: 940-952.

Yang F., Rustad T., Xu Y., Jiang Q., and Xia W. (2015). Endogenous proteolytic enzymes–A study of their impact on cod (*Gadus morhua*) muscle proteins and textural properties in a fermented product. *Food Chemistry*. 172: 551-558.

Yang J., Gao R., Zhou Y., Anankanbil S., Li J., Xie G., and Guo Z. (2018). β-Glucosidase from *Thermotoga naphthophila* RKU-10 for exclusive synthesis of galactotrisaccharides: Kinetics and thermodynamics insight into reaction mechanism. *Food Chemistry*. 240: 422-429.

Yang M.-T., Chang C.-H., Wang J. M., Wu T. K., Wang Y.-K., Chang C.-Y., and Li T. T. (2011). Crystal structure and inhibition studies of transglutaminase from *Streptomyces mobaraense*. *Journal of Biological Chemistry*. 286: 7301-7307.

Yasueda H., Kumazawa Y., and Motoki M. (1994). Purification and characterization of a tissue-type transglutaminase from red sea bream (*Pagrus major*). *Bioscience, biotechnology, and biochemistry*. 58: 2041-2045.

Yasueda H., Nakanishi K., Kumazawa Y., Nagase K., Motoki M., and Matsui H. (1995). Tissue-type transglutaminase from red sea bream (*Pagrus major*). *European Journal of Biochemistry*. 232: 411-419.

Yee V. C., Pedersen L. C., Le Trong I., Bishop P. D., Stenkamp R. E., and Teller D. C. (1994). Three-dimensional structure of a transglutaminase: human blood coagulation factor XIII. *Proceedings of the National Academy of Sciences*. 91: 7296-7300.

Yokoyama K., Nio N., and Kikuchi Y. (2004). Properties and applications of microbial transglutaminase. *Applied Microbiology and Biotechnology*. 64: 447-454.

Yokoyama K., Utsumi H., Nakamura T., Ogaya D., Shimba N., Suzuki E., and Taguchi S. (2010). Screening for improved activity of a transglutaminase from *Streptomyces mobaraensis* created by a novel rational mutagenesis and random mutagenesis. *Applied Microbiology and Biotechnology*. 87: 2087-2096.

You L., Zhao M., Regenstein J. M., and Ren J. (2011). *In vitro* antioxidant activity and in vivo anti-fatigue effect of loach (*Misgurnus anguillicaudatus*) peptides prepared by papain digestion. *Food Chemistry*. 124: 188-194.

Yu J., Pian Y., Ge J., Guo J., Zheng Y., Jiang H., Hao H., Yuan Y., Jiang Y., and Yang M. (2015). Functional and structural characterization of the antiphagocytic properties of a novel transglutaminase from *Streptococcus suis*. *Journal of Biological Chemistry*. 290: 19081-

19092.

Yu S., Zhang Y., Zhu Y., Zhang T., Jiang B., and Mu W. (2017a). Improving the catalytic behavior of DFA I-forming inulin fructotransferase from *Streptomyces davawensis* with site-directed mutagenesis. *Journal of Agricultural and Food Chemistry*. 65: 7579-7587.

Yu X.-W., Yang M., Jiang C., Zhang X., and Xu Y. (2017b). *N*-Glycosylation Engineering to Improve the Constitutive Expression of *Rhizopus oryzae* Lipase in *Komagataella phaffii*. *Journal of Agricultural and Food Chemistry*. 65: 6009-6015.

Yu Y.-J., Wu S.-C., Chan H.-H., Chen Y.-C., Chen Z.-Y., and Yang M.-T. (2008). Overproduction of soluble recombinant transglutaminase from *Streptomyces netropsis* in *Escherichia coli*. *Applied Microbiology and Biotechnology*. 81: 523-532.

Yu Z., Alsammarraie F. K., Nayigiziki F. X., Wang W., Vardhanabhuti B., Mustapha A., and Lin M. (2017c). Effect and mechanism of cellulose nanofibrils on the active functions of biopolymer-based nanocomposite films. *Food Research International*. 99: 166-172.

Zaroog M. S., and Tayyab S. (2012). Formation of molten globule-like state during acid denaturation of *Aspergillus niger* glucoamylase. *Process Biochemistry*. 47: 775-784.

Zhang D., Zhu Y., and Chen J. (2009). Microbial transglutaminase production: understanding the mechanism. *Biotechnology and Genetic Engineering Reviews*. 26: 205-222.

Zhang P., Hu T., Feng S., Xu Q., Zheng T., Zhou M., Chu X., Huang X., Lu X., and Pan S. (2016a). Effect of high intensity ultrasound on transglutaminase-catalyzed soy protein isolate cold set gel. *Ultrasonics Sonochemistry*. 29: 380-387.

Zhang Q.-X., Fu R.-J., Yao K., Jia D.-Y., He Q., and Chi Y.-L. (2018a). Clarification effect of collagen hydrolysate clarifier on chrysanthemum beverage. *LWT - Food Science and Technology*. 91: 70-76.

Zhang S., Zeng X., Ren M., Mao X., and Qiao S. (2017a). Novel metabolic and physiological functions of branched chain amino acids: A review. *Journal of Animal Science and Biotechnology*. 8: 10.

Zhang W., Jia M., Yu S., Zhang T., Zhou L., Jiang B., and Mu W. (2016b). Improving the thermostability and catalytic efficiency of the D-psicose 3-epimerase from *clostridium bolteae* ATCC BAA-613 using site-directed mutagenesis. *Journal of Agricultural and Food Chemistry*. 64: 3386-3393.

Zhang W., Lu P., Qian L., and Xiao H. (2014). Fabrication of superhydrophobic paper surface via

wax mixture coating. *Chemical Engineering Journal*. 250: 431-436.

Zhang X., Wang W., Wang Y., Wang Y., Wang X., Gao G., Chen G., and Liu A. (2018b). Effects of nanofiber cellulose on functional properties of heat-induced chicken salt-soluble meat protein gel enhanced with microbial transglutaminase. *Food Hydrocolloids*. 84: 1-8.

Zhang Y., Dutilleul P., Li C., and Simpson B. K. (2019). Alcalase-assisted production of fish skin gelatin rich in high molecular weight (HMW) polypeptide chains and their characterization for film forming capacity. *LWT*. 110: 117-125.

Zhang Y., Dutilleul P., Orsat V., and Simpson B. K. (2018c). Alcalase assisted production of novel high alpha-chain gelatin and the functional stability of its hydrogel as influenced by thermal treatment. *International journal of biological macromolecules*. 118: 2278-2286.

Zhang Y., He S., and Simpson B. K. (2017b). A cold active transglutaminase from Antarctic krill (*Euphausia superba*): Purification, characterization and application in the modification of cold-set gelatin gel. *Food Chemistry*. 232: 155-162.

Zhang Y., Simpson B. K., and Dumont M.-J. (2018d). Effect of beeswax and carnauba wax addition on properties of gelatin films: A comparative study. *Food Bioscience*. 26: 88-95.

Zhao H.-Y., and Feng H. (2018). Engineering *Bacillus pumilus* alkaline serine protease to increase its low-temperature proteolytic activity by directed evolution. *BMC biotechnology*. 18: 34.

Zheng J. P., Li P., Ma Y. L., and Yao K. D. (2002). Gelatin/montmorillonite hybrid nanocomposite. I. Preparation and properties. *Journal of Applied Polymer Science*. 86: 1189-1194.

Zheng Z., Xu W., Aweya J. J., Zhong M., Liu S., Lun J., Chen J., and Zhang Y. (2018). Functional domains of *Litopenaeus vannamei* transglutaminase and their involvement in immunoregulation in shrimp. *Fish & Shellfish Immunology*. 81: 168-175.

Zhong Y., Khan M. A., and Shahidi F. (2007). Compositional characteristics and antioxidant properties of fresh and processed sea cucumber (*Cucumaria frondosa*). *Journal of Agricultural and Food Chemistry*. 55: 1188-1192.

Zhou L., Li S., Zhang T., Mu W., and Jiang B. (2016). Properties of a novel polydatin-β-d-glucosidase from *Aspergillus niger* SK34. 002 and its application in enzymatic preparation of resveratrol. *Journal of the Science of Food and Agriculture*. 96: 2588-2595.

Zhu F., Jiang T., Wu B., and He B. (2018). Enhancement of *Z*-aspartame synthesis by rational engineering of metalloprotease. *Food Chemistry*. 253: 30-36.

Zhu Y., and Tramper J. (2008). Novel applications for microbial transglutaminase beyond food

processing. *Trends in Biotechnology*. 26: 559-565.

Zilhao R., Isticato R., Martins L. O., Steil L., Völker U., Ricca E., Moran C. P., and Henriques A. O. (2005). Assembly and function of a spore coat-associated transglutaminase of *Bacillus subtilis*. *Journal of Bacteriology*. 187: 7753-7764.